AN EXPERIMENTAL INVESTIGATION ON THE SHEAR STRENGTH AT THE MONOLITHIC INTERFACES OF THE FLY ASH AND GGBS BASED GEOPOLYMER CONCRETE AND ITS APPLICATION IN THE CORBELS

Submitted in partial fulfilment of the requirements

for the award of the degree of

DOCTOR OF PHILOSOPHY

in

CIVIL ENGINEERING

by

SUMANTH KUMAR BANDARU

(Roll No: 717 001)

Supervisor

Prof. D. RAMA SESHU

STRUCTURES DIVISION

DEPARTMENT OF CIVIL ENGINEERING

NATIONAL INSTITUTE OF TECHNOLOGY

WARANGAL- 506 004 (T.S.) INDIA

OCTOBER 2020

NATIONAL INSTITUTE OF TECHNOLOGY
WARANGAL

CERTIFICATE

This is to certify that the thesis entitled **"AN EXPERIMENTAL INVESTIGATION ON THE SHEAR STRENGTH AT THE MONOLITHIC INTERFACES OF THE FLY ASH AND GGBS BASED GEOPOLYMER CONCRETE AND ITS APPLICATION IN THE CORBELS"** being submitted by **Mr. SUMANTH KUMAR BANDARU** for the award of the degree of **DOCTOR OF PHILOSOPHY** to the Faculty of Engineering and Technology of **NATIONAL INSTITUTE OF TECHNOLOGY, WARANGAL** is a record of bonafide research work carried out by him under my supervision and it has not been submitted elsewhere for award of any degree.

Prof. D RAMA SESHU
Thesis Supervisor

Department of Civil Engineering
National Institute of Technology
Warangal (T.S.) – INDIA

APPROVAL SHEET

This Thesis entitled **"AN EXPERIMENTAL INVESTIGATION ON THE SHEAR STRENGTH AT THE MONOLITHIC INTERFACES OF THE FLY ASH AND GGBS BASED GEOPOLYMER CONCRETE AND ITS APPLICATION IN THE CORBELS"** by **Mr. SUMANTH KUMAR BANDARU** is approved for the degree of Doctor of Philosophy.

Examiners

_____

_____

_____

Supervisor

_____

Chairman

_____

Date: _____

DECLARATION

This is to certify that the work presented in the thesis entitled **"AN EXPERIMENTAL INVESTIGATION ON THE SHEAR STRENGTH AT THE MONOLITHIC INTERFACES OF THE FLY ASH AND GGBS BASED GEOPOLYMER CONCRETE AND ITS APPLICATION IN THE CORBELS"** is a bonafide work done by me under the supervision of **Prof. D RAMA SESHU** and was not submitted elsewhere for the award of any degree. I declare that this written submission represents my ideas in my own words and where others' ideas or words have been included, I have adequately cited and referenced the original sources. I also declare that I have adhered to all principles of academic honesty and integrity and have not misrepresented or fabricated or falsified any idea / data / fact / source in my submission. I understand that any violation of the above will be a cause for disciplinary action by the Institute and can also evoke penal action from the sources which have thus not been properly cited or from whom proper permission has not been taken when needed.

_____

(Name of the Student: **Sumanth Kumar B**)

(Roll No: **717 001**)

Date: 07-05-2021

With Blessings of
Goddess Bhadrakali
&
Influential Mentors

Start now.

Start where you are.

Start with fear.

Start with pain.

Start with doubt.

Start with hands shaking.

Start with voice trembling but start.

Start and don't stop.

Start where you are, with what you have.

Just…start.

~ Ijeoma Umebinyuo

Dedicated to

My Beloved Parents,

Wife and Son *Tejas*

ACKNOWLEDGEMENTS

Foremost, I would like to express my sincere gratitude to my research supervisor, **Prof. D Rama Seshu**, Department of Civil Engineering, for his continuous support of my research, for his patience, motivation, enthusiasm, and immense knowledge in bringing out this research work with artistry. I could not have imagined having a better advisor and mentor for my research study.

I would like to express my deepest indebtedness to **Prof. C B Kameshwara Rao,** Chairman Doctoral Scrutiny Committee for his enlightening guidance and immense help rendered in bringing out this work. My sincere gratefulness to **Prof. P Rathish Kumar**, Head, Department of Civil Engineering for his constant encouragement and support during the research.

I would like to be grateful to **Prof. G Rajesh Kumar**, Department of Civil Engineering, **Prof. T D Gunneswara Rao**, Department of Civil Engineering, **Prof. Adepu Kumar**, Department of Mechanical Engineering, **Prof. G Amba Prasad Rao**, Department of Mechanical Engineering (NIT AP) of Doctoral Scrutiny Committee for their guidance and help during the investigation.

I am also thankful to Sri M. Sudhakar, Dr. S Venkateswara Rao, Dr. D Ravi Prasad, Dr. K. Gopi Krishna, Dr. M.V.N. Siva Kumar, Dr. T.P. Tezaswi, Dr. S. Anitha Priyadharshani, Dr. B Kavitha, Dr. B Umesh, Dr. Akshay Venkateshwaran and Dr. P. Ravi Prakash, the faculty members of Structures Division, NITW for the moral support given during the period of research work.

I am thankful to **JSW Cements Pvt ltd**, Bilakalagudur, India in providing ground granulated blast furnace slag for the research work.

I thank all my fellow research scholars for their direct or indirect suggestions throughout the period of my research work. I am thankful to Sri A Chandra Narayana, Sri A Laxman and Mechanics in Structural Engineering Laboratories, Sri P Rajendra Prasad, Smt. G. Padmaja, Sri Md. Hussain and Administrative staff for the help done during the research period.

Above all, I am forever indebted to my Parents, my wife and son for their personal support and great patience at all times.

Finally I thank everyone, who contributed either directly or indirectly in successful completion of this work.

~ Sumanth Kumar B

ABSTRACT

The steep rise in the infrastructure development has led to the huge consumption of various building materials in general and cement in particular. The production of Cement involves high CO_2 emissions into the atmosphere, which in turn has created an imbalance in the environment, causing a greenhouse effect and also depletion of natural resources. To reduce this negative impact on the atmosphere, new environmentally friendly building materials are being developed all over the world. The main aspect in achieving environmentally friendly building materials is to reduce the excessive use of virgin materials used to make concrete. In this context, the conventional Portland cement (OPC) is being replaced with large volumes of supplementary cementitious materials or binders. These binders used are mainly industrial waste by-products that are rich in silica and alumina, such as fly ash, rice husk ash, ground granulated blast furnace slag (GGBS), metakaolin, etc.

Using fly ash, GGBS, etc. as binders along with alkaline activated solution forms a matrix called Geopolymer concrete (GPC). Geopolymer concrete with a relatively lower environmental impact compared to conventional Portland cement, holds great promise as a suitable alternative in the construction industry. As the Geopolymers made using fly ash requires high curing temperatures (60–90°c) to achieve strength (Hardjito, D et al., 2004), the GGBS and fly ash combination along alkaline activator solution is being promoted as alternate binders in producing geopolymer concrete at ambient temperatures.

There are numerous studies about the geopolymer concrete. The focus of these studies has been mainly oriented towards material characterization, physical, chemical properties and the associated polymerisation reaction, mix-proportioning of geo polymeric concrete, etc. In the recent past, several investigations reported various parameters affecting the strength of GPC. Some of the identified parameters which are affecting the strength of GPC include the the ratio of sodium silicate to sodium hydroxide, the concentration of sodium hydroxides, the fly ash and GGBS ratio etc. Several investigations have reported the effects of these identified variables on strength of GPC in an isolated manner. Keeping in view of the different identified parameters an attempt has been made in the first phase of this investigation, to introduce a single parameter that can be taken into account in controlling the strength of GPC.

Despite the advantages, the use of geopolymer concrete in practice is significantly limited. This is mainly due to a lack of research in terms of structural elements, design, and

applications. The use of geopolymer concrete as structural concrete calls for studies on its behavior under different structural actions such as compression, tension, flexure, shear, etc. The review of the literature indicated the requirement of studies on shear strength and shear transfer characteristics of GPC. A study on the shear strength at the monolithic interface of GGBS and fly ash-based GPC and its application to the GPC corbels have been carried out in the present investigation.

Keeping in view of the identified gaps in the literature, the investigation reported in the present work has been carried out in three phases. In the first phase of the investigation, based on the analytical study of the published strength results of GPC, a new parameter termed as 'Binder Index (Bi)' has been proposed as a unique parameter influencing the compressive strength of the GPC. The binder index has been further used in the development of a phenomenological model for the strength of GPC.

The second phase of the study is focussed on the assessment of the shear strength of the GPC at monolithic interfaces. The experimental study is carried out taking into account three different strengths of GPC and three different percentages of reinforcement at the interface of the push-off samples. The results obtained from the experimental work are analyzed based on the concept of shear friction, which includes the components of cohesion, friction, and dowel action as proposed by Randl, 1997. The GPC shear strength obtained from the experimental study is compared with conventional concrete shear design theories and design codes.

The third phase of the investigation involved the validation of the equation developed for the shear strength of GPC by testing the geopolymer reinforced concrete corbels. The parameters of the experimental study are the compressive strength of GPC and the reinforcement crossing the shear interface of corbels. Experimental results are also compared with various design theories and codes of corbels.

Based on the analytical and experimental investigation carried out, it is concluded that the new parameter called "Binder Index (Bi)" which combines the different parameters such as alkaline to binder content ratio, GGBS to fly ash ratio and molarity of sodium hydroxide, can be considered as a unique parameter to control the compressive strength of GPC. A non-linear variation exists between the binder index and the compressive strengths f_{gpc} of GPC and can be indicated by a power equation.

The experimental investigation on GPC push-off specimens indicated that the shear strength of the monolithic GPC interface has increased with an increase in the compressive strength of GPC. The rate of increase of shear strength has decreased for compressive strength of GPC more than 40 MPa. The shear (V_u) across the reinforced monolithic interface in GPC specimens is resisted by the combined action of cohesion, friction, and dowel action. Further it is observed that the available conventional concrete shear strength prediction models are highly conservative in estimating the shear strength of unreinforced and reinforced monolithic shear interfaces in GPC.

The experimental study on the GPC corbels indicated that the ultimate load capacity of corbels increased with an increase in the compressive strength of GPC. Also, the ultimate load of corbels was increased by the increase in the percentage of closed-loop stirrups (secondary reinforcement). Further the shear capacity as obtained from different codes and theories is underestimating the interface shear capacity of reinforced GPC corbels.

CONTENTS

LIST OF FIGURES

LIST OF TABLES

CHAPTER 1
INTRODUCTION

1.1 GENERAL

The phenomenal growth in infrastructure development has led to huge consumption of building materials in general and concrete in particular. The amount of cement consumed is likely to increase by 25% over the next 10 years (Rajamane et al., 2012). It is a known fact that cement production not only accounts for global CO_2 emissions but also consumes a significant amount of natural resources. Approximately one ton of CO_2 is emitted for every ton of cement produced. Keeping in mind current climatic conditions and global warming phenomena, there is an urgent need for construction industry to adopt sustainable and environmental friendly alternatives.

One way to achieve this being finding an alternative material to cement, coal-fired power plants and steel industries have led to the generation of huge quantities of industrial waste (by-products) such as fly ash and round granulated blast furnace slag (GGBS), posing problems with regard to safe disposal. Several efforts are being made in direction of effective use such by-products in the development of new binders in concrete production and reducing to some extent environmental pollution. The new binders are viewed as an alternative to Portland cement without compromising durability and strength. In this regard, geopolymer concrete with a relatively low environmental impact compared to conventional Portland cement offers fine prospects as a suitable alternative in the concrete industry (Nugteren et al., 2005).

1.2 GEOPOLYMER CONCRETE – A SUSTAINABLE MATERIAL

Geopolymers are inorganic polymers that are made using locally available industrial by-products, which are rich in silica and alumina, along with alkaline activators to form a sodium

alumino-silicate hydrate gel that binds the aggregates to form geopolymer concrete (Davidovits, 1999, Palomo et al., 1999, Lăzărescu et al., 2017). Another key property of geopolymer mixtures is that they don't require water for curing. The mixtures are cured either in an oven or cured in the open air. The use of geopolymer concrete helps in reducing carbon footprint while developing infrastructure (Gartner, 2004, Palomo et al., 2004). Thus, geopolymer is slowly emerging as an alternative to conventional cementitious materials for application in a wide range of civil engineering works.

1.3 CONSTITUENTS OF GEOPOLYMER CONCRETE (GPC)

The main constituents of geopolymer concrete are materials (Fig.1.1) rich in silicon (Si) and aluminum (Al) like fly ash, GGBS, etc., and Catalytic Liquid Solution (CLS) i.e. an Alkaline Activator Solution (AAS) which is a combination of alkali hydroxide and silicate. Alkaline Activator Solution activates the primary source materials to form a geopolymer mix.

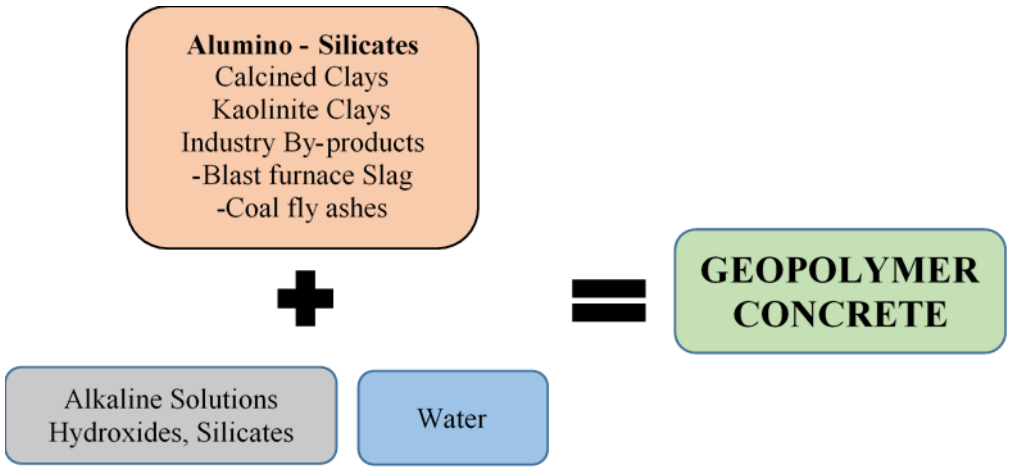

Figure 1.1: Constituents of geopolymer concrete

Fly Ash (F): It is a by-product of a coal-fired power plant that comes from dry bottom boilers. In India, 16% of fly ash is used and the rest is disposed as a landfills causing environmental concerns (Rajamane et al., 2012).

Ground Granulated Blast Furnace Slag (GGBS or G): It is a by-product from blast furnace used in steel production. GGBS is a glassy, granular, non-metallic consists of silicates and aluminates of calcium and other bases.

Alkaline Activator / Liquid (A): This is a combination of alkali silicate (sodium silicate) and hydroxide (sodium hydroxide) solution. This combines with silicon and aluminum present in fly ash and GGBS to form a binder that binds the aggregates to form geopolymer concrete.

High Range Water Reducer and Extra water (or) Superplasticiser: To improve the workability of the mix, a high range water reducer or superplasticizer like naphthalene sulphonate can be used.

Coarse (CA) and Fine Aggregate (FA): Coarse and fine aggregate can be used for producing geopolymer concrete like in ordinary Portland cement concrete. The aggregates in general occupies 75% to 80% of the mass of geopolymer concrete.

Curing: Heat curing is recommended for assisting chemical reactions in fly ash-based geopolymer concretes. Both the temperature and time of curing have an effect on the compressive strength of fly ash-based geopolymer concrete. However, partial replacement of fly ash with GGBS referred to as GGBS and fly ash-based geopolymer concrete or GGBS based geopolymer concrete, can help in avoiding heat curing and also enhance compressive strengths.

1.4 GEOPOLYMERISATION

Geopolymerisation involves the formation of complex polymers through the chemical reaction of alumina-silicate present in source materials with alkaline activators. Sodium hydroxide (NaOH)) and sodium silicate (Na_2SiO_3) are regularly used in the preparation of alkaline activator solution. Generally, activation can be done by hydroxides like sodium hydroxide, but

the reaction process happens at a slower phase. Thus, to accelerate the reaction rate and polymerisation process, hydroxides combined with silicates are used. Also, an increase in the concentration of hydroxide leads to greater dissolution of alumino-silicate and results in faster geopolymerisation process. (Davidovits, 1991). Geopolymerisation procedure involves the chemical response of alumino silicate with alkaline solutions, forming polymeric bonds (Si –O –Al –O) whose chemical representation is given below (Davidovits, 1999).

$$n(Si_2O_5, Al_2O_2) + 2nSiO_2 + 4nH_2O + (Na^+, K^+) \longrightarrow n(OH)_3 - Si - O - \underset{\substack{|\\(OH)_2}}{Al^-} - O - Si - (OH)_3$$

$$n(OH)_3 - Si - O - \underset{\substack{|\\(OH)_2}}{Al^-} - O - Si - (OH)_3 \longrightarrow (Na^+, K^+) - (-\underset{\substack{|\\O\\|}}{\overset{|}{Si}} - O - \underset{\substack{|\\O\\|}}{\overset{|}{Al^-}} - O - \underset{\substack{|\\O\\|}}{\overset{|}{Si}} - O-)n + 4nH_2O$$

Based on the above chemical representation, it is understood that water is expelled through geopolymerisation. During curing and drying time leaves nano-pores in the medium, which in turn benefits geopolymers performance. This is reverse to the reaction of water with Portland cement hydration process (Davidovits, 1999).

In ordinary Portland cement concrete, achievement of strength is due to the hydration process, which involves the formation of calcium silicate Hydrate (C-S-H) and calcium hydroxides in presence of water during curing. In geopolymer concrete the geopolymerisation process is responsible for the strength. Geopolymers are also stated to be zeolite precursors (Duxson et al., 2007, Grutzeck et al., 2004) because of similar composition and 3D network.

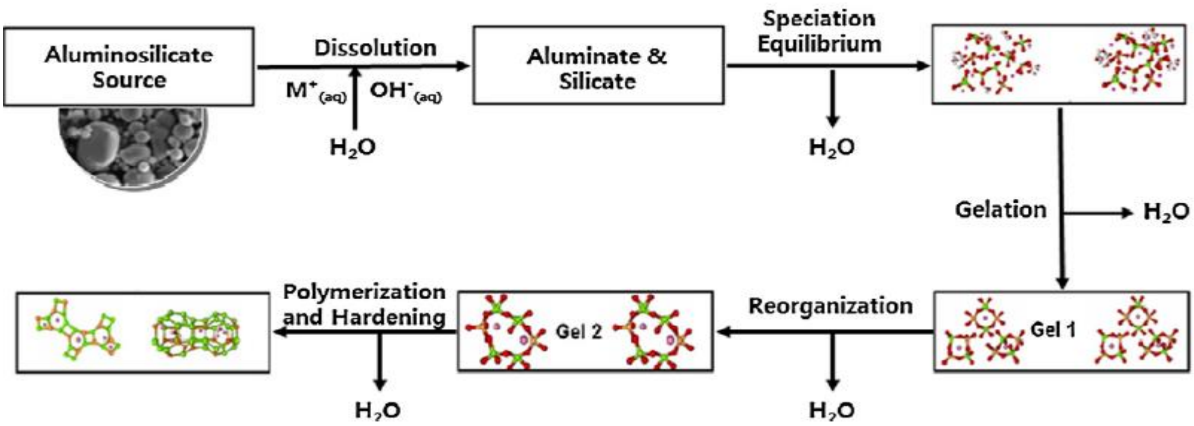

Figure 1.2: Schematic diagram of the polymerisation process (Duxson et al., 2007)

Geopolymers has amorphous structure and use poly-condensation of silica and alumina precursors to attain structural strength. The geopolymerisation process was detailed by Glukhovsky (1959) in three stages **a.** Destruction – Coagulation, **b.** Coagulation – Condensation, **c.** Condensation – Crystallisation. A similar process was also reported by Duxson et al., 2007, shown in figure 1.2.

1.5 SALIENT FEATURES AND PROPERTIES OF GPC

Engineering properties of GPC: Several researchers (Hardjito and Rangan, 2005, Wallah and Rangan, 2006, Rangan, 2009, Sofi et al., 2007, Collins and Sanjayan, 1999) have reported various engineering properties of geopolymer concrete such as compressive strength, indirect tensile strength, modules of elasticity, and Poisson's ratio. Geopolymer concrete has lower elastic modulus than OPC (Hardjito and Rangan, 2005). Strain at peak stress ranges from 0.0024 to 0.0026 and Poisson's ratio ranges from 0.12 to 0.16 for fly ash-based geopolymer concrete (Rangan, 2009). Geopolymer concrete has good gel-aggregate interface (Song et al., 2005). Geopolymer concrete undergoes very little shrinkage and shows good resistance to sulphate (Wallah and Rangan, 2006). Also, researchers have discovered that geopolymer concrete showed good response in terms of properties like permeation, elevated temperature, sulfate attack, and fire attack (Chi et al., 2013, Ismail et al., 2013).

Structural performance of GPC: Load deflection behavior of geopolymer concrete is similar to that of OPC (Sumajouw et al., 2005, Yost et al., 2013). Higher shear strength was observed for geopolymer concrete under flexural and shear loading (Mourougane et al., 2012, Chang, 2009, Visintin et al., 2017). Geopolymer concrete columns perform better than ordinary RC columns and structural failure occurred crushing upon concrete on the compressive side similar to conventional RC columns (Sujatha et al., 2012, Rahman and Sarker, 2011, Sumajouw et al., 2006).

1.6 SHEAR STRENGTH

The strength of reinforced concrete structures is critical in the transfer of shear force across the concrete interface. Shear transfer across an interface between two members that slip relative to one another is due to shear-friction, and aggregate interlock. These planes or interfaces where shear acts are known as a *shear plane* or *slip plane*. The relative contribution of friction, cohesion, and dowel action at the interface depends on the applied shear force and slip displacement between interfaces (Zilch and Reinecke, 2000). Based on the predominance of a particular mechanism, shear transfer is accordingly classified. If cohesion force predominates, it is termed *aggregate interlock*, friction between layers are predominate then it is known as *shear-friction* and all three plays important role then this shear transfer is known as *Interface shear transfer*.

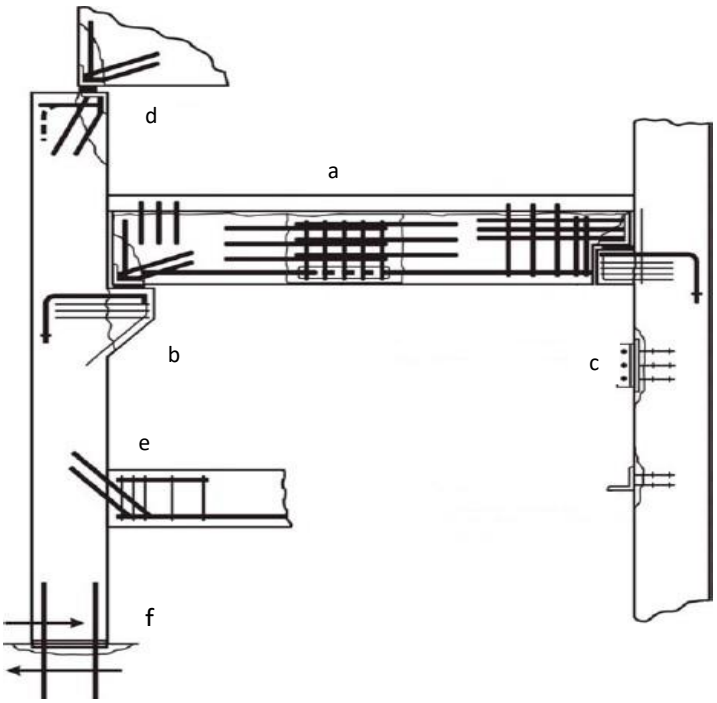

a) The interface between precast elements with cast-in-place parts;
b) Corbels;
c) Metallic supports subjected mainly to shear forces;
d) Regions near supports;
e) The connection between precast elements and existing concrete; and
f) The connection between columns and foundations.

Figure 1.3 Possible locations of shear-friction theory (CIRSOC 201, 2005)

In general, shear friction theory is used in predicting the shear strength of concrete (Santos and Júlio, 2012). CIRSOC 201, 2005 gives several zones in a typical structure where shear friction

zones are considered, shown in figure 1.3. In general, corbels are considered to study the transfer of shear along an interface.

1.7 CORBELS (BRACKETS)

Corbels (Brackets) are a reinforced element projecting from the face of the column and cast monolithically with column or wall to support primary beams or girders. The shear span-to-depth (a/d) of corbels is often less than one. The typical corbel and its free body force diagram are shown in Fig.1.4.

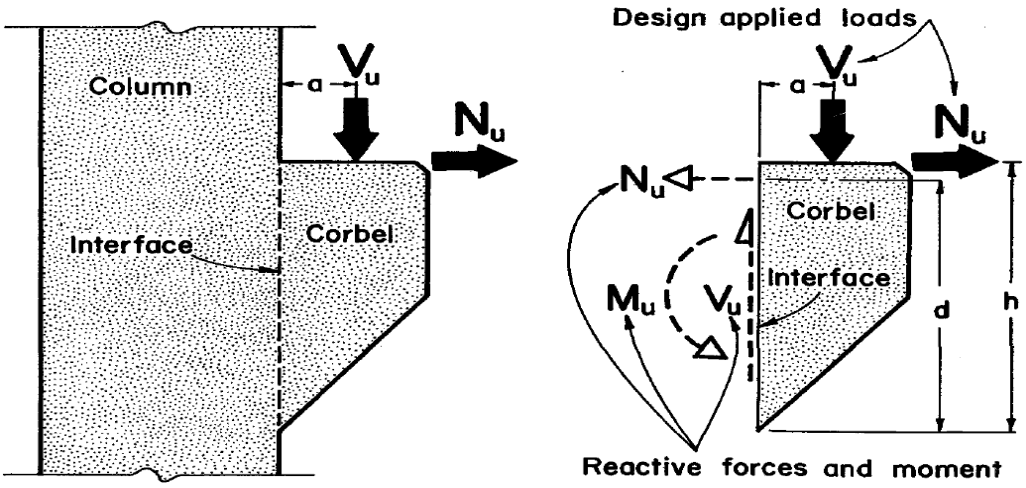

Figure 1.4 Typical corbel and free body force diagram (Mattock, 1976)

The principal failure modes for corbels without stirrups consist of: shear failure, yielding of the principal reinforcement (flexural tension), crushing of concrete strut (flexural compression), and diagonal splitting. In brackets or corbels with secondary reinforcement (stirrups), which is always suggested, all the failure modes stated earlier tend to converge into a single typology of failure mode called **beam-shear failure**. The last one is characterized by the opening of one or more diagonal cracks followed by shear failure in the compressed zone of the strut.

Due to inconsistency in failure modes, mechanical behavior of corbels at failure and the assessment of their shear strength are very complex. The assessment of corbels is evaluated

using the following methods: shear-friction method, shear due to flexural behavior, and strut and tie models (Yassin and Hasan, 2015).

1.8 RATIONALE FOR THE PRESENT RESEARCH

Although numerous studies have been carried out on geopolymer concrete, the primary focus has been on material characterization, physical and chemical properties, associated polymerisation reactions, and mix-proportioning of geopolymer concrete.

Different parameters such as the quantity of source materials, activator to binder ratio, molarities of activator solution have been identified as sources affecting the strength of geopolymer concrete. Literature review has shown that there is a wide variation in geopolymer concrete strength results when the parameters identified are considered in isolation. A brief review of the parametric study on geopolymer concrete study conducted as part of this thesis revealed the scope for introducing a unique parameter that can account for the combined effect of different parameters on the strength of the geopolymer concrete.

Further, the use of geopolymer concrete in practice is rather limited despite having several advantages. This is mainly due to a lack of research in the structural performance of geopolymer concrete design, and its applications. The use of geopolymer concrete as structural concrete calls for studies on its behavior under different structural actions such as compression, tension, flexure, shear, etc... Very few studies have been carried out on shear transfer in geopolymer concrete.

The requirement of studies on shear strength and shear transfer characteristics of geopolymer concrete has been urgent. Therefore, the present research is dedicated to the study of interfacial shear strength of fly ash and GGBS based geopolymer concrete. The investigation reported in

the work presents an experimental investigation on the shear strength at the monolithic interfaces of fly ash and GGBS based geopolymer concrete and its application to corbels.

1.9 THESIS ORGANIZATION

The present thesis is organised in the following way

i. The study begins with an introduction to geopolymer concrete, salient features of geopolymer concrete and its structural performances, shear transfer, and its application to corbel/bracket design.

ii. The next section includes literature review on shear transfer for conventional concrete, evaluation of geopolymer concrete, different parameters for varying the strength of geopolymer concrete, shear strength of geopolymer concrete, and identifying gaps in the literature review.

iii. The third chapter presents the scope and objectives of the investigation.

iv. The fourth section includes the study of the cumulative effect of various parameters on the strength of GGBS and fly ash-based geopolymer concrete. A unified parameter called '*Binder Index (Bi)*' is proposed which influences the strength of geopolymer concrete and its variation with the strength of geopolymer concrete.

v. The fifth chapter involves experimental investigation on shear strength at the monolithic interface of GGBS based geopolymer concrete and a comparison of different design shear theories and codes for conventional concrete.

vi. The sixth chapter includes applying the equation developed for the shear strength of geopolymer concrete to reinforced geopolymer concrete corbels. The experimental results are also compared with different design theories and codes on corbels.

vii. Conclusions, scope for further investigation and limitations of the present study figure in the seventh chapter along with references.

CHAPTER 2
LITERATURE REVIEW

2.1 LITERATURE REVIEW ON SHEAR STRENGTH OF CONCRETE

The strength of reinforced concrete structures is critical in the transfer of shear force across the concrete interface. Based on the nature of surfaces in contact, friction coefficient (tan φ) is considered. From applied mechanics, shear transferred between surfaces is $V_u = N \tan \varphi$. Where V_u is the maximum shear force transferred and N is the normal force acting on the interface.

Shear friction theory is used for predicting longitudinal shear stress of concrete from the 1960s. Before 1960, all the surfaces were roughened, for achieving adequate shear strength along with shear keys for prevention of slippage at construction joint. The research significantly started in 1960s in this area because accurate test data fits this analogy. Research on composite beams regarding horizontal shear and push-off specimens was first introduced by Anderson in 1960 for evaluating shear transfer at the interface and later these specimens were widely used. In the tests, pure shear and normal force can be introduced on the failure plane.

Table 2.1 presents the year of publication and the researchers' data on the shear strength of concrete based on shear friction. Several researchers have arrived at design expression on the longitudinal shear strength of concrete interfaces assuming monolithic concrete; composite concrete with rough or smooth surface at interface; material density, different geometrics. The mechanical properties of adopted materials, concrete and steel reinforcement are different. The majority researchers concluded that shear transfer is directly proportional to steel reinforcement crossing interface by proposing linear and non-linear models. Some researchers also proposed factoring concrete strength and reinforcement as vital parameters while considering the shear strength of concrete (Refer Annexure – 1).

Table 2.1 Researchers' data on the shear strength of concrete based on shear-friction.

1960 - 1969	1970 - 1979	1980 - 1989	1990 - 1999	2000 - 2009	2010 -
1960 Anderson Hanson	**1972** Mattock and Hawkins	**1981** Mattock	**1992** Patnaik	**2000** Patnaik	**2011** Constantinescu horia, Măgureanu cornelia
1961 Mattock and Kaar	**1974** Mattock Hermansen and Cowan	**1986** Vecchio and Collins	**1993** Hoff	**2001** Patnaik Mattock	**2012** Harries, Zeno and Shahrooz Keun-Hyeok Yang
1964 Saemann and Washa Gaston and Kriz	**1975** Mattock, Johal and Chow	**1987** Walraven, Frenay and Pruijssers	**1994** Loov and Patnaik Mattock	**2002** Kahn and Mitchell Papanicolaou and Triatafillou	**2013** Randl Benny Joseph and George Mathew
1966 Birkeland and Birkeland	**1976** Mattock, Li and Wang	**1988** Mattock Mau and Hsu	**1995** Walraven and Stroband	**2003** Gohnert	**2014** Shaw and Sneed
1967 Badoux and Hulsbos	**1977** Raths	**1989** Lin and Chen Tsoukantas and Tassios	**1997** Randl	**2008** Mansur, Vinayagam and Tan	**2015** Rahal KN and Khaleefi AL Rahal KN, Khaleefi AL and Sanee AL
1968 Mast Birkeland	**1978** Shaikh Loov		**1999** Ali and White Valluvan, Kreger and Jirsa	**2009** Santos and Julio	**2016** Alkatan
1969 Hofbeck, Ibrahim and Mattock					**2017** Barbosa, Trejo and Neilson Robert M Foster Seung-Jun Kwon

Birkeland and Birkeland, 1966 were the first to propose a theory of shear friction. This model is also known as the Saw-tooth friction model. An initial hypothesis is made to describe mechanisms by which shear is transferred by pre-cracked concrete joints (Figure 2.1).

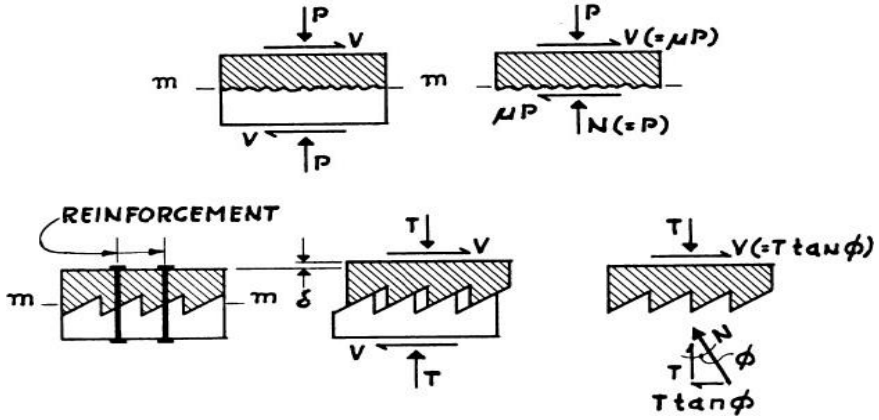

Figure 2.1 Shear-friction model (Birkeland and Birkeland (1966))

As per the model, interface shear is transferred by means of friction produced due to clamping stress generated by reinforcement crossing interface. Shear causes relative slip-causing surfaces to separate with reinforcement crossing both layers being elongated i.e., causing tension in bars so that for equilibrium compressive stress is induced at the slip surface.

$$v_u = \rho f_y \mu \qquad \text{Eq. – 2.1}$$

Where, v_u- Ultimate longitudinal shear stress at the interface;

μ - Coefficient of friction;

μ = 1.7 for monolithic concrete;

μ = 1.4 for artificially roughened joints;

μ = 0.8 - 1.0 for ordinary construction joints.

ρ - Reinforcement ratio;

f_y - Characteristic value of yield strength of the reinforcement;

The normal force to this compression force is a frictional force that is induced between two rough surfaces for the transfer of shear force. Birkeland and Birkeland suggested at the ultimate load, crack width would be large enough to stress to its yield stress 'f_y'

Mattock and Hawkins, 1972 investigated the role of compressive strength of concrete, shear plane characteristics, reinforcement, and direct stress on shear transfer, and their work was based on monolithically cast push-off, pull-off, and modified push-off specimens. Mattock and Hawkins observed that further deformation of push-off specimens cast monolithically with transverse reinforcement across slip plane fails with the formation of inclined cracks crossing the shear plane, forming compression struts rotated at their ends. Crack width increases, causing stretch in transverse reinforcement. This tension in bars equilibrium by compression in struts. A truss-like action is developed by concrete between cracks as compression struts and the reinforcement across the interface as tension members. These specimens fail either due to yielding of reinforcement or crushing of struts (Figure 2.2). They also suggested that the shear is carried by friction and is independent of concrete strength.

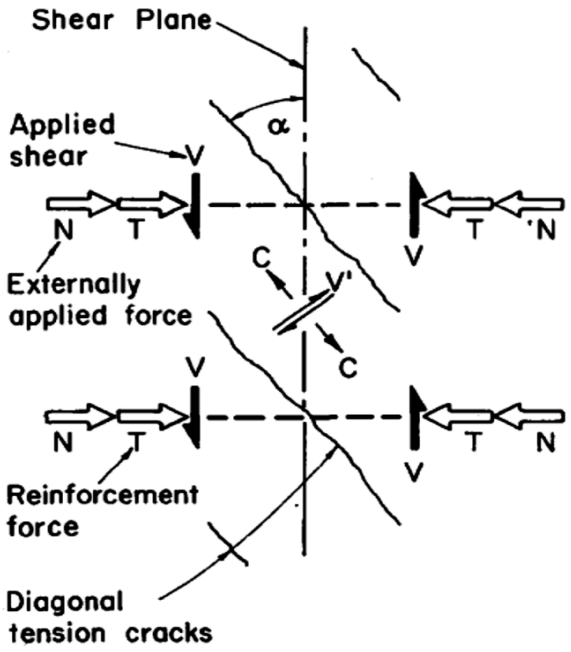

Figure 2.2 Shear transfer in initially uncracked concrete (Mattock and Hawkins, 1972)

Lower Bound of test results

$$v_u = 1.38 + 0.8\left(\rho f_y + \sigma_n\right) \qquad \text{Eq. – 2.2}$$

Where, v_u- Ultimate longitudinal shear stress at the interface;

ρ - Reinforcement ratio;

f_y - Characteristic value of yield strength of the reinforcement;

σ_n- normal stress at the interface.

Equation 2.2 shows that in addition to internal compressive stresses of reinforcement, external clamping stresses by an external force normal to the shear plane are effective. The first-term in the equation is interface surface contribution to shear transfer by cohesion and the second term is friction shear transfer which depends on the general roughness of the shear plane. Small shear force along layers is resisted by cohesion and after crack, cohesion is lost and the transfer is a combination of shear-friction and dowel action. Mattock, 1974 developed average values of the earlier experimental results of Mattock and Hawkins, 1972 which was based on lower bound. Also they introduced a modified equation based on the orientation of reinforcement crossing interface.

Developed for the mean values of the results of the tests

$$v_u = 2.76 + 0.8\left(\rho f_y + \sigma_n\right) \qquad \text{Eq. – 2.3}$$

$$v_u = 2.76\, sin^2\theta + \rho f_s\,(0.8\, sin^2\theta - 0.5 sin2\theta) \qquad \text{Eq. – 2.4}$$

Where, v_u- Ultimate longitudinal shear stress at the interface;

ρ - Reinforcement ratio;

f_y - Characteristic value of yield strength of the reinforcement;

θ is the angle between the reinforcement and the shear plane;

σ_n- normal stress at the interface.

Loov, 1978 was the first to include concrete strength in the design expression of ultimate longitudinal shear strength and he also proposed a non-dimensional equation. The design expression below is used with any consistent system of units.

$$\frac{v_u}{f_c} = k\sqrt{\frac{\rho f_y + \sigma_n}{f_c}} \qquad \text{Eq. – 2.5}$$

Where, v_u- Ultimate longitudinal shear stress at the interface;

ρ - Reinforcement ratio;

f_c - is the concrete compressive strength;

f_y - Characteristic value of yield strength of the reinforcement;

k – Constant, for initially uncracked interfaces, k = 0.50

σ_n- normal stress at the interface.

Walraven, Frenay, and Pruijssers, 1987 investigated push-off specimens for evaluating a non-linear expression for predicting the shear strength of an initially cracked interface. The design equation is a function of reinforcement ratio, concrete strength, and yield strength of reinforcement. The design model was based on *Walraven, 1981* where the concept of shear transfer along cracks and aggregate interlock was introduced. This comprehensive model is based on experimental data which consists of normal stress, shear stress, crack width, and shear displacement. It was assumed that concrete with different size graded spherical coarse aggregates was surrounded by hardened cement matrix. A crack was idealized such that it crosses the matrix and follows the interface around the aggregate (Figure 2.3).

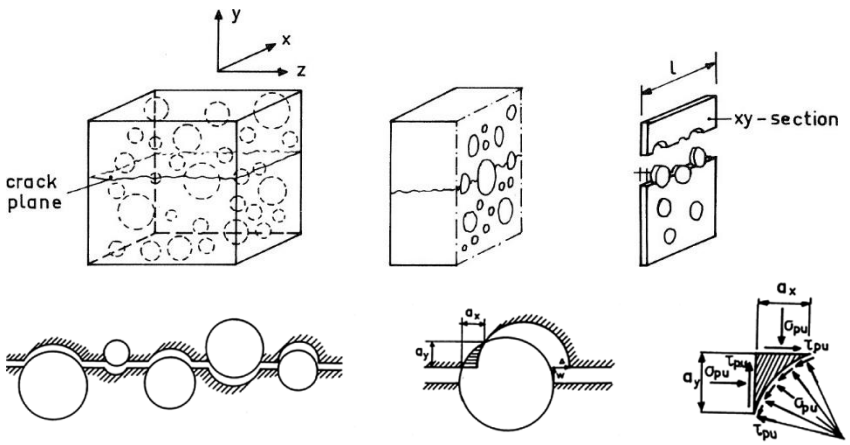

Figure 2.3 Modelling of aggregate interlock by Walraven, 1981

After a small slip, spherical aggregate comes into the matrix which allows shear to transfer across the crack by sliding and overriding between aggregate particles and this concrete matrix is known as aggregate interlock. Due to high contact stresses, irreversible plastic deformations occur. This phenomenon is continuous till the crack surface weakens. For the higher grade of concrete, cracks tend to cross the aggregate rather than going around them, making crack surfaces smoother.

$$v_u = C_1(\rho f_y)^{C_2} \qquad \text{Eq. – 2.6}$$

$$C_1 = 0.822 f_c^{0.406} \qquad \text{Eq. – 2.7}$$

$$C_2 = 0.159 f_c^{0.303} \qquad \text{Eq. – 2.8}$$

Where, v_u- Ultimate longitudinal shear stress at the interface;

ρ - Reinforcement ratio;

f_c - Concrete compressive strength;

f_y - Characteristic value of yield strength of the reinforcement;

Randl, 1997 advanced the idea that full yield strength of reinforcement cannot be the same as tension clamping force across the interface. This theory considers cohesion, friction, and dowel action. If surfaces are rough, steel reinforcement stresses result in tension and if surfaces are smooth, dowel action i.e. shear resistance of steel predominates. When reinforcement is not provided, the shear transfer can occur due to good interlocking effect of the interface surfaces.

Randl proposed that the tensile load in steel doesn't reach full yield strength at the failure of the specimen. Under load-bearing behavior, slip in horizontal and vertical directions shows that interface separation under shear leads to lack of roughness, loss of contact between the shear surfaces and shear transfer comes from dowel action. With an increase in surface roughness, shear transfer and stiffness improves predominantly.

$$v_u = c f_c^{1/3} + \mu\left[\sigma_n + \rho k f_y\right] + \alpha\rho\sqrt{f_y f_c} \qquad \text{Eq. – 2.9}$$

$$v_u \leq \beta v f_c \qquad \text{Eq. – 2.10}$$

Where, v_u- Ultimate longitudinal shear stress at the interface;

c - Coefficient of cohesion;

μ - Coefficient of friction;

For water blasted surfaces (R ≥ 3.0 mm);

c = 0.4, μ = 0.8 to 1.0

For sand blasted surfaces (R ≥ 0.5 mm);

c = 0, μ = 0.7

For smooth surfaces;

c = 0, μ = 0.5

ρ - Reinforcement ratio;

k - Coefficient of efficiency for shear reinforcement to transmit the tensile force;

f_c - Characteristic value of concrete compressive strength;

f_y - Characteristic value of yield strength of the reinforcement;

σ_n - normal stress at the interface due to external loading;

α - Coefficient for dowel action (flexural resistance of reinforcement);

β - Coefficient allowing for angle of concrete diagonal strut; and

ν - Reduction factor for strength of concrete diagonal strut.

Several milestones have been identified. The first one is the shear friction model by Birkeland and Birkeland, 1966. The second milestone model was by Mattock and Hawkins, 1972 known as modified shear friction model, where the cohesion of particles is considered. The third one is the explicit inclusion of concrete strength by Loov, 1978. The fourth milestone is an approach to quantify shear stress at the interface by Walraven et al., 1987. The fifth breakthrough is an expression proposed by Randl, 1997, considering dowel action for all shear friction and cohesion referring as interface shear transfer along with friction between surfaces.

Types of Test Specimens

Chmielewska, 2008 presented four categories of tests for in testing bond strength, namely, direct tension test (pull-off test), bending test (beam), splitting and shearing test (push-off, slant shear test). Momayez et al., 2005 classified bond tests into three categories depending on shear state application, namely, tension stress (pull-off test, splitting), shear stress (push-off test), and a combination of shear and compression test (slant shear test). Test specimens used for shear transfer are shown in figure 2.4.

The splitting test measures the tensile bond between two different types of concrete. When compressive forces are applied on composite specimen, failure results from tension normal to the interface due to Poisson's effect. Splitting tests do not generate shear forces along the interface. Slant Shear test was proposed by Kreigh in 1976 and is done for composite concrete cylinders which simulate actual stress strata and failure mode.

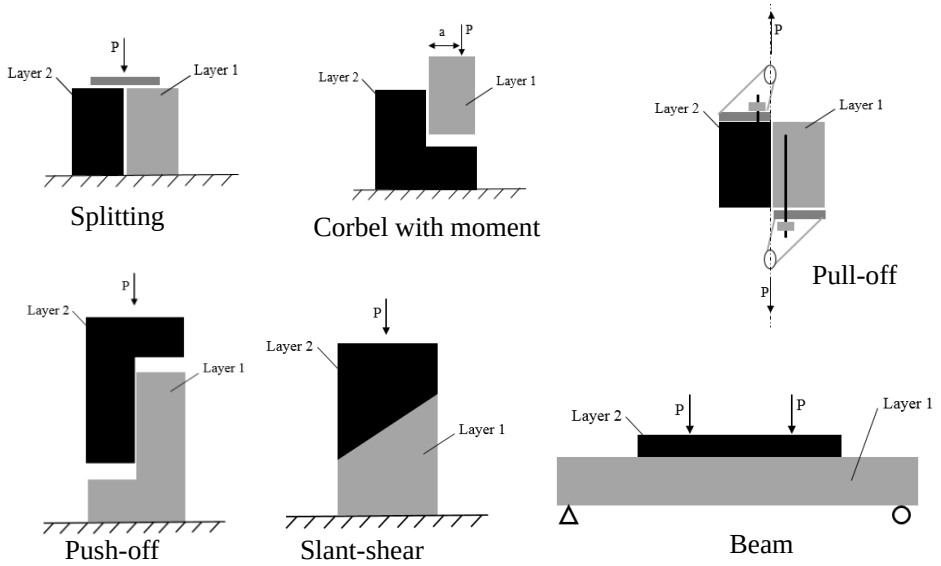

Figure 2.4 Test specimens used for shear transfer

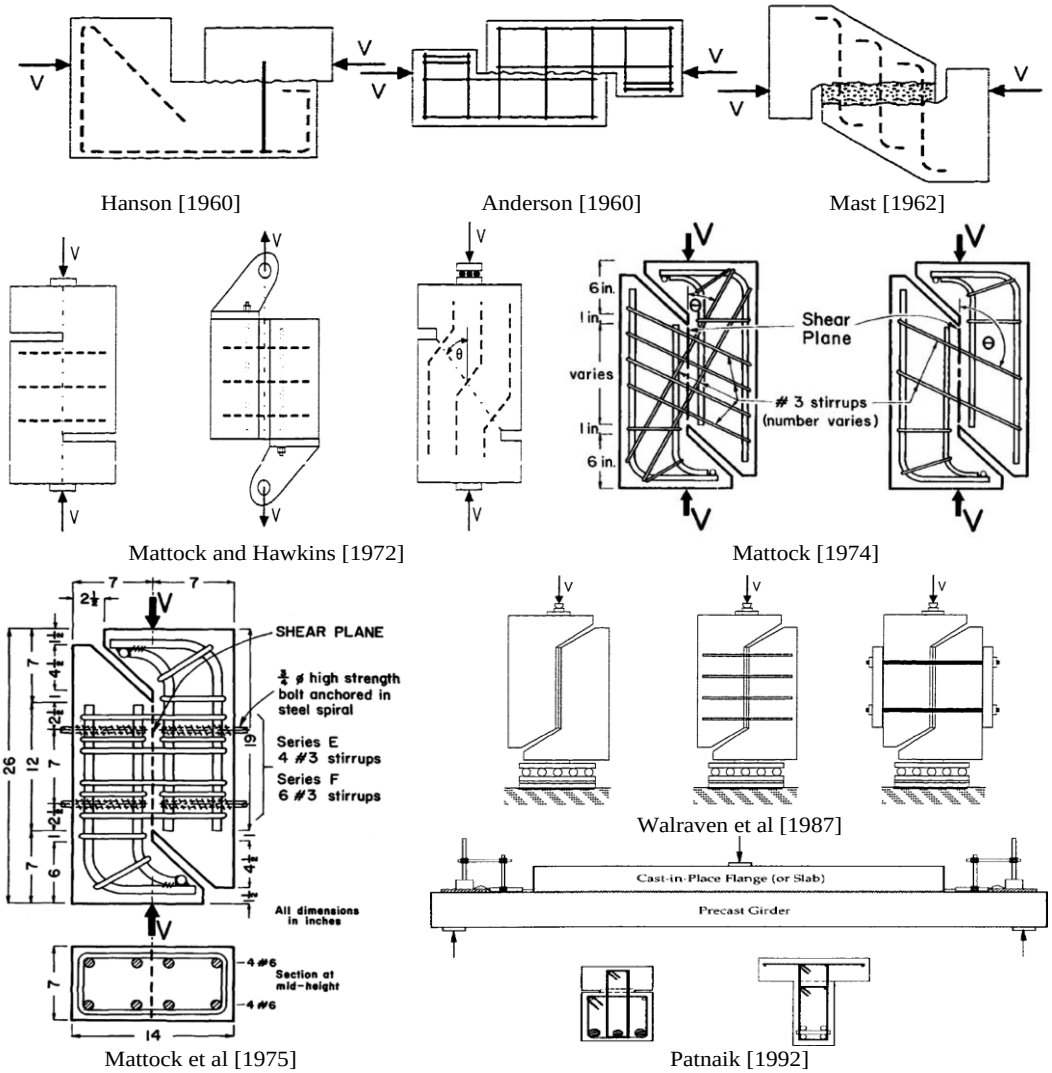

Figure 2.5 Test specimens of shear transfer models (Extracted from respective works)

The push-off method, also known as the L-shaped test was used by majority of researchers for analyzing the shear friction model. In the test, direct shear is generated through compression loads applied at the ends of test specimens. In these tests, pure shear and normal force can be introduced on a failure plane. In the four-point bending test (beam method), assembly of the specimen is easier and interface shear transfer is uniformly distributed. This is ideal for the testing of composite beams. Corbel tests induce both shear and moment. Pull-off tests depend on the reinforcement parallel and near the interface for tensile forces to transfer. Test specimens used by different researchers are shown in figure 2.5.

2.2 LITERATURE REVIEW ON GEOPOLYMER CONCRETE

Cement manufacturing has undergone a great evolution from its early stages. The use of cement in concrete has been there for a very long period from the time industrial manufacture of cement happened in the middle of 19^{th} century. With infrastructure growth, the development of smart cities in India led to a boom in the housing sector which increased the demand for cement and it is estimated that there would be 25% increase in demand for cement in the next decade (Rajamane et al., 2012).

The production of cement is the most energy-intensive process. Production of 1Kg of cement requires 2.8kg raw material, including fuel and other ingredients, and the process produces 5 to 10% of dust i.e., 60 – 140 m^3 of 0.7 to 800 g/m^3 of dust and emits 0.8 to 1kg of CO_2 from the time of production to maintenance (Habert et al., 2010). At the same time, the cement industry has been facing challenges like increased cost of fuel, compulsion to reduce CO_2 emissions, and supply of quality and adequate raw materials. (Lund, 2007, WBCSD, 2008).

Increasing economic factors also impel the industry to look forward to using recycling and reuse of waste material. Mehta, 2002 recommended that for producing environmentally friendly

concrete, there ought to be less use of natural resources, less energy and reduction in CO_2 emissions and he also advised that to fulfill the long term goal of reducing the impact of by-products of an industry, should kick in industrial ecology.

The necessity of new technology which is economically viable and can handle huge quantities of waste and by-products as an alternate to OPC was mooted. Fly ash, which is abundantly available worldwide, is replaced with Portland cement as a binder and activated using alkaline solutions. Palomo et al., 1999 developed two models for activation of fly ash and other similar pozzolanic materials. He suggested the use of blast furnace slag by complete replacement of OPC activated with alkaline liquids to form binders. In this model, silicon and calcium in slags are activated by a low or mild concentration of alkaline solution to produce C-S-H gel as a result of the hydration process. On the contrary, in other models, silicon and aluminum-rich binders are activated with an alkaline solution to form polymeric Si-O-Al bonds as a result of polymerisation. The first model is called alkali activated slag cement and the latter model as inorganic alumino silicate polymers and these were named geopolymers by Davidovits in 1979 (Davidovits. 1991).

In the early thirties, sodium and potassium hydroxide alkalis were used in iron slag which would set firmly when added to Portland cement. In evolving testing methodology for slags, Purdon, 1940 discovered that alkali, when added to slag, produced a rapid hardening binder, termed alkali-activated slag cement. Glukhovsky, 1957 discovered that both calcium silicate hydrates and calcium and zeolites i.e. sodium alumino – silicate hydrates contributed to solidification process and termed this “soil silicate concrete” and binders as “soil cement”. Davidovits, 1985 discovered an inorganic polymer material with a 3D cross-linked polysialate chain formed from Calcined kaolin (metakaolin). This inorganic polymer which is the result of hydroxylation and

Polycondensation reaction of waste by-products or natural materials on alkaline activation below 160°C was termed polysialate in 1976 and later geopolymers in 1979.

Several studies were carried out on the strength, durability, and workability of geopolymer concrete (Wang et al., 1995) and it was concluded that fly ash-based geopolymers exhibit better strength. Puertas et al., 2000 reported that higher temperature and higher concentration of the alkaline solution can result in higher strength of geopolymer concrete i.e. about 50 MPa. Fly ash-based geopolymer concrete has rapid setting, low workability, and no curing regime (Fernández-Jiménez et al., 2002); to enhance workability Naphthalene based super plasticizer was used (Hardjito et al., 2004).

For common use of geopolymer concrete, mix proportion in line with OPC was proposed by Rangan, 2008, and based on the alkaline liquid to fly ash ratio, mix proportions had been developed by Junaid et al., 2015). To avoid heat curing, trails with alkali-activated slag were considered by Nath et al., 2014). In the present scenario, the research has shifted towards fly ash and GGBS based geopolymer concrete.

Jumppanen, 1986, was the first to study the fire resistance performance of alkali-activated concrete developed using sodium hydroxide. Experiments showed excellent resistance for aging, freeze-thaw cycling, salt scaling, and carbonation (Shi et al., 2003, Krivenko, 1994, and Douglas, 1992). Geopolymer Gel is highly resistant to acid attack because of a high degree of cross-linking present with acid-resistant leached silica formed. Also the strong bond between gels and aggregates enhances flexural and tensile strength.

Fly ash-based geopolymer concrete showed better durability against sulphuric attack, nitric and hydrochloric attack along with low creep and little drying shrinkage when compared with ordinary Portland cement. (Rostami et al., 1996, Hardjito et al., 2005, Bakharev et al., 2005).

Samples with fly ash-based geopolymer concrete which were exposed to sodium sulfate and sulphuric acid did not affect mass loss or reduction of compressive strength. But mass and strength reduction was observed when the samples were exposed to sulphuric acid (Wallah et al., 2005). Fly ash-based geopolymer concrete specimens show better performance than OPC specimens under elevated temperatures. (Sarker et al., 2014, Rashad et al., 2019).

It can be concluded that geopolymer concrete shows significant potential to be material of next-generation since it is not only environmentally friendly but also has better mechanical and durability properties. Details showing the evaluation of geopolymer concrete, its properties, and durability aspects, etc. figure in Table 2.2 and one can conclude the emergence of geopolymer concrete as one of the alternatives to ordinary Portland cement.

2.3 LITERATURE REVIEW ON STRENGTH OF GPC

This review is targeted to contribute an all-encompassing understanding and assessment of geopolymer concrete. Against this background, comprehensive data based on the past literature is listed in Table 2.2. Assessment and analysis are conducted on the variables that impact the properties performances of geopolymer concrete.

Table 2.2 Summary of various investigators worked on strength of geopolymer concrete

Investigator (s) and year	Parameters of investigation	Observations
Davidovits, J. and Cordi, S.A., 1979	Investigation on Calcined kaolin (metakaolin) with alkaline activator.	Discovered an inorganic polymer material with 3D cross-linked polysialate chain formed. Termed as polysialate in 1976 and later named as geopolymers in 1979.
Wang et al., 1995	Several studiess were carried out on the strength, durability, and workability of GPC	Concluded GPC has better properties than OPC.
Rostami et al., 1996	Developed chemically activated fly ash (CAFA) and investigated durability performance by immersing	Reported that GPC has better resistance than the Portland cement concrete

Investigator (s) and year	Parameters of investigation	Observations
	the specimens in acids like sulphuric, hydrochloric, and nitric.	
Palomo, 1999	Investigation on strength of fly ash-based geopolymers with varying parameters like alkaline to fly ash ratio, curing temperatures (65°C and 85°C), the period of curing (2h, 5h and 24 hours), the molarity of NaOH and KOH as 12M and 18M respectively.	Reported that the formation of alumino silicate hydrate gel was found to be responsible for the strength. The period of curing can be limited to 2h - 5h for fly ash-based geopolymer pastes for better strengths.
Puertas et al., 2000	Experimental works on different temperatures and concentrations of alkaline solution on fly ash-based geopolymer concrete.	Reported that higher temperature and higher concentration of alkaline solution can result in higher strength of GPC i.e. about 50 MPa.
Fernández-Jiménez et al., 2002	Study of the setting, curing regime, and workability on different binder materials.	Fly ash based GPC has rapid setting, low workability, curing regime
Pinto et al., 2002	Studied the effect of compressive strength of geopolymers on the molar ratio of Na_2SiO_3/NaOH.	Concluded that maximum strength can be achieved at a ratio of 2.5 at constant binder content.
Hardjito et al., 2004, 2005	Studied parameters impacting the compressive strength of fly ash-based GPC with varying higher molarity of sodium hydroxide solution (8M to 16M), higher curing temperature (30 - 90°C), curing period (6 hours to 96 hours), and low water to binder ratio.	This resulted in higher compressive strength of GPC with the increase of sodium silicate to sodium hydroxide ratio with less curing time and lower concentration of NaOH. To enhance workability Naphthalene based super plasticizer can be used
Hardjito et al., 2005	Studied the behavior of fly ash-based geopolymer concrete to acid attack, creep, and shrinkage	Summarized that GPC has excellent resistance to sulfate attack, low creep, and little drying shrinkage
Bakharev, 2005	Investigated fly ash-based geopolymer with pre-curing and alkaline solution with only NaOH or sodium silicate. Also studied the durability aspects of acetic and sulphuric acid exposure	Reported that application of heat at room temperature for a longer duration gave better performance for strength development than pre-curing of fly ash-based GPC. Also concluded that the geopolymers activated with NaOH had more strength than those activated by sodium silicate

Investigator (s) and year	Parameters of investigation	Observations
		solution. GPC performed better against acidic exposure.
Wallah et al., 2005	Worked on durability studies on fly ash-based geopolymer concrete-like mass loss and compressive strength when exposed to two different solutions: sodium sulfate and sulphuric acid.	Specimens exposed to sulphuric acid showed a reduction of about 30% in strength after 12 weeks of exposure whereas specimens have exposed to sodium sulfate did not have any effect on mass loss and compressive strength.
Chindaprasirt et al., 2007	The behavior of class C fly ash-based geopolymer mortars using different duration of oven curing (1, 2, 3, and 4 days), delay time (0, 1, 3, and 6 hours), sodium silicate /NaOH ratio (0.67, 1, 1.5 and 3), the concentration of sodium hydroxide (10, 15 and 20M) and curing temperatures (30°C, 45°C, 60°C, 75°C, and 90°C)	It has been concluded that the maximum compressive strength was witnessed at sodium silicate to sodium hydroxide ratio 0.67 and 1, at 1 h of oven curing at 75° C for no fewer less than two days.
Hardjito et al., 2008	The study is based on the compressive strength of fly ash-based geopolymers for varying parameters like molarity of sodium hydroxide, the alkaline solution to fly ash ratio, curing temperature, and the ratio of water to geopolymer solids.	The outcome of this work is that increased molarity of sodium hydroxide increases the compressive strength while curing temperature plays a vital role in achieving strength.
Thokchom et al., 2009	Investigated the tests of sorptivity, water absorption, porosity and compared residual properties of fly ash-based geopolymer mortars exposed to sulphuric acid with varying $\%Na_2O$ (5, 6.5, and 8%) in the activator solution.	Reported that water absorption, sorptivity, porosity is lower for Higher the $\%Na_2O$ content and better the performance under sulphuric acid attack.
Reddy et al., 2010	Studied the fresh and hardened properties of low calcium fly ash-based geopolymer concrete with varying concentrations of the sodium hydroxide taken were 10M, 12M, 14M, and 16M and the ratio of sodium hydroxide and sodium silicate was 2.5 with oven curing 60°C for 24 hours.	Concluded that an increase in molarity of sodium hydroxide led to increase in compressive strength and decrease in workability of GPC. For each NaOH concentration as age increases, improvement was observed in compressive strength.
Kumar et al., 2010	To arrive at a better combination of parameters for maximum compression strength for fly ash-	Concluded that optimum contents of parameters are geopolymer solids to water ratio

Investigator (s) and year	Parameters of investigation	Observations
	based geopolymer considering fly ash to alkaline solution ratio, the concentration of sodium hydroxide, sodium silicate, and geopolymer solids to water ratio.	as 2.15, fly ash to alkaline solution as 60:40, the concentration of NaOH as 12M, the concentration of sodium silicate as 2M, and sodium silicate to sodium hydroxide ratio as 2.5.
Somna et al., 2011	The behavior of ground fly ash (mean size of 10.5 mm) and fly ash varying the concentration of NaOH (4.5, 7, 9.5, 12, 14, and 16.5) cured under ambient and hot oven conditions.	It has been concluded that compressive strength has been increased with an increase in the concentration of NaOH (7.9-14M). Further increase in molarity of NaOH, was observed decrease in compressive strength due to early precipitation of the alumino-silicate products.
Rajamane et al., 2011	Conducted rapid chloride penetrability test on fly ash-based geopolymer concrete for chloride ion permeability to compare it with conventional concrete (OPC).	Test outcomes revealed that geopolymer concrete and conventional concrete have shown the similar performance of chloride ion penetrability.
Bakri et al., 2011	Studied the properties of fly ash-based GPC	Reported that with increase in fineness of fly ash, the porosity GPC reduced and its compressive strength increased. It was also concluded that GPC performed better in an aggressive environment and at elevated temperatures than normal concrete.
Bakri et al., 2012	Studied the strength of fly ash-based geopolymer pastes by changing molarity of sodium hydroxide (6M, 8M, 10M, 12M, 14M, and 16M), sodium silicate to sodium hydroxide ratio (0.5, 1.0, 1.5, 2 and 2.5), fly ash to the alkaline ratio (1.5, 2 and 2.5) and oven curing temperature (40°C, 50°C, 60°C, 70°C, and 80°C) for a period of 24 hrs.	Compressive strength achieved at fly ash to alkaline ratio as 2 with the molarity of NaOH being 12M, sodium silicate to sodium hydroxide ratio 2.5, and curing temperature as 60°C for 24 hours.
Joseph et al., 2012	Studied compressive strength of fly ash-based geopolymer concrete by varying the parameters, like total aggregate content (60%, 65%, 70%,	It has been reported that maximum compressive strength, poisons ratio, modulus of elasticity is achieved with the

Investigator (s) and year	Parameters of investigation	Observations
	and 75%), the ratio of sodium silicate to sodium hydroxide (1.5, 2.2, 2.5, and 3.0), oven temperature for curing (30°C to 120°C) for 24 hours and the ratio of alkaline solution to fly ash (0.35, 0.45, 0.55 and 0.65).	mix at a total aggregate content 70%, for a the ratio of sodium silicate to sodium hydroxide of 2.5, molarity of sodium hydroxide being 10M at 100°C for 24 hours.
Ganapati Naidu P et al., 2012	Study of strength properties for fly ash and GGBS based GPC with different percentages of fly ash and GGBS with constant molarity of NaOH (8M) and Na_2Si_{O3}/NaOH as 2.5.	Concluded that compressive strength increased with an increase in percentage replacement of fly ash with GGBS. 90% of compressive strength is achieved in 14days and also average density is equal to OPC.
Rajamane et al., 2012	A study of sulfate resistance of fly ash and GGBS based geopolymer concrete was prepared by replacing fly ash with GGBS as 50% and 75% and cured under outdoor conditions. The sulfate resistance was assessed by submerging the specimens in 5% Na_2SO_4 and 5% $MgSO_4$ solutions separately for 90 days by comparing results with Portland Pozzolanic Cement Concrete (PPCC).	Results after 90days of sulfate exposure found only 2% mass loss. The decrease in compressive strength was about 2% to 29% for geopolymer concrete against 9% to 38% for PPCC based on the exposure time and type of sulfate solution. It has been concluded that GPC has better performance than conventional concrete.
Parthiban et al., 2013	Investigated the performance of fly ash and GGBS GPC with varying % of GGBS from 0 to 100%. Also studied the effect of alkaline ratio (sodium silicate to sodium hydroxide ratio) of 1 to 1.5 by a constant concentration of sodium hydroxide as 10M.	The study concluded that the compressive strength of GPC has increased with an increase in GGBS content and alkaline ratio.
Madheswaran et al., 2013	The investigation covers the effect of GGBS to fly ash combination with 100%, 75% 50% GGBS based geopolymer concrete by varying the concentration of Sodium Hydroxide solution (3M, 5M, and 7M),	It was reported that strength increased with an increase in molarity and maximum compressive strength was achieved for 100% GGBS with 7M of NaOH at 28 Days.
Deepa Balakrishnan et al., 2013	Investigation of the mechanical properties of fly ash-based geopolymer concrete considering parameters like binder content (395 kg/m^3, 410 kg/m^3, and 450 kg/m^3),	Concluded that the binder content of 410 kg/m^3 attained the maximum compressive strength and it was also witnessed that there was about 60% gain in the

Investigator (s) and year	Parameters of investigation	Observations
	fine aggregate (100% sand, sand, and sand stone: 50% each and; 100% sand stone), curing (outdoor and hot air oven 72 hrs.) and the ratio of sodium hydroxide/sodium silicate 1:2.5.	strength at 90 days than that of 28 days.
Ganesan N et al., 2014	Studied the effect of confinement on the behavior of GPC and OPC concrete.	Result concluded that confinement reinforcement improved the strength and ductility of GPC.
Morsy et al., 2014	Examined the behavior of fly ash-based geopolymers by changing the ratio of sodium silicate to sodium hydroxide (0.5, 1, 1.5, 2, and 2.5) with oven curing at 800C for 24 hours.	Maximum compressive strength was attained at sodium silicate to sodium hydroxide ratio of 1, due to its homogenous and less porous matrix, and found strength was increasing with increase in age.
Deb et al., 2014	Investigated the effect of GGBS content on compressive strength and setting time of fly ash and GGBS based geopolymer concrete with varying replacement percentage of GGBS (0%, 10%, and 20%) and different ratios of sodium silicate to sodium hydroxide (1.5-2.5).	Reported that with an increase in the GGBS quantity, there was an enhancement in the mechanical properties of GPC, while the workability reduced with a decrease in the alkaline to binder ratio.
Rajini B and Narasimha Rao AV 2014	Worked on mechanical properties of GPC with replacement of fly ash by GGBS of 0 to 100% and at ambient outdoor curing for a number of days.	Concluded that with an increase in the GGBS quantity, there was an improvement in the mechanical properties of GPC.
Dutta and Somnath Gosh 2014	Studied the effect of the composition of alkaline activator with a combination of only fly ash and fly ash + GGBS. Effect on the strength of concrete with varying percentage of Na_2O content (6% and 8%), silicate modulus (0.5, 1 and 1.5), and curing temperatures (55°C, 65°C, 75°C, and 85°C).	The study was concluded that $\%Na_2O$ content ought to be lower in the presence of the fly ash and GGBS combination and $\%Na_2O$ should be more to achieve better strength for the fly ash-based samples.
Krishnaraja A R et al., 2014	Study of compressive strength of GPC with replacement of fly ash by GGBS of 0 to 50% and at ambient outdoor curing	Concluded that the addition of GGBS performed better than OPC. Also with the increase in GGBS will increase the strength of GPC.
Rao et al., 2014	Experimental work of fly ash-based geopolymer pastes on normal	The study concluded that an increase in setting time occurred

Investigator (s) and year	Parameters of investigation	Observations
	consistency and setting times by varying the concentration of sodium hydroxide (8M – 16M), sodium silicate to sodium hydroxide ratio (1.5, 2.0, 2.5 and 3), and curing temperature (30°C, 60°C, and 90°C).	with an increase in molarity of sodium hydroxide (8M-12M) for alkaline liquid ratio 1.5 and 2. On further increase in molarity of the sodium hydroxide, setting time decreased. It was concluded that temperature plays a vital role in decreasing the setting times i.e., reasonable decrease in setting time till 60°C, thereafter the setting time decreased significantly.
Nematollahi and Sanjayan et al., 2014	An experimental study is based on the workability of fly ash-based geopolymer pastes with different types of superplasticizers like naphthalene, melamine, and modified polycarboxylate and also with varying alkaline solution i.e., only sodium hydroxide (8M) and a combination of sodium hydroxide and sodium silicate. The flow ability of paste with 1% of superplasticizer is compared with no superplasticizer paste.	It has been concluded that naphthalene based superplasticizer performed well without compromising strength and a combination of sodium hydroxide and sodium silicate showed better results.
Nath and Sarker, 2014	Study of fly ash-based geopolymer concrete suitable curing without using high temperature.	Reported that fly ash-based geopolymer concrete can be cured at ambient temperature by replacing fly ash with GGBS at optimal proportions for desirable workability, setting time, and strength. Na2SiO3/NaOH ratio can be maintained from 1.5 to 2.5.
Deb et al., 2014	Study of mechanical properties by considering 0, 10, and 20% replacement of fly ash with GGBS with a varying activator content (40% & 35% of binder content) and changing Na2SiO3/NaOH ratio (1.5 – 2.5)	Workability decreased with the increase of GGBS content and also decreased with the activator to binder ratio decreased. Compressive strength increased with an increase in GGBS quantity. Tensile strength is in line with OPC concrete as per AS 3600 (2009) and ACI 318 (2008).

Investigator (s) and year	Parameters of investigation	Observations
Sarker et al., 2014	Study of fly ash-based geopolymer concrete exposed under elevated temperatures (400°C, 650°C, 800°C, and 1000°C) and compared with OPC concrete.	Fly ash-based geopolymer concrete performed better than OPC.
Zende R and Mamatha A, 2015	Study of compressive strength of GPC with replacement of fly ash by GGBS (25, 50, and 75%) with 11M and 13M concentration of Alkaline activator.	Observed that an increase in the percentage of GGBS decreases workability and increases the strength of GPC.
Mallikarjuna Rao G and Gunneswara Rao T D, 2015	Considered the behavior of fly ash and GGBS based geopolymer pastes and mortars for different concentrations of sodium hydroxide (8M, 12M, and 16M) and two curing regimes i.e., outdoor and oven curing at 60°C for 24 hours.	Concluded that addition of GGBS reduced setting time and also excluded oven curing and required strength can be achieved under ambient curing outside.
Phoo - ngernkham, et al., 2015	Study of compressive strength and shear bond strength of FA-GGBS geopolymer for three types of pastes made of FA, GGBS, and FA+GGBS and varying with alkaline activators of Na_2SiO_3, NaOH and combination of both with 10M of NaOH and alkaline to the binder of 0.6 ratios cured at ambient temperature.	An increase of GGBS enhanced the compressive strength of paste. Shear bond strength is maximum for the FA – GGBS based paste and combination of Na_2SiO_3, NaOH alkaline solution.
Prasanna K et al., 2016	Study of compressive strength of GPC with replacement of fly ash by GGBS of 25 to 45% and at ambient outdoor curing	Concluded that the addition of GGBS performed better than OPC. Also, GGBS will omit heat curing.
Bhikshma and Naveen Kumar T, 2016	Work on mechanical properties of GPC with fly ash and partial replacement of GGBS (9, 20, 27.5, 38, and 43%) with 8M of NaOH, sodium silicate to sodium hydroxide ratio as 2.5, alkaline to binder content as 0.5 under ambient curing.	Mechanical properties are better than OPC, workability and average density are the same as OPC. Compressive strength is more than recommended than IS: 456, 2000.
Rajarajeswari and Dhinkaran, 2016	Investigation of compressive strength with change in A/B Ratio, Curing temperature, and sodium silicate to sodium hydroxide ratio.	An increase in curing temperature (up to 80°c), sodium silicate to sodium hydroxide, and A/B ratio increase the strength of GPC.

Investigator (s) and year	Parameters of investigation	Observations
Mallikarjuna Rao G et al., 2016	The investigation looked at the influence of different parameters like a binder, binder content, alkaline to binder ratio with 8M of NaOH concentration, and sodium silicate to sodium hydroxide ratio as 2.5 on strength and durability properties of geopolymer.	Reported that an increase of percentage of GGBS reduces setting time and increases the strength of the mix. Strength decreased with an increase in alkaline to binder ratio.
Muthadhi et al, 2016	Study of strength by varying Alkaline content to binder ratio, curing method, and NaOH concentration	An increase in alkaline content to binder ratio and NaOH concentration enhances the strength of GPC.
Jawahar et al., 2016	Investigated mechanical properties of fly ash and GGBS based geopolymer concrete.	Concluded that the mechanical properties improve with increase of GGBS content and that outdoor curing at ambient temperature is sufficient for GGBS based GPC.
Rafeel et al., 2017	Study of mechanical properties and suitable mix proportioning of GGBS based GPC varying from 0 to 100% replacement of fly ash by GGBS.	Reported that 30 – 33% of paste volume did not affect the strength but influenced the consistency of mixes. Water to binder content ratio influence compressive strength but the effect was reduced with GGBS content increase. Strength increases with increase in GGBS.
Rama Seshu et al., 2017	Study of the combined effect of GGBS, fly ash, and molarity of alkaline activator on compressive strength. Also, a parameter was introduced considering the effect of GGBS to fly ash ratio and molarity of activator.	Reported that compressive strength of GPC increases with increase of GGBS to fly ash for specific molarity of activator. An increase of strength is not proportionate to the increase of molarity of the activator. A new parameter binder index was established where the increase in binder index shows increase in compressive strength.
Ibrahim et al, 2017	Investigation of strength by varying sodium silicate to sodium hydroxide ratio and alkaline to binder ratio	Reported that an increase in sodium silicate to sodium hydroxide up to 2.5 increased in strength. Also concluded that the increase in alkaline to binder ratio increased strength.

Investigator (s) and year	Parameters of investigation	Observations
Annapurna and Kishore, 2017	Investigation of strength related properties on GGBS based GPC with 20 to 60% replacement of fly ash with GGBS for constant alkaline concentration and ratio.	An increase in strengths was observed with replacement of GGBS, while Poisson's ratio decreased.
Nath and Sarker, 2017	Study of strength by a change in A/B ratio and GGBS to FA ratio	An increase in A/B ratio and GGBS to FA ratio enhanced the mechanical properties of GPC.
Prasad and Kumar, 2017	Worked on assessment of strength by varying FA to GGBS and NaOH molarity	An increase in FA to GGBS ratio or lower molarity of NaOH results in a reduction in the strength of GPC.
Mallikarjuna Rao and T.D Gunneswara Rao, 2018	Developed mix proportions for fly ash and GGBS based GPC. Considering Sodium silicate to sodium hydroxide ratio as 2.5, and concentration of NaOH is 8M. Variables are binder content (360, 420, and 450 kg/m3) with proportions of fly ash to GGBS as 70-30, 60-40, and 50-50 and alkaline solution to binder content as 0.45, 0.50, 0.55, and 0.60 with outdoor curing.	Maximum strength is at alkaline to binder ratio of 0.5 for all three binder contents; however, 50-50 proportion of fly ash to GGBS given superior strength. GGBS content, alkaline to binder content ratio, and the curing regime are found to be more influential on the compressive and workability of GPC.
Nagaraj and Babu, 2018	Studied the mechanical properties of GPC by changing Na_2SiO_3/NaOH ratio and concentration of NaOH.	An increase in concentration reduces workability and enhances strength. The ratio of sodium silicate to sodium hydroxide increases the strength of GPC.
Rai et al., 2018	Studied the mechanical properties by varying alkaline to binder ratio, Na_2SiO_3 / NaOH, NaOH concentration, and curing temperature	The strength of GPC increases with curing temperature and also with the increase sodium silicate to sodium hydroxide and NaOH concentration up to 14.
Ramamohana B et al., 2019	Studied the strengths of GGBS based GPC for varying percentages from 30% to 70% replacement with fly ash with dissimilar curing conditions and varying concentration of alkaline activators.	Reported that GGBS with 70% performed better for all strengths (compressive, split tensile and Flexural strength) under ambient outdoor curing for 14M activator concentration.
Rajagopalan Gopalakrishna 2019	Carried out experimental study on durability of GPC with GGBS to class F fly ash from 50 to 0% for the	Concluded that mix with 100% GGBS performed well and achieved maximum compressive strength; however, mix with 40%

Investigator (s) and year	Parameters of investigation	Observations
	constant concentration of 12M alkaline activator	fly ash performed well under severe environmental conditions.
Rama Seshu D et al., 2019	Examined the influence of GGBS to fly ash ratios (0.25, 0.43, 0.67, 1.0, 1.5, and 2.3), the concentration of alkaline activator (6, 8, 10, and 12) on strength of GPC and a parameter binder index.	Compressive strength and modulus of rupture increase with increase in GGBS to fly ash ratio for a particular concentration of alkaline activator. The relation between the binder index with the strength of GPC is nonlinear.

Geopolymer binders are sustainable building materials since they utilizes by-products and can be an alternate building material to OPC as GPC synthesis competes with OPC from characterization, where geopolymerisation of the inorganic polymer formed of alumino-silicate rich material is activated with alkaline solution producing three - dimensional alumino-silicate gel compared to C-S-H gel formation due to hydration in OPC. GPC has superior features than OPC such as higher early strength, better mechanical and durability properties, better dimensional stability, better bond to reinforcement and aggregates, superior fire resistance, etc.

Based on the investigations, Geopolymer Concrete strengths vary based on different parameters like mass and ratio of binder materials, the concentration of alkali hydroxides, and alkaline solutions. Thus, the existing investigation pursues parameters considering the effects of binder material, concentration of sodium hydroxide, alkaline solution for fly ash and GGBS-based geopolymer concrete.

2.4 LITERATURE REVIEW ON SHEAR STRENGTH OF GPC

Literature available on geopolymer concrete has mainly dwelt on the manufacturing aspect along with physical, mechanical, and durability properties and it has been found that geopolymer concrete performed better than conventional concrete. However, inadequate attention was given to reinforced geopolymer concrete behavior and structural applications. The

minimal research on geopolymer concrete has been extended to beams, columns, and slabs. Some of the investigations are tabulated in Table 2.3. General structural behavior of geopolymer concrete such as load-deflection, cracking characteristics and the failure mode is similar to conventional concrete members. Due to this, researchers agree that geopolymer concrete members could be designed the same as conventional concrete members.

Table 2.3 Summary of the structural performance of geopolymer concrete

Investigator (s) and year	Testing variable / Type of loading	Remarks
	Beams	
Sumajouw et al., 2005	Tensile reinforcement ratio to flexural loading.	Flexural strength improved when the reinforcement ratio is increased as in conventional RC beams.
Sumajouw et al., 2006	Tensile reinforcement ratio, concrete strength to flexural loading.	The effect of reinforcement ratio on GPC beams is similar to conventional RC beams and also with regard to flexural capacity and ductility.
Dattatreya et al., 2011	Fly-ash slag ratio to flexural loading.	Lower post-peak ductility was observed.
Mourougan et al., 2012	Different reinforcing configuration to flexural loading / shear loading.	Higher shear strength was observed for geopolymer concrete.
Ng et al., 2013	Steel fiber content with fly ash-based geopolymer concrete.	Shear capacity was delayed due to fiber; finer cracks were observed.
Yost et al., 2013	Tensile reinforcement ratio to flexural & shear loading.	No significant difference found between geopolymer concrete beam and ordinary RC beam in the shear behavior.
Andalib et al., 2014	POFA – Fly ash ratio to flexural loading.	Similar cracking pattern as RC beam.
Srinivasan et al., 2014	Glass fiber content to flexural loading.	Flexural capacity increased nearly 35% with glass fiber. Over-utilization of fiber led to capacity reduction.
Devika and Deepthi, 2015	The proportion of steel fiber and hybrid polypropylene to flexural loading.	Flexural capacity enhanced 30% with the incorporation of hybrid steel polypropylene fiber.
Kathirvel and Kaliyaperumal, 2016	Proportions of recycled aggregate to flexural loading.	Higher number of cracks and greater crack width but there was better deflection and ductility.
Chang, 2009	Tensile reinforcement ratio, transverse reinforcement ratio/shear loading.	The modes of failure and crack patterns were generally similar to Portland cement concrete beams.
Visintin et al., 2017	Shear span ratio	Experimental results of the direct shear tests showed shear-friction properties for geopolymer concrete which fall within

Investigator (s) and year	Testing variable / Type of loading	Remarks
		the range of shear-friction properties of established OPC concrete.
Columns		
Sumajouw et al., 2006	Longitudinal reinforcement ratio and concrete strength / axial loading.	Similar failure by crushing it in a brittle manner.
Rahman and Sarker, 2011	Reinforcement ratio and biaxial load eccentricities.	The failure occurred by crushing concrete on the compressive side similar to conventional RC columns
Sujatha et al., 2012	Concrete strength.	Geopolymer concrete columns are better than RC columns for up to 34% in ultimate strength
Nagan and Karthiyaini, 2014	Effect of confinement.	The ultimate strength of the geopolymer concrete column improved by 30%. Confinement further enhanced the load-carrying capacity and ductility.
Ganesan et al., 2015	Steel fibers volume and aspect ratio / axial loading.	The inclusion of steel fibers increased the load carrying capacity by up to 56%.
.Albitar et al., 2017	Eccentricity and slenderness ratio.	Results reveal that fly ash and GGBS based geopolymer concrete exhibit the same structural behavior as ordinary Portland cement (OPC) concrete.
Slabs		
Rajendran and Soundarapandian, 2013	The volume fraction of reinforcement and types of reinforcement.	Enhanced ductility and energy absorption compared to Ferro cement slabs.
Nagan and Mohana, 2014	The volume fraction of reinforcement and types of reinforcement.	An increase in volume fraction can improve about 10 times of impact energy absorption.

Research on direct shear strength on GPC is minimal. This is because the main cause of failure for bearing shoes, corbel, etc. is predominantly interfacial shear strength or shear friction.

Joseph et al., 2013 worked on interface shear strength of fly ash-based geopolymer concrete and compared it with conventional concrete along with different shear equations of ACI 318, 1999, Mast, 1968, and Mattock et al., 1976. It was concluded that geopolymer concrete specimens showed more slip than OPC concrete specimens. The study reported that the interface shear strength of geopolymer concrete is inferior to OPC concrete for both unreinforced and reinforced specimens and just above 60% of the value was obtained when compared with different shear equations for geopolymer concrete.

The above study concluded that shear strength is less for geopolymer concrete when compared to OPC concrete. This resembles the bond strength between reinforcement and geopolymer concrete which is inferior to OPC concrete since the structural performance of concrete depends on the bond between the concrete and reinforcing bar. This performance influences the load-bearing capacity of elements, embedded length, etc. Based on the observations from Table 2.3 it is understood that the bonding between steel reinforcement with geopolymer concrete was superior to that of ordinary Portland cement concrete. To assess this bond strength of geopolymer concrete, the literature on bond strength has been reviewed.

Sofi et al., 2007 started research on bond behavior between concrete and reinforcement through-beam end testing and direct pull-out testing and concluded that fly ash and slag geopolymer concrete perform better than conventional concrete. He also compared the same with AS 3600, 2004, ACI 318, 2002, and EC2, 2004 and found these codes are more conservative in predicting the bond strength for geopolymer concrete.

Sarker, 2011 evaluated bond strength of fly ash-based geopolymer concrete by pull-out test using ASTM A944, 1999 with a varying diameter of the bar (20 and 24 mm) and concrete cover to diameter ratio (1.71 to 3.62) for different grades of concrete. The same was compared with conventional concrete. From the study, it was concluded that geopolymer concrete showed a similar cracking pattern to OPC concrete failing in a brittle manner by splitting concrete along the bond length of the pull-out bar. Geopolymer concrete has higher splitting tensile strength than OPC concrete of the same compressive strength i.e. bond strength of geopolymer concrete was found to be higher than conventional concrete. (Chang et al., 2009, Ganesan et al., 2015)

D Rama Seshu, 2015 investigated the bond strength of GGBS, fly ash-based concrete, and conventional concrete. He concluded that geopolymer concrete exhibited higher bond strength than corresponding conventional concrete.

Tanakorn Phoo et al., 2015 reported details of shear bond length (slant angle 45°) between Portland cement paste and geopolymer paste which increased with an increase in compressive strength. It had been reported that the bonding and tensile strength of geopolymer were higher than OPC pastes. Out of geopolymer pastes, FA-GGBS paste was better than other pastes. (FA Only, GGBS Only). It is understood that geopolymer structural members exhibit better ductile behavior and bond strength. However, based on interfacial shear strength of fly ash geopolymer concrete shown reduced shear strength leading to lower bond strength. Considering this lacuna, research on interfacial shear strength of GGBS, fly ash-based GPC is very much required.

2.5 CONCLUSION OF LITERATURE REVIEW

From the review of literature, it is observed that geopolymers are among viable alternatives to Portland cement as binder material because of their eco-friendly properties, superior strength, better durability, and being cost effective. The evaluation of mechanical and durability characteristics of geopolymer concrete paves the way for its structural use for an environmental friendly, and sustainable construction industry. The following conclusions emerge from the literature review:

i. The chemical composition of the source material affects the mechanical properties of geopolymer concrete.
ii. Alkaline activator composed of sodium hydroxide solution and sodium silicate solution leads to better mechanical properties (including compressive strengths) than using only NaOH solution as an activator since Na_2SiO_3 solution favors the polymerization process adding more silicon (Si) atoms to the product, better leading to mechanical strength.
iii. To avoid heat curing, slag is considered a partial replacement to fly ash. Since then research has shifted fly ash and GGBS based geopolymer concrete.

iv. The compressive strength of geopolymer concrete witnessed an increase with increase in GGBS to fly ash ratio for a particular molarity of activator and particular Na_2SiO_3 to NaOH ratio.

v. General behavior and failure mode of reinforced geopolymer concrete members such as beams, columns, slabs, etc. were similar to those of ordinary Portland cement concrete.

vi. Reinforced geopolymer concrete member design based on the design codes for conventional cement concrete gave a more conservative estimate of the ultimate load-carrying capacity.

vii. The interfacial shear strength of fly ash-based geopolymer concrete is inferior to conventional concrete.

viii. Geopolymer concrete exhibits higher bond strength compared to corresponding conventional concrete strength.

Based on the literature review, the following gaps/shortfall have been identified for the use of geopolymer concrete.

i. There is no single unified parameter; instead, several parameters control the strength of geopolymer concrete.

ii. There are limited studies on the quantification of parameters affecting the shear transfer across monolithic interfaces in geopolymer concrete. There is a need for a design model for establishing shear strength at the monolithic interface of fly ash and GGBS based geopolymer concrete.

iii. There are limited studies on the applicability of existing design theories and design codes on conventional concrete to predict the shear strength of geopolymer concrete.

CHAPTER 3
OBJECTIVES AND SCOPE OF INVESTIGATION

From the standpoint of sustainability, geopolymer concrete is considered an alternative to conventional cement concrete as a building material. It consumes less energy during the manufacturing process and also gets cured under ambient conditions without any need for water curing. Further, geopolymers are considered promising binders, which are rich in silica and alumina and form inorganic polymers during geopolymerisation when activated with alkaline solution.

From the literature review it is apparent that the strength of geopolymer concrete varies with composition and the quantity of source or binder material along with alkaline solution and its concentration. It is also indicated in the literature that there are several variables that affect the strength of geopolymer concrete such as molarity of NaOH, the quantity of fly ash, GGBS, activation solution, etc. Many investigations reported the effects of these variables in an isolated manner. There is no single parameter identified/reported which controls the strength of geopolymer concrete. Hence in this investigation, an attempt is made to introduce a single unified parameter that can be taken into count in controlling the strength of geopolymer concrete. This parameter helps in assessing the strength of geopolymer concrete based on the constituents considered.

Further, an attempt is made to study the interfacial shear strength of fly ash and GGBS based geopolymer concrete experimentally by testing push-off specimens. The experimental results are validated with the proposed analytical model and compared with existing codes of practice / analytical models on the shear strength of OPC concrete. This will be a constructive step forward to use geopolymer concrete for structural application.

Keeping above aspects in view, investigations were conducted in different phases. The objectives of different phases of work are mentioned below.

Phase I:

1. To conduct an analytical study on the parameters affecting the strength of fly ash, GGBS based geopolymer concrete and establish unique parameters controlling the strength of geopolymer concrete.

Phase II:

2. To investigate the Interfacial shear strength in monolithic geopolymer concrete on Push-off Specimens.
3. To compare the results of shear strength of geopolymer concrete with design theories and design codes of conventional concrete.

Phase III:

4. To apply interfacial shear strength equation formulated to the reinforced geopolymer concrete corbel to validate and compare the same with different design models and codes of conventional concrete.

To fulfill the above objectives, the present analytical and experimental investigation was carried out in three phases and the same is explained in brief in the following sections.

PHASE – I

In this phase of the investigation, a review of the different mix proportions and corresponding strength of different investigators on fly ash and GGBS based geopolymer concrete was made. A study of factors affecting the strength of geopolymer concrete reveals that there are three important parameters, **i**. Concentration/molarity of NaOH solution, **ii**. Effect of alkaline to binder ratio and **iii**. GGBS to fly ash ratio. A new unified parameter "Binder Index (Bi)" which

combines the effect of different parameters influencing the compressive strength of geopolymer concrete was proposed and this helps in the development of binder index-based criteria for controlling the strength of geopolymer concrete. The relations between compressive strength (f_{gpc}) and binder index (Bi) of geopolymer concrete were developed. The same was validated by conducting an experimental study by casting, testing geopolymer concrete cubes.

PHASE – II

The second phase of the investigation looked at the shear strength of geopolymer concrete at monolithic interfaces, by casting and testing push-off specimens. Experimental work was carried out by considering three grades and three varying percentages of reinforcement across the interface of push-off specimens. The results obtained from the experimental work were analyzed based on the shear transfer mechanism that includes cohesion, friction, and dowel action components. The shear strength of geopolymer concrete obtained from the experimental study was compared with conventional concrete design theories and design codes on the shear.

PHASE – III

The third phase of the investigation was devoted to applying the equation developed for the shear strength of fly ash and GGBS based geopolymer concrete to reinforced geopolymer concrete corbels. The parameters of the experimental study were compressive strength of geopolymer concrete and reinforcement crossing the shear interface of corbels. The experimental results were then compared with different design theories and codes on corbels.

The methodology of the investigation carried out is illustrated in the following flow chart.

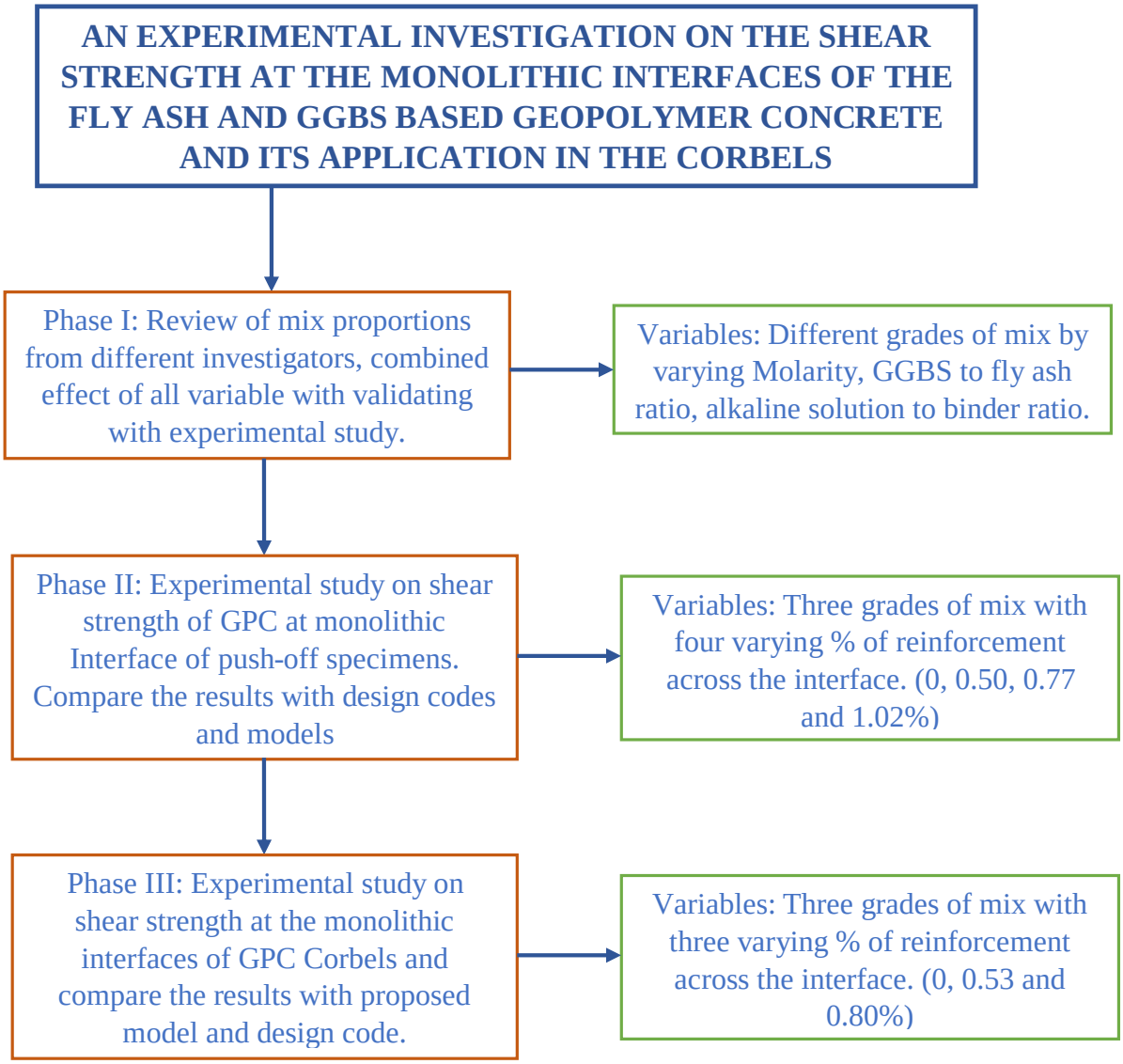

Figure 3.1: Flowchart for the proposed methodology

Scope of Investigation

- To review the factors affecting the strength of GGBS and fly ash-based geopolymer concrete of previous investigators.
- Compare the strengths of geopolymer concrete of different works and propose a unique parameter termed “Binder Index (Bi)” that controls the strength of geopolymer concrete.
- The binder material considered includes Class F Fly ash, GGBS, Alkaline activators – a combination of Na_2SiO_3 and NaOH solutions in the ratio of 2.5:1 and 8 molar concentration of NaOH solution.

- Experimental study on interfacial shear strength of GGBS and fly ash-based geopolymer concrete push-off specimens.
- Compare the experimental shear strength results with that from different design theories and design codes (ACI 318, 2019, Euro Code 2, 2004, FIB Model Code, 2010 and CSA A23.3, 2019)
- Experimental study of reinforced geopolymer concrete corbels by varying three strength grades of geopolymer concrete and varying % of reinforcement across the interface and to validate the results with shear strength equation of geopolymer concrete developed and compare the results with shear strength provisions provided by different design theories and codes on corbels.

CHAPTER 4
AN ANALYTICAL STUDY ON THE PARAMETERS AFFECTING THE STRENGTH OF THE GEOPOLYMER CONCRETE

4.1 PARAMETERS AFFECTING STRENGTH OF GGBS AND FLY ASH BASED GEOPOLYMER CONCRETE

The production of Geopolymer Concrete (GPC) involves the use of source materials such as fly ash (F), ground granulated blast furnace slag (GGBS), which are rich in silicon and aluminum, along with alkaline liquids such as sodium hydroxide and/or sodium silicate solution. In recent past, several investigations reported various parameters affecting the strength of geopolymer concrete, such as sodium hydroxide solution concentration i.e. molarity of NaOH solution, the ratio of sodium silicate to sodium hydroxide, alkaline activator solution to binder (F + GGBS), binder content, curing temperature, the content of coarse and fine aggregate.

The review of literature also indicated that the parameters listed above were considered either in an isolated manner or as a group of a few parameters in the strength studies on geopolymer concrete. No unique parameter, which can be used as a controlling parameter for the strength of geopolymer concrete was reported. Hence in this investigation, an attempt was made to identify a unique parameter affecting the strength of geopolymer concrete rationally.

For this purpose, an analytical study on the published strength related results of geopolymer concrete was made. This analytical study included the collection and analysis of data related to compressive strength, flexural strength, and split tensile strength of geopolymer concrete, reported by 13 different investigators. The data collected consisted of strength related results of about 215 concrete mixes and 25 mortar mixes and are shown in table 4.1.

From the geopolymer concrete mix proportions (table 4.1) adopted by different investigators along with corresponding strength, the following points were observed with respect to the quantity of materials adopted for producing geopolymer concrete.

1) It is observed that the quantity of fly ash varied from 40 kg to 808 kg and the GGBS quantity varied from 35 kg to 808 kg. The GGBS to fly ash ratio adopted was between 0.1 and 9.
2) The total alkaline activator solution (i.e. a combined mixture of sodium silicate and sodium hydroxide solution) varied from 133 kg to 404 kg.
3) In most of the investigations, the ratio of sodium silicate to sodium hydroxide was 2.5. However very few investigations (Rafeel et al., 2017) included the ratio of sodium silicate to sodium hydroxide as 1.2.
4) The molarity of NaOH varied from 6 to 16.
5) The total amount of aggregate in geopolymer concrete concrete varied from 1655 kg to 1913 kg per cubic meter of concrete. The fine aggregate to coarse aggregate ratio adopted varied between 0.43 and 0.82.
6) The total aggregate quantity in the investigation related to geopolymer concrete mortars was around 890 kg.

The effect of different parameters such as GGBS to fly ash ratio, molarity, and alkaline activator to binder (GGBS + fly ash) quantity ratio on the variation of different strengths of geopolymer concrete such as compressive strength, flexural strength and split tensile strength is shown in figure 4.1 and discussed in the following sections.

Table 4.1 Mix proportions and strengths of geopolymer concrete reported in different investigations

Inv (Yr)	F (Kg/Cum)	G (Kg/Cum)	Na_2SiO_3 (Kg/Cum)	NaOH (Kg/Cum)	M	CA ((Kg/Cum)	FA (Kg/Cum)	f_{gpc} (N/mm^2)	f_{cr} (N/mm^2)	f_{st} (N/mm^2)	*Bi*
Bhikshma et al., 2016	437.00	43.00	171.43	68.57	8	915.00	740.00	28.33	3.01	1.88	0.39
	384.00	96.00	171.43	68.57	8	926.00	749.00	40.40	3.67	2.55	1.00
	348.00	132.00	171.43	68.57	8	933.00	756.00	50.46	4.27	3.11	1.52
	298.00	182.00	171.43	68.57	8	943.00	763.00	59.90	4.93	3.63	2.44
	274.00	206.00	171.43	68.57	8	948.00	767.00	71.07	5.43	4.24	3.01
Annapurna et al., 2017	432.00	48.00	171.00	69.00	8	1090.00	590.00	27.30	2.90	2.50	0.44
	384.00	96.00	171.00	69.00	8	1090.00	590.00	40.50	4.10	3.50	1.00
	336.00	144.00	171.00	69.00	8	1090.00	590.00	49.30	4.50	4.00	1.71
	288.00	192.00	171.00	69.00	8	1090.00	590.00	60.40	4.90	4.50	2.67
	240.00	240.00	171.00	69.00	8	1090.00	590.00	70.80	5.30	4.80	4.00
Ganapati Naidu et al., 2012	370.09	37.91	116.57	46.63	8	961.00	554.00	24.29	1.00	2.30	0.33
	340.00	68.00	116.57	46.63	8	961.00	554.00	41.04	5.00	3.45	0.64
	313.85	94.15	116.57	46.63	8	961.00	554.00	45.76	5.77	5.17	0.96
	291.43	116.57	116.57	46.63	8	961.00	554.00	57.33	7.06	9.05	1.28
Rama Seshu et al., 2017 & 2019	301.92	76.92	173.08	69.23	6	692.31	507.69	16.30	1.77	NR	0.98
	265.38	113.46	173.08	69.23	6	692.31	507.69	17.80	2.10	NR	1.64
	227.31	151.54	173.08	69.23	6	692.31	507.69	24.50	2.48	NR	2.56
	189.62	189.23	173.08	69.23	6	692.31	507.69	37.10	2.70	NR	3.83
	151.54	227.31	173.08	69.23	6	692.31	507.69	40.90	3.00	NR	5.76
	113.46	265.38	173.08	69.23	6	692.31	507.69	44.80	3.36	NR	8.98
	301.92	76.92	173.08	69.23	8	692.31	507.69	18.90	1.83	NR	1.30
	265.38	113.46	173.08	69.23	8	692.31	507.69	23.00	2.19	NR	2.19
	227.31	151.54	173.08	69.23	8	692.31	507.69	29.60	2.55	NR	3.41
	189.62	189.23	173.08	69.23	8	692.31	507.69	37.80	2.93	NR	5.11
	151.54	227.31	173.08	69.23	8	692.31	507.69	41.90	3.09	NR	7.68

Table 4.1 Mix proportions and strengths of geopolymer concrete reported in different investigations

Inv (Yr)	F (Kg/Cum)	G (Kg/Cum)	Na_2SiO_3 (Kg/Cum)	NaOH (Kg/Cum)	M	CA ((Kg/Cum)	FA (Kg/Cum)	f_{gpc} (N/mm^2)	f_{cr} (N/mm^2)	f_{st} (N/mm^2)	*Bi*
	113.46	265.38	173.08	69.23	8	692.31	507.69	48.40	3.59	NR	11.97
	301.92	76.92	173.08	69.23	10	692.31	507.69	22.10	2.06	NR	1.63
	265.38	113.46	173.08	69.23	10	692.31	507.69	25.50	2.29	NR	2.73
	227.31	151.54	173.08	69.23	10	692.31	507.69	36.70	2.61	NR	4.26
	189.62	189.23	173.08	69.23	10	692.31	507.69	38.80	2.99	NR	6.38
	151.54	227.31	173.08	69.23	10	692.31	507.69	43.00	3.12	NR	9.59
	113.46	265.38	173.08	69.23	10	692.31	507.69	52.90	3.66	NR	14.96
	301.92	76.92	173.08	69.23	12	692.31	507.69	27.40	2.16	NR	1.96
	265.38	113.46	173.08	69.23	12	692.31	507.69	29.50	2.36	NR	3.28
	227.31	151.54	173.08	69.23	12	692.31	507.69	38.90	2.64	NR	5.12
	189.62	189.23	173.08	69.23	12	692.31	507.69	40.30	3.05	NR	7.66
	151.54	227.31	173.08	69.23	12	692.31	507.69	43.90	3.36	NR	11.51
	113.46	265.38	173.08	69.23	12	692.31	507.69	56.90	3.75	NR	17.95
Rajagopalan Gopalakrishnan et al., 2019	40.00	360.00	120.00	48.00	12	1124.00	688.00	46.19	NR	NR	45.36
	80.00	320.00	120.00	48.00	12	1124.00	688.00	45.24	NR	NR	20.16
	120.00	280.00	120.00	48.00	12	1124.00	688.00	44.29	NR	NR	11.76
	160.00	240.00	120.00	48.00	12	1124.00	688.00	43.33	NR	NR	7.56
	200.00	200.00	120.00	48.00	12	1124.00	688.00	42.38	NR	NR	5.04
Zende et al., 2015	295.71	98.57	112.65	45.06	11	1293.60	554.40	33.00	3.10	3.20	1.47
	197.14	197.14	112.65	45.06	11	1293.60	554.40	35.00	3.88	3.95	4.40
	98.57	295.71	112.65	45.06	11	1293.60	554.40	40.00	4.10	4.40	13.20
	295.71	98.57	112.65	45.06	13	1293.60	554.40	35.00	3.70	3.92	1.73
	197.14	197.14	112.65	45.06	13	1293.60	554.40	38.00	4.01	4.30	5.20
	98.57	295.71	112.65	45.06	13	1293.60	554.40	43.00	4.20	4.94	15.60
	102.30	306.70	102.00	41.00	10	1293.00	554.00	58.12	NR	3.23	10.49

Table 4.1 Mix proportions and strengths of geopolymer concrete reported in different investigations

Inv (Yr)	F (Kg/Cum)	G (Kg/Cum)	Na_2SiO_3 (Kg/Cum)	NaOH (Kg/Cum)	M	CA ((Kg/Cum)	FA (Kg/Cum)	f_{gpc} (N/mm^2)	f_{cr} (N/mm^2)	f_{st} (N/mm^2)	*Bi*
Rajini et al., 2014	204.50	204.50	102.00	41.00	10	1293.00	554.00	46.32	NR	2.03	3.50
	306.70	102.30	102.00	41.00	10	1293.00	554.00	15.55	NR	1.36	1.17
Krishnaraja et al., 2014	315.00	35.00	100.00	40.00	14	1081.00	483.00	29.52	3.60	3.28	0.62
	280.00	70.00	100.00	40.00	14	1081.00	483.00	32.86	3.65	4.04	1.40
	245.00	105.00	100.00	40.00	14	1081.00	483.00	35.73	3.83	4.36	2.40
	210.00	140.00	100.00	40.00	14	1081.00	483.00	36.93	3.86	4.69	3.73
	175.00	175.00	100.00	40.00	14	1081.00	483.00	39.23	4.01	4.94	5.60
Rafeel et al., 2017	318.00	79.00	93.00	77.00	10	1111.00	721.00	37.67	NR	NR	1.06
	309.00	77.00	91.00	75.00	10	1111.00	721.00	38.72	NR	NR	1.07
	301.00	75.00	89.00	73.00	10	1111.00	721.00	38.20	NR	NR	1.07
	294.00	73.00	86.00	71.00	10	1111.00	721.00	31.40	NR	NR	1.06
	291.00	73.00	85.00	70.00	10	1145.00	742.00	40.81	NR	NR	1.07
	283.00	71.00	83.00	68.00	10	1145.00	742.00	35.06	NR	NR	1.07
	276.00	69.00	81.00	67.00	10	1145.00	742.00	31.40	NR	NR	1.07
	289.00	72.00	85.00	70.00	10	1160.00	753.00	39.77	NR	NR	1.07
	281.00	70.00	83.00	68.00	10	1160.00	753.00	40.81	NR	NR	1.07
	274.00	68.00	81.00	66.00	10	1160.00	753.00	35.58	NR	NR	1.07
	267.00	67.00	79.00	64.00	10	1160.00	753.00	31.92	NR	NR	1.07
	239.00	159.00	94.00	77.00	10	1111.00	721.00	60.19	NR	NR	2.86
	230.00	153.00	90.00	74.00	10	1111.00	721.00	57.38	NR	NR	2.85
	227.00	151.00	89.00	73.00	10	1111.00	721.00	60.75	NR	NR	2.85
	218.00	145.00	86.00	70.00	10	1111.00	721.00	50.63	NR	NR	2.86
	219.00	146.00	86.00	70.00	10	1145.00	742.00	57.38	NR	NR	2.85
	216.00	144.00	85.00	69.00	10	1145.00	742.00	55.13	NR	NR	2.85
	213.00	142.00	84.00	69.00	10	1145.00	742.00	56.25	NR	NR	2.87

Table 4.1 Mix proportions and strengths of geopolymer concrete reported in different investigations

Inv (Yr)	F (Kg/Cum)	G (Kg/Cum)	Na_2SiO_3 (Kg/Cum)	NaOH (Kg/Cum)	M	CA ((Kg/Cum)	FA (Kg/Cum)	f_{gpc} (N/mm^2)	f_{cr} (N/mm^2)	f_{st} (N/mm^2)	*Bi*
	209.00	139.00	82.00	67.00	10	1160.00	753.00	56.25	NR	NR	2.85
	203.00	136.00	80.00	65.00	10	1160.00	753.00	55.13	NR	NR	2.87
	198.00	132.00	78.00	64.00	10	1160.00	753.00	54.00	NR	NR	2.87
	113.00	264.00	89.00	73.00	10	1111.00	721.00	77.44	NR	NR	10.04
	108.00	251.00	84.00	69.00	10	1111.00	721.00	71.16	NR	NR	9.90
	105.00	245.00	82.00	68.00	10	1111.00	721.00	64.88	NR	NR	10.00
	106.00	248.00	83.00	68.00	10	1145.00	742.00	72.21	NR	NR	9.98
	101.00	236.00	79.00	65.00	10	1145.00	742.00	69.07	NR	NR	9.98
	99.00	230.00	77.00	63.00	10	1145.00	742.00	68.02	NR	NR	9.89
	103.00	240.00	81.00	66.00	10	1160.00	753.00	74.30	NR	NR	9.99
	98.00	228.00	77.00	63.00	10	1160.00	753.00	69.07	NR	NR	9.99
	95.00	223.00	75.00	61.00	10	1160.00	753.00	63.84	NR	NR	10.04
Prasanna et al., 2016	324.52	108.17	192.31	67.31	12	1057.69	432.69	37.50	NR	NR	2.40
	281.25	151.44	192.31	67.31	12	1057.69	432.69	44.90	NR	NR	3.88
	237.98	194.71	192.31	67.31	12	1057.69	432.69	48.00	NR	NR	5.89
Ramamohana et al., 2019	267.10	114.47	95.90	37.92	6	787.30	339.36	20.00	3.65	0.88	0.90
	228.94	152.63	95.90	37.92	8	787.30	339.36	24.23	4.42	1.97	1.87
	190.78	190.78	95.90	37.92	10	787.30	339.36	28.75	5.16	2.50	3.51
	152.63	228.94	95.90	37.92	12	787.30	339.36	33.25	6.67	3.10	6.31
	114.47	267.10	95.90	37.92	14	787.30	339.36	44.16	7.48	3.98	11.46
Mallikarjuna Rao et al., 2018 & 2017	315.00	135.00	144.64	57.86	8	972.00	760.50	20.76	NR	NR	1.54
	308.00	132.00	141.43	56.57	8	969.47	777.33	22.40	NR	NR	1.54
	301.00	129.00	138.21	55.29	8	989.04	773.96	23.62	NR	NR	1.54
	294.00	126.00	135.00	54.00	8	966.00	810.60	25.11	NR	NR	1.54
	287.00	123.00	131.79	52.71	8	1026.66	769.14	25.20	NR	NR	1.54

Table 4.1 Mix proportions and strengths of geopolymer concrete reported in different investigations

Inv (Yr)	F (Kg/Cum)	G (Kg/Cum)	Na_2SiO_3 (Kg/Cum)	NaOH (Kg/Cum)	M	CA ((Kg/Cum)	FA (Kg/Cum)	f_{gpc} (N/mm^2)	f_{cr} (N/mm^2)	f_{st} (N/mm^2)	*Bi*
	280.00	120.00	128.57	51.43	8	1042.93	773.07	25.30	NR	NR	1.54
	273.00	117.00	125.36	50.14	8	1057.64	775.36	25.40	NR	NR	1.54
	266.00	114.00	122.14	48.86	8	1070.59	776.21	25.50	NR	NR	1.54
	259.00	111.00	118.93	47.57	8	1081.56	775.84	25.60	NR	NR	1.54
	315.00	135.00	160.71	64.29	8	972.00	760.50	25.71	NR	NR	1.54
	252.00	108.00	115.71	46.29	8	1090.80	774.00	25.71	NR	NR	2.40
	308.00	132.00	157.14	62.86	8	969.47	777.33	25.88	NR	NR	2.40
	301.00	129.00	153.57	61.43	8	989.04	773.96	26.01	NR	NR	2.40
	294.00	126.00	150.00	60.00	8	966.00	810.60	26.17	NR	NR	2.40
	287.00	123.00	146.43	58.57	8	1026.66	769.14	26.95	NR	NR	2.40
	280.00	120.00	142.86	57.14	8	1042.93	773.07	27.77	NR	NR	2.40
	273.00	117.00	139.29	55.71	8	1057.64	775.36	28.60	NR	NR	2.40
	266.00	114.00	135.71	54.29	8	1070.59	776.21	29.43	NR	NR	2.40
	259.00	111.00	132.14	52.86	8	1081.56	775.84	30.27	NR	NR	2.40
	252.00	108.00	128.57	51.43	8	1090.80	774.00	31.11	NR	NR	2.40
	315.00	135.00	176.79	70.71	8	972.00	760.50	33.81	NR	NR	3.60
	252.00	108.00	141.43	56.57	8	1090.80	774.00	33.83	NR	NR	3.60
	259.00	111.00	145.36	58.14	8	1081.56	775.84	34.31	NR	NR	3.60
	266.00	114.00	149.29	59.71	8	1070.59	776.21	34.79	NR	NR	3.60
	308.00	132.00	172.86	69.14	8	969.47	777.33	34.89	NR	NR	3.60
	273.00	117.00	153.21	61.29	8	1057.64	775.36	35.27	NR	NR	3.60
	301.00	129.00	168.93	67.57	8	989.04	773.96	35.70	NR	NR	3.60
	280.00	120.00	157.14	62.86	8	1042.93	773.07	35.76	NR	NR	3.60
	252.00	108.00	154.29	61.71	8	1090.80	774.00	36.19	NR	NR	3.60
	287.00	123.00	161.07	64.43	8	1026.66	769.14	36.24	NR	NR	3.60

Table 4.1 Mix proportions and strengths of geopolymer concrete reported in different investigations

Inv (Yr)	F (Kg/Cum)	G (Kg/Cum)	Na_2SiO_3 (Kg/Cum)	NaOH (Kg/Cum)	M	CA ((Kg/Cum)	FA (Kg/Cum)	f_{gpc} (N/mm^2)	f_{cr} (N/mm^2)	f_{st} (N/mm^2)	*Bi*
	259.00	111.00	158.57	63.43	8	1081.56	775.84	36.52	NR	NR	1.71
	294.00	126.00	165.00	66.00	8	966.00	810.60	36.69	NR	NR	1.71
	266.00	114.00	162.86	65.14	8	1070.59	776.21	36.85	NR	NR	1.71
	273.00	117.00	167.14	66.86	8	1057.64	775.36	37.18	NR	NR	1.71
	280.00	120.00	171.43	68.57	8	1042.93	773.07	37.52	NR	NR	1.71
	287.00	123.00	175.71	70.29	8	1026.66	769.14	37.85	NR	NR	1.71
	294.00	126.00	180.00	72.00	8	966.00	810.60	38.16	NR	NR	1.71
	301.00	129.00	184.29	73.71	8	989.04	773.96	38.43	NR	NR	1.71
	308.00	132.00	188.57	75.43	8	969.47	777.33	38.66	NR	NR	1.71
	315.00	135.00	192.86	77.14	8	972.00	760.50	38.96	NR	NR	1.71
	270.00	180.00	176.79	70.71	8	972.00	760.50	41.85	NR	NR	2.67
	216.00	144.00	115.71	46.29	8	1090.80	774.00	42.32	NR	NR	2.67
	264.00	176.00	172.86	69.14	8	969.47	777.33	42.91	NR	NR	2.67
	222.00	148.00	118.93	47.57	8	1081.56	775.84	42.95	NR	NR	2.67
	216.00	144.00	128.57	51.43	8	1090.80	774.00	43.38	NR	NR	2.67
	228.00	152.00	122.14	48.86	8	1070.59	776.21	43.58	NR	NR	2.67
	258.00	172.00	168.93	67.57	8	989.04	773.96	43.71	NR	NR	2.67
	234.00	156.00	125.36	50.14	8	1057.64	775.36	44.21	NR	NR	2.67
	252.00	168.00	165.00	66.00	8	966.00	810.60	44.67	NR	NR	2.67
	240.00	160.00	128.57	51.43	8	1042.93	773.07	44.85	NR	NR	2.67
	246.00	164.00	161.07	64.43	8	1026.66	769.14	45.02	NR	NR	4.00
	240.00	160.00	157.14	62.86	8	1042.93	773.07	45.38	NR	NR	4.00
	246.00	164.00	131.79	52.71	8	1026.66	769.14	45.48	NR	NR	4.00
	270.00	180.00	160.71	64.29	8	972.00	760.50	45.68	NR	NR	4.00
	234.00	156.00	153.21	61.29	8	1057.64	775.36	45.75	NR	NR	4.00

Table 4.1 Mix proportions and strengths of geopolymer concrete reported in different investigations

Inv (Yr)	F (Kg/Cum)	G (Kg/Cum)	Na_2SiO_3 (Kg/Cum)	NaOH (Kg/Cum)	M	CA ((Kg/Cum)	FA (Kg/Cum)	f_{gpc} (N/mm^2)	f_{cr} (N/mm^2)	f_{st} (N/mm^2)	*Bi*
	270.00	180.00	144.64	57.86	8	972.00	760.50	45.88	NR	NR	4.00
	264.00	176.00	141.43	56.57	8	969.47	777.33	45.96	NR	NR	4.00
	258.00	172.00	138.21	55.29	8	989.04	773.96	46.01	NR	NR	4.00
	264.00	176.00	157.14	62.86	8	969.47	777.33	46.01	NR	NR	4.00
	252.00	168.00	135.00	54.00	8	966.00	810.60	46.08	NR	NR	4.00
	228.00	152.00	149.29	59.71	8	1070.59	776.21	46.12	NR	NR	1.89
	222.00	148.00	132.14	52.86	8	1081.56	775.84	46.20	NR	NR	1.89
	228.00	152.00	135.71	54.29	8	1070.59	776.21	46.27	NR	NR	1.89
	258.00	172.00	153.57	61.43	8	989.04	773.96	46.27	NR	NR	1.89
	234.00	156.00	139.29	55.71	8	1057.64	775.36	46.35	NR	NR	1.89
	240.00	160.00	142.86	57.14	8	1042.93	773.07	46.42	NR	NR	1.89
	210.00	210.00	165.00	66.00	8	966.00	810.60	46.48	NR	NR	1.89
	222.00	148.00	145.36	58.14	8	1081.56	775.84	46.49	NR	NR	1.89
	246.00	164.00	146.43	58.57	8	1026.66	769.14	46.50	NR	NR	1.89
	252.00	168.00	150.00	60.00	8	966.00	810.60	46.57	NR	NR	1.89
	180.00	180.00	154.29	61.71	8	1090.80	774.00	46.68	NR	NR	2.93
	185.00	185.00	158.57	63.43	8	1081.56	775.84	46.84	NR	NR	2.93
	216.00	144.00	141.43	56.57	8	1090.80	774.00	46.87	NR	NR	2.93
	190.00	190.00	162.86	65.14	8	1070.59	776.21	46.98	NR	NR	2.93
	195.00	195.00	167.14	66.86	8	1057.64	775.36	47.13	NR	NR	2.93
	215.00	215.00	168.93	67.57	8	989.04	773.96	47.15	NR	NR	2.93
	205.00	205.00	161.07	64.43	8	1026.66	769.14	47.28	NR	NR	2.93
	200.00	200.00	171.43	68.57	8	1042.93	773.07	47.28	NR	NR	2.93
	205.00	205.00	175.71	70.29	8	1026.66	769.14	47.43	NR	NR	2.93
	210.00	210.00	180.00	72.00	8	966.00	810.60	47.57	NR	NR	2.93

Table 4.1 Mix proportions and strengths of geopolymer concrete reported in different investigations

Inv (Yr)	F (Kg/Cum)	G (Kg/Cum)	Na_2SiO_3 (Kg/Cum)	NaOH (Kg/Cum)	M	CA ((Kg/Cum)	FA (Kg/Cum)	f_{gpc} (N/mm^2)	f_{cr} (N/mm^2)	f_{st} (N/mm^2)	*Bi*
	215.00	215.00	184.29	73.71	8	989.04	773.96	47.59	NR	NR	4.40
	220.00	220.00	188.57	75.43	8	969.47	777.33	47.61	NR	NR	4.40
	225.00	225.00	192.86	77.14	8	972.00	760.50	47.64	NR	NR	4.40
	220.00	220.00	172.86	69.14	8	969.47	777.33	47.71	NR	NR	4.40
	228.00	152.00	162.86	65.14	8	1070.59	776.21	47.91	NR	NR	4.40
	216.00	144.00	154.29	61.71	8	1090.80	774.00	47.92	NR	NR	4.40
	200.00	200.00	157.14	62.86	8	1042.93	773.07	48.14	NR	NR	4.40
	225.00	225.00	176.79	70.71	8	972.00	760.50	48.45	NR	NR	4.40
	222.00	148.00	158.57	63.43	8	1081.56	775.84	48.47	NR	NR	4.40
	234.00	156.00	167.14	66.86	8	1057.64	775.36	48.75	NR	NR	4.40
	225.00	225.00	144.64	57.86	8	972.00	760.50	48.91	NR	NR	2.06
	195.00	195.00	153.21	61.29	8	1057.64	775.36	49.00	NR	NR	2.06
	240.00	160.00	171.43	68.57	8	1042.93	773.07	49.59	NR	NR	2.06
	190.00	190.00	149.29	59.71	8	1070.59	776.21	49.86	NR	NR	2.06
	246.00	164.00	175.71	70.29	8	1026.66	769.14	50.43	NR	NR	2.06
	270.00	180.00	192.86	77.14	8	972.00	760.50	50.69	NR	NR	2.06
	185.00	185.00	145.36	58.14	8	1081.56	775.84	50.73	NR	NR	2.06
	264.00	176.00	188.57	75.43	8	969.47	777.33	50.89	NR	NR	2.06
	258.00	172.00	184.29	73.71	8	989.04	773.96	51.04	NR	NR	2.06
	252.00	168.00	180.00	72.00	8	966.00	810.60	51.22	NR	NR	2.06
	180.00	180.00	141.43	56.57	8	1090.80	774.00	51.61	NR	NR	3.20
	220.00	220.00	141.43	56.57	8	969.47	777.33	51.90	NR	NR	3.20
	215.00	215.00	138.21	55.29	8	989.04	773.96	54.14	NR	NR	3.20
	180.00	180.00	115.71	46.29	8	1090.80	774.00	55.37	NR	NR	3.20
	185.00	185.00	118.93	47.57	8	1081.56	775.84	55.62	NR	NR	3.20

Table 4.1 Mix proportions and strengths of geopolymer concrete reported in different investigations

Inv (Yr)	F (Kg/Cum)	G (Kg/Cum)	Na_2SiO_3 (Kg/Cum)	NaOH (Kg/Cum)	M	CA ((Kg/Cum)	FA (Kg/Cum)	f_{gpc} (N/mm^2)	f_{cr} (N/mm^2)	f_{st} (N/mm^2)	*Bi*
	190.00	190.00	122.14	48.86	8	1070.59	776.21	55.85	NR	NR	3.20
	195.00	195.00	125.36	50.14	8	1057.64	775.36	56.11	NR	NR	3.20
	200.00	200.00	128.57	51.43	8	1042.93	773.07	56.36	NR	NR	3.20
	205.00	205.00	131.79	52.71	8	1026.66	769.14	56.62	NR	NR	3.20
	210.00	210.00	135.00	54.00	8	966.00	810.60	56.86	NR	NR	3.20
	225.00	225.00	160.71	64.29	8	972.00	760.50	58.53	NR	NR	4.80
	220.00	220.00	157.14	62.86	8	969.47	777.33	59.23	NR	NR	4.80
	215.00	215.00	153.57	61.43	8	989.04	773.96	59.75	NR	NR	4.80
	180.00	180.00	128.57	51.43	8	1090.80	774.00	59.79	NR	NR	4.80
	185.00	185.00	132.14	52.86	8	1081.56	775.84	59.88	NR	NR	4.80
	190.00	190.00	135.71	54.29	8	1070.59	776.21	59.98	NR	NR	4.80
	195.00	195.00	139.29	55.71	8	1057.64	775.36	60.08	NR	NR	4.80
	200.00	200.00	142.86	57.14	8	1042.93	773.07	60.18	NR	NR	4.80
	205.00	205.00	146.43	58.57	8	1026.66	769.14	60.28	NR	NR	4.80
	210.00	210.00	150.00	60.00	8	966.00	810.60	60.38	NR	NR	4.80
Mallikarjuna Rao et al., 2015	808.24	89.80	289.74	115.50	8	--	898.04	44.00	NR	NR	0.40
	718.43	179.61	289.74	115.50	8	--	898.04	46.00	NR	NR	0.90
	628.63	269.41	289.74	115.50	8	--	898.04	49.00	NR	NR	1.55
	538.82	359.22	289.74	115.50	8	--	898.04	50.00	NR	NR	2.41
	449.02	449.02	289.74	115.50	8	--	898.04	50.00	NR	NR	3.61
	359.22	538.82	289.74	115.50	8	--	898.04	52.00	NR	NR	5.41
	269.41	628.83	289.74	115.50	8	--	898.04	57.00	NR	NR	8.42
	179.61	718.43	289.74	115.50	8	--	898.04	63.00	NR	NR	14.44
	89.80	808.24	289.74	115.50	8	--	898.04	69.00	NR	NR	32.49
	808.24	89.80	289.74	115.50	12	--	898.04	45.00	NR	NR	0.60

Table 4.1 Mix proportions and strengths of geopolymer concrete reported in different investigations

Inv (Yr)	F (Kg/Cum)	G (Kg/Cum)	Na_2SiO_3 (Kg/Cum)	NaOH (Kg/Cum)	M	CA ((Kg/Cum)	FA (Kg/Cum)	f_{gpc} (N/mm^2)	f_{cr} (N/mm^2)	f_{st} (N/mm^2)	*Bi*
	718.43	179.61	289.74	115.50	12	--	898.04	47.00	NR	NR	1.35
	628.63	269.41	289.74	115.50	12	--	898.04	50.00	NR	NR	2.32
	538.82	359.22	289.74	115.50	12	--	898.04	52.00	NR	NR	3.61
	449.02	449.02	289.74	115.50	12	--	898.04	53.00	NR	NR	5.41
	359.22	538.82	289.74	115.50	12	--	898.04	55.00	NR	NR	8.12
	269.41	628.83	289.74	115.50	12	--	898.04	62.00	NR	NR	12.64
	179.61	718.43	289.74	115.50	12	--	898.04	65.00	NR	NR	21.66
	89.80	808.24	289.74	115.50	12	--	898.04	72.00	NR	NR	48.74
	808.24	89.80	289.74	115.50	16	--	898.04	47.00	NR	NR	0.80
	718.43	179.61	289.74	115.50	16	--	898.04	52.00	NR	NR	1.81
	628.63	269.41	289.74	115.50	16	--	898.04	56.00	NR	NR	3.09
	538.82	359.22	289.74	115.50	16	--	898.04	59.00	NR	NR	4.81
	449.02	449.02	289.74	115.50	16	--	898.04	63.00	NR	NR	7.22
	359.22	538.82	289.74	115.50	16	--	898.04	65.00	NR	NR	10.83
	269.41	628.83	289.74	115.50	16	--	898.04	67.00	NR	NR	16.85
	179.61	718.43	289.74	115.50	16	--	898.04	69.00	NR	NR	28.88
	89.80	808.24	289.74	115.50	16	--	898.04	75.00	NR	NR	64.98

Where, Inv – Investigator (s) and year, F – Quantity of fly Ash in Kg/Cum, G – Quantity of GGBS in Kg/Cum, SS – Quantity of sodium silicate solution in Kg/Cum, SH – Quantity of sodium hydroxide solution in Kg/Cum, A = SS + SH - Combination of the quantity of Na_2SiO_3 and NaOH in Kg/Cum, M – Molarity of NaOH, CA - Quantity of coarse aggregate in Kg/Cum, FA - Quantity of fine aggregate in Kg/Cum, f_{gpc} - Compressive strength in N/mm^2, f_{cr} – Flexural strength in N/mm^2, f_{st} – Split tensile strength in N/mm^2, Bi – Proposed Binder Index, NR – Not reported.

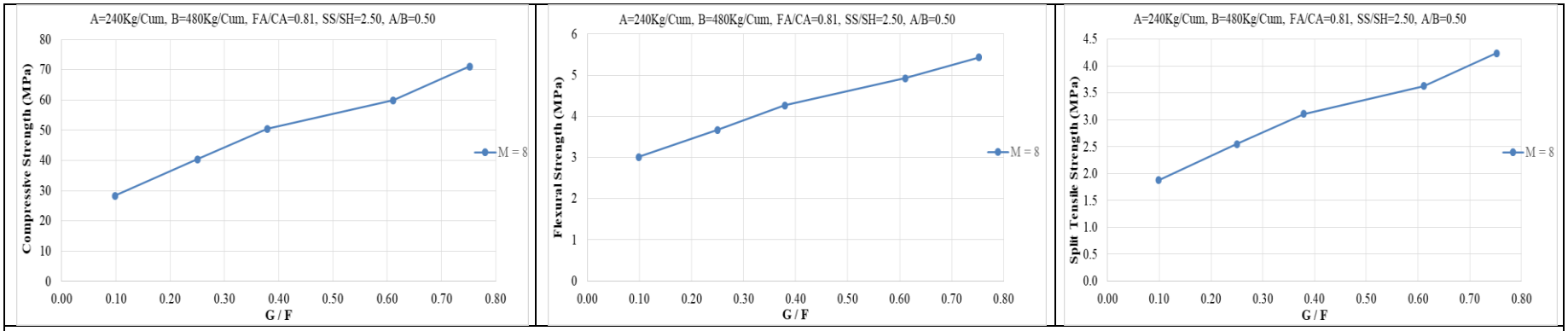

Figure 4.1 (a) Strengths of GPC vs. GGBS to fly ash (G / F) - Bhikshma et al, 2016

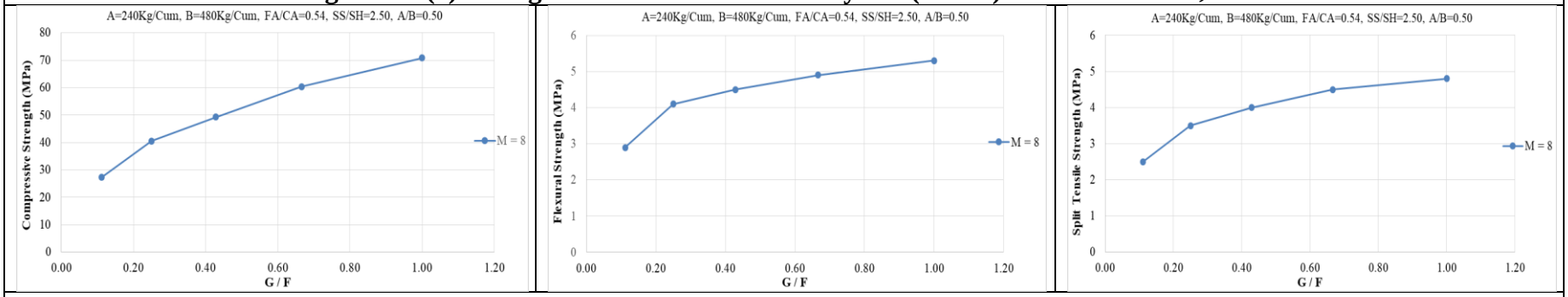

4.1 (b) Strengths of GPC vs. GGBS to fly ash (G / F) - Annapurna et al., 2017

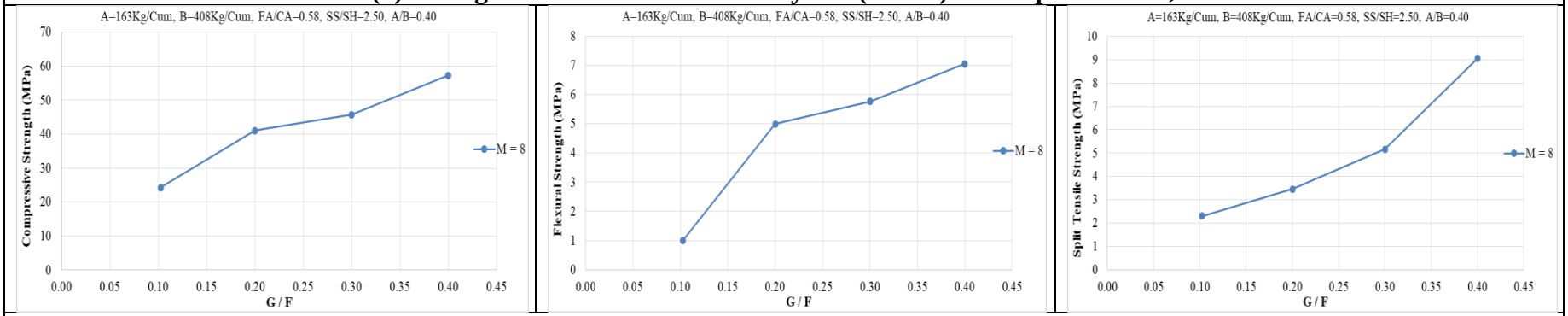

Figure 4.1 (c) Strengths of GPC vs. GGBS to fly ash (G / F) - Ganapati Naidu et al., 2012

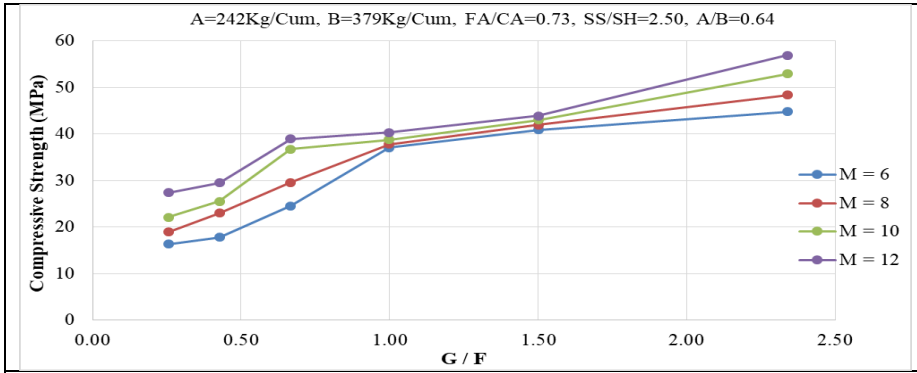

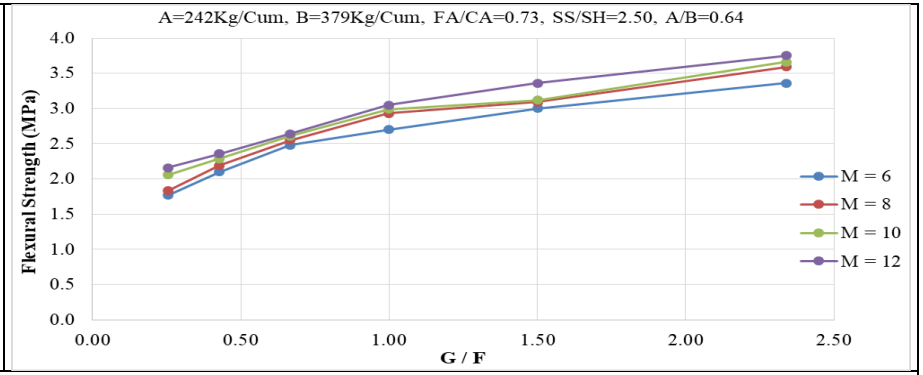

Figure 4.1 (d) Strengths of GPC vs. GGBS to fly ash (G / F) - Rama Seshu et al., 2017 & 2019

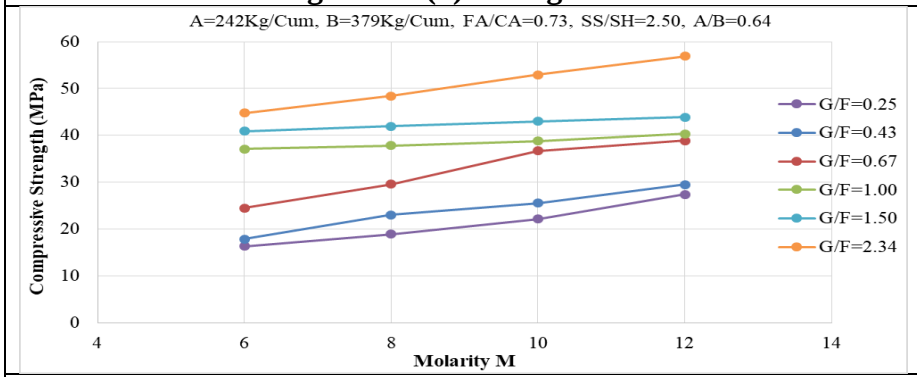

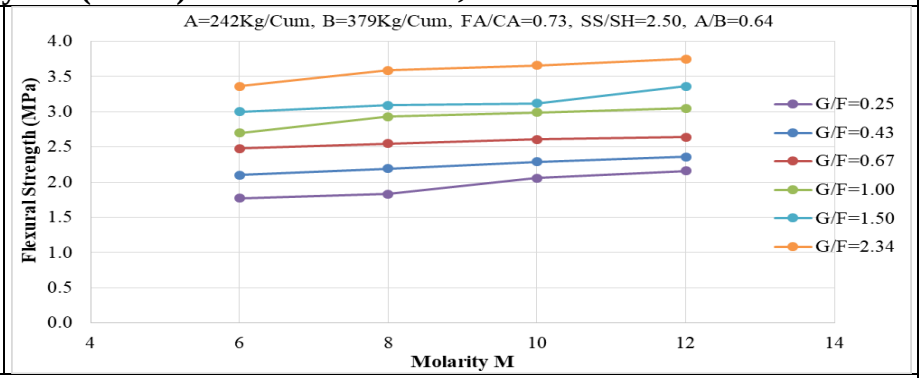

Figure 4.1 (e) Strengths of GPC vs. molarity of NaOH Solution (M) - Rajagopalan Gopalakrishnan et al., 2019

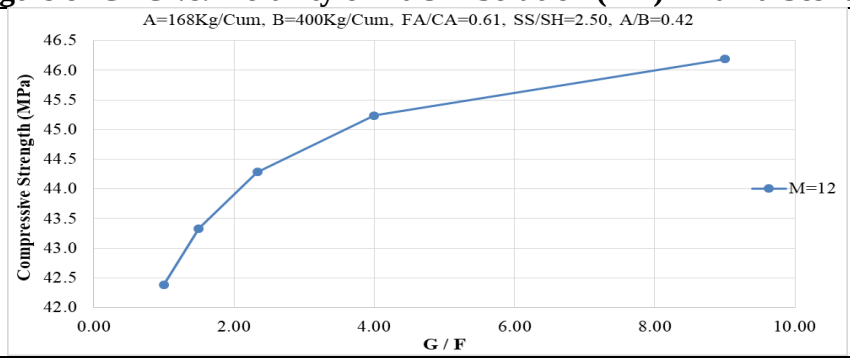

Figure 4.1 (f) Compressive strength of GPC vs. GGBS to fly ash (G / F) - Rajagopalan Gopalakrishnan et al., 2019

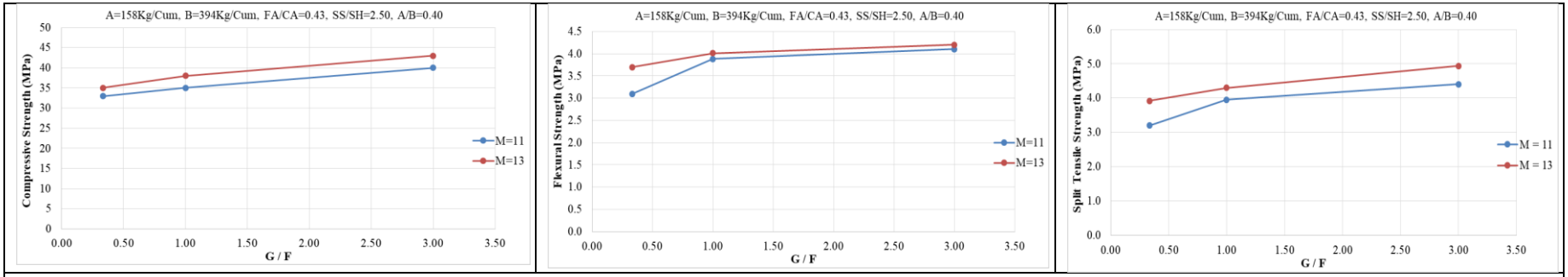

Figure 4.1 (g) Strengths of GPC vs. GGBS to fly ash (G / F) – Zende et al., 2015

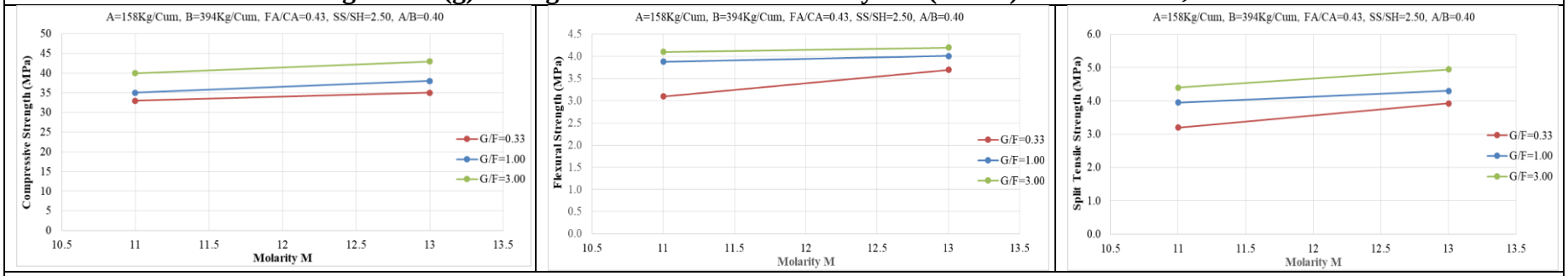

Figure 4.1 (h) Strengths of GPC vs. molarity of NaOH Solution (M) - Zende et al., 2015

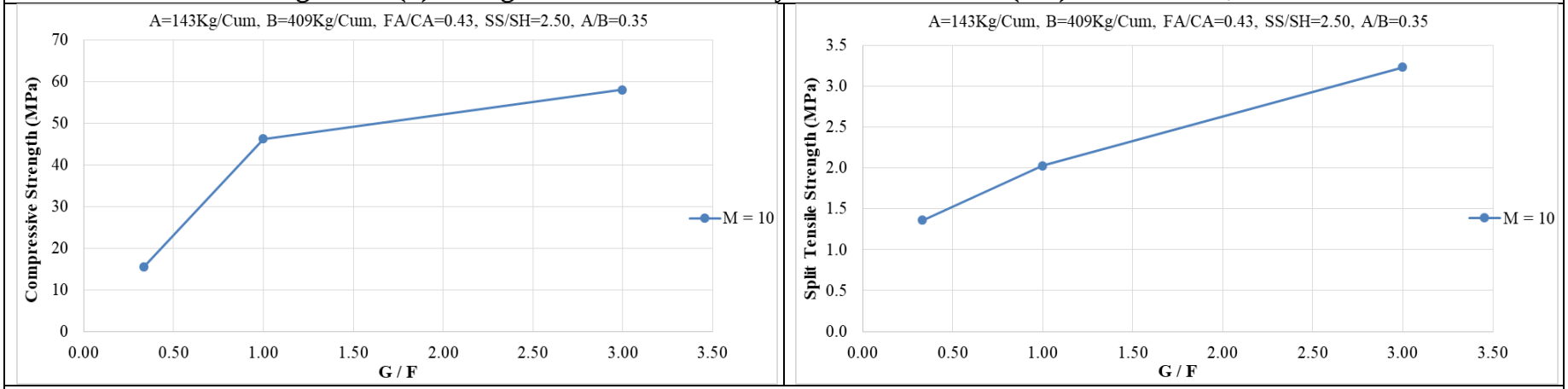

Figure 4.1 (i) Strengths of GPC vs. GGBS to fly ash (G / F) – Rajini et al., 2014

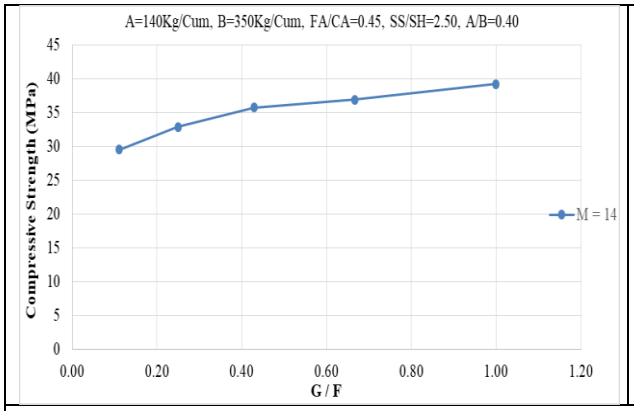

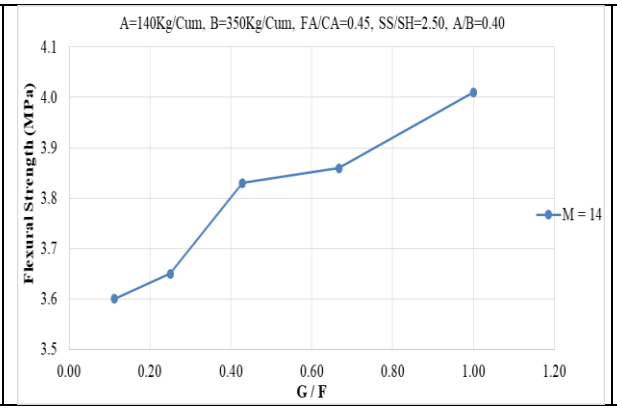

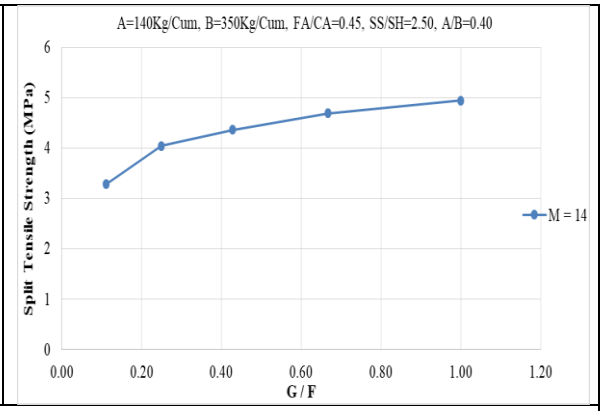

Figure 4.1 (j) Strengths of GPC vs. GGBS to fly ash (G / F) – Krishnaraja et al., 2014

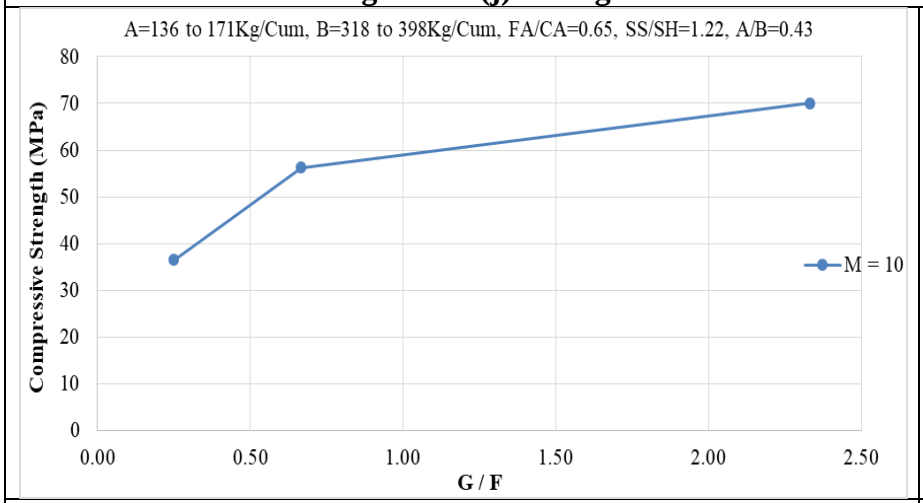

Figure 4.1 (k) Avg. Compressive strength of GPC vs. GGBS to fly ash (G / F) – Rafeel et al., 2017

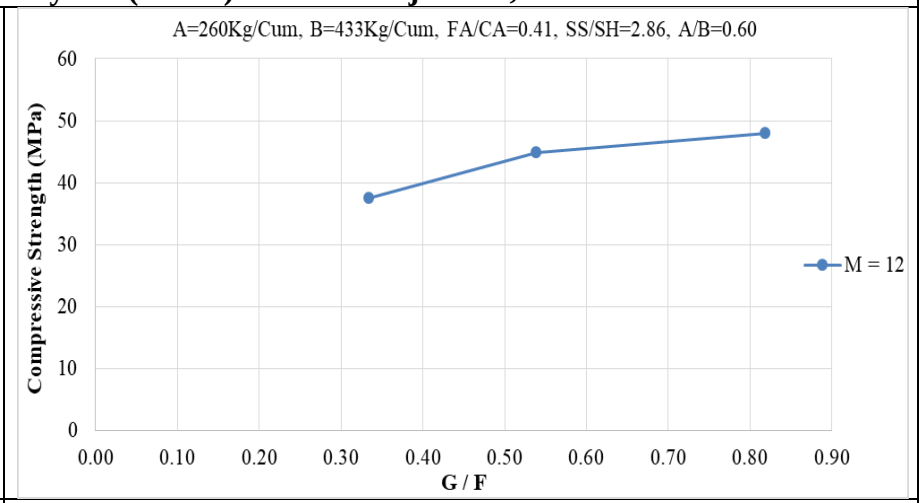

Figure 4.1 (l) Compressive strength of GPC vs. GGBS to fly ash (G / F) – Prasanna et al., 2016

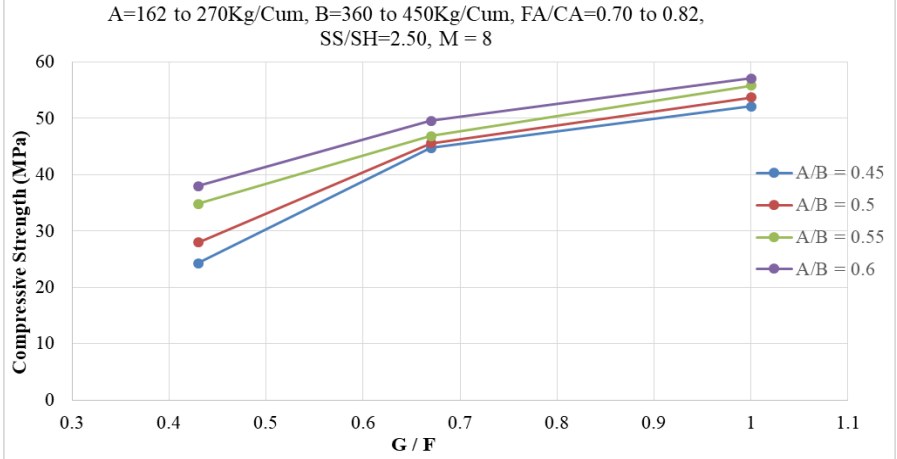

Figure 4.1 (m) Avg. compressive strength of GPC vs. GGBS to fly ash (G / F) – Mallikarjuna Rao et al., 2018 & 2017

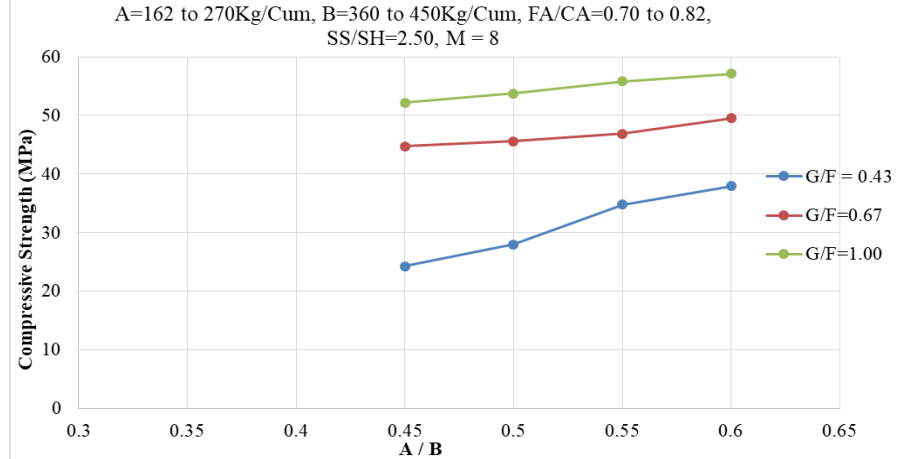

Figure 4.1 (n) Avg. compressive strength of GPC vs. alkaline activator to binder ratio (A / B) – Mallikarjuna Rao et al., 2018 & 2017

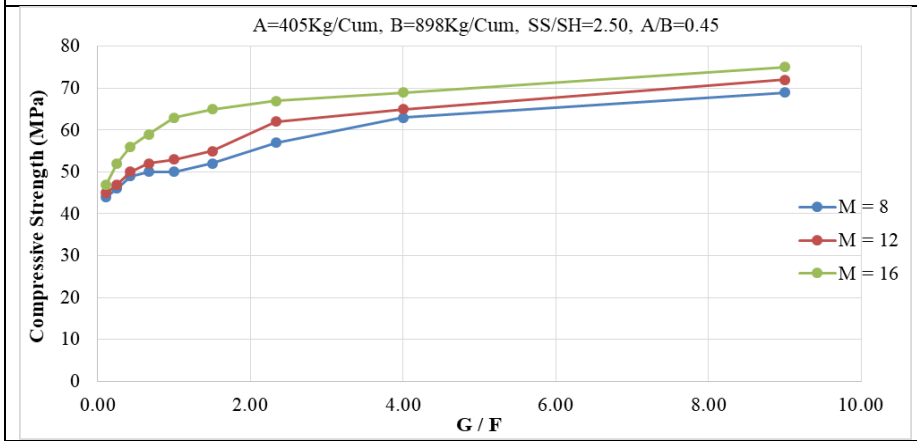

Figure 4.1 (o) Avg. compressive strength of GPC vs. GGBS to fly ash (G / F) – Mallikarjuna Rao et al., 2015 on GP mortars

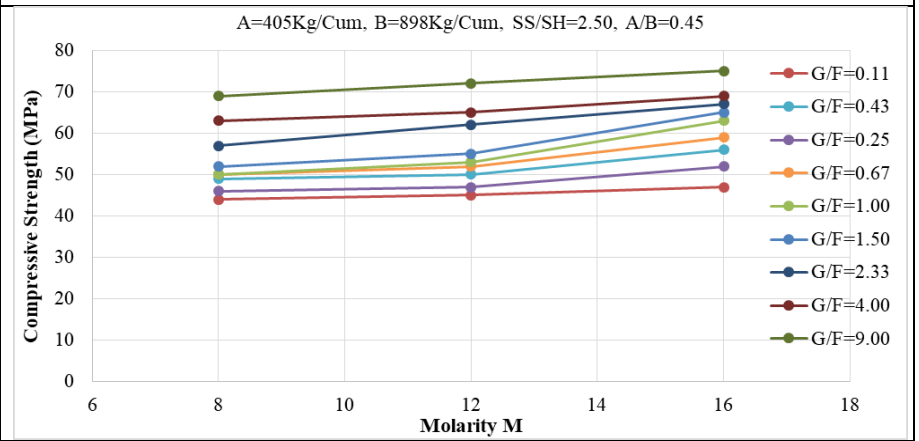

Figure 4.1 (p) Avg. compressive strength of GPC vs. molarity (M) of NaOH solution – Mallikarjuna Rao et al., 2015 on GP mortars

Figure 4.1 Variation of strengths of GPC with parameters like GGBS to fly ash (G/F), alkaline activator to binder ratio (A/B), and molarity (M) of NaOH solution of published works (table 4.1)

4.1.1 Effect of GGBS to fly ash ratio (G/F)

The investigations presented in Table 4.1, considered the GGBS to fly ash ratio as an important parameter affecting the strength of geopolymer concrete. It was observed from figures 4.1 (a), (d), (f), (g), (i), (j), (l), (m), and (o) that the strength of geopolymer concrete such as compressive strength, flexural and split tensile strength increased with increase in the GGBS to fly ash ratio (G/F) for constant alkaline activator to binder content ratio (A/B) and constant molarity. The variation in the strength of geopolymer concrete with GGBS to fly ash ratio was observed to be non-linear (Fig 4.1 (d), (f), (o)) at lower values of GGBS to fly ash ratio and became linear at higher values of GGBS to fly ash ratio. The rate of increase in the strength of geopolymer concrete was observed to be decreasing as GGBS to fly ash ratio increased (4.1 (d), (f), (g), (i)).

It was observed from figure 4.1 (d) that the compression and flexural strengths were compared with varying GGBS to fly ash ratio (G/F) for different molarities (6 to 12) and constant alkaline activator solution (A), binder content (B), alkaline to binder content ratio (A/B), fine aggregate to the coarse aggregate ratio (FA/CA) and sodium silicate to sodium hydroxide ratio SS/SH. It was observed that the rate of increase in the strengths was higher for GGBS to fly ash ratios less than 1.0 and later the rate of increase was reduced.

From figure 4.1 (f), it was observed the strengths increased with GGBS to fly ash ratios (G/F) for molarity of M = 12 and with other constant parameters. It was also observed that the rate of increase in the strengths was negligible compared to earlier observations. This may be due to low alkaline activation solution. The same can be seen from figure 4.1 (g) for molarity of M = 11 and 13 and figure 4.1 (j) for molarity of M=14 for constant binder content, alkaline activator, and alkaline solution to binder ratio.

From figure 4.1 (i) it was observed that the rate of increase in the strength decreased after GGBS to fly ash ratios of more than 1.0. Also it was observed that the alkaline activator solution

quantity was low when compared to binder quantity. However, there was reasonable growth in strength which was not the case in earlier observations, figures 4.1 (g) and 4.1 (j).

From figure 4.1 (k), it was observed that alkaline solution quantity varied from 136 to 171kg/cum, binder content quantity from 318 to 398 kg/cum with constant sodium silicate to sodium hydroxide of 1.22 and molarity of M = 10. It was observed that the strengths of geopolymer concrete increased with an increase in GGBS to fly ash ratio. It was also observed that an the increase in strength was attained with a low alkaline activator solution and a lower ratio of sodium silicate to sodium hydroxide.

It was observed from figure 4.1 (m) that the alkaline activator solution was varied from 162 to 270 kg/cum, binder quantity from 360 to 450 kg/cum, constant sodium silicate to sodium hydroxide ratio of 2.5, and molarity of NaOH solution to 8. From the figure, we can observe that compression strength increased with an increase in GGBS to fly ash ratio. It was also evident that there was an increase in compressive strength with an increase in alkaline activator solution to binder content ratio (0.45 to 0.60).

From figure 4.1 (o), the compressive strength increases with an increase in GGBS to fly ash ratio for geopolymer mortars. Also, the rate of increase in the strength of mortar is higher for the GGBS to fly ash ratios is less than 1.0, and later the rate increase is considerably reduced.

4.1.2 Effect of molarity (M) / concentration of sodium hydroxide (NaOH) solution

The molarity/concentration of NaOH solution for preparation of alkaline activator solution and considered by different investigators is another important parameter affecting the strength of geopolymer concrete. Form figure 4.1 (e) it can observe that compression and flexural strength of geopolymer concrete increased as the molarity of NaOH increased for different GGBS to fly ash ratio, varying from 0.25 to 2.34 for the same alkaline activator solution, binder quantity,

sodium silicate to sodium hydroxide ratio and alkaline activator solution to binder ratio. The same trend was reported in figure 4.1 (h) for strengths with varying molarity of NaOH solution.

It was observed from figure 4.1 (p) that the compressive strength increased with an increase in molarity of NaOH, for different GGBS to fly ash ratios for geopolymer mortars. However, the increase in strength was low when compared with geopolymer concrete (From figure 4.1 (e) and 4.1 (h)).

4.1.3 Effect of alkaline activator to binder ratio (A/B)

Some of the investigations presented in table 4.1, considered the alkaline to binder ratio as another important parameter affecting the strength of geopolymer concrete. It was observed from figure 4.1 (n), the compressive strength increased with an increase in alkaline activator solution to binder content ratio for different GGBS to fly ash ratios for constant molarity. From figure 4.1(n), it was observed that low alkaline activator solution to binder content ratio leads to low increase in strength of geopolymer concrete.

In keeping with the above discussion, the following facts are noted:

1) The strengths of geopolymer concrete were observed to increase with an increase in GGBS to fly ash (G/F) ratio for a particular molarity of activator used.
2) An increase in molarity/concentration of NaOH increases different strengths of geopolymer concrete.
3) It was also observed that an increase in alkaline activator composed of sodium hydroxide solution and sodium silicate solution, to binder ratio led to better strengths.
4) Several investigators conducted experimental investigation on geopolymer concrete considering different parameters in an isolated manner. Further, the results reported presented different strength of geopolymer concrete though parameters such as molarity while GGBS to fly ash was constant. No parameter was used that considers the

combined effect of different parameters identified on the strength of geopolymer concrete.

Given the above-listed facts based on analytical study, this investigation presents a new and unified parameter representing the combined effect of different parameters identified on the strength of fly ash and GGBS based geopolymer concrete.

4.2 UNIFIED PARAMETER

The major observations made in the analytical study are presented in section 4.1: the observations claim that increase in strength of geopolymer concrete occurs with increase in molarity of sodium hydroxide solution, alkaline activator to binder ratio, and GGBS to fly ash ratio. Considering the important parameters such as molarity (M) of sodium hydroxide solution, alkaline activator (A) solution to binder quantity (B = F + G), and GGBS to fly ash (G/F) ratio, the following new parameter termed **'Binder Index (Bi)'** was proposed based on phenomenological behavior of geopolymer concrete by grouping all parameters thus:

$$\boldsymbol{Bi} = \frac{\boldsymbol{MA}}{\boldsymbol{G}+\boldsymbol{F}}\left[\frac{\boldsymbol{G}}{\boldsymbol{F}}\right] \qquad \text{- Eq. 4.1}$$

Where, M = molarity of NaOH, A = alkaline activator (both NaOH and Na_2SiO_3 together) content, G = GGBS content, F = fly ash content.

The 'Binder Index (Bi)' was calculated using geopolymer concrete mix proportions adopted by different investigators and is tabulated in table 4.1. The effect of the above proposed 'Binder index' on the strengths of geopolymer concrete reported by different investigators is shown in figure 4.2. The best-fit equation for the variation of the strength of geopolymer concrete with binder index and the corresponding coefficient of correlation (R^2) value obtained are given in table 4.2. This proposed equation is valid for GGBS and fly ash geopolymer concrete only.

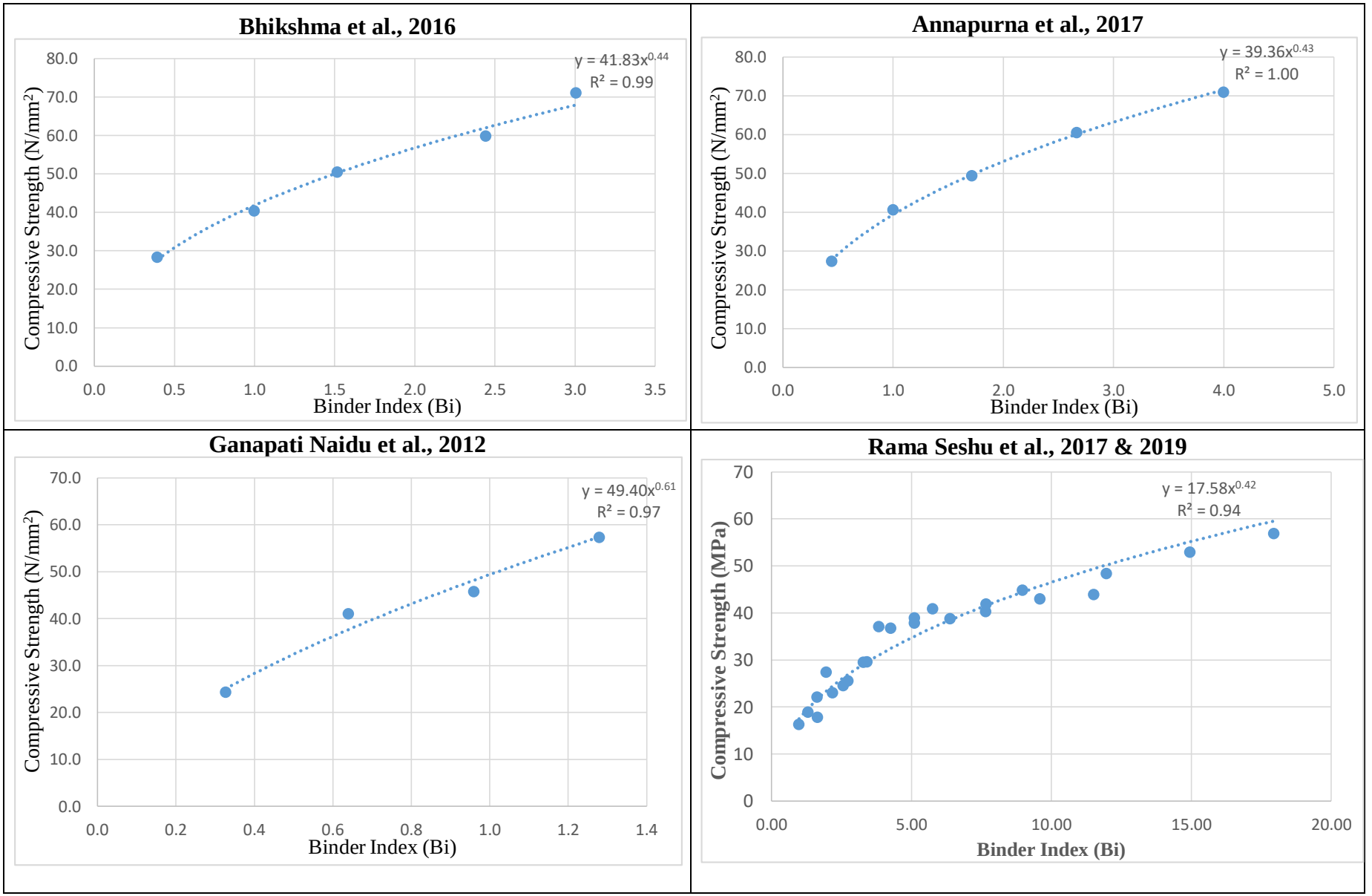
Bhikshma et al., 2016
y = 41.83x^0.44
R² = 0.99
Compressive Strength (N/mm²)
Binder Index (Bi)
Annapurna et al., 2017
y = 39.36x^0.43
R² = 1.00
Compressive Strength (N/mm²)
Binder Index (Bi)
Ganapati Naidu et al., 2012
y = 49.40x^0.61
R² = 0.97
Compressive Strength (N/mm²)
Binder Index (Bi)
Rama Seshu et al., 2017 & 2019
y = 17.58x^0.42
R² = 0.94
Compressive Strength (MPa)
Binder Index (Bi)

Rajagopalan Gopalakrishnan et al., 2019

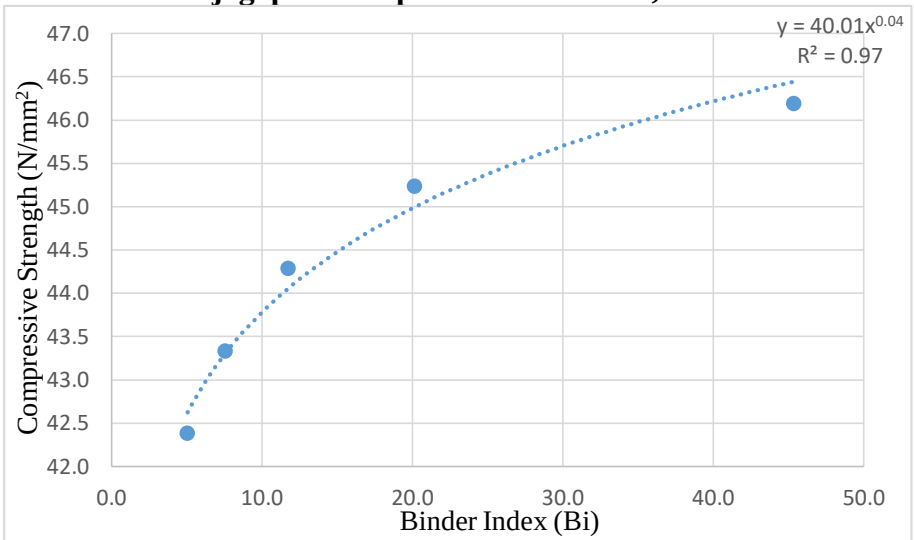

Zende et al., 2015

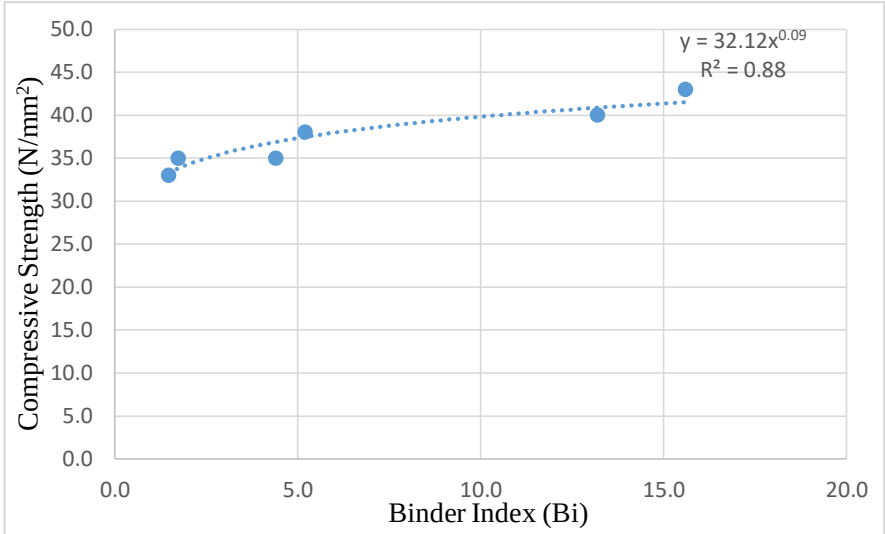

Rajini et al., 2014

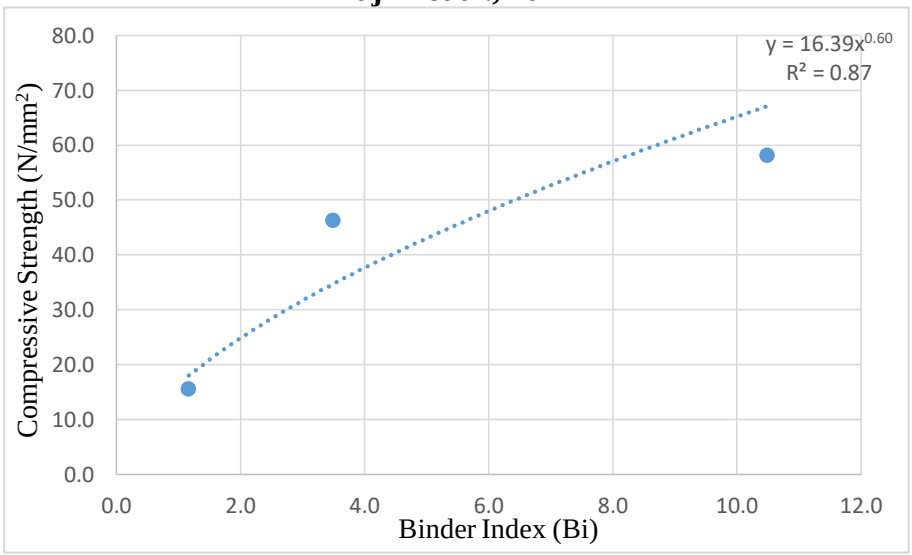

Krishnaraja et al., 2014

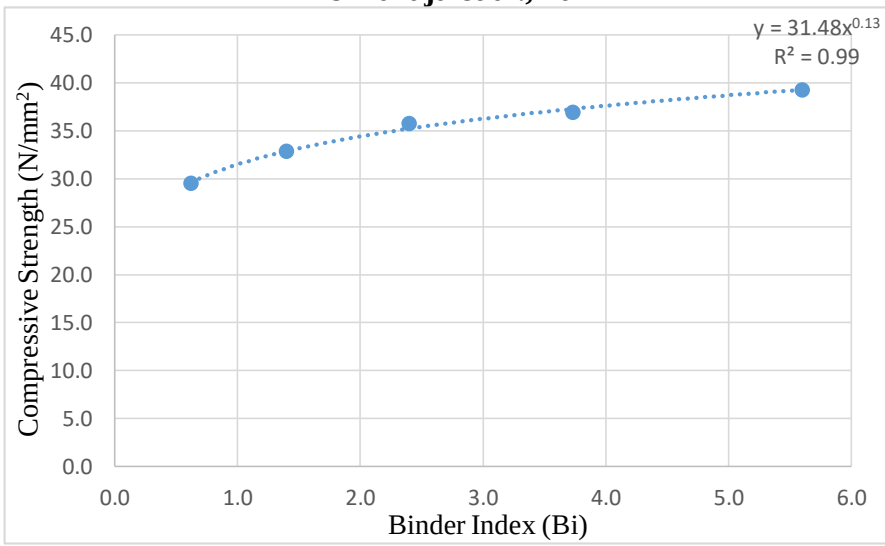

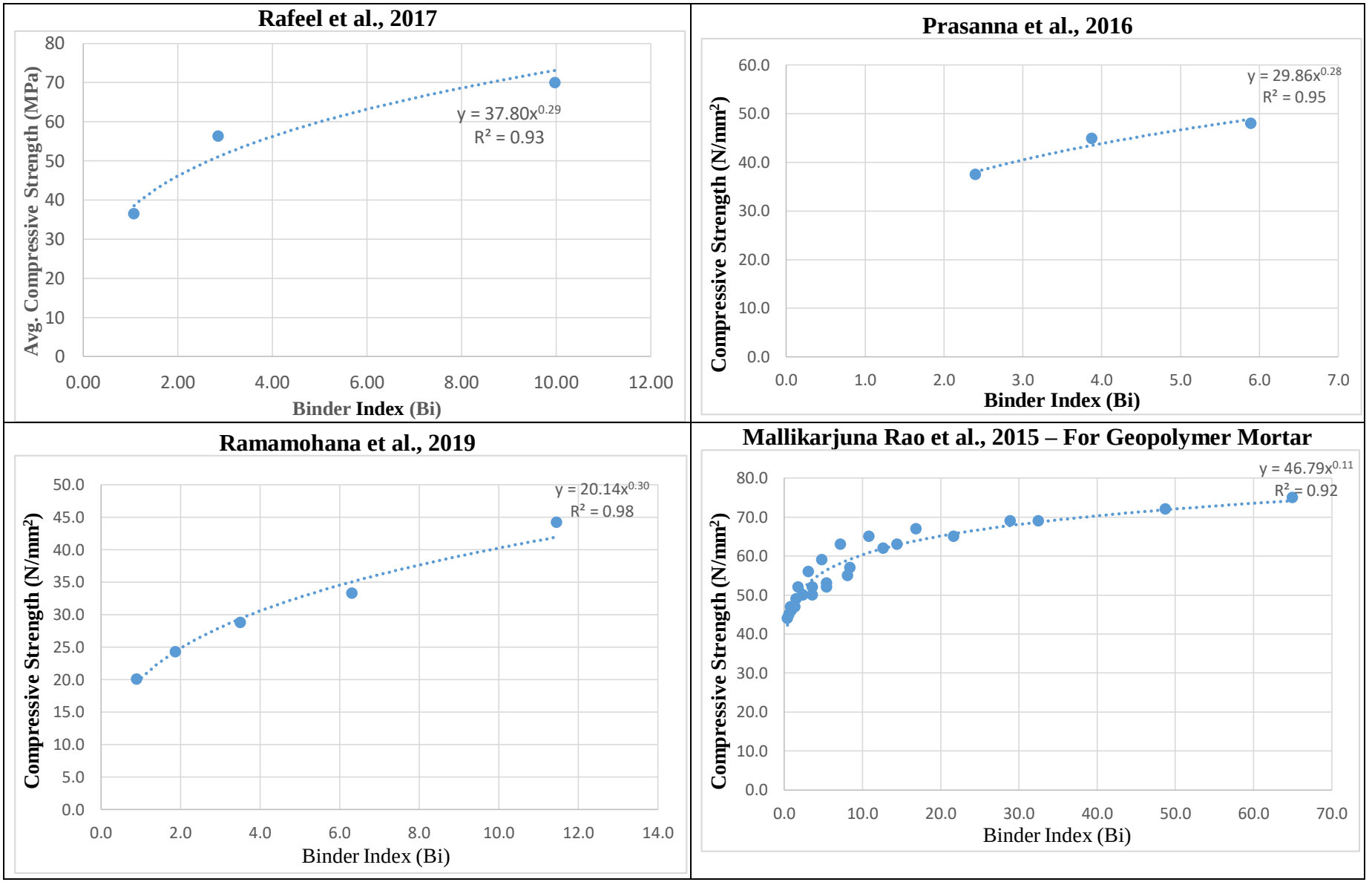
Rafeel et al., 2017
Avg. Compressive Strength (MPa)
y = 37.80x^0.29
R² = 0.93
Binder Index (Bi)
Prasanna et al., 2016
Compressive Strength (N/mm²)
y = 29.86x^0.28
R² = 0.95
Binder Index (Bi)
Ramamohana et al., 2019
Compressive Strength (N/mm²)
y = 20.14x^0.30
R² = 0.98
Binder Index (Bi)
Mallikarjuna Rao et al., 2015 – For Geopolymer Mortar
Compressive Strength (N/mm²)
y = 46.79x^0.11
R² = 0.92
Binder Index (Bi)

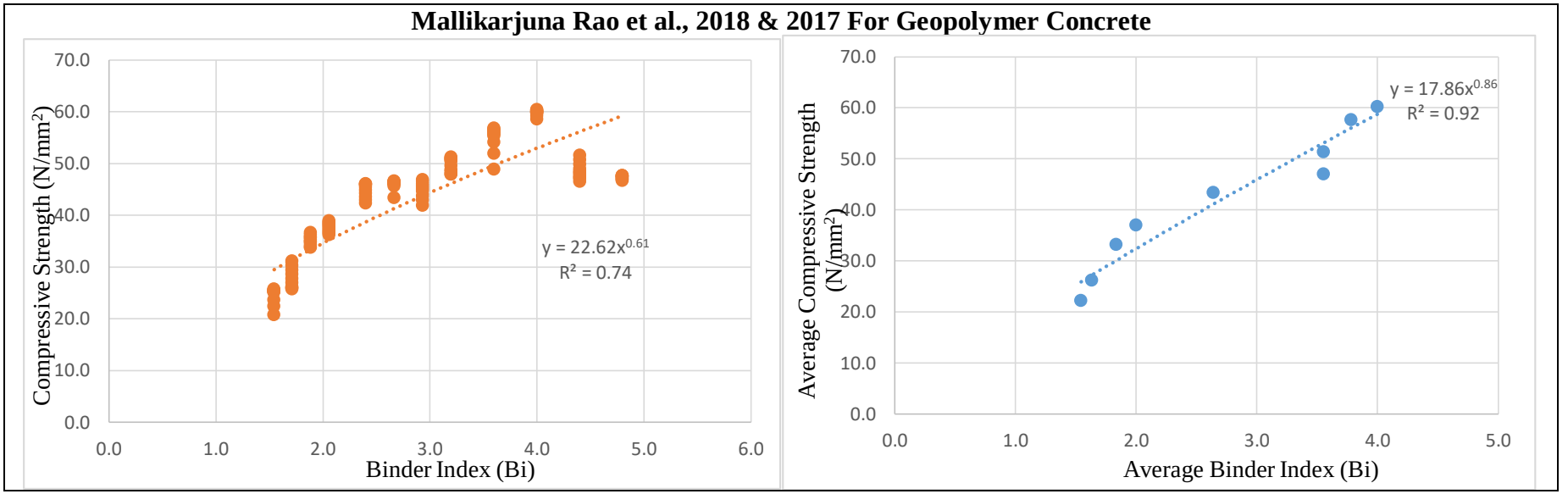

Figure 4.2 (a): Variation of compressive strength of GPC (f_{gpc}) with the proposed Binder index (Bi) for the mix proportions reported in Table 4.1

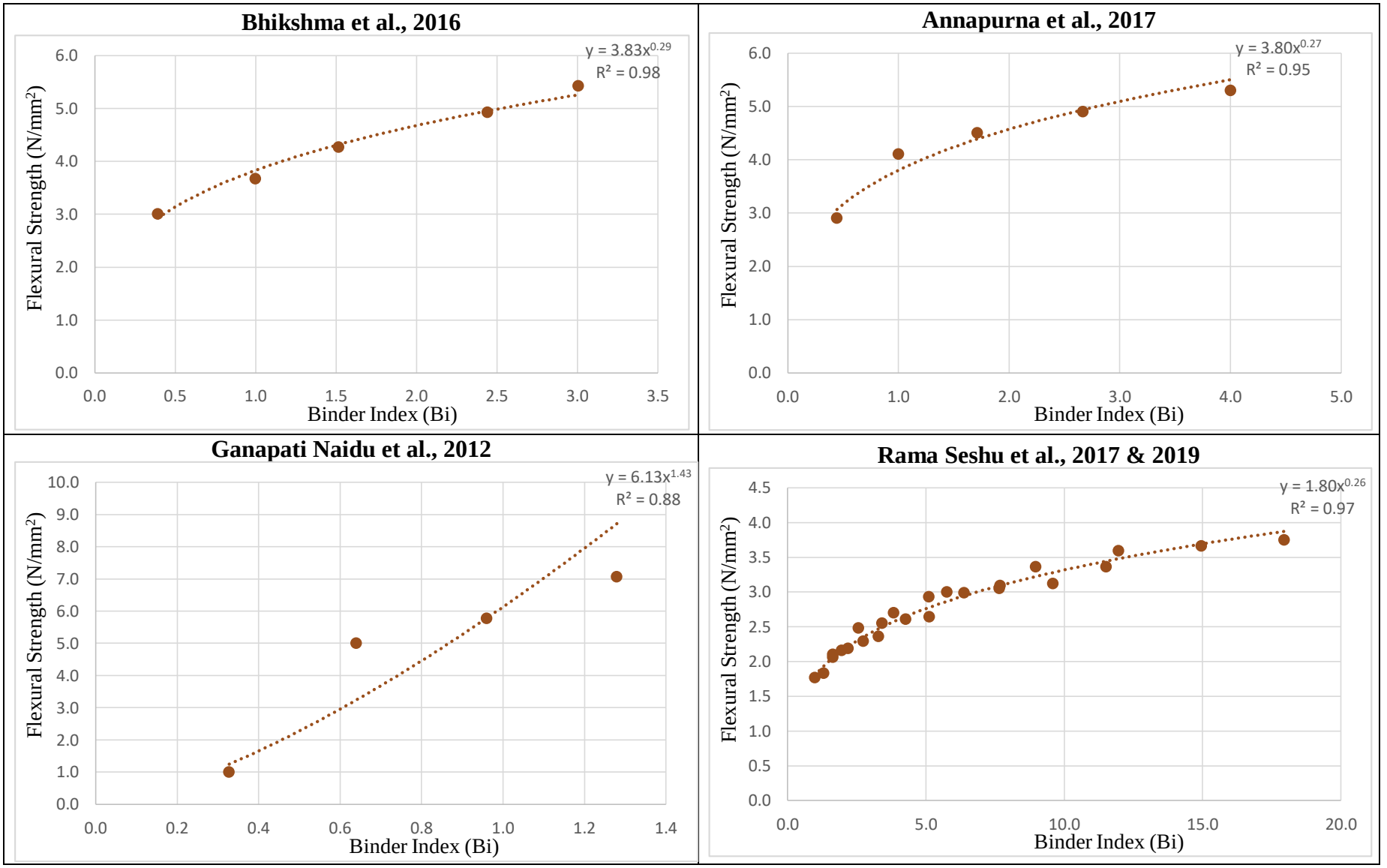
Bhikshma et al., 2016
y = 3.83x^0.29
R² = 0.98
Flexural Strength (N/mm²)
Binder Index (Bi)
Annapurna et al., 2017
y = 3.80x^0.27
R² = 0.95
Flexural Strength (N/mm²)
Binder Index (Bi)
Ganapati Naidu et al., 2012
y = 6.13x^1.43
R² = 0.88
Flexural Strength (N/mm²)
Binder Index (Bi)
Rama Seshu et al., 2017 & 2019
y = 1.80x^0.26
R² = 0.97
Flexural Strength (N/mm²)
Binder Index (Bi)

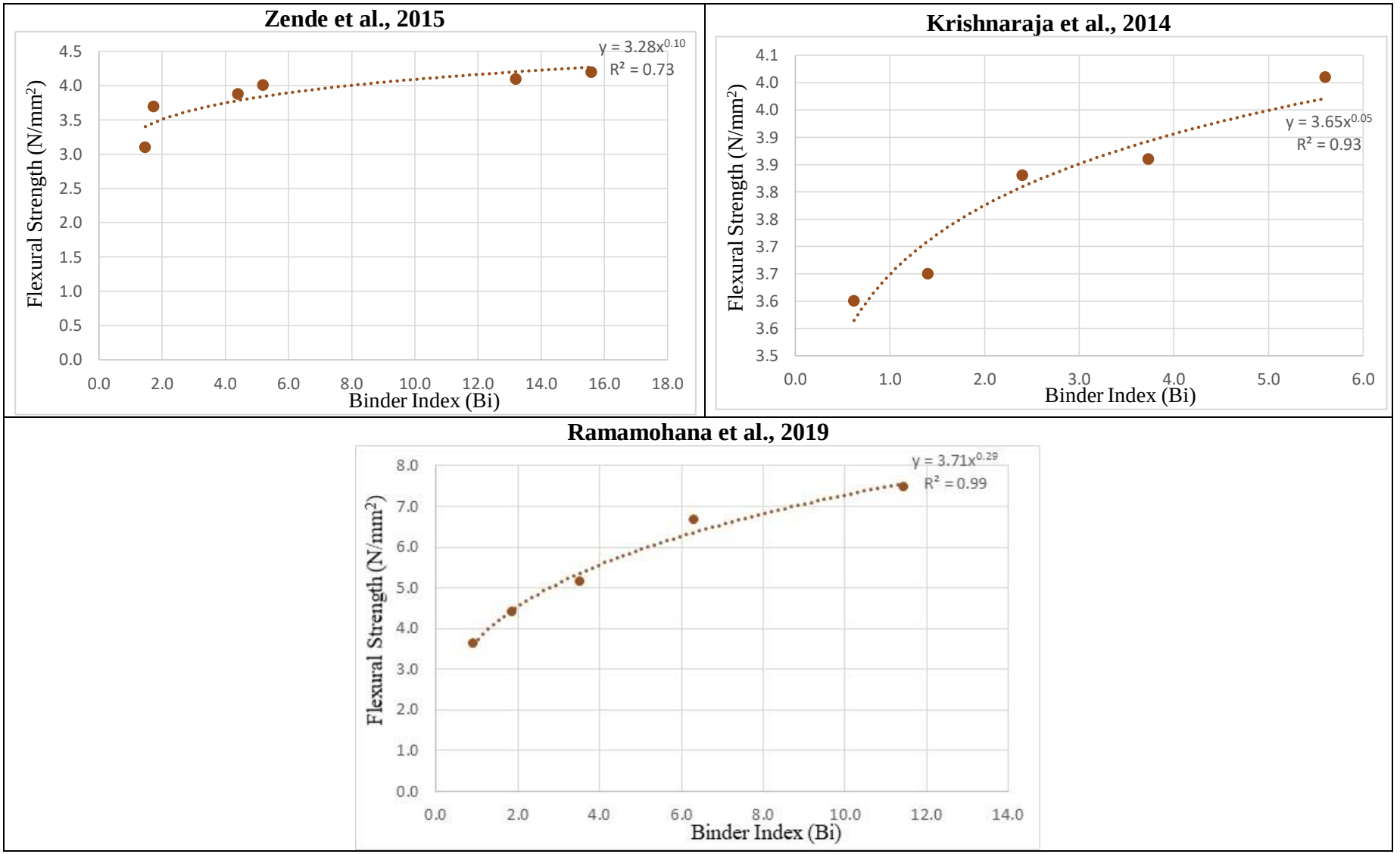

Figure 4.2 (b): Variation of flexural strength of GPC (f_{cr}) with the proposed Binder index (Bi) for the mix proportions reported in Table 4.1

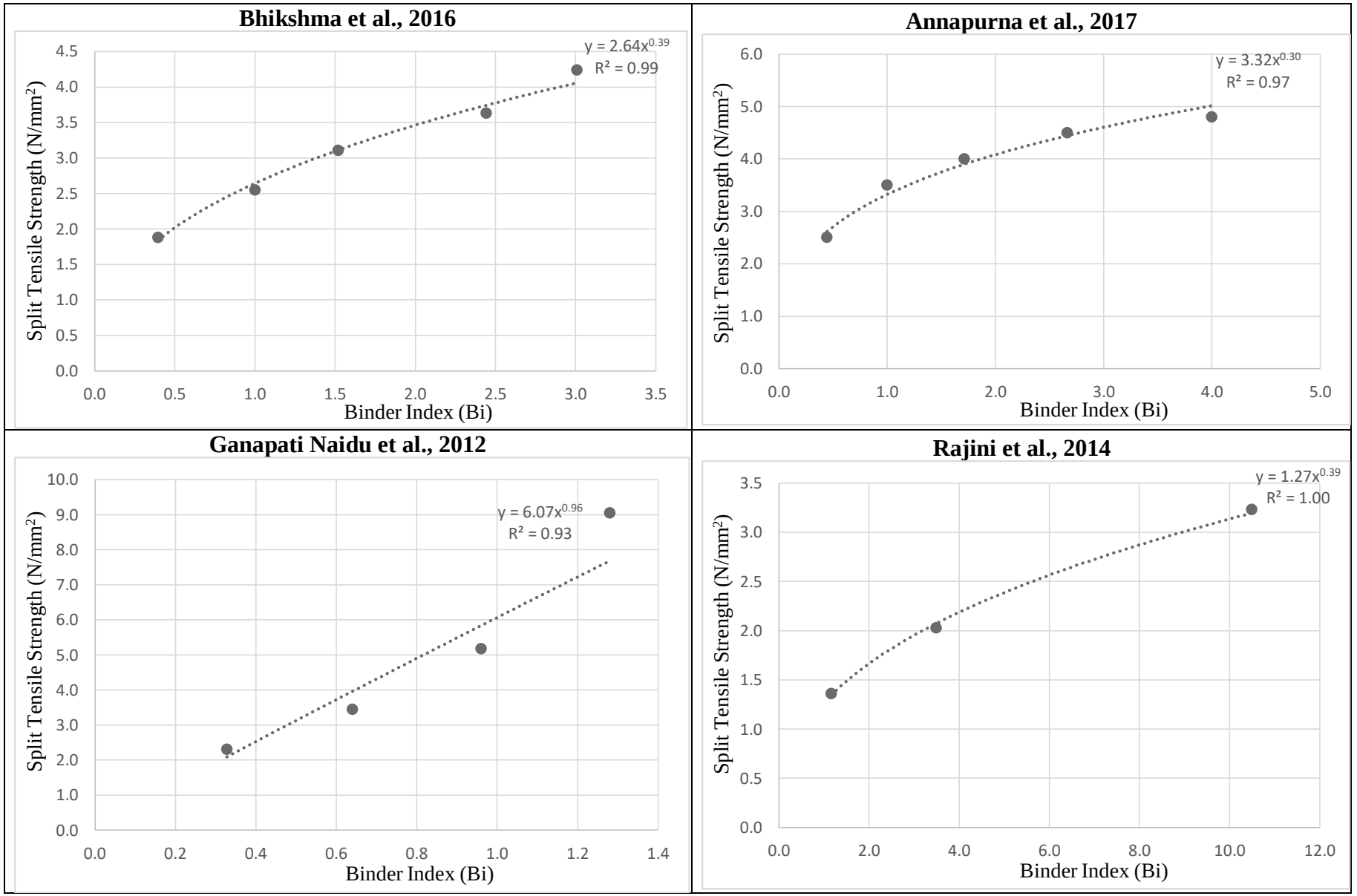
Bhikshma et al., 2016
y = 2.64x^0.39
R² = 0.99
Split Tensile Strength (N/mm²)
Binder Index (Bi)
Annapurna et al., 2017
y = 3.32x^0.30
R² = 0.97
Split Tensile Strength (N/mm²)
Binder Index (Bi)
Ganapati Naidu et al., 2012
y = 6.07x^0.96
R² = 0.93
Split Tensile Strength (N/mm²)
Binder Index (Bi)
Rajini et al., 2014
y = 1.27x^0.39
R² = 1.00
Split Tensile Strength (N/mm²)
Binder Index (Bi)

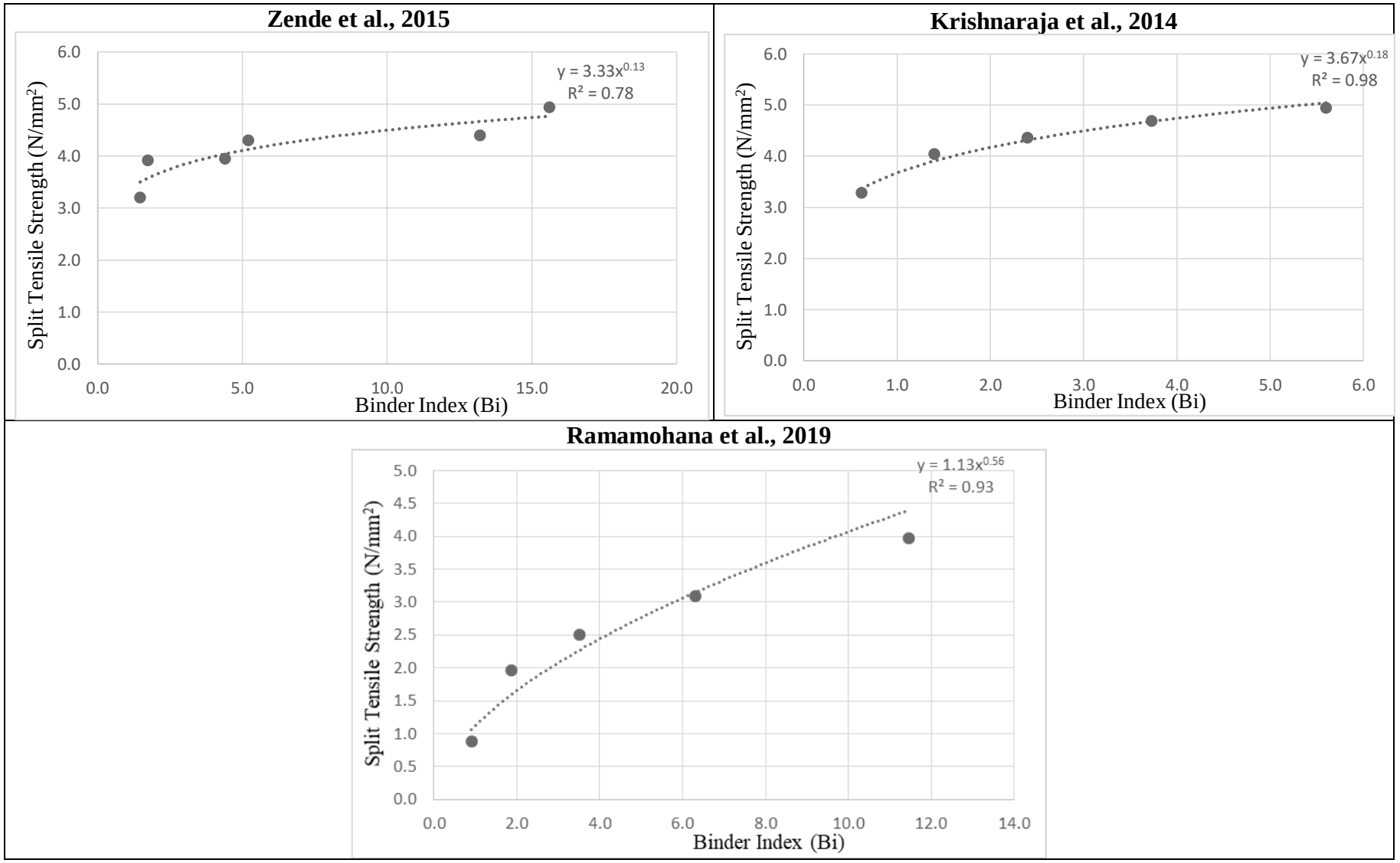

Figure 4.2 (c): Variation of split tensile strength of GPC (f_{st}) with the proposed Binder index (Bi) for the mix proportions reported in Table 4.1

Table 4.2: The best fit equation and corresponding correlation coefficient (R^2) value obtained for the compressive strength test results of GPC mixes reported by different investigators.

Investigator (s)	Equation	R^2
Bhikshma et al., 2016	$f_{gpc} = 41.83\ Bi^{0.44}$	$R^2 = 0.99$
Annapurna et al., 2017	$f_{gpc} = 39.36\ Bi^{0.43}$	$R^2 = 1.00$
Ganapati Naidu et al., 2012	$f_{gpc} = 49.40\ Bi^{0.61}$	$R^2 = 0.97$
Rama Seshu et al., 2017 & 2019	$f_{gpc} = 17.58\ Bi^{0.42}$	$R^2 = 0.94$
Rajagopalan Gopalakrishnan et al., 2019	$f_{gpc} = 40.01\ Bi^{0.04}$	$R^2 = 0.97$
Zende et al., 2015	$f_{gpc} = 32.12\ Bi^{0.09}$	$R^2 = 0.88$
Rajini et al., 2014	$f_{gpc} = 16.39\ Bi^{0.60}$	$R^2 = 0.87$
Krishnaraja et al., 2014	$f_{gpc} = 31.48\ Bi^{0.13}$	$R^2 = 0.99$
Rafeel et al., 2017	$f_{gpc} = 37.80\ Bi^{0.29}$	$R^2 = 0.93$
Prasanna et al., 2016	$f_{gpc} = 29.86\ Bi^{0.28}$	$R^2 = 0.95$
Ramamohana et al., 2019	$f_{gpc} = 20.14\ Bi^{0.30}$	$R^2 = 0.98$
Mallikarjuna Rao et al., 2018 & 2017	$f_{gpc} = 17.86\ Bi^{0.86}$	$R^2 = 0.92$
Mallikarjuna Rao et al., 2015 – For Geopolymer Mortar	$f_{gpc} = 46.79\ Bi^{0.11}$	$R^2 = 0.92$

It is observed from figure 4.2, that there is an increase in compressive strength of GPC with an increase in binder index. Further, the increase in strength is non-linear in proportion to the increase in binder index. The observed variation of compressive strength of GPC (f_{gpc}) with binder index (Bi) indicates that the proposed form of binder index which combines the effects of molarity of NaOH, alkaline to binder ratios, and GGBS to fly ash ratio, can be considered a single parameter influencing the compressive strength of geopolymer concrete mixes.

Hence the variation of compressive strength of geopolymer concrete (f_{gpc}) with binder index (Bi) can be represented by a simple power equation of the following form:

$$\mathbf{f_{gpc} = N[Bi]^{L}} \qquad \text{- Eq. 4.2}$$

Where N and L are constants.

The above form of the equation could be the basis for the initial estimation of strength in the mix design of geopolymer concrete. The non-linear relation proposed for GPCas above is similar to the variation of strength of ordinary concrete with its water to cement ratio following by Abram's law. However, the difference in the strength variation relation between GPC and ordinary concrete is that in geopolymer concrete the strength increases with an increase in

binder index whereas in ordinary concrete, the strength decreases with an increase in water to cement ratio.

4.3 PHENOMENOLOGICAL MODEL

A phenomenological model is a model that can be used to test several combinations of parameters within the framework of basic scientific laws. The use of the phenomenological model requires experimental input from a single trial to account for interactions between various constituents of a given set of materials. If any parameter changes concerning a set of ingredients, new inputs must be generated again to use the phenomenological model to arrive at appropriate proportions /properties of the mixture to meet specific requirements. This is similar to adjusting the trial mix until the specified requirements are met. Instead of repeated laboratory tests, the desired results can be achieved by simple calculations by introducing an experimentally determined reference strength value in a phenomenological model.

This quick exercise has the added potential of identifying parameters that will result in a wide range of mixes that have strengths in the desired range for a given set of materials. Now it is proposed to formulate a phenomenological model for assessing the development of compressive strength geopolymer concrete for various binder indexes. The compressive strength of geopolymer concrete reported by different investigators and the corresponding binder index listed in table 4.1 is considered for proposing the phenomenological model for geopolymer concrete. All geopolymer concrete compressive strengths are rearranged in increasing order of binder index and tabulated in table 4.3. In this study, the compressive strength at a binder index of 5.41 is considered as a reference for normalizing the corresponding compressive strengths. The chosen binder index value is purely arbitrary and is a matter of convenience. Geopolymer concrete compressive strengths tabulated in table 4.3 are normalized vis-à-vis geopolymer concrete compressive strength at a binder index of 5.41. Accordingly, the

strength ratio has been obtained by dividing geopolymer concrete strength values for different binder indexes, by the reference strength, which is taken as the strength corresponding to the binder index of 5.41, i.e. 52 N/mm^2. The strength ratios (SR) for different binder indexes of geopolymer concrete are shown in table 4.3.

Table 4.3. Data for Phenomenological model

Bi	f_{gpc}	SR	Bi	f_{gpc}	SR	Bi	f_{gpc}	SR	Bi	f_{gpc}	SR
0.33	24.29	0.47	1.89	26.01	0.50	2.93	45.75	0.88	4.80	46.68	0.90
0.39	28.33	0.54	1.89	30.27	0.58	2.93	45.38	0.87	4.80	46.84	0.90
0.40	44.00	0.85	1.89	29.43	0.57	2.93	45.02	0.87	4.80	46.98	0.90
0.44	27.30	0.53	1.89	26.95	0.52	2.93	44.67	0.86	4.80	47.13	0.91
0.60	45.00	0.87	1.89	26.17	0.50	2.93	43.71	0.84	4.80	47.28	0.91
0.62	29.52	0.57	1.89	25.88	0.50	2.93	42.91	0.83	4.80	47.43	0.91
0.64	41.04	0.79	1.89	25.71	0.49	2.93	41.85	0.80	4.80	47.57	0.91
0.80	47.00	0.90	1.89	31.11	0.60	3.01	71.07	1.37	4.80	47.59	0.92
0.90	20.00	0.38	1.96	27.40	0.53	3.09	56.00	1.08	4.80	47.61	0.92
0.90	46.00	0.88	2.06	25.60	0.49	3.20	43.38	0.83	4.80	47.64	0.92
0.96	45.76	0.88	2.06	25.50	0.49	3.20	46.20	0.89	4.81	59.00	1.13
0.98	16.30	0.31	2.06	25.40	0.49	3.20	46.27	0.89	5.04	42.38	0.82
1.00	40.40	0.78	2.06	25.30	0.49	3.20	46.35	0.89	5.11	37.80	0.73
1.00	40.50	0.78	2.06	25.20	0.48	3.20	46.42	0.89	5.12	38.90	0.75
1.06	31.40	0.60	2.06	25.11	0.48	3.20	46.50	0.89	5.20	38.00	0.73
1.06	37.67	0.72	2.06	23.62	0.45	3.20	46.57	0.90	**5.41**	**52.00**	**1.00**
1.07	35.58	0.68	2.06	22.40	0.43	3.20	46.27	0.89	5.41	53.00	1.02
1.07	40.81	0.78	2.06	20.76	0.40	3.20	46.01	0.88	5.60	39.23	0.75
1.07	39.77	0.76	2.06	25.71	0.49	3.20	45.68	0.88	5.76	40.90	0.79
1.07	35.06	0.67	2.19	23.00	0.44	3.28	29.50	0.57	5.89	48.00	0.92
1.07	38.72	0.74	2.32	50.00	0.96	3.41	29.60	0.57	6.31	33.25	0.64
1.07	40.81	0.78	2.40	35.73	0.69	3.50	46.32	0.89	6.38	38.80	0.75
1.07	31.40	0.60	2.40	42.32	0.81	3.51	28.75	0.55	7.22	63.00	1.21
1.07	38.20	0.73	2.40	42.95	0.83	3.60	55.37	1.06	7.56	43.33	0.83
1.07	31.92	0.61	2.40	43.58	0.84	3.60	55.62	1.07	7.66	40.30	0.78
1.17	15.55	0.30	2.40	44.21	0.85	3.60	55.85	1.07	7.68	41.90	0.81
1.28	57.33	1.10	2.40	44.85	0.86	3.60	56.11	1.08	8.12	55.00	1.06
1.30	18.90	0.36	2.40	45.48	0.87	3.60	56.36	1.08	8.42	57.00	1.10
1.35	47.00	0.90	2.40	46.08	0.89	3.60	56.62	1.09	8.98	44.80	0.86
1.40	32.86	0.63	2.40	46.01	0.88	3.60	56.86	1.09	9.59	43.00	0.83
1.47	33.00	0.63	2.40	45.96	0.88	3.60	54.14	1.04	9.89	68.02	1.31
1.52	50.46	0.97	2.40	45.88	0.88	3.60	51.90	1.00	9.90	71.16	1.37
1.54	34.31	0.66	2.40	37.50	0.72	3.60	48.91	0.94	9.98	72.21	1.39
1.54	34.79	0.67	2.41	50.00	0.96	3.61	50.00	0.96	9.98	69.07	1.33

Bi	f_{gpc}	SR	Bi	f_{gpc}	SR	Bi	f_{gpc}	SR	Bi	f_{gpc}	SR
1.54	35.27	0.68	2.44	59.90	1.15	3.61	52.00	1.00	9.99	74.30	1.43
1.54	35.76	0.69	2.56	24.50	0.47	3.73	36.93	0.71	9.99	69.07	1.33
1.54	34.89	0.67	2.67	49.59	0.95	3.83	37.10	0.71	10.00	64.88	1.25
1.54	33.81	0.65	2.67	60.40	1.16	3.88	44.90	0.86	10.04	63.84	1.23
1.54	33.83	0.65	2.67	47.92	0.92	4.00	70.80	1.36	10.04	77.44	1.49
1.54	36.24	0.70	2.67	48.47	0.93	4.00	59.79	1.15	10.48	58.12	1.12
1.54	36.69	0.71	2.67	47.91	0.92	4.00	59.88	1.15	10.83	65.00	1.25
1.54	35.70	0.69	2.67	48.75	0.94	4.00	59.98	1.15	11.46	44.16	0.85
1.55	49.00	0.94	2.67	50.43	0.97	4.00	60.08	1.16	11.51	43.90	0.84
1.63	22.10	0.43	2.67	51.22	0.99	4.00	60.18	1.16	11.76	44.29	0.85
1.64	17.80	0.34	2.67	51.04	0.98	4.00	60.28	1.16	11.97	48.40	0.93
1.71	38.96	0.75	2.67	50.89	0.98	4.00	60.38	1.16	12.64	62.00	1.19
1.71	49.30	0.95	2.67	50.69	0.97	4.00	59.75	1.15	13.20	40.00	0.77
1.71	36.52	0.70	2.73	25.50	0.49	4.00	59.23	1.14	14.44	63.00	1.21
1.71	37.18	0.72	2.85	56.25	1.08	4.00	58.53	1.13	14.96	52.90	1.02
1.71	37.52	0.72	2.85	57.38	1.10	4.26	36.70	0.71	15.60	43.00	0.83
1.71	37.85	0.73	2.85	57.38	1.10	4.40	35.00	0.67	16.85	67.00	1.29
1.71	38.16	0.73	2.85	60.75	1.17	4.40	51.61	0.99	17.95	56.90	1.09
1.71	38.43	0.74	2.85	55.13	1.06	4.40	50.73	0.98	20.16	45.24	0.87
1.71	38.66	0.74	2.86	60.19	1.16	4.40	49.86	0.96	21.66	65.00	1.25
1.71	36.19	0.70	2.86	50.63	0.97	4.40	49.00	0.94	28.88	69.00	1.33
1.71	36.85	0.71	2.87	55.13	1.06	4.40	48.14	0.93	32.49	69.00	1.33
1.73	35.00	0.67	2.87	54.00	1.04	4.40	47.28	0.91	45.36	46.19	0.89
1.81	52.00	1.00	2.87	56.25	1.08	4.40	46.48	0.89	48.74	72.00	1.38
1.87	24.23	0.47	2.93	46.87	0.90	4.40	47.15	0.91	64.98	75.00	1.44
1.89	28.60	0.55	2.93	46.49	0.89	4.40	47.71	0.92			
1.89	27.77	0.53	2.93	46.12	0.89	4.40	48.45	0.93			

The variation of strength ratio with binder index, in general, is shown in figure 4.3 (a). The variation of strength ratio with binder index (up to 10) is shown in figure 4.3 (b). The variation of strength ratio with binder index (>10) is shown in figure 4.3 (c). The best-fit equation between the strength ratio ($\frac{f_{gpc}}{f_{gpc,5.41}}$) and binder index (Bi) is as follows:

For Binder Index Bi ≤ 10, $\frac{f_{gpc}}{f_{gpc,5.41}} = 0.63\ Bi^{0.25}$ - Eq. 4.3

For Binder Index Bi > 10, $\frac{f_{gpc}}{f_{gpc,5.41}} = 0.81\ Bi^{0.10}$ - Eq. 4.4

Where f_{gpc} is the compressive strength for any specified Binder Index and $f_{gpc,\ 5.41}$ is the reference strength and is equal to experimentally evaluated geopolymer concrete compressive strength for a binder index of 5.41.

To use this relation for a given set of materials, initially, the compressive strength needs to be determined experimentally for a binder index of 5.41. Using this as an input, the compressive strength of geopolymer concrete for any other binder index can be determined using the best-fit equations given above as part of the phenomenological model. Thus, the model will be useful in reducing the number of trial mixes required.

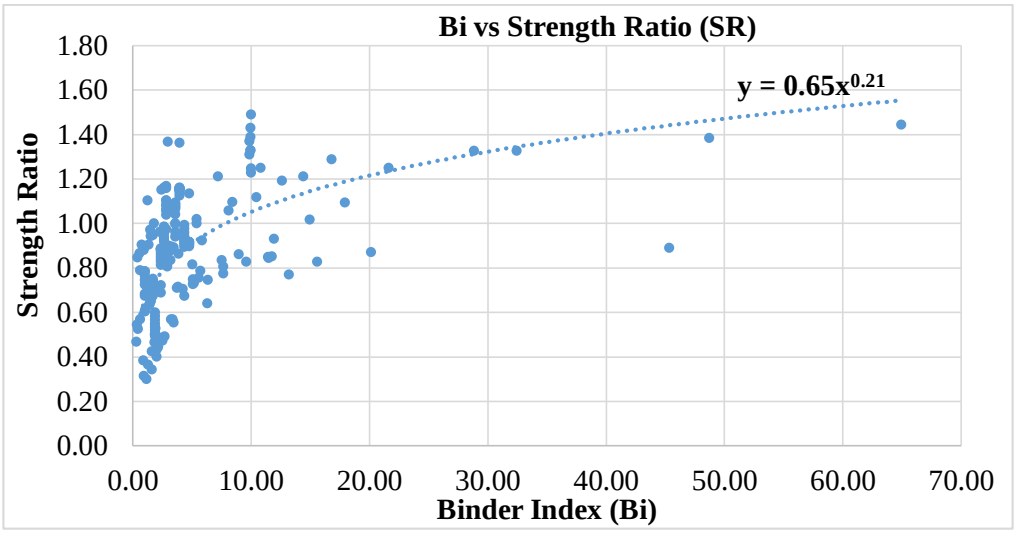

Figure 4.3 (a) Variation between Binder index (Bi) vs. Strength ratio for mix proportions shown in Table 4.1

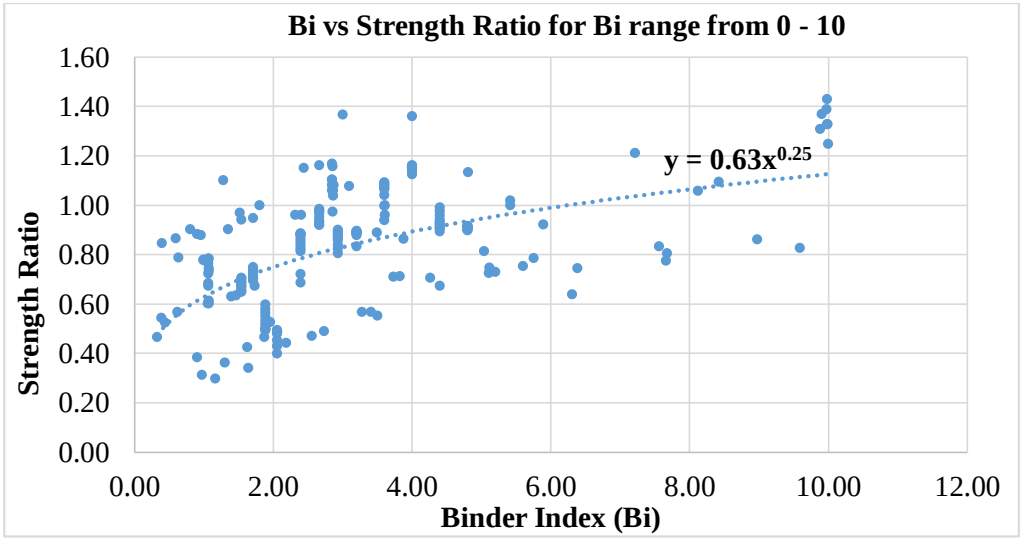

Figure 4.3 (b) Variation between Binder index (Bi) vs. Strength ratio for mix proportions of Binder Index range from 0 – 10 from Table 4.1

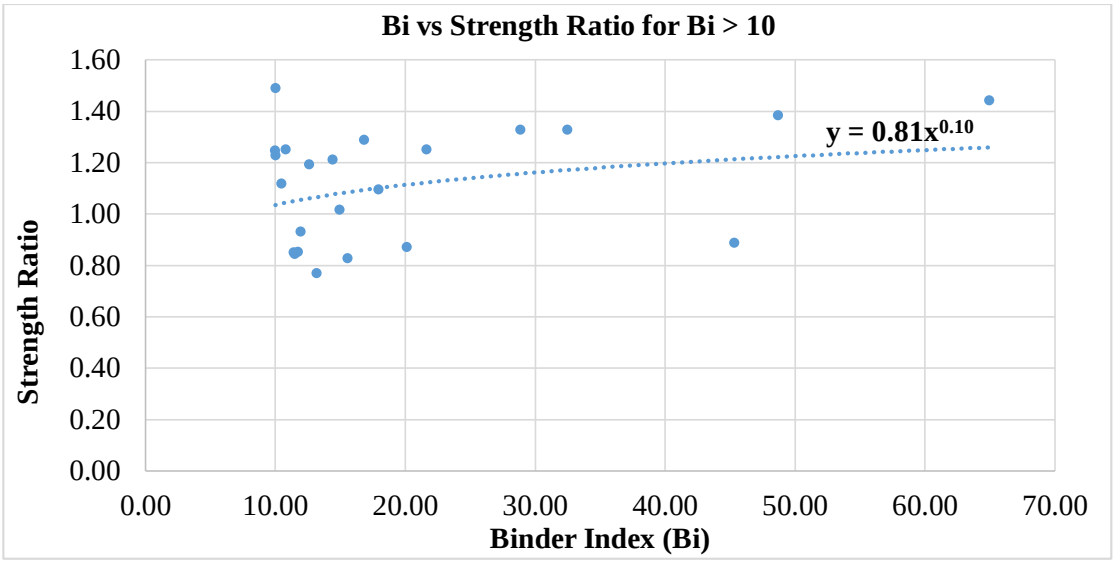

Figure 4.3 (c) Variation between Binder index (Bi) vs. Strength ratio for mix proportions of Binder Index range greater than 10 from Table 4.1

Figure 4.3 Variation between Binder index (Bi) vs. Strength ratio

To further validate the proposed new parameter "Binder Index (Bi)" of geopolymer concrete and phenomenological model proposed, an experimental study was conducted and is detailed in the following section.

4.4 EXPERIMENTAL PROCEDURE

The objective of this experimental investigation was to validate the proposed unified parameter 'Binder Index (BI)' establish its influence on the strengths of geopolymer concrete and validate the phenomenological model. The binder index of each of the considered geopolymer concrete mix was varied by varying the alkaline activator to binder content ratio, GGBS to fly ash ratio, and the molarity of NaOH solution.

The experimental program consisted of casting and testing cubes of size 150 mm x 150 mm x 150 mm and prisms of size 100 mm x 100 mm x 400 mm for determining the compressive strength and flexural strength i.e., modulus of rupture (tensile strength in bending) of fly ash and GGBS based geopolymer concrete. Figure 4.4 gives the flow chart of the experimental program conducted on geopolymer concrete.

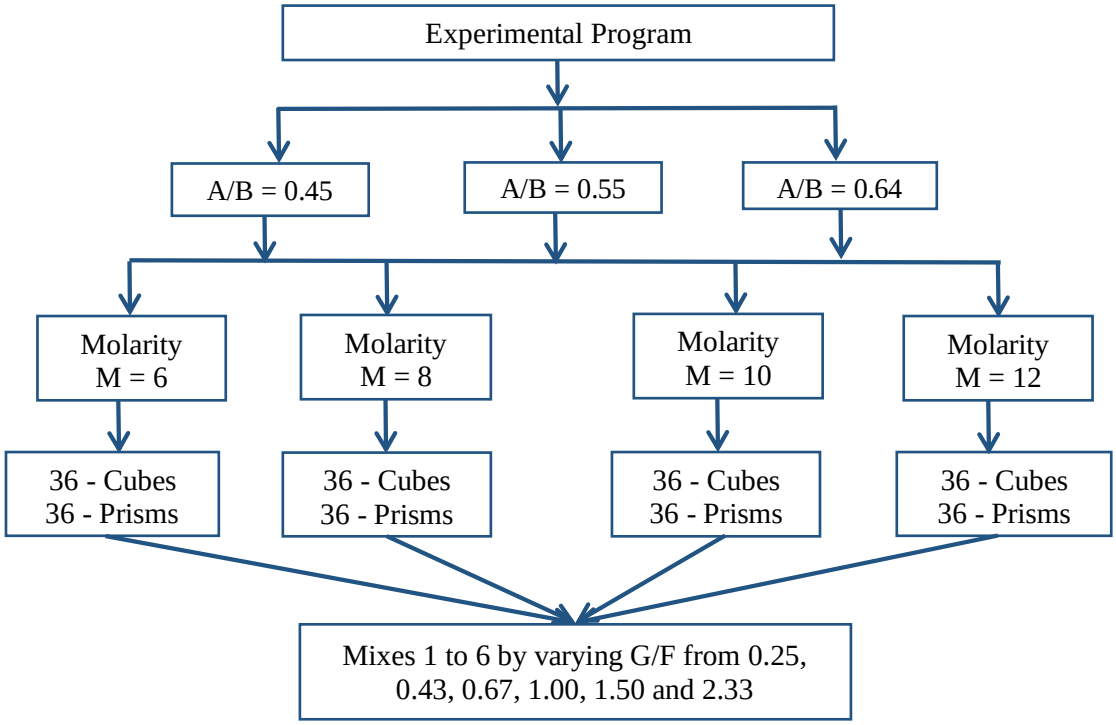

Figure 4.4 Schematic diagram of the experimental program

4.5 DETAILS OF MATERIALS USED IN THE STUDY

4.5.1 Fly ash and GGBS

Fly ash and **GGBS** were used as binders and these were obtained from NTPC Ramagundam thermal power plant, Ramagundam, India, and JSW Cements Pvt ltd, Bilakalagudur, India with a specific gravity of 2.17 and 2.90 respectively. Table 4.4, shows the details of chemical compositions of the binders.

Table 4.4: Chemical composition of fly ash and GGBS (% by mass)

Binder Material	SiO_2	Al_2O_3	Fe_2O_3	SO_3	CaO	MgO	Na_2O	LOI
Fly ash	60.11	26.53	4.25	0.35	4.00	1.25	0.22	0.88
GGBS	37.73	14.42	1.11	0.39	37.34	8.71	--	1.41

4.5.2 Aggregates

River sand conforming to Zone-II of IS: 383, 2016 was used as fine aggregate. The specific gravity and bulk density of sand are 2.65 & 1.45 g/cm^3 respectively. Well-graded aggregate conforming to IS: 383, 2016 with 20 mm nominal size of granite was used as coarse aggregate of 2.80 and 1.5 g/cm^3 with specific gravity and bulk density respectively.

4.5.3 Alkaline activator solution

A combination of sodium hydroxide and sodium silicate solutions was used to form an alkaline activator solution. Sodium hydroxide in the form of pellets with 98% purify was used for the study. Sodium hydroxide pellets were dissolved in portable water to prepare solutions of different molarity (M = 6, 8, 10, and 12). After cooling, sodium hydroxide solution was mixed with sodium silicate in the form of liquid with a mixing ratio of 1:2.5, and the prepared alkaline activator solution thus prepared was stored at an ambient temperature for 24 hrs. at a relative humidity of 65 - 75% before using it in the casting of geopolymer concrete specimens.

4.5.4 Superplasticizer

Sulphonate naphthalene polymers (Conplast SP 430 Fosroc make) based superplasticizer was used.

4.6 MIX PROPORTIONS

The geopolymer concrete mix proportions adopted in the study are shown in table 4.5. These mixes were designed to facilitate the study of the effect of various parameters on fly ash and GGBS based geopolymer concrete. Molarity of sodium hydroxide varied from 6M, 8M, 10M, and 12M, while sodium silicate to sodium hydroxide ratio was fixed at 2.5.

Table 4.5: Mix proportions of geopolymer concrete

A / B	G / F	Fly ash (kg/m^3) (F)	GGBS (kg/m^3) (G)	Coarse Aggregate (kg/m^3)	Fine Aggregate (kg/m^3)	NaOH (kg/m^3)	Na_2SiO_3 (kg/m^3)	Alkaline liquid (kg/m^3) (A)
0.64	0.25	354.80	90.40	813.56	596.61	81.36	203.39	284.75
	0.43	311.86	133.33	813.56	596.61	81.36	203.39	284.75
	0.67	267.12	178.08	813.56	596.61	81.36	203.39	284.75
	1.00	222.82	222.37	813.56	596.61	81.36	203.39	284.75
	1.50	178.08	267.12	813.56	596.61	81.36	203.39	284.75
	2.3	133.33	311.86	813.56	596.61	81.36	203.39	284.75
0.55	0.25	354.80	90.40	813.56	596.61	69.96	174.90	244.86
	0.43	311.86	133.33	813.56	596.61	69.96	174.90	244.86
	0.67	267.12	178.08	813.56	596.61	69.96	174.90	244.86
	1.00	222.82	222.37	813.56	596.61	69.96	174.90	244.86
	1.50	178.08	267.12	813.56	596.61	69.96	174.90	244.86
	2.3	133.33	311.86	813.56	596.61	69.96	174.90	244.86

A / B	G / F	Fly ash (kg/m^3) (F)	GGBS (kg/m^3) (G)	Coarse Aggregate (kg/m^3)	Fine Aggregate (kg/m^3)	NaOH (kg/m^3)	Na_2SiO_3 (kg/m^3)	Alkaline liquid (kg/m^3) (A)
0.45	0.25	354.80	90.40	813.56	596.61	57.24	143.10	200.34
	0.43	311.86	133.33	813.56	596.61	57.24	143.10	200.34
	0.67	267.12	178.08	813.56	596.61	57.24	143.10	200.34
	1.00	222.82	222.37	813.56	596.61	57.24	143.10	200.34
	1.50	178.08	267.12	813.56	596.61	57.24	143.10	200.34
	2.3	133.33	311.86	813.56	596.61	57.24	143.10	200.34

4.7 CASTING AND CURING OF GPC CUBES

For determining the compressive and flexural strength of geopolymer concrete, a total of 72 cubes and 72 prisms representing six different mixes with different GGBS to fly ash ratios (0.25, 0.43, 0.67, 1.0, 1.5, and 2.3), four different molarities (6, 8, 10, and 12) of NaOH alkaline solution were considered. In all the above specimens, the alkaline activator solution to binder content ratio was maintained constant at 0.64. Additionally, to study the effect of alkaline activator solution to binder content ratio on the compressive and flexural strength of geopolymer concrete, 72 cubes and 72 prism specimens were cast and tested. The parameters varied include two different alkaline activator solution to binder content ratios (0.55 and 0.45), three different GGBS to fly ash ratios (0.25, 0.67, and 1.5), and four different molarities (6, 8, 10, and 12) of NaOH alkaline solution. Three identical specimens were cast and tested for each variation.

A rotating drum-type pan mixer of 100kg capacity was used to mix the dry materials. After uniform mixing of dry materials, an alkaline activator solution of a specified quantity and a superplasticizer (Conplast SP 430 Fosroc make) at optimal dosage were added. A consistent mixture was obtained after mixing it for about 5 – 7 minutes. The fresh mixes that were prepared were cohesive and there was no segregation of the mix. The mixture was placed in cubes and prisms moulds and compacted by placing it on the jolted table. After compaction, the top surface of the moulds was leveled with a trowel. The cubes and prisms were de-moulded after 24 hours of casting. The specimens are air-cured at room temperature of 35 ± 2ºC and relative humidity of 75% for 28 days.

4.8 TESTING PROCEDURE FOR COMPRESSIVE STRENGTH TEST

The geopolymer concrete cube specimens of size 150 mm x 150 mm x 150 mm and prisms of size 100 mm x 100 mm x 400 mm that were cast, were tested on a 2000 kN Tinius Olsen Testing machine and failure loads were recorded and tabulated in table 4.6. The testing of cube and prism specimens was carried out at the end of 28 days of curing outdoors. The testing was done conforming to IS: 516, 1959.

Compressive strength of geopolymer concrete

From the recorded maximum load or failure loads of three identical cube specimens, the average compression strength of geopolymer concrete for different GGBS to fly ash ratios and for different molarities of NaOH alkaline activator were calculated and tabulated in table 4.6.

Flexural strength or modulus of rupture (tensile strength in bending) of GPC

After outdoor curing for 28 days, the prism specimens were tested under standard four point bending in accordance with IS: 516, 1959. The load applied was increased continuously at a constant rate until the resistance of the specimen to the increasing load broke down and it could no longer be sustained. The maximum load applied to the specimen was recorded. From the recorded maximum load or failure loads of three identical prism specimens, the average flexural strength of geopolymer concrete for different GGBS to fly ash ratios and for different molarities of the NaOH alkaline activator was tabulated. This data figures in table 4.6.

4.9 TESTS RESULTS AND DISCUSSIONS

Compressive and flexural strength for different mix proportions and the corresponding average binder index are tabulated in table 4.6.

The variation in compressive strength, flexural strength with different molarity of NaOH, alkaline to binder ratio, GGBS to fly ash ratio, and binder index of geopolymer concrete is plotted and discussed in the following sections.

Table 4.6. Test results on geopolymer concrete cubes

Molarity of NaOH Solution (M)	GGBS / Fly ash (G / F)	A / B =0.64			A / B =0.55			A / B =0.45		
		Binder Index (Bi)	Comp. Strength (MPa)	Flex. Strength (Mpa)	Binder Index (Bi)	Comp. Strength (MPa)	Flex. Strength (Mpa)	Binder Index (Bi)	Comp. Strength (MPa)	Flex. Strength (Mpa)
6	0.25	0.96	**16.62**	**1.77**	0.83	**13.33**	**1.65**	0.68	**12.62**	**1.50**
6	0.43	1.65	18.14	2.10	-	-	-	-	-	-
6	0.67	2.57	**24.97**	**2.48**	2.21	**20.00**	**2.40**	1.81	**17.11**	**2.25**
6	1.00	3.84	37.82	2.70	-	-	-	-	-	-
6	1.50	5.76	**41.69**	**3.00**	4.95	**33.33**	**2.73**	4.05	**28.44**	**2.55**
6	2.33	8.95	45.67	3.36	-	-	-	-	-	-
8	0.25	1.28	**19.27**	**1.83**	1.10	**19.10**	**1.71**	0.90	**19.02**	**1.59**
8	0.43	2.20	23.45	2.19	-	-	-	-	-	-
8	0.67	3.43	**30.17**	**2.55**	2.95	**28.88**	**2.46**	2.41	**25.77**	**2.40**
8	1.00	5.12	38.53	2.93	-	-	-	-	-	-
8	1.50	7.68	**42.71**	**3.09**	6.60	**35.55**	**2.92**	5.40	**28.88**	**2.85**
8	2.33	11.93	49.34	3.59	-	-	-	-	-	-
10	0.25	1.60	**22.53**	**2.06**	1.38	**21.33**	**1.80**	1.13	**20.08**	**1.74**
10	0.43	2.75	25.99	2.29	-	-	-	-	-	-
10	0.67	4.29	**37.41**	**2.61**	3.69	**33.33**	**2.55**	3.02	**28.44**	**2.46**
10	1.00	6.40	39.55	2.99	-	-	-	-	-	-
10	1.50	9.60	**43.83**	**3.12**	8.25	**37.33**	**3.00**	6.75	**30.53**	**2.92**
10	2.33	14.91	53.92	3.66	-	-	-	-	-	-
12	0.25	1.92	**27.93**	**2.16**	1.65	**25.77**	**2.10**	1.35	**24.44**	**1.95**
12	0.43	3.30	30.07	2.36	-	-	-	-	-	-
12	0.67	5.15	**39.65**	**2.64**	4.42	**34.22**	**2.58**	3.62	**31.11**	**2.52**
12	1.00	7.68	41.08	3.05	-	-	-	-	-	-
12	1.50	11.52	**44.75**	**3.36**	9.90	**40.44**	**3.27**	8.10	**36.13**	**3.15**
12	2.33	17.89	58.00	3.75	-	-	-	-	-	-

Note: Binder Index (Bi) = M x (G/F) x (A/B), where A / B = Alkaline activator to binder ratio
Binder B = Sum quantity of GGBS and Fly ash (G + F)

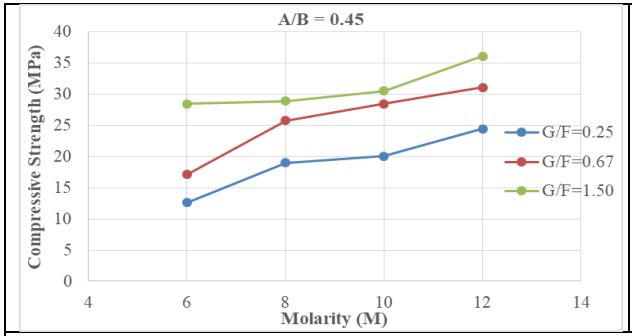

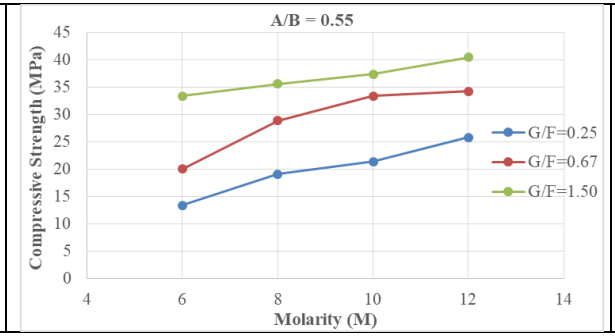

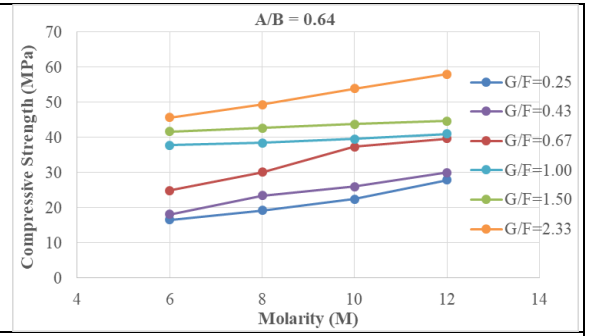

Figure 4.5 (a) Compression strength of the GPC vs. molarity of NaOH for different GGBS to fly ash ratio and different alkaline activator to binder ratio

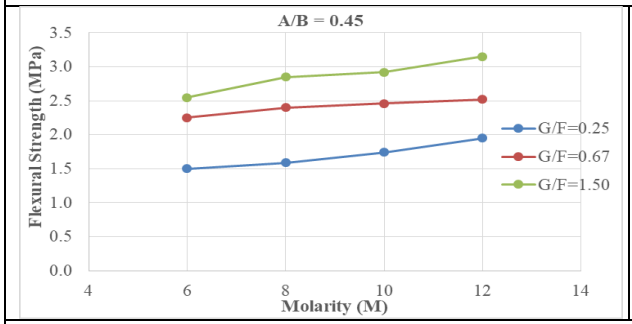

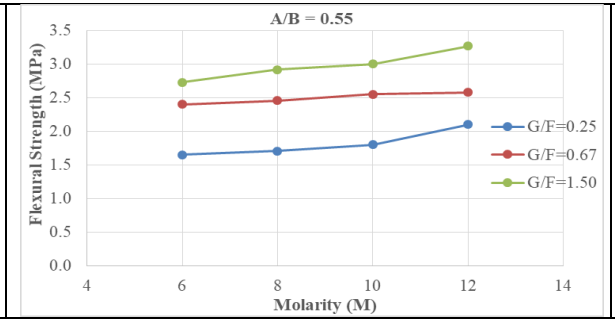

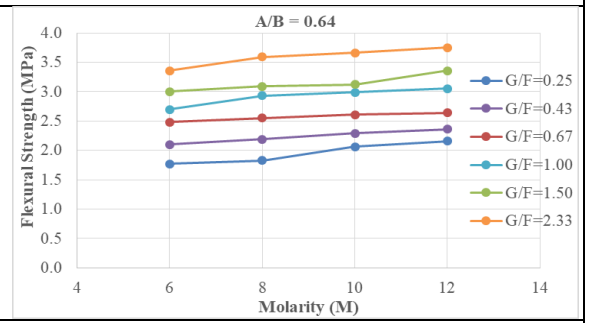

Figure 4.5 (b) Flexural strength of the GPC vs. molarity of NaOH for different GGBS to fly ash ratio and different alkaline activator to binder ratio

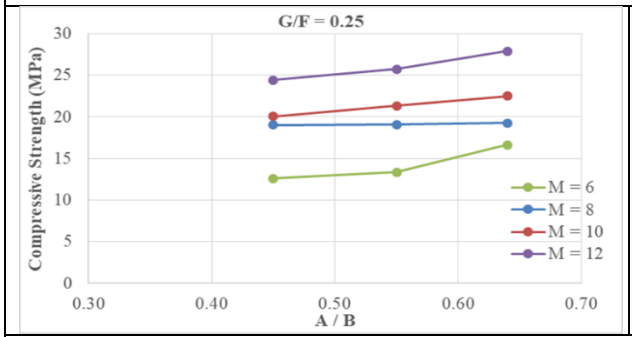

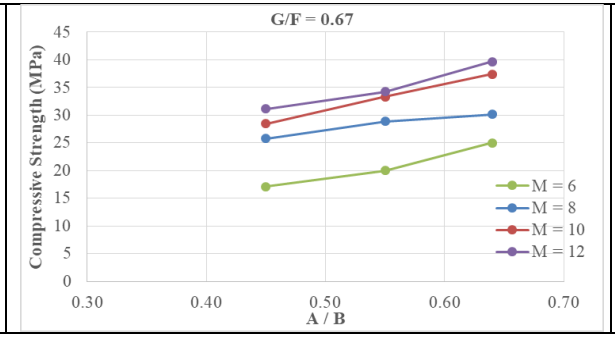

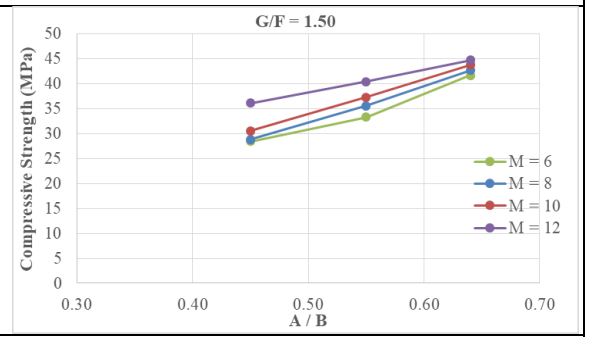

Figure 4.5 (c) Compression strength of the GPC vs. alkaline activator to binder ratio for different molarity of NaOH and different GGBS to fly ash ratios

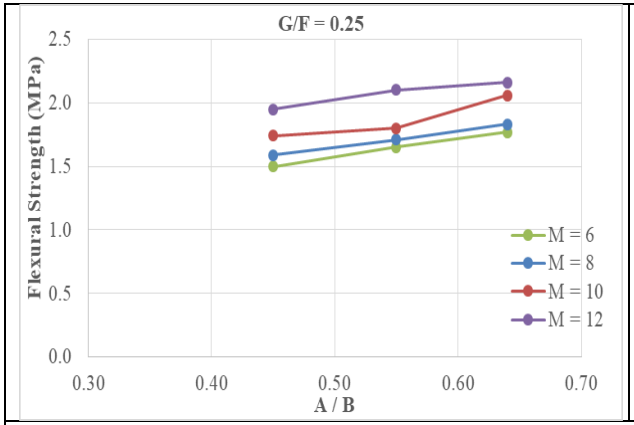

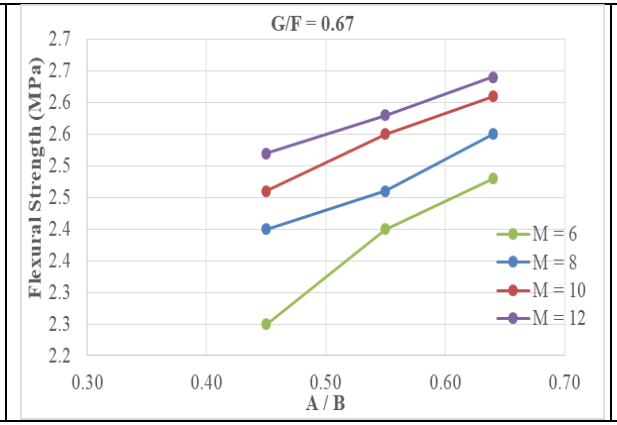

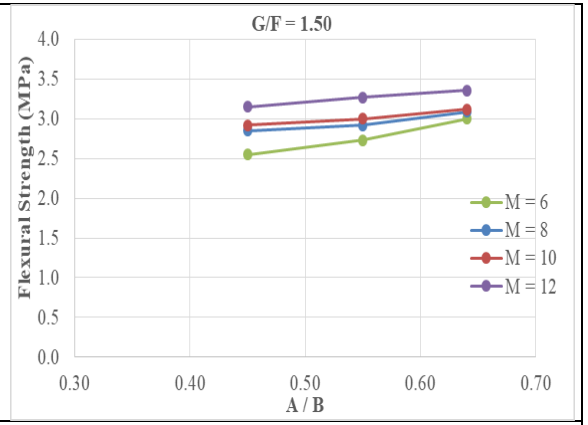

Figure 4.5 (d) Flexural strength of the GPC vs. alkaline activator to binder ratio for different molarity of NaOH and different GGBS to fly ash ratios

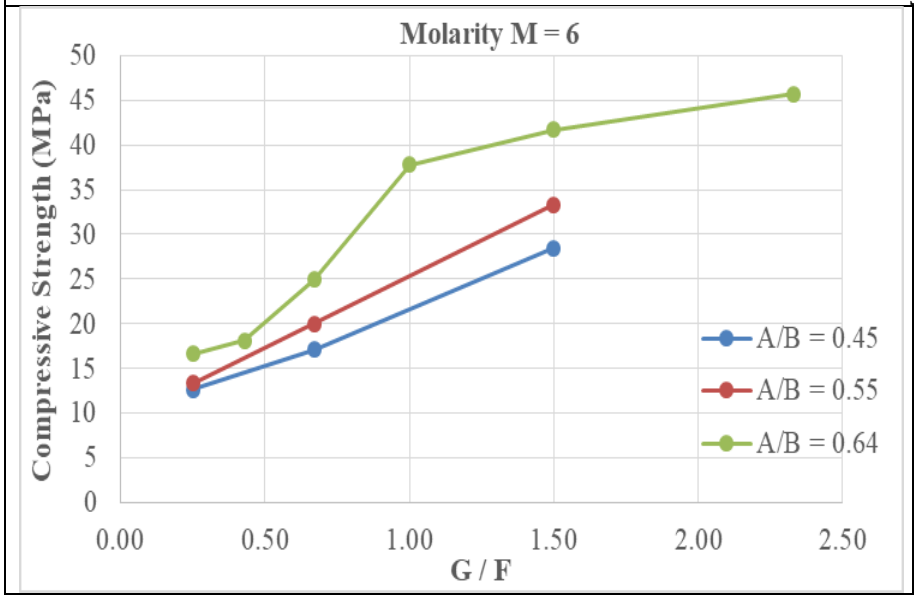

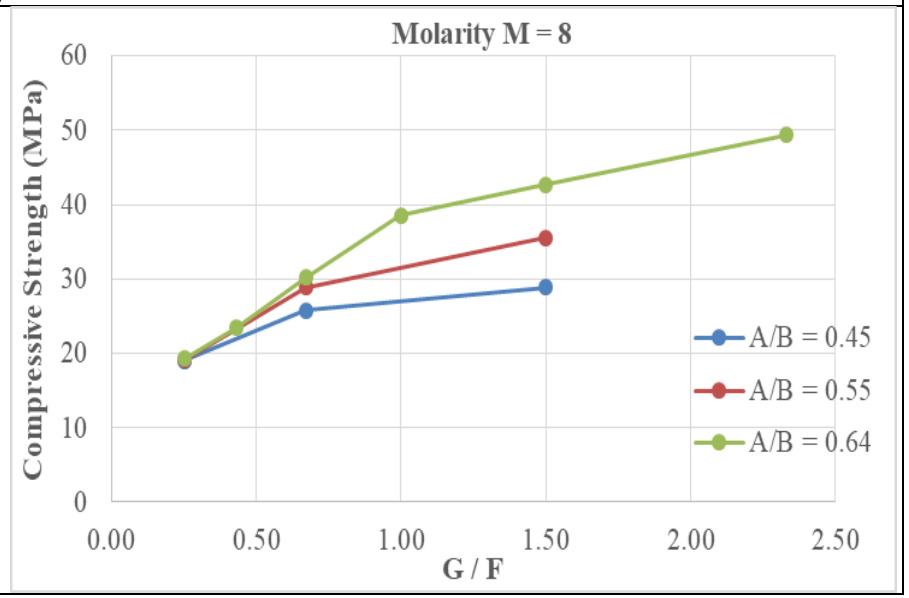

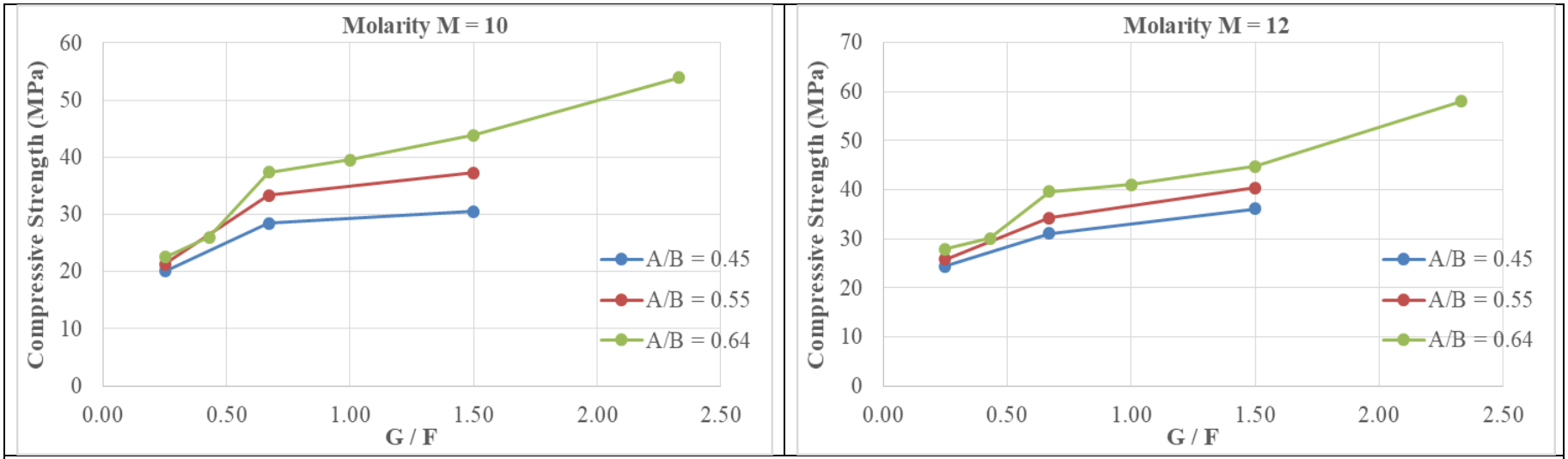

Figure 4.5 (e) Compression strength of the GPC vs. GGBS to fly ash ratios for the different alkaline activator to binder ratio and different molarity of NaOH

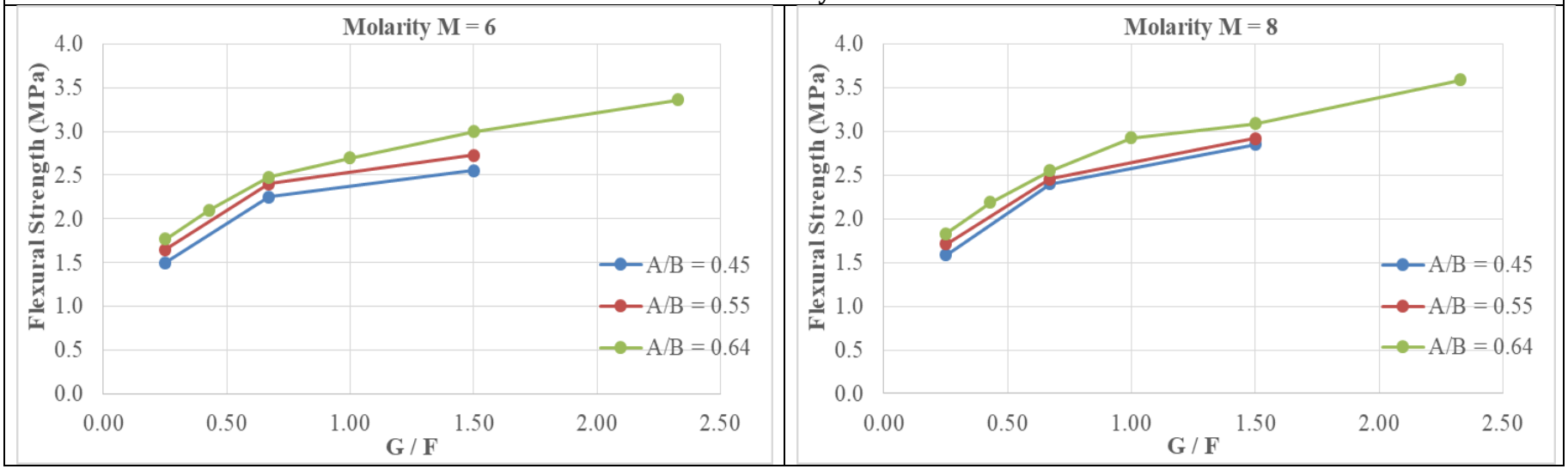

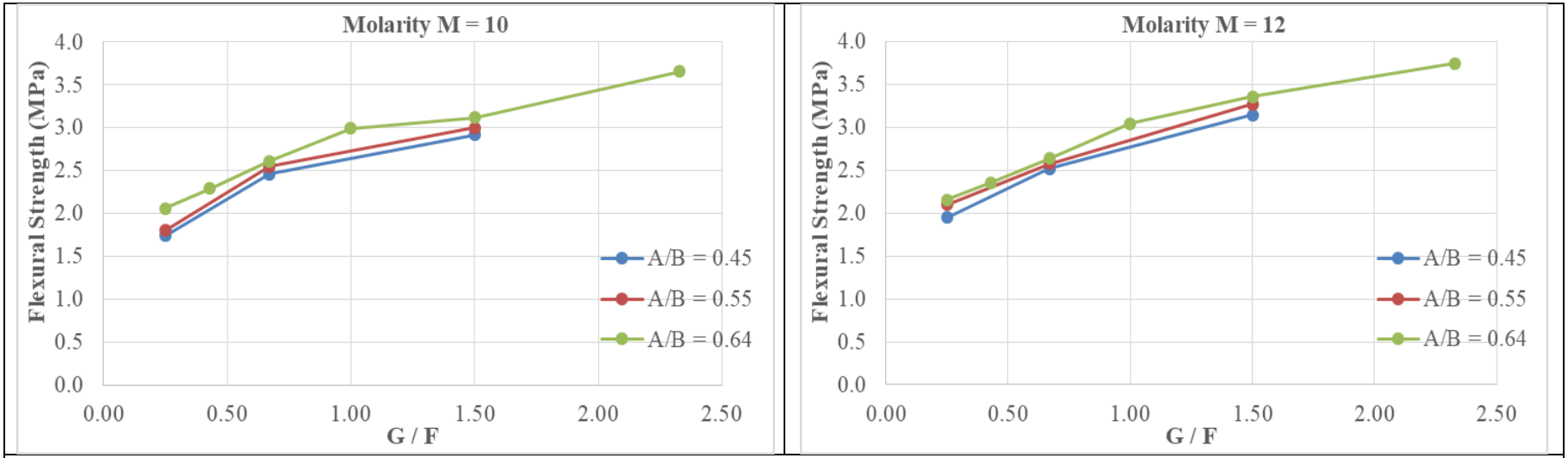

Figure 4.5 (f) Flexural strength of the GPC vs. GGBS to fly ash ratios for the different alkaline activator to binder ratio and different molarity of NaOH

Figure 4.5 Variation of strengths of the GPC vs. GGBS to fly ash ratios, alkaline activator to binder ratio, and molarity of NaOH

4.9.1 Effect of molarity (M) / concentration of Sodium hydroxide (NaOH) solution

On the compressive strength of geopolymer concrete

The effect of molarity of NaOH solution on different GGBS to fly ash ratios on the compressive strength of geopolymer concrete is shown in figure 4.5 (a). It was observed that as molarity increase the compressive strength of geopolymer concrete also increased. However, the increase in strength was not in proportion to increase in molarity. For a particular alkaline activator to binder ratio (i.e. A/B = 0.64), as the GGBS to fly ash ratio increased from 0.25 to 2.3 the compressive strength of geopolymer concrete increased by 175%, 156%, 139%, and 107% for molarity of NaOH solution of 6M, 8M, 10M, and 12M respectively.

On the flexural strength of geopolymer concrete

The effect of the molarity of NaOH solution for the different GGBS to fly ash ratios on the flexural strength of geopolymer concrete is shown in Figure 4.5 (b). It was observed that as the molarity increase the flexural strength of geopolymer concrete also increased. However, the increase in strength was not in proportion to the increase in molarity. For a particular alkaline activator to binder ratio (i.e. A/B = 0.64), as the GGBS to fly ash ratio increased from 0.25 to 2.3, the flexural strength of geopolymer concrete increased by 89.8%, 96.1%, 77.6%, and 73.6% for a molarity of 6M, 8M, 10M, and 12M respectively of the NaOH solution.

4.9.2 Effect of the alkaline activator to binder ratio (A/B)

On the compressive strength of geopolymer concrete

The effect of alkaline activator to binder ratio (A/B) and molarity of the NaOH solution on the compressive strength of geopolymer concrete for a particular GGBS to fly ash ratio is shown in figure 4.5 (c). From the figures, it can be observed that the compression strength of

geopolymer concrete increased with an increase in the alkaline activator to binder content ratio. However, the rate of increase of the compressive strength was higher for higher GGBS to fly ash ratios. For a particular GGBS to fly ash ratio (i.e. G/F = 0.67) as the alkaline activator to binder ratio increased from 0.25 to 1.50 the compressive strength of geopolymer concrete increased by 150%, 121%, 94%, and 60% for a molarity 6M, 8M, 10M, and 12M respectively of the alkaline activator.

For a constant value of low molarity (6M) and GGBS to fly ash ratio (0.67), increasing the alkaline activator to binder content ratio from 0.45 to 0.64 the compressive strength of geopolymer concrete increased from 125% to 150%. However, in the case of high molarity (12M) and GGBS to fly ash ratio (0.67), increasing the alkaline activator to binder content ratio from 0.45 to 0.64 increased the compressive strength of geopolymer concrete from 48% to 60%. Hence the use of a stronger alkaline activator to binder content ratio is beneficial in increasing the strength of geopolymer concrete prepared with low molarity NaOH solution.

On the flexural strength of geopolymer concrete

The effect of alkaline activator to binder content ratio (A/B) and molarity of NaOH solution on the flexural strength of geopolymer concrete for a particular GGBS to fly ash ratio is shown in figure 4.5 (d). From the figure, it can be seen that the flexural strength of geopolymer concrete increases with an increase in the alkaline activator to binder content ratio. However, the rate of increase of flexural strength is more or less uniform as the alkaline activator to binder content ratio (A/B) increased for the same molarity of NaOH solution. For a particular GGBS to fly ash ratio (i.e. G/F = 0.67), as the alkaline activator solution to binder ratio increased from 0.25 to 1.50 the flexural strength of geopolymer concrete increased by 70%, 69%, 51%, and 55% for the molarity of NaOH solutions of 6M, 8M, 10M, and 12M respectively. However, in the case of constant low or high molarity (6M or 12M) and for constant GGBS to fly ash ratio (0.67),

increasing A/B ratio from 0.45 to 0.64 led to percent increase in flexural strength of geopolymer concrete and this varied from 51% to 70%.

4.9.3 Effect of GGBS to fly ash ratio (G/F)

On the compressive strength of geopolymer concrete

The effect of GGBS to fly ash ratio and molarity of the alkaline activator on the compressive strength of geopolymer concrete for a particular alkaline activator solution to binder content ratio is shown in figure 4.5 (e). From the figure, it can be observed that the compression strength of geopolymer concrete increased with an increase in GGBS to fly ash ratio. However, the rate of increase of the compressive strength was higher for GGBS to fly ash ratios lower than 1.0, as indicated by larger increase of compressive strength when there was a changes in molarity. The same is also observed in figure 4.1.

On the flexural strength of geopolymer concrete

The effect of GGBS to fly ash ratio and molarity of the alkaline activator on the flexural strength of geopolymer concrete for a particular alkaline activator to binder ratio is shown in figure 4.5 (f). From the figure, it can be observed that the flexural strength of geopolymer concrete increased with an increase in GGBS to fly ash ratio. However, the rate of increase of flexural strength was lower compared to that of the compression strength of geopolymer concrete for all GGBS to fly ash ratios considered in the investigation.

4.9.4 Validation of Binder Index (Bi)

In the present study, the concept of a unified parameter called 'Binder Index (Bi)' is proposed which includes the effect of GGBS to fly ash ratio (G/F), alkaline activator solution to binder content ratio (A/B), and the molarity of NaOH solution (M) controlling the strength of GGBS

and fly ash based geopolymer concrete. The values of the compressive strength of geopolymer concrete at 28 days (f_{gpc}) and the corresponding binder index (Bi) are given in table 4.6, and a variation between them is shown in figure 4.6. This variation indicates that the compressive strength of geopolymer concrete increased with an increase in binder index. However, the increase in strength was not in proportion to an increase in binder index. A non-linear variation exists between the binder index and the compressive strength of geopolymer concrete. A similar variation was also observed from the test results of various investigators shown in figure 4.2 and table 4.2. The following best-fit equation gives the relation between the compressive strength of the fly ash and GGBS based Geopolymer Concrete at 28 days with binder index (Bi). The equation was represented by a single power equation with an acceptable correlation with the experimental values.

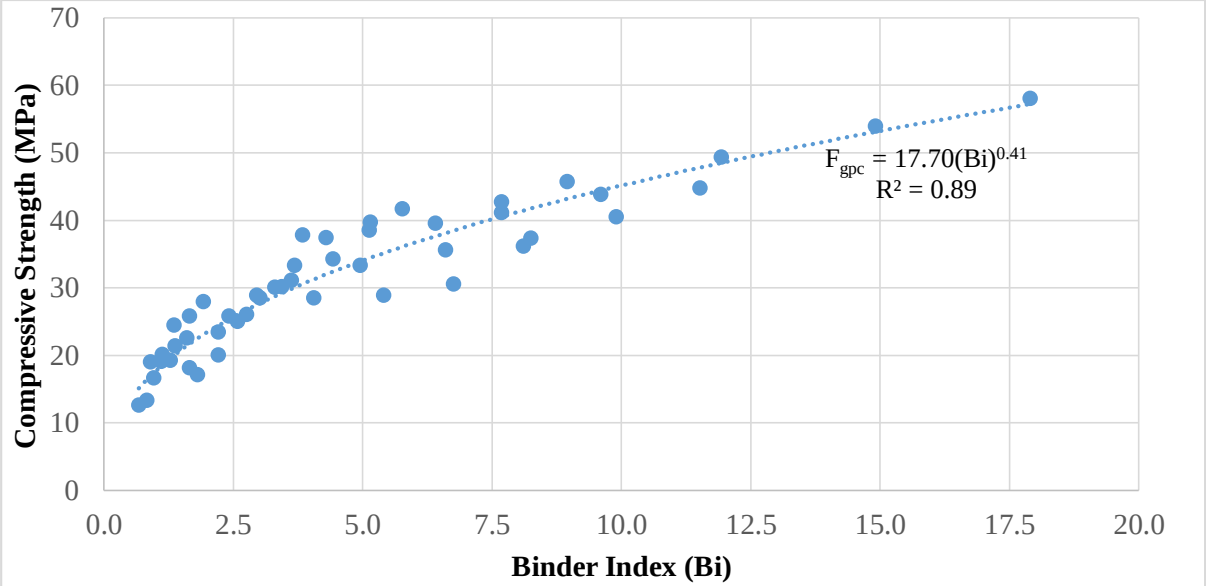

Figure 4.6: Variation of compressive strength w.r.t Binder Index

$$\mathbf{f_{gpc} = 17.70[Bi]^{0.41}} \quad \text{- Eq. 4.5}$$

Where f_{gpc} is the compressive strength of geopolymer concrete at 28 days and Bi is Binder Index. The values of the flexural strength of geopolymer concrete at 28 days and corresponding binder index (Bi) are given in table 4.6, and the variation between them is shown in figure 4.7. This variation indicates that the flexural strength of geopolymer concrete increased with an

increase in the binder index and is along similar lines to the compressive strength of geopolymer concrete. A similar trend can be observed from the flexural strength results of various investigators, shown in figure 4.2 and table 4.2. The following best-fit equation gives the relation between the flexural strength of the fly ash and GGBS based Geopolymer Concrete at 28 days with the binder index (Bi).

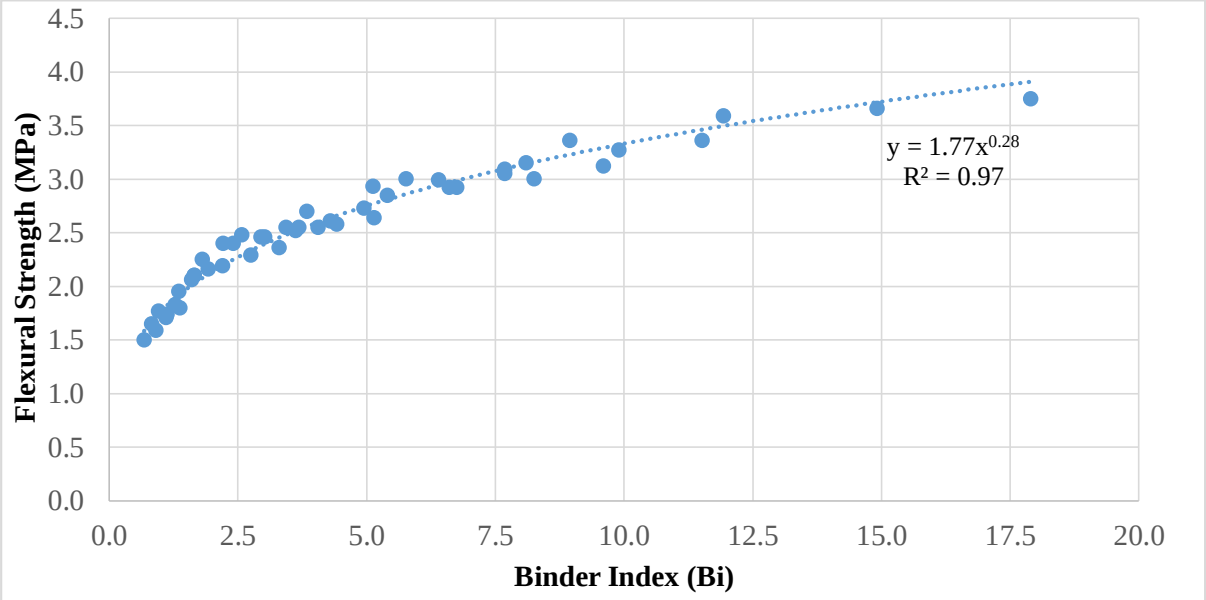

Figure 4.7: Variation of flexural strength w.r.t Binder Index

$$\mathbf{f_{flexural} = 1.77[Bi]^{0.28}} \quad \text{- Eq. 4.6}$$

Where $f_{flexural}$ is the flexural strength of geopolymer concrete at 28 days and Bi is Binder Index. It can be noted that the variation of strengths with binder index is in line with the proposed equation for geopolymer mixes and follows the non-linear power equation. Given the above discussions, the newly proposed parameter called "Binder Index (Bi)" combines the effects of alkaline to binder content ratio, GGPS to fly ash ratio, and molarity of sodium hydroxide and can be considered a single unique parameter to control the compressive strength of geopolymer concrete.

4.9.5 Validation of the phenomenological model

Table 4.7 shows the experimental data extracted from table 4.6, which was used to validate the predictions made with the phenomenological model. For each of these sets, the compressive strength at a binder index of 5.40 was considered as reference strength in the phenomenological model proposed in section 4.3. The compressive strength corresponding to each binder index value was calculated using the proposed phenomenological model (Eq. 5.3 and Eq. 5.4) and tabulated in Table 4.7 for comparison with experimental values. There is a close agreement between the experimental and predicted values, which enhances the applicability of the phenomenological model with a 0.911 correlation between them.

Table 4.7. Experimental results for validating the phenomenological model

Binder Index (Bi)	**Experimental compressive strength (N/mm^2) ($f_{gpc\ e}$)**	**Predicted compressive strength * (N/mm^2) ($f_{gpc\ p}$)**
0.96	16.62	18.01
1.65	18.14	20.62
2.57	24.97	23.04
3.84	37.82	25.47
5.76	41.69	28.19
8.95	45.67	31.47
1.28	19.27	19.35
2.20	23.45	22.16
3.43	30.17	24.76
5.12	38.53	27.37
7.68	42.71	30.29
11.93	49.34	29.97
1.60	22.53	20.46
2.75	25.99	23.43
4.29	37.41	26.18
6.40	39.55	28.94
9.60	43.83	32.03
14.91	53.92	30.65
1.92	27.93	21.42
3.30	30.07	24.53
5.15	39.65	27.40
7.68	41.08	30.29
11.52	44.75	29.87
17.89	58.00	31.21
0.83	13.33	17.34
2.21	20.00	22.19

Binder Index (Bi)	Experimental compressive strength (N/mm^2) ($f_{gpc\ e}$)	Predicted compressive strength * (N/mm^2) ($f_{gpc\ p}$)
4.95	33.33	27.14
1.10	19.10	18.63
2.95	28.88	23.84
6.60	35.55	29.16
1.38	21.33	19.70
3.69	33.33	25.21
8.25	37.33	30.84
1.65	25.77	20.62
4.42	34.22	26.38
9.90	40.44	32.27
0.68	12.62	16.49
1.81	17.11	21.10
4.05	28.44	25.81
0.90	19.02	17.72
2.41	25.77	22.67
5.40	**28.88**	27.74
1.13	20.08	18.74
3.02	28.44	23.98
6.75	30.53	29.33
1.35	24.44	19.61
3.62	31.11	25.09
8.10	36.13	30.69

*Note:
Predicted compressive strength of geopolymer concrete:
From Eq. 4.3, For Bi $\leq$10, $f_{gpc,\ p} = 28.88 \times 0.63 \times (Bi)^{0.25}$
From Eq. 4.4, For Bi >10, $f_{gpc,\ p} = 28.88 \times 0.81 \times (Bi)^{0.10}$
Where, 28.88 used in the above equation is the reference compressive strength of geopolymer concrete in MPa, corresponding to the binder index of 5.40.

4.10 CONCLUSIONS

The following are the conclusions derived from the analytical and experimental study of different variables affecting the compressive strength of Geopolymer concrete mixes.

1. The compression strength of the fly ash and GGBS based geopolymer concrete increases with an increase in GGBS to fly ash ratio. However, the rate of increase of the compressive strength is higher for the GGBS to fly ash ratios lower than 1.0.

2. Flexural strength of the fly ash and GGBS based geopolymer concrete increases with an increase in the GGBS to fly ash ratio. However, the rate of increase of flexural strength is lower compared to that of the compression strength of geopolymer concrete.
3. The compression strength of geopolymer concrete increases with an increase in the alkaline activator to binder content ratio. However, the rate of increase of the compressive strength is higher for higher GGBS to fly ash ratios for constant molarity of NaOH solution in an alkaline activator.
4. The use of a higher alkaline activator to binder content ratio (A/B) is beneficial in increasing the strength of geopolymer concrete prepared with low molarity NaOH.
5. The flexural strength of geopolymer concrete increases with an increase in alkaline activator to binder content ratio (A/B). However, the rate of increase of the flexural strength is more or less uniform with increase in alkaline activator to binder ratio (A/B) for a constant molarity of the alkaline activator.
6. The newly proposed parameter called "Binder Index (Bi)" which combines the effects of alkaline to binder content ratio, GGBS to fly ash ratio, and molarity of sodium hydroxide can be considered as a single unique parameter to control the compressive strength of geopolymer concrete.

$$\boldsymbol{Bi = \frac{MA}{G+F}\left[\frac{G}{F}\right]}$$

Where, M= molarity of NaOH, A=alkaline activator (Both NaOH and Na_2SiO_3 together) content, G= GGBS content, F= fly ash content.

7. The strength of geopolymer concrete (both compression and flexural strengths) increases with an increase of binder index.
8. A non-linear variation exists between the binder index and the strengths (both compression and flexural strengths) f_{gpc} of geopolymer concrete and can be signified by a power equation.

$$\mathbf{f_{gpc} = N[Bi]^{L}}$$

Where N and L are constants.

9. Based on the phenomenological model, the compressive strength of geopolymer concrete for any binder index can be estimated as follows.

For Binder Index Bi ≤ 10, $\frac{f_{gpc}}{f_{gpc,5.41}} = 0.63\ Bi^{0.25}$

For Binder Index Bi > 10, $\frac{f_{gpc}}{f_{gpc,5.41}} = 0.81\ Bi^{0.10}$

Where f_{gpc} is the Compressive Strength for any specified Binder Index required and $f_{gpc5.41}$ is the experimentally evaluated strength for a binder index of 5.41.

CHAPTER 5
EXPERIMENTAL INVESTIGATION ON THE SHEAR STRENGTH AT THE MONOLITHIC INTERFACE OF GEOPOLYMER CONCRETE

5.1 INTRODUCTION

Geopolymer concrete is slowly gaining significance from the sustainability point of view in the concrete industry. Hence the evaluation of mechanical properties of geopolymer concrete is becoming important to gain acceptance as a structural material. The review of literature revealed that the number of investigations on shear strength of geopolymer concrete in general and shear strength at the monolithic interfaces of geopolymer concrete, in particular, are fewer in number compared to the investigations related to the mechanical properties such as compressive strength and the tensile strength of geopolymer concrete. The evaluation of shear friction characteristics of geopolymer concrete assumes significance from the point of its use as structural material and finds application at the critical shear locations of concrete corbels, beam-column junction, beam-slab interface, etc.

In this chapter, a study on the shear capacity of monolithically cast geopolymer concrete interface is evaluated by testing push-off specimens. The shear strength of geopolymer concrete was analyzed based on the shear friction concept that includes cohesion, friction, and dowel action components

5.2 RESEARCH SIGNIFICANCE

Shear capacity at the interface, in general, depends on parameters like the roughness of the interface, amount of reinforcement crossing the interface or shear reinforcement, and strength

of concrete. The review of literature indicated that the shear strength at the interfaces is influenced by three shear load carrying mechanisms i.e., cohesion (due to interlocking between aggregates), friction (because of slip among different concrete layers and is affected by normal stress and roughness at the interface) and the dowel resistance of steel connectors i.e., dowel action (due to the presence of reinforcement crossing the interface).

Several types of test specimens such as push-off specimens, corbel specimens subjected to transverse loading, pull-off, etc. were used to determine the shear strength of concrete. The push-off specimens being most suitable are commonly used due to direct shear transfer across interfaces against other types of specimens, which induces both shear and moment (Mattock, 2001, Xiao J et al., 2016).

The results of push-off tests were used in proposing shear transfer models for concrete (ACI 318, 2019, PCI, 2010 and CSA A23.3, 2019). Different models were available in the literature for calculating the concrete shear transfer strength (Birkeland and Birkeland, 1966, Mattock and Hawkins, 1972, Mattock, 1974, Loov, 1978, Walraven et al., 1987 and Randl, 1997).

In the present study, the shear capacity of the monolithically cast geopolymer concrete interface was evaluated by testing push-off specimens. The shear strength was analyzed based on shear friction concept that includes cohesion, friction, and dowel action components (CSA A23.3, 2019, Euro code 2, 2004, Randl, 1997). The variables considered in the investigation are the strength of GPC with and without the reinforcement crossing the monolithic shear interface.

The coefficient of cohesion for geopolymer concrete has been predicted based on tests conducted on push-off specimens without reinforcement across the interface (unreinforced geopolymer concrete) in relation to the strength of geopolymer concrete. Further, the tests were conducted on push-off specimens with varying percent of reinforcement across the monolithic

geopolymer concrete interface to determine the shear strength of geopolymer concrete with reinforced interfaces.

5.3 EXPERIMENTAL PROCEDURE

5.3.1 Binder materials

Fly ash and GGBS, which are rich in silica (Si) and aluminum (Al) were used as source materials in the present study. GGBS was acquired from Jindal Steel Works, Bhopal, and fly ash from National Thermal Power Plant (NTPC), Ramagundam with a specific gravity of 2.90 and 2.17 respectively. Table 5.1 shows the chemical composition details of fly ash and GGBS used in the study.

Table 5.1: Chemical composition of fly ash and GGBS (% by mass)

Binder material	Fly ash	GGBS
SiO_2	60.11	37.73
Al_2O_3	26.53	14.42
Fe_2O_3	4.25	1.11
SO_3	0.35	0.39
CaO	4	37.34
MgO	1.25	8.71
Na_2O	0.22	--
LOI	0.88	1.41

5.3.2 Fine aggregate

River sand was considered for investigation. Different lab tests were conducted on fine aggregate as per IS: 2386, 1963. Fine aggregate properties are tabulated in Table 5.2. River sand was sieved as per IS sieves (i.e. 2.36, 1.18, 0.6, 0.3, and 0.15 mm). The gradation curve from figure 5.1 and table 5.3 shows that river sand considered falls in Zone – II as per IS: 383, 2016.

Table 5.2: Physical properties of fine aggregate

Test Conducted	Result
Specific Gravity	2.65
Fineness Modulus	3.35
Bulk Density	1.45 g/cm^3

Table 5.3: Proportions of different size fractions of sand

Sieve size (mm)	Weight retained in grams	% Weight retained	Cumulative % weight retained	% Passing	% Passing as per for Zone II - IS 383 (2016) – Upper Limit	% Passing as per for Zone II - IS 383 (2016) – Lower Limit
10-4.75	-	-	-	100	100	100
4.75-2.36	55	5.5	5.5	94.5	100	90
2.36-1.18	190	19	24.5	75.5	90	75
1.18-0.60	235	23.5	48	52	59	55
0.60-0.30	435	43.5	91.5	8.5	30	35
0.30-0.15	60	6	97.5	2.5	10	8
0.15 - Pan	25	2.5	100	0	0	0

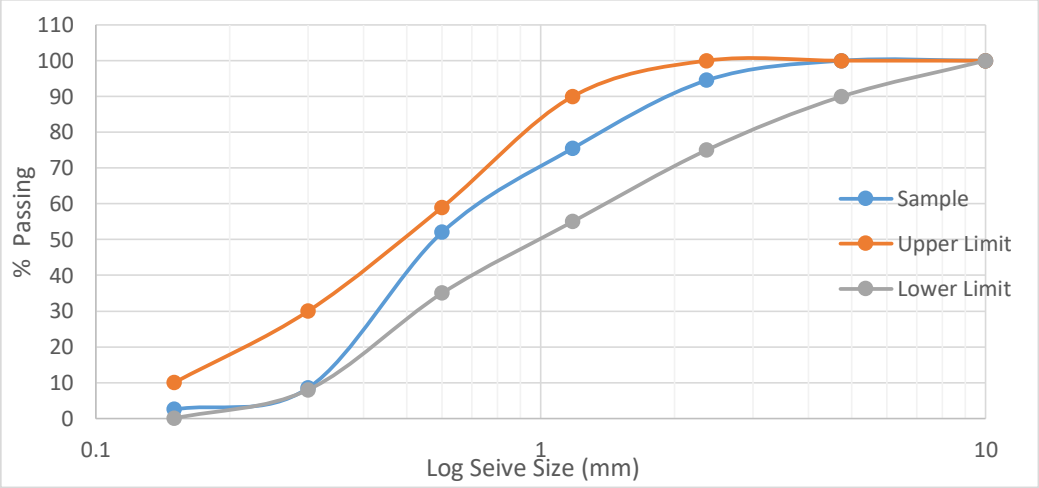

Figure 5.1: Gradation curve for fine aggregate

5.3.3 Coarse aggregate

Well-graded crushed granite conforming to IS 383: 2016 was considered as coarse aggregate. The coarse aggregate was acquired from a local crushing plant with 20 mm being the nominal size. Different tests conforming to IS: 2386, 1963 were conducted to attain physical properties and these are tabulated in table 5.4. Figure 5.2 and Table 5.5 show the proportions with sieves of different sizes: 20, 16, 12.5, 10, and 4.75 mm, respectively.

Table 5.4: Physical properties of coarse aggregate

Test conducted	Result
Specific Gravity	2.80
Fineness Modulus	7.30
Bulk Density	1.5 g/cm^3

Table 5.5: Proportions of different size fractions of coarse aggregate

Sieve size (mm)	Weight retained in grams	% Weight retained	Cumulative % weight retained	% Passing	% Passing for graded aggregate - IS 383 (2016) – Upper Limit	% Passing for graded aggregate - IS 383 (2016) – Lower Limit
80	-	-	-	100	100	100
40	-	-	-	100	100	100
20	42	4.2	4.2	95.8	100	90
16	66	6.6	10.8	89.2	-	-
12.5	312	31.2	42	58	-	-
10	318	31.8	73.8	26.2	35	25
4.75	262	26.2	100	0	10	0

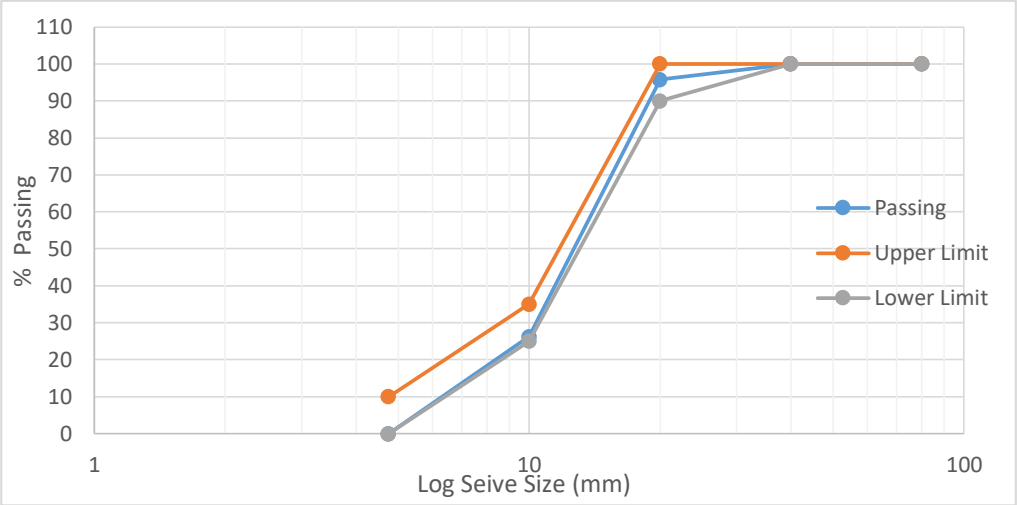

Figure 5.2: Gradation curve for coarse aggregate

5.3.4 Preparation of alkaline solution

For the experimental study, an alkaline solution having a concentration of NaOH solution equal to 8 moles / L was considered i.e., the molarity of 8 for NaOH solution. 320 g of NaOH pellets were liquefied in potable water to make one liter of 8M NaOH solution. The ratio of sodium silicate solution to sodium hydroxide solution was maintained constant at 2.5 and the same was stored for 24 hours at ambient temperature (25±2^{o}C) before used for casting, since the dissolution of NaOH is an exothermic reaction and a considerable amount of heat is generated when added in concrete. Hence the heat liberated has to be tamed and the solution maintained at room temperature.

5.3.5 Water

Potable water was used for the preparation of alkaline solution.

5.3.6 Superplasticizer

No additional water was used in geopolymer concrete apart from that used in the alkaline solution preparation; instead, a superplasticizer was used. Sulphonated naphthalene formaldehyde (Conplast SP 430 of Fosroc make) based superplasticizer is used for improving the workability. Conplast SP 430 is a brown color liquid and immediately dispersible in water and conforms to IS: 9103, 1999.

Table 5.6: Physical properties of superplasticizer

Chemical Base	Sulphonated naphthalene formaldehyde
Air entrainment (approx.)	1% additional air is entrained
Chloride content	Nil to IS:456, 2000
Specific gravity	1.15

5.4 PARAMETERS STUDIED

The following were the outcomes based on a preliminary study on the shear strength of ordinary Portland cement concrete using a push-off specimen.

- Size of push-off specimen i.e., 500 mm x 200 mm x 100 mm with 2nos 16 mm notches were considered.
- Test Setup was established.

For evaluating the shear strength of monolithic fly ash and GGBS based geopolymer concrete, the following parameters were considered. The flow chart indicating the experimental program is given in figure 5.3.

- Three different ranges of compressive strengths of geopolymer concrete (20-25 MPa, 40-45 MPa, and 50-55 MPa).
- With and without shear reinforcement crossing the interface (0.0%, 0.51%, 0.77% and 1.02%).

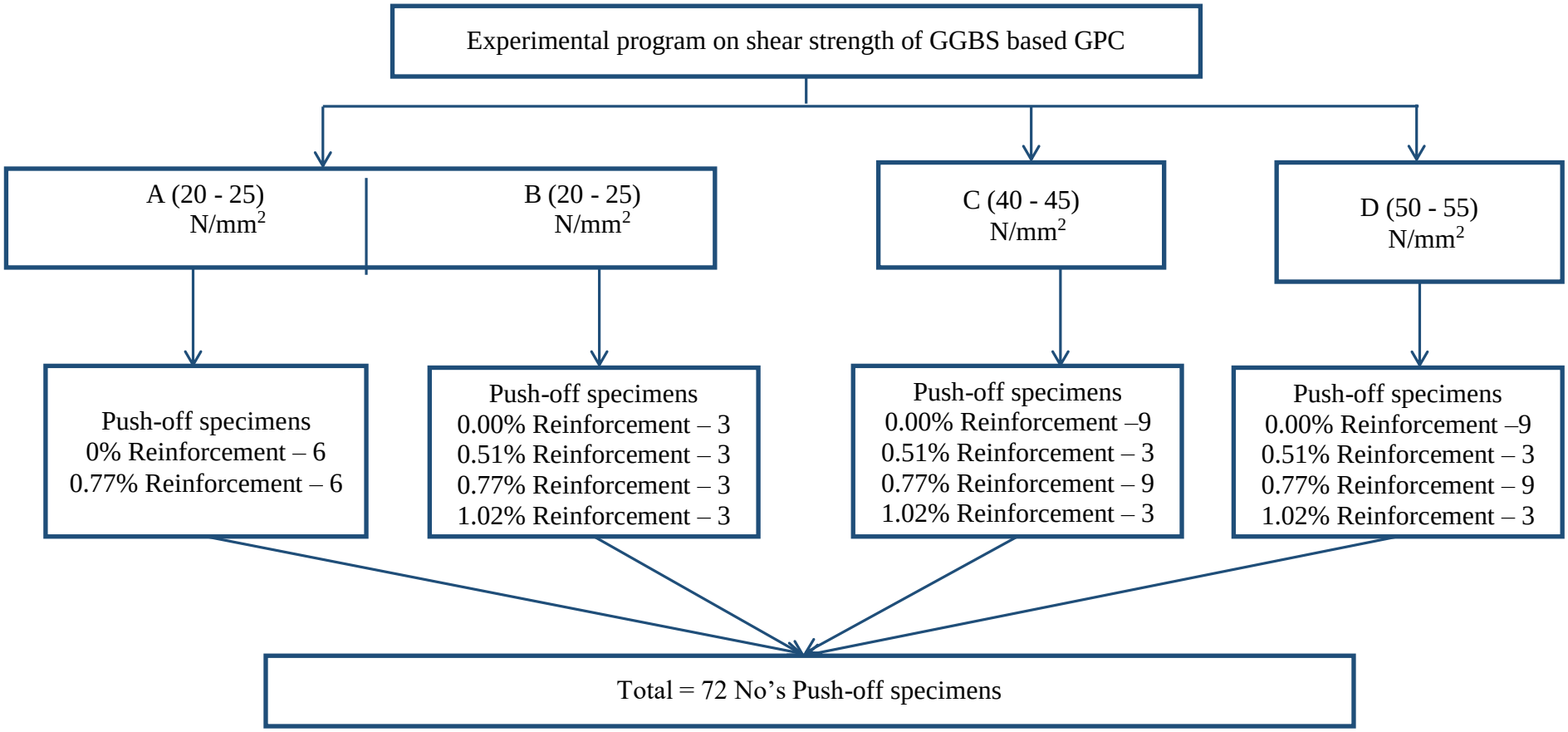

Figure 5.3: Schematic diagram of the experimental program

Specimen Identity is given as TBSGBN, where T – **T**ype of concrete, B – **B**atch, **S** – Type of Specimen, G – **G**rade of concrete, B – No of bars, N – Specimen **N**umber. For Example: For ID – G1SA21, G – **G**eopolymer concrete, 1 – Batch **1**, C – Specimen type **P**ush-off, **A** – Grade between 20 – 25 N/mm^2, 2 – **2** nos. of 6 mm bars as shear reinforcement, 1 – **1**st no. push-off specimen.

5.5 MIX PROPORTIONS

The geopolymer concrete mix proportion procedure proposed by Mallikarjuna Rao et al., 2016 was considered for our study. The mix proportions shown in table 5.7 were adopted after making different trials, in casting geopolymer concrete push-off specimens, with different strengths.

Table 5.7: Mix proportions of geopolymer concrete

Mix Type (Range for Grade of Concrete) N/mm^2	Fly ash (kg/m^3) (F)	GGBS (kg/m^3) (G)	Fine aggregate (kg/m^3)	Coarse aggregate (kg/m^3)	NaOH (kg/m^3) M = 8	Na_2SiO_3 (kg/m^3)	Alkaline liquid (kg/m^3) (A)	Superplasticiser (kg/m^3)
	Na_2SiO_3/NaOH = 2.5							
A (20 - 25)	294	126	812	965	66	165	231	4.20
B (20 - 25)	294	126	812	965	72	180	252	8.82
C (40 - 45)	252	168	812	965	66	165	231	12.60
D (50 - 55)	210	210	812	965	60	150	210	14.70

5.6 SPECIMEN PREPARATION

5.6.1 Push-off specimen - size and reinforcement details

The geopolymer concrete push-off specimen shown in figure 5.4 has been used to study the shear transfer behavior. The push-off specimen consists of two identical “L” shaped halves with an overall size of 500 mm x 200 mm x 100 mm. The reinforcement in each L-shaped half consists of four 10 mm diameter bars having a yield strength of 500 MPa as main reinforcement and 6 mm diameter rings as stirrups. The amount of reinforcement adopted was based on the criteria of avoiding flexural failure of the cantilever part of the push-off specimen. The reinforcement crossing the monolithic interface of the geopolymer concrete push-off specimen consists of varying numbers (two, three, and four) of 2 legged 6 mm diameter mild steel horizontal ties representing 0.51, 0.77, and 1.02% respectively. The reinforcement crossing the interface has a yield strength of 250 MPa and they were placed across the shear plane in the form of closed links. The details of reinforcement of push-off specimen are shown in figure

5.5. V grooves of 4 mm deep were made on either side of the push-off specimen along the shear plane for ensuring the formation and direction of the shear crack.

5.6.2 Mixing, casting, and curing of geopolymer concrete specimens

The mix considered for the specimen preparation is in accordance with mix proportions given in table 5.7. A rotational drum-type pan mixer of 100 kg capacity was used to mix the dry materials for three minutes, which was later mixed with an alkaline solution and superplasticizer. A homogenous mixture was achieved after mixing it for five minutes. Fresh geopolymer concrete mixture was placed in push-off moulds and compacted on a jolting table. The top surface of moulds was levelled with a trowel after compaction. The push-off specimens were cast with and without reinforcement across the shear interface (figure 5.6).

After 24 hrs. of casting, specimens were de-moulded and air-cured for 28 days. The average room temperature and relative humidity measured during the period of curing were 35±5 ºC and 75% respectively (figure 5.7).

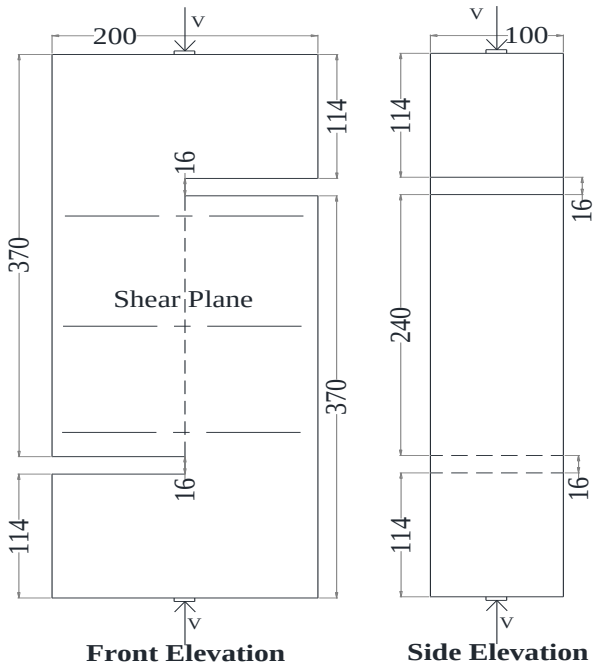

Figure 5.4: The push-off specimen

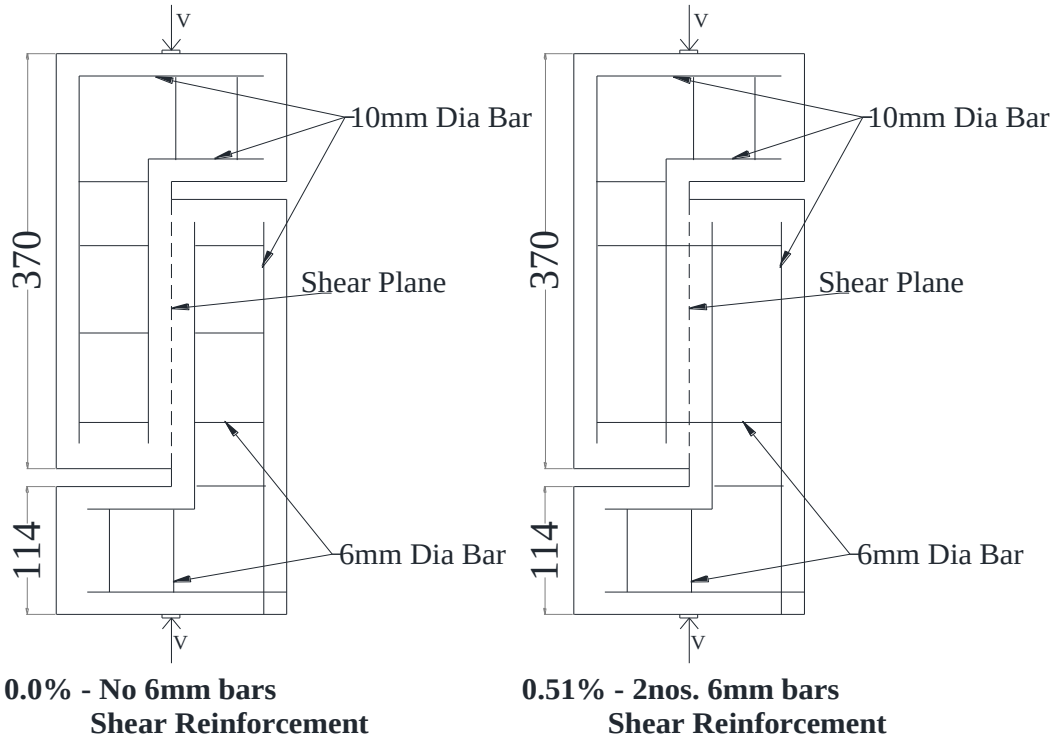

a. 0% and 0.51% of shear reinforcement

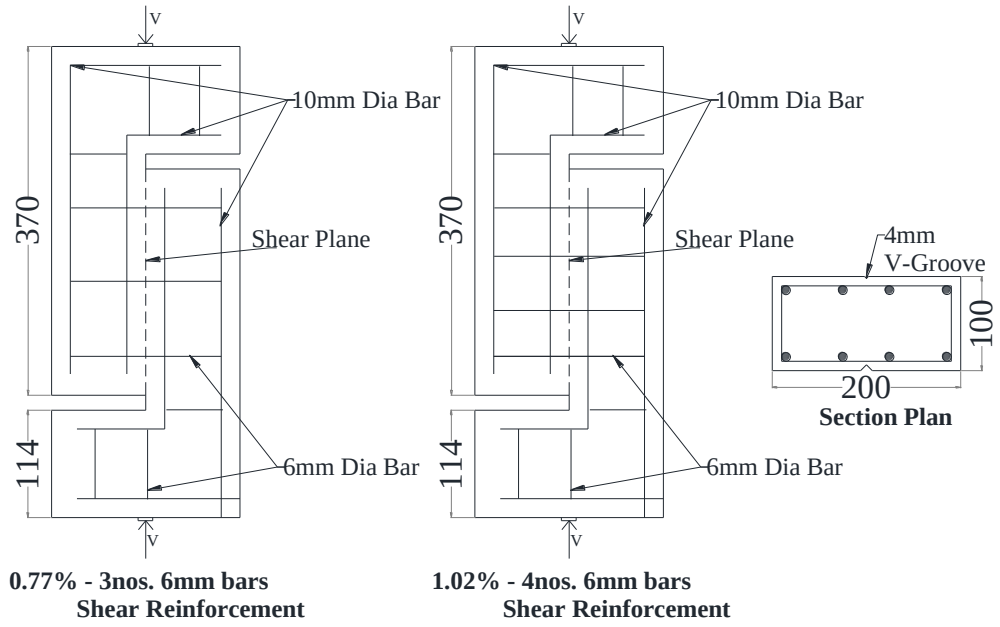

b. 0.77% and 1.02% of shear reinforcement

Figure 5.5: Reinforcement details for push-off specimen

Push-off specimen mould

Push-off specimen with reinforcement before casting

Reinforcement configuration

The casting of push-off specimens and cubes

Figure 5.6: Push-off specimen casting details

Figure 5.7: Ambient temperature curing for 28 days

5.6.3 Testing of geopolymer concrete push-off specimen

The experimental setup in testing the push-off specimens is shown in figure 5.8. The samples were loaded axially using a 2000 kN Tinius Olsen Testing machine. The push-off specimens were accurately aligned. LVDT's (Linear Variable Differential Transformer or Linear Displacement Transducer) and load cell of capacity 2000 kN were used to record the displacement and load respectively, which were connected to data acquisition and control system.

Figure 5.8: Test setup

The push-off specimens with and without reinforcement across the interface tested failed by developing cracks along with the interface. The experimental shear strength of push-off specimens with and without reinforcement across the interface (ν_{ur}, ν_{up}) was calculated by dividing the failure load (P_u) by the cross-sectional area of the interface. The failure patterns of the push-off specimens are shown in figure 5.9. The axial loads at failure (ultimate load) were recorded and tabulated in table 5.8.

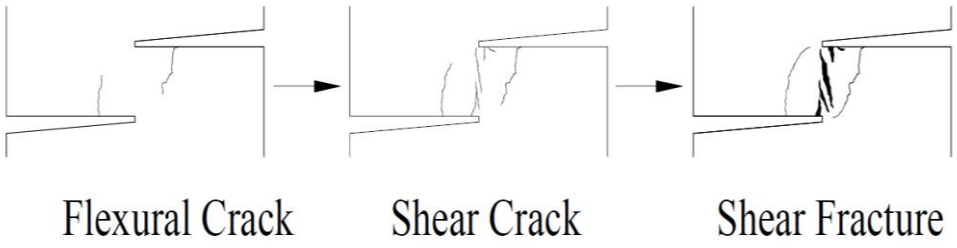

Cracking pattern sequence of the push-off specimen by Kaneko et al., 2003

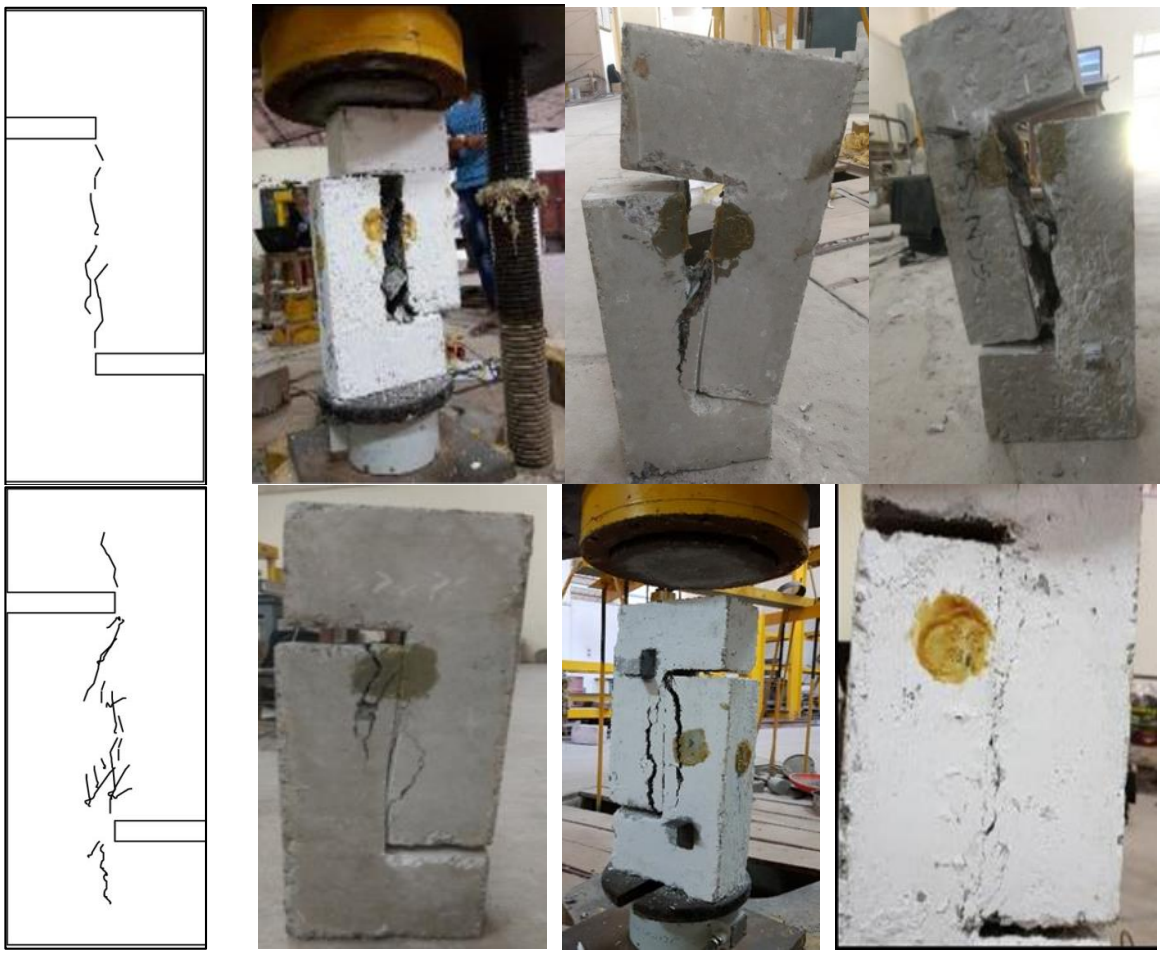

Figure 5.9: Failure pattern for unreinforced and reinforced across the shear plane

Table. 5.8. The Ultimate loads, Shear strength of GPC push-off specimens

Average compressive strength (f_{gpc}) N/mm^2	Designation	Shear strength P_u kN	Shear stress υ_{up} N/mm^2	υ_{up} / f_{gpc}		Average compressive strength (f_{gpc}) N/mm^2	Designation	Shear strength P_u kN	Shear stress υ_{ur} N/mm^2	υ_{ur} / f_{gpc}	(υ_{ur} - υ_{up}) / υ_{up}
With no reinforcement across the shear Interface						With 0.51% of reinforcement across the shear Interface					
27.68	G3SB01	60.26	2.73	0.10		27.68	G3SB21	96.31	4.36	0.16	0.60
27.68	G3SB02	61.37	2.78	0.10		27.68	G3SB22	99.11	4.49	0.16	0.62
27.68	G3SB03	60.80	2.75	0.10		27.68	G3SB23	98.21	4.45	0.16	0.62
40.30	G3SC01	95.97	4.35	0.11		40.30	G3SC21	140.53	6.36	0.16	0.46
40.30	G3SC02	98.42	4.46	0.11		40.30	G3SC22	144.80	6.56	0.16	0.47
40.30	G3SC03	96.06	4.35	0.11		40.30	G3SC23	138.88	6.29	0.16	0.45
53.81	G3SD01	108.00	4.89	0.09		53.81	G3SD21	172.95	7.83	0.15	0.60
53.81	G3SD02	105.61	4.78	0.09		53.81	G3SD22	177.15	8.02	0.15	0.68
53.81	G3SD03	110.38	5.00	0.09		53.81	G3SD23	171.25	7.76	0.14	0.55
Total				**0.10**		**Total**				**0.16**	**0.56**
With no reinforcement across the shear Interface						With 0.77% of reinforcement across the shear Interface					
27.29	G1SA01	62.30	2.82	0.10		27.29	G1SA31	142.39	6.45	0.24	1.29
32.04	G1SA02	71.20	3.22	0.10		32.04	G1SA32	155.74	7.05	0.22	1.19
35.99	G1SA03	80.10	3.63	0.10		35.99	G1SA33	186.89	8.46	0.24	1.33
26.50	G2SA01	61.56	2.79	0.11		26.50	G2SA31	127.92	5.79	0.22	1.08
28.88	G2SA02	64.91	2.94	0.10		28.88	G2SA32	137.61	6.23	0.22	1.12
31.29	G2SA03	66.50	3.01	0.10		31.29	G2SA33	156.64	7.09	0.23	1.36
27.68	G3SB01	60.26	2.73	0.10		30.26	G3SB31	144.94	6.56	0.22	1.20
27.68	G3SB02	61.37	2.78	0.10		30.26	G3SB32	147.71	6.69	0.22	1.20
27.68	G3SB03	60.80	2.75	0.10		30.26	G3SB33	146.65	6.64	0.22	1.21
37.28	G1SC01	89.00	4.03	0.11		37.28	G1SC31	213.59	9.67	0.26	1.40
37.77	G1SC02	93.45	4.23	0.11		37.77	G1SC32	213.59	9.67	0.26	1.29

Table. 5.8. The Ultimate loads, Shear strength of GPC push-off specimens

Average compressive strength (f_{gpc}) N/mm^2	Designation	Shear strength P_u kN	Shear stress υ_{up} N/mm^2	υ_{up} / f_{gpc}		Average compressive strength (f_{gpc}) N/mm^2	Designation	Shear strength P_u kN	Shear stress υ_{ur} N/mm^2	υ_{ur} / f_{gpc}	(υ_{ur} - υ_{up}) / υ_{up}
38.57	G1SC03	97.90	4.43	0.11		38.57	G1SC33	222.49	10.08	0.26	1.27
38.57	G2SC01	95.45	4.32	0.11		38.57	G2SC31	215.27	9.75	0.25	1.26
40.65	G2SC02	98.72	4.47	0.11		40.65	G2SC32	228.14	10.33	0.25	1.31
41.76	G2SC03	101.16	4.58	0.11		41.76	G2SC33	225.62	10.22	0.24	1.23
40.30	G3SC01	95.97	4.35	0.11		41.90	G3SC31	206.48	9.35	0.22	1.07
40.30	G3SC02	98.42	4.46	0.11		41.90	G3SC32	208.50	9.44	0.23	1.04
40.30	G3SC03	96.06	4.35	0.11		41.90	G3SC33	205.84	9.32	0.22	1.06
41.10	G1SD01	102.35	4.64	0.11		41.10	G1SD31	226.94	10.28	0.25	1.22
48.11	G1SD02	106.80	4.84	0.10		48.11	G1SD32	241.39	10.93	0.23	1.26
52.86	G1SD03	111.25	5.04	0.10		52.86	G1SD33	258.09	11.69	0.22	1.32
48.04	G2SD01	107.69	4.88	0.10		48.04	G2SD31	238.02	10.78	0.22	1.21
53.69	G2SD02	121.41	5.50	0.10		53.69	G2SD32	265.74	12.04	0.22	1.19
54.09	G2SD03	127.92	5.79	0.11		54.09	G2SD33	276.68	12.53	0.23	1.16
53.81	G3SD01	108.00	4.89	0.09		55.70	G3SD31	262.44	11.89	0.21	1.35
53.81	G3SD02	105.61	4.78	0.09		55.70	G3SD32	259.29	11.74	0.21	1.37
53.81	G3SD03	110.38	5.00	0.09		55.70	G3SD33	261.22	11.83	0.21	1.29
Total				**0.10**		**Total**				**0.23**	**1.23**
With no reinforcement across the shear Interface						With 1.02% of reinforcement across the shear Interface					
27.68	G3SB01	60.26	2.73	0.10		30.26	G3SB41	178.46	8.08	0.27	1.71
27.68	G3SB02	61.37	2.78	0.10		30.26	G3SB42	183.14	8.29	0.27	1.73
27.68	G3SB03	60.80	2.75	0.10		30.26	G3SB43	177.85	8.05	0.27	1.68
40.30	G3SC01	95.97	4.35	0.11		41.90	G3SC41	249.05	11.28	0.27	1.50
40.30	G3SC02	98.42	4.46	0.11		41.90	G3SC42	252.00	11.41	0.27	1.46

Table. 5.8. The Ultimate loads, Shear strength of GPC push-off specimens

Average compressive strength (f_{gpc}) N/mm^2	Designation	Shear strength P_u kN	Shear stress υ_{up} N/mm^2	υ_{up} / f_{gpc}		Average compressive strength (f_{gpc}) N/mm^2	Designation	Shear strength P_u kN	Shear stress υ_{ur} N/mm^2	υ_{ur} / f_{gpc}	(υ_{ur} - υ_{up}) / υ_{up}
40.30	G3SC03	96.06	4.35	0.11		41.90	G3SC43	255.10	11.55	0.28	1.55
53.81	G3SD01	108.00	4.89	0.09		55.70	G3SD41	324.30	14.69	0.26	1.90
53.81	G3SD02	105.61	4.78	0.09		55.70	G3SD42	320.77	14.53	0.26	1.93
53.81	G3SD03	110.38	5.00	0.09		55.70	G3SD43	322.88	14.62	0.26	1.83
Total				**0.10**		**Total**				**0.27**	**1.70**

Notation:

f_{gpc}	=	Concrete compressive strength of 150 mm cube (MPa)	ν_{up}	=	Shear stress at the unreinforced interface (MPa) = P_u/bh
P_u	=	Average experimental peak load (kN)	ν_{ur}	=	Shear stress at the reinforced interface (MPa) = P_u/bh
bh	=	Cross sectional area of the interface = 92 x 240 mm^2			

5.6.4 Observations during the test

During testing, the crack along the shear plane was nearly sudden in the case of push-off specimens with no reinforcement across the interface. However, in the case of push-off specimens having reinforcement across the shear interface, a noticeable crack along the shear plane was observed at about 70 to 80 percent of the ultimate loads. Due to the provision of adequate reinforcement in both halves of the push-off specimen, none of the specimens failed prematurely due to flexure in horizontal or vertical arms of the push-off specimen. The variation of shear strength of geopolymer concrete obtained by testing the push-off specimens (with and without reinforcement across the monolithic interface) with the compressive strength of geopolymer concrete is shown in figure 5.10. It is observed that the shear strength of geopolymer concrete increased with an increase in the compressive strength of GPC.

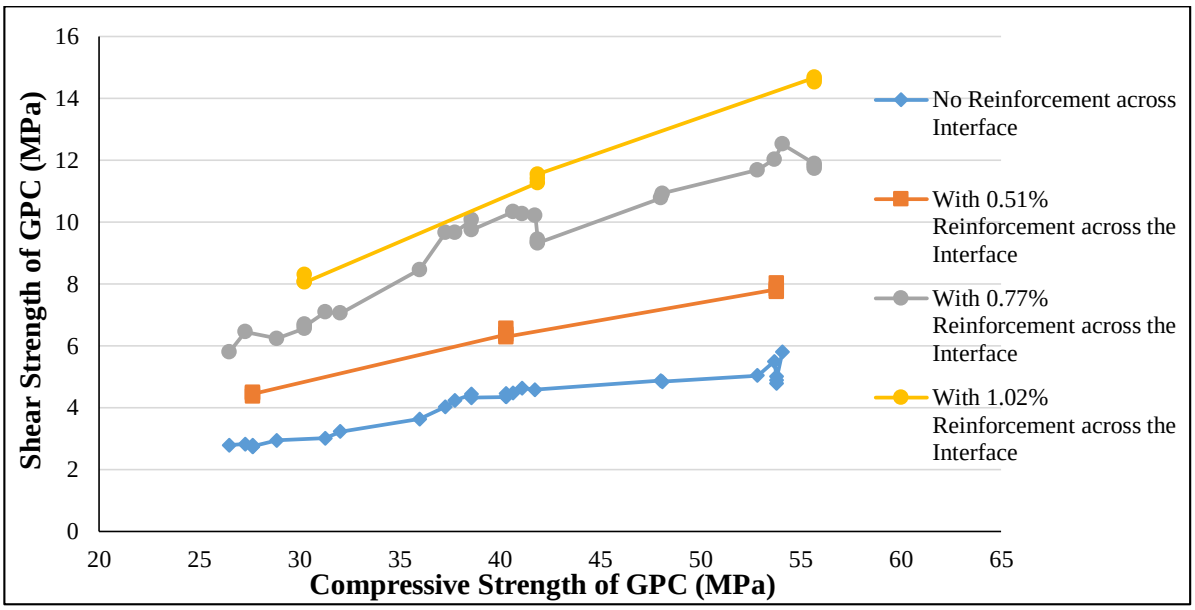

Figure 5.10: Shear strength vs. Compressive strength of GPC

5.7 RESULTS AND DISCUSSIONS

From the test results shown in table 5.8, it is observed that the average shear strength of geopolymer concrete at the unreinforced monolithic interface is about 10% of its compressive strength. In the case of reinforced interfaces, the shear strength of geopolymer concrete was

observed to be about 16%, 23%, and 27% of its compressive strength for 0.51%, 0.77%, and 1.02% percentage of reinforcement (ρ) crossing the interface respectively.

In the uncracked stage, the shear across the interface in the push-off specimen was assumed to be resisted predominantly by the cohesion due to the aggregate interlock of the concrete. After the initiation of the crack along the shear plane, the cohesion of concrete reduces and other mechanisms such as friction and resistance (dowel action) of reinforcement across the interface come into action. Eventually, the shear strength at the interface is mainly resisted by the bending resistance of reinforcement across the interface. This may be attributed to the diminishing effect of aggregate interlock with an increase in concrete strength (Walraven, 1981). There is a marked increase of shear strength with compressive strength in the presence of reinforcement across the interface. The higher increase is due to the bending resistance (dowel action) of reinforcement across the interface. The shear strength of the reinforced interface when compared with that of the unreinforced one indicates that the shear strength of geopolymer concrete at the interface increased with the provision of reinforcement. The increase in the shear strength of reinforced geopolymer concrete is about 56 %, 123 %, and 170 % to the corresponding unreinforced geopolymer concrete shear strength of 0.51 %, 0.77 %, and 1.02 % percentage of reinforcement (ρ) crossing the interface respectively.

In the following sections, the shear strength of the unreinforced GPC interface was used to arrive at the cohesion factor of GPC. In the case of reinforced interfaces of GPC, the added contribution to the shear strength of GPC due to friction was evaluated based on different theories available in the literature. Further, the coefficient of dowel action (α) that influences the contribution of dowel action in enhancing the shear strength of reinforced interfaces of GPC was evaluated. Finally, the shear strength (V_u) across the monolithic interface of GPC was expressed as a summation of strength due to cohesion, friction, and dowel action which is in line with the shear strength expression given by Randl, 1997 for ordinary concrete.

Therefore the shear strength of reinforced interface of GPC was given by Randl, 1997 as:

$$V_u = \underbrace{cf_c^{1/3}}_{\text{Cohesion}} + \underbrace{\mu[\sigma_n + \rho k f_y]}_{\text{Friction}} + \underbrace{\alpha\rho\sqrt{f_y f_c}}_{\text{Dowel Action}} \quad \text{- Eq. 5.1}$$

Where, v_u- Ultimate longitudinal shear stress at the interface;

c - Coefficient of cohesion; μ - Coefficient of friction; ρ - Reinforcement ratio;

k - Coefficient of efficiency for shear reinforcement to transmit the tensile force;

f_c - Characteristic value of concrete compressive strength;

f_y - Characteristic value of yield strength of the reinforcement;

σ_n - normal stress at the interface due to external loading;

α - Coefficient for dowel action (flexural resistance of reinforcement);

5.7.1 Geopolymer concrete shear strength at the interface due to cohesion

In the push-off specimens without reinforcements across the interface, the shear force was resisted by cohesion i.e. bond between geopolymer products and aggregate which indirectly depends on the compressive strength of geopolymer concrete. From the analytical and experimental investigation presented in chapter 4, it is concluded that the compressive strength of geopolymer concrete can be correlated to the binder index of geopolymer concrete. The shear strength of the unreinforced geopolymer concrete interface was used to arrive at the coefficient of cohesion (c) of GPC and the same is given in Table 5.9. A plot between average compressive strength and average coefficient of friction for geopolymer concrete is shown in figure. 5.11.

It is observed that the compressive strength of geopolymer concrete varies bi-linearly with coefficient of cohesion i.e. "c". The compressive strength of geopolymer concrete is linearly increasing up to 40 MPa and thereafter the rate at which it increases is lower compared with earlier change. However, two linear equations for measuring the coefficient of cohesion are provided. Based on the graph, coefficient of cohesion c is predicted as:

For $f_{gpc} \leq 40$ MPa, $c = 0.031f_{gpc}+0.06$ - Eq. 5.2

For $f_{gpc} > 40$ MPa, $c = 0.0054f_{gpc}+1.0809$ - Eq. 5.3

The correlation coefficient between the predicted values with respect to experimentally obtained values of the coefficient of cohesion is 0.992.

Table. 5.9. Coefficient of cohesion for GPC specimens unreinforced across the shear plane

Specimen ID	f_{gpc} MPa	P_u kN	ν_{up} N/mm^2	$c = \nu_{up}/(f_{gpc})^{1/3}$ MPa	Avg f_{gpc}	Avg "c"	Predicted c For $f_{gpc} < 40$ MPa, $c = 0.031 f_{gpc} + 0.06$ For $f_{gpc} \geq 40$ MPa, $c = 0.0054 f_{gpc} + 1.0809$
G2SA01	26.50	61.56	2.79	0.935	27.62	0.93	0.92
G1SA01	27.29	62.30	2.82	0.937			
G3SB01	27.68	60.26	2.73	0.902			
G3SB02	27.68	61.37	2.78	0.919			
G3SB03	27.68	60.80	2.75	0.910			
G2SA02	28.88	64.91	2.94	0.958			
G2SA03	31.29	66.50	3.01	0.956	31.66	0.99	1.04
G1SA02	32.04	71.20	3.22	1.015			
G1SA03	35.99	80.10	3.63	1.099	37.64	1.23	1.23
G1SC01	37.28	89.00	4.03	1.207			
G1SC02	37.77	93.45	4.23	1.261			
G1SC03	38.57	97.90	4.43	1.312			
G2SC01	38.57	95.45	4.32	1.279			
G3SC01	40.30	95.97	4.35	1.268	40.74	1.30	1.30
G3SC02	40.30	98.42	4.46	1.300			
G3SC03	40.30	96.06	4.35	1.269			
G2SC02	40.65	98.72	4.47	1.300			
G1SD01	41.10	102.35	4.64	1.343			
G2SC03	41.76	101.16	4.58	1.321			
G2SD01	48.04	107.69	4.88	1.342	48.07	1.34	1.34
G1SD02	48.11	106.80	4.84	1.330			
G1SD03	52.86	111.25	5.04	1.342	53.68	1.37	1.37
G2SD02	53.69	121.41	5.50	1.458			
G3SD01	53.81	108.00	4.89	1.296			
G3SD02	53.81	105.61	4.78	1.267			
G3SD03	53.81	110.38	5.00	1.324			
G2SD03	54.09	127.92	5.79	1.532			

Notation:

f_{gpc} = Concrete compressive strength of 150 mm cube (MPa)

P_u = Average experimental peak load (kN)

c = Coefficient of cohesion.

ν_{up} = Shear Stress at the unreinforced interface (MPa) = P_u/bh

bh = Cross sectional area of the interface = 92 x 240 mm^2

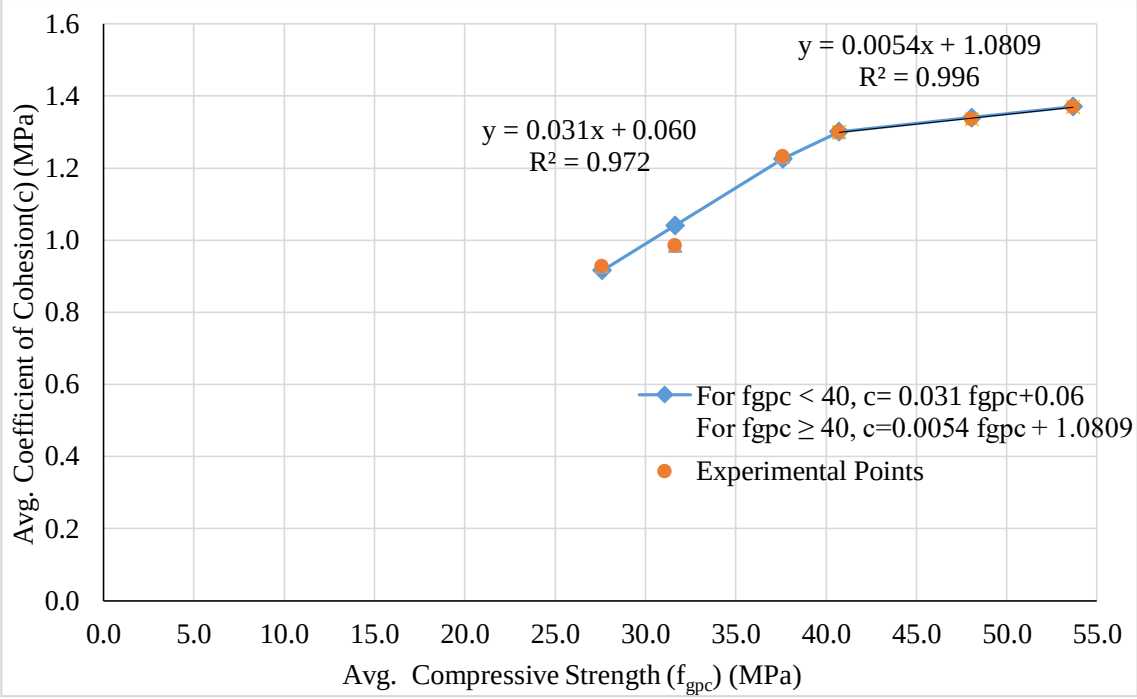

Figure 5.11: Coefficient of cohesion vs. Compressive strength of GPC

5.7.2 Evaluation of coefficient of dowel action influencing the shear strength of reinforced geopolymer concrete interface

The reinforced push-off specimens tested in this study consisted of varying shear reinforcements across the interface in the form of two, three, and four equally spaced 6 mm diameter closed rectangular stirrups representing percentage steel equal to 0.51%, 0.77%, and 1.02% respectively. The shear across the interface in these specimens was resisted by the combined action of cohesion, friction, and bending resistance (dowel action) of steel across the shear plane. The shear strength of the monolithic GPC interface (V_u) is determined as follows:

$$V_u = V_c + V_f + V_d \quad \text{- Eq. 5.4}$$

Where,

V_c = Shear strength of unreinforced GPC due to cohesion = c $(f_{gpc})^{(1/3)}$ bh, where For $f_{gpc} \leq 40$ MPa, c = 0.031 f_{gpc}+0.06, For f_{gpc}>40 MPa, c = 0.0054f_{gpc}+1.0809

V_f = Shear strength of reinforced GPC due to friction = $\mu[\sigma_n+\rho k f_y]$ bh, where k=0.5 and $f_{gpc} \geq 20$ MPa μ =0.8, $f_{gpc} \geq 35$ MPa μ =1.0, $\rho = \rho_{Main} + \rho_{Stirrups}$ (Randl, 1997)

V_d = Shear strength of reinforced GPC due to dowel action = $\alpha\rho\sqrt{f_y f_{gpc}}$ bh

$\rho = \rho_{Stirrups}$

Cohesion contribution is evaluated by considering the coefficient of cohesion from unreinforced geopolymer concrete specimens developed via equations 5.2 and 5.3. Friction contribution was calculated by considering friction coefficient and 'k' in line with Randl, 1997 assumptions as it is derived based on the yield strength of reinforcement steel and the percentage of steel involved which is the sum of both closed and open-ended bars (A_{main} + $A_{stirrups}$). The normal stress, σ_n at the interface at failure is taken as zero as there are no clamping forces in the push-off specimens tested.

Dowel resistance (dowel action) of reinforcement across the interface contribution is calculated by deducting cohesion and friction contributions from the experimental shear strength of the reinforced geopolymer concrete push-off specimen. Accordingly, the coefficient of dowel action (α) is calculated and the same is tabulated in table 5.10. In this case, reinforcement across the interface is provided in the form of closed stirrups/ties. $A = A_{stirrups}$

It is observed from figure 5.12 that the coefficient of dowel action in geopolymer concrete linearly varies with $\rho\sqrt{(f_y f_c)}$ and the coefficient of dowel action $\alpha = 6.338\ \rho\sqrt{f_y f_{gpc}}$ with R^2 of 0.932.

Table. 5.10. Cohesion contribution, Friction contribution, and calculation of the coefficient of dowel action of GPC

Specimen ID	f_{gpc} MPa	P_u kN	% of Stirrups	c MPa	V_c kN	V_f kN	V_d kN	$\alpha = V_d / \rho\sqrt{(fyfc)bd}$	$\rho\sqrt{f_y f_{gpc}}$	Predicted $\alpha = 6.338\ \rho\sqrt{f_y f_{gpc}}$
UNREINFORCED GPC INTERFACE										
G1SA01	27.29	62.30	0.00	0.906	60.23	0.00	0.00	0.00	0.000	0.00
G1SA02	32.04	71.20	0.00	1.053	73.86	0.00	0.00	0.00	0.000	0.00
G1SA03	35.99	80.10	0.00	1.176	85.70	0.00	0.00	0.00	0.000	0.00
G2SA01	26.50	61.56	0.00	0.881	58.02	0.00	0.00	0.00	0.000	0.00
G2SA02	28.88	64.91	0.00	0.955	64.70	0.00	0.00	0.00	0.000	0.00
G2SA03	31.29	66.50	0.00	1.030	71.65	0.00	0.00	0.00	0.000	0.00
G3SB01	27.68	60.26	0.00	0.918	61.33	0.00	0.00	0.00	0.000	0.00
G3SB02	27.68	61.37	0.00	0.918	61.33	0.00	0.00	0.00	0.000	0.00
G3SB03	27.68	60.80	0.00	0.918	61.33	0.00	0.00	0.00	0.000	0.00
G3SC01	40.30	95.97	0.00	1.299	98.30	0.00	0.00	0.00	0.000	0.00
G3SC02	40.30	98.42	0.00	1.299	98.30	0.00	0.00	0.00	0.000	0.00
G3SC03	40.30	96.06	0.00	1.299	98.30	0.00	0.00	0.00	0.000	0.00
G1SC01	37.28	89.00	0.00	1.216	89.67	0.00	0.00	0.00	0.000	0.00
G1SC02	37.77	93.45	0.00	1.231	91.20	0.00	0.00	0.00	0.000	0.00
G1SC03	38.57	97.90	0.00	1.256	93.66	0.00	0.00	0.00	0.000	0.00
G2SC01	38.57	95.45	0.00	1.256	93.68	0.00	0.00	0.00	0.000	0.00
G2SC02	40.65	98.72	0.00	1.300	98.73	0.00	0.00	0.00	0.000	0.00
G2SC03	41.76	101.16	0.00	1.306	100.08	0.00	0.00	0.00	0.000	0.00
G1SD01	41.10	102.35	0.00	1.303	99.28	0.00	0.00	0.00	0.000	0.00
G1SD02	48.11	106.80	0.00	1.341	107.66	0.00	0.00	0.00	0.000	0.00
G1SD03	52.86	111.25	0.00	1.366	113.22	0.00	0.00	0.00	0.000	0.00
G2SD01	48.04	107.69	0.00	1.340	107.58	0.00	0.00	0.00	0.000	0.00
G2SD02	53.69	121.41	0.00	1.371	114.19	0.00	0.00	0.00	0.000	0.00

Table. 5.10. Cohesion contribution, Friction contribution, and calculation of the coefficient of dowel action of GPC

Specimen ID	f_{gpc} MPa	P_u kN	% of Stirrups	c MPa	V_c kN	V_f kN	V_d kN	$\alpha = V_d / \rho\sqrt{(fyfc)bd}$	$\rho\sqrt{f_y f_{gpc}}$	Predicted $\alpha = 6.338\ \rho\sqrt{f_y f_{gpc}}$
G2SD03	54.09	127.92	0.00	1.373	114.65	0.00	0.00	0.00	0.000	0.00
G3SD01	53.81	108.00	0.00	1.371	114.33	0.00	0.00	0.00	0.000	0.00
G3SD02	53.81	105.61	0.00	1.371	114.33	0.00	0.00	0.00	0.000	0.00
G3SD03	53.81	110.38	0.00	1.371	114.33	0.00	0.00	0.00	0.000	0.00
REINFORCED GPC INTERFACE										
G3SB21	27.68	96.31	0.51	0.918	61.33	11.31	23.68	2.52	0.426	2.70
G3SB22	27.68	99.11	0.51	0.918	61.33	11.31	26.48	2.81	0.426	2.70
G3SB23	27.68	98.21	0.51	0.918	61.33	11.31	25.58	2.72	0.426	2.70
G3SC21	40.30	140.53	0.51	1.299	98.30	14.14	28.09	2.47	0.514	3.26
G3SC22	40.30	144.80	0.51	1.299	98.30	14.14	32.36	2.85	0.514	3.26
G3SC23	40.30	138.88	0.51	1.299	98.30	14.14	26.44	2.33	0.514	3.26
G3SD21	53.81	172.95	0.51	1.371	114.33	14.14	44.48	3.39	0.594	3.77
G3SD22	53.81	177.15	0.51	1.371	114.33	14.14	48.69	3.71	0.594	3.77
G3SD23	53.81	171.25	0.51	1.371	114.33	14.14	42.79	3.26	0.594	3.77
G2SA31	26.50	127.92	0.77	0.881	58.02	16.96	52.93	3.83	0.625	3.96
G1SA31	27.29	142.39	0.77	0.906	60.23	16.96	65.20	4.65	0.635	4.02
G2SA32	28.88	137.61	0.77	0.955	64.70	16.96	55.94	3.88	0.653	4.14
G3SB31	30.26	144.94	0.77	0.998	68.66	16.96	59.31	4.02	0.668	4.24
G3SB32	30.26	147.71	0.77	0.998	68.66	16.96	62.08	4.21	0.668	4.24
G3SB33	30.26	146.65	0.77	0.998	68.66	16.96	61.02	4.14	0.668	4.24
G2SA33	31.29	156.64	0.77	1.030	71.65	16.96	68.02	4.53	0.680	4.31
G1SA32	32.04	155.74	0.77	1.053	73.86	16.96	64.92	4.28	0.688	4.36
G1SA33	35.99	186.89	0.77	1.176	85.70	21.21	79.99	4.97	0.729	4.62

Table. 5.10. Cohesion contribution, Friction contribution, and calculation of the coefficient of dowel action of GPC

Specimen ID	f_{gpc} MPa	P_u kN	% of Stirrups	c MPa	V_c kN	V_f kN	V_d kN	$\alpha = V_d / \rho\sqrt{(fyfc)bd}$	$\rho\sqrt{f_y f_{gpc}}$	Predicted $\alpha = 6.338\ \rho\sqrt{f_y f_{gpc}}$
G1SC31	37.28	213.59	0.77	1.216	89.67	21.21	102.72	6.27	0.742	4.70
G1SC32	37.77	213.59	0.77	1.231	91.20	21.21	101.19	6.14	0.747	4.73
G1SC33	38.57	222.49	0.77	1.256	93.66	21.21	107.63	6.46	0.754	4.78
G2SC31	38.57	215.27	0.77	1.256	93.68	21.21	100.38	6.03	0.754	4.78
G2SC32	40.65	228.14	0.77	1.300	98.73	21.21	108.21	6.33	0.775	4.91
G1SD31	41.10	226.94	0.77	1.303	99.28	21.21	106.46	6.19	0.779	4.94
G2SC33	41.76	225.62	0.77	1.306	100.08	21.21	104.34	6.02	0.785	4.98
G3SC31	41.90	206.48	0.77	1.307	100.24	21.21	85.04	4.90	0.786	4.98
G3SC32	41.90	208.50	0.77	1.307	100.24	21.21	87.05	5.01	0.786	4.98
G3SC33	41.90	205.84	0.77	1.307	100.24	21.21	84.39	4.86	0.786	4.98
G2SD31	48.04	238.02	0.77	1.340	107.58	21.21	109.23	5.88	0.842	5.34
G1SD32	48.11	241.39	0.77	1.341	107.66	21.21	112.52	6.05	0.843	5.34
G1SD33	52.86	258.09	0.77	1.366	113.22	21.21	123.66	6.34	0.883	5.60
G2SD32	53.69	265.74	0.77	1.371	114.19	21.21	130.35	6.63	0.890	5.64
G2SD33	54.09	276.68	0.77	1.373	114.65	21.21	140.83	7.14	0.893	5.66
G3SD31	55.70	262.44	0.77	1.382	116.51	21.21	124.73	6.23	0.907	5.75
G3SD32	55.70	259.29	0.77	1.382	116.51	21.21	121.58	6.07	0.907	5.75
G3SD33	55.70	261.22	0.77	1.382	116.51	21.21	123.50	6.17	0.907	5.75
G3SB41	30.26	178.46	1.02	0.998	68.66	22.62	87.18	4.43	0.891	5.65
G3SB42	30.26	183.14	1.02	0.998	68.66	22.62	91.86	4.67	0.891	5.65
G3SB43	30.26	177.85	1.02	0.998	68.66	22.62	86.57	4.40	0.891	5.65
G3SC41	41.90	249.05	1.02	1.307	100.24	28.27	120.54	5.21	1.048	6.64
G3SC42	41.90	252.00	1.02	1.307	100.24	28.27	123.49	5.33	1.048	6.64
G3SC43	41.90	255.10	1.02	1.307	100.24	28.27	126.59	5.47	1.048	6.64

Table. 5.10. Cohesion contribution, Friction contribution, and calculation of the coefficient of dowel action of GPC

Specimen ID	f_{gpc} MPa	P_u kN	% of Stirrups	c MPa	V_c kN	V_f kN	V_d kN	$\alpha = V_d / \rho\sqrt{(fyfc)}bd$	$\rho\sqrt{f_y f_{gpc}}$	Predicted $\alpha = 6.338\,\rho\sqrt{f_y f_{gpc}}$
G3SD41	55.70	324.30	1.02	1.382	116.51	28.27	179.52	6.73	1.209	7.66
G3SD42	55.70	320.77	1.02	1.382	116.51	28.27	175.99	6.59	1.209	7.66
G3SD43	55.70	322.88	1.02	1.382	116.51	28.27	178.10	6.67	1.209	7.66

Notation:

f_{gpc} = Concrete compressive strength of 150 mm cube (MPa) f_y = Yield strength of reinforcement across interface = 250 MPa

P_u = Experimental peak load (kN) bh = Cross sectional area of the interface = 92 x 240 mm^2

V_c = Cohesion contribution, c $(f_{gpc})^{(1/3)}$ bh (kN), where For $f_{gpc} \leq 40$ MPa, c = 0.031 f_{gpc}+0.06, For f_{gpc}>40 MPa, c = 0.005f_{gpc}+1.0809

V_f = Friction contribution, $\mu[\sigma_n+\rho k f_y]$ bh (kN) V_d = Dowel contribution, $\alpha\rho\sqrt{f_y f_{gpc}}$ bh (kN)

V_d = **For the reinforced GPC interface: $V_d = P_u - V_c - V_f$**
For the unreinforced GPC interface: Vd=0

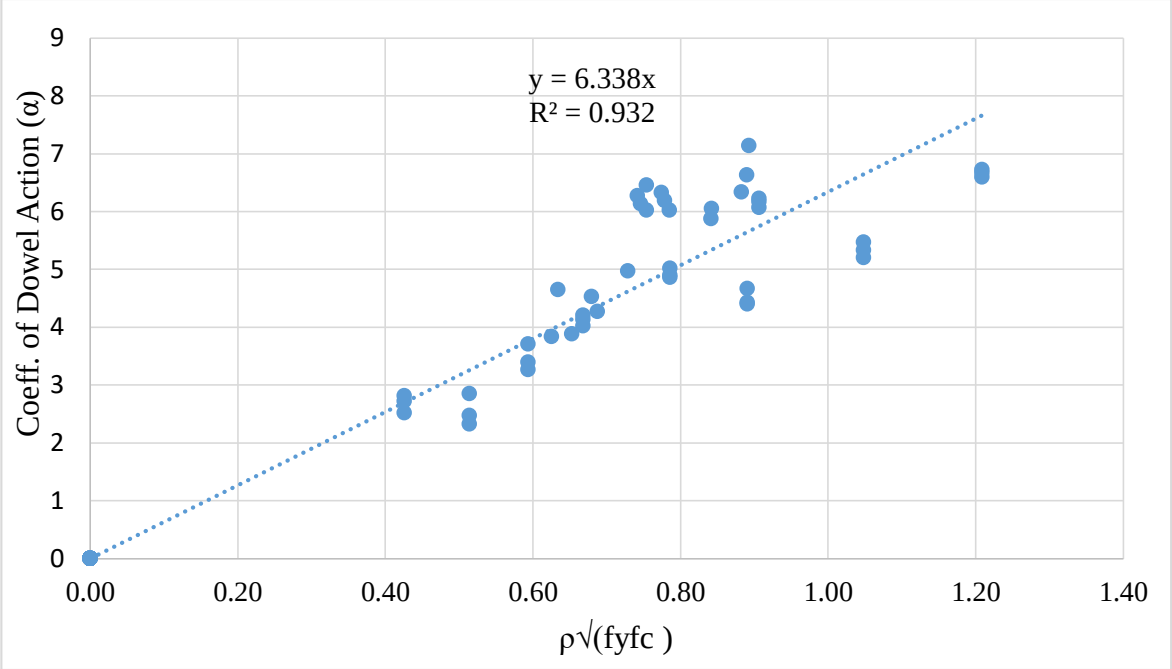

Figure 5.12: Variation of coefficient of dowel action in GPC

Therefore, the shear strength of the monolithic geopolymer concrete interface (Vu) is given as Eq. 5.4 is as follows:

$$V_u = V_c + V_f + V_d$$

Where,

V_c = Shear strength of unreinforced GPC due to cohesion = c $(f_{gpc})^{(1/3)}$ bh, where For $f_{gpc} \leq 40$ MPa, c = 0.031 f_{gpc}+0.06, For f_{gpc}>40 MPa, c = 0.0054f_{gpc}+1.0809

V_f = Shear strength of reinforced GPC due to friction = $\mu[\sigma_n+\rho k f_y]$ bh, where k=0.5 and $f_{gpc} \geq 20$ MPa μ =0.8, $f_{gpc} \geq 35$ MPa μ =1.0, $\rho = \rho_{Main} + \rho_{Stirrups}$ (Randl, 1997)

V_d = Shear Strength due to Dowel contribution = $\alpha\rho\sqrt{f_y f_{gpc}}$bh, $\rho = \rho_{Stirrups}$ where $\alpha = 6.338\,\rho\sqrt{f_y f_{gpc}}$

The proposed shear strength equations are based on Cube strength and SI units.

5.7.3 Comparison of experimental with a predicted shear strength of GPC

From the above equation, shear strength due to cohesion, friction, and bending resistance i.e., dowel action of reinforcement across the interface has been calculated and tabulated in table 5.11. A graph between the predicted shear strength model to experimental shear strength has been plotted and the shear strength was found to correlate with $R^2 = 0.965$.

Table. 5.11. Comparison between experimental vs. predicted shear strength

Specimen ID	f_{gpc} MPa	Experimental P_u kN	% of Stirrups @ interface $A_{stirrups}$	V_c kN	V_f kN	V_d kN	Predicted shear strength kN	Experimental / Predicted
G1SA01	27.29	62.30	0.00	60.23	0.00	0.00	60.23	1.03
G1SA02	32.04	71.20	0.00	73.86	0.00	0.00	73.86	0.96
G1SA03	35.99	80.10	0.00	85.70	0.00	0.00	85.70	0.93
G2SA01	26.50	61.56	0.00	58.02	0.00	0.00	58.02	1.06
G2SA02	28.88	64.91	0.00	64.70	0.00	0.00	64.70	1.00
G2SA03	31.29	66.50	0.00	71.65	0.00	0.00	71.65	0.93
G3SB01	27.68	60.26	0.00	61.33	0.00	0.00	61.33	0.98
G3SB02	27.68	61.37	0.00	61.33	0.00	0.00	61.33	1.00
G3SB03	27.68	60.80	0.00	61.33	0.00	0.00	61.33	0.99
G3SC01	40.30	95.97	0.00	98.30	0.00	0.00	98.30	0.98
G3SC02	40.30	98.42	0.00	98.30	0.00	0.00	98.30	1.00
G3SC03	40.30	96.06	0.00	98.30	0.00	0.00	98.30	0.98
G1SC01	37.28	89.00	0.00	89.67	0.00	0.00	89.67	0.99
G1SC02	37.77	93.45	0.00	91.20	0.00	0.00	91.20	1.02
G1SC03	38.57	97.90	0.00	93.66	0.00	0.00	93.66	1.05
G2SC01	38.57	95.45	0.00	93.68	0.00	0.00	93.68	1.02
G2SC02	40.65	98.72	0.00	98.73	0.00	0.00	98.73	1.00
G2SC03	41.76	101.16	0.00	100.08	0.00	0.00	100.08	1.01
G1SD01	41.10	102.35	0.00	99.28	0.00	0.00	99.28	1.03
G1SD02	48.11	106.80	0.00	107.66	0.00	0.00	107.66	0.99
G1SD03	52.86	111.25	0.00	113.22	0.00	0.00	113.22	0.98
G2SD01	48.04	107.69	0.00	107.58	0.00	0.00	107.58	1.00
G2SD02	53.69	121.41	0.00	114.19	0.00	0.00	114.19	1.06
G2SD03	54.09	127.92	0.00	114.65	0.00	0.00	114.65	1.12
G3SD01	53.81	108.00	0.00	114.33	0.00	0.00	114.33	0.94
G3SD02	53.81	105.61	0.00	114.33	0.00	0.00	114.33	0.92
G3SD03	53.81	110.38	0.00	114.33	0.00	0.00	114.33	0.97
G3SB21	27.68	96.31	0.51	61.33	11.31	25.41	98.04	0.98
G3SB22	27.68	99.11	0.51	61.33	11.31	25.41	98.04	1.01
G3SB23	27.68	98.21	0.51	61.33	11.31	25.41	98.04	1.00
G3SC21	40.30	140.53	0.51	98.30	14.14	36.99	149.43	0.94
G3SC22	40.30	144.80	0.51	98.30	14.14	36.99	149.43	0.97
G3SC23	40.30	138.88	0.51	98.30	14.14	36.99	149.43	0.93
G3SD21	53.81	172.95	0.51	114.33	14.14	49.39	177.86	0.97
G3SD22	53.81	177.15	0.51	114.33	14.14	49.39	177.86	1.00
G3SD23	53.81	171.25	0.51	114.33	14.14	49.39	177.86	0.96
G2SA31	26.50	127.92	0.77	58.02	16.96	54.73	129.71	0.99
G1SA31	27.29	142.39	0.77	60.23	16.96	56.37	133.56	1.07
G2SA32	28.88	137.61	0.77	64.70	16.96	59.64	141.30	0.97
G3SB31	30.26	144.94	0.77	68.66	16.96	62.49	148.12	0.98
G3SB32	30.26	147.71	0.77	68.66	16.96	62.49	148.12	1.00

Specimen ID	f_{gpc} MPa	Experimental P_u kN	% of Stirrups @ interface $A_{stirrups}$	V_c kN	V_f kN	V_d kN	Predicted shear strength kN	Experimental / Predicted
G3SB33	30.26	146.65	0.77	68.66	16.96	62.49	148.12	0.99
G2SA33	31.29	156.64	0.77	71.65	16.96	64.61	153.23	1.02
G1SA32	32.04	155.74	0.77	73.86	16.96	66.17	156.99	0.99
G1SA33	35.99	186.89	0.77	85.70	21.21	74.32	181.23	1.03
G1SC31	37.28	213.59	0.77	89.67	21.21	76.99	187.87	1.14
G1SC32	37.77	213.59	0.77	91.20	21.21	78.01	190.42	1.12
G1SC33	38.57	222.49	0.77	93.66	21.21	79.65	194.51	1.14
G2SC31	38.57	215.27	0.77	93.68	21.21	79.66	194.55	1.11
G2SC32	40.65	228.14	0.77	98.73	21.21	83.95	203.88	1.12
G1SD31	41.10	226.94	0.77	99.28	21.21	84.89	205.37	1.11
G2SC33	41.76	225.62	0.77	100.08	21.21	86.25	207.53	1.09
G3SC31	41.90	206.48	0.77	100.24	21.21	86.53	207.97	0.99
G3SC32	41.90	208.50	0.77	100.24	21.21	86.53	207.97	1.00
G3SC33	41.90	205.84	0.77	100.24	21.21	86.53	207.97	0.99
G2SD31	48.04	238.02	0.77	107.58	21.21	99.22	228.00	1.04
G1SD32	48.11	241.39	0.77	107.66	21.21	99.35	228.22	1.06
G1SD33	52.86	258.09	0.77	113.22	21.21	109.16	243.59	1.06
G2SD32	53.69	265.74	0.77	114.19	21.21	110.89	246.28	1.08
G2SD33	54.09	276.68	0.77	114.65	21.21	111.71	247.56	1.12
G3SD31	55.70	262.44	0.77	116.51	21.21	115.03	252.75	1.04
G3SD32	55.70	259.29	0.77	116.51	21.21	115.03	252.75	1.03
G3SD33	55.70	261.22	0.77	116.51	21.21	115.03	252.75	1.03
G3SB41	30.26	178.46	1.02	68.66	22.62	111.09	202.38	0.88
G3SB42	30.26	183.14	1.02	68.66	22.62	111.09	202.38	0.90
G3SB43	30.26	177.85	1.02	68.66	22.62	111.09	202.38	0.88
G3SC41	41.90	249.05	1.02	100.24	28.27	153.82	282.34	0.88
G3SC42	41.90	252.00	1.02	100.24	28.27	153.82	282.34	0.89
G3SC43	41.90	255.10	1.02	100.24	28.27	153.82	282.34	0.90
G3SD41	55.70	324.30	1.02	116.51	28.27	204.51	349.29	0.93
G3SD42	55.70	320.77	1.02	116.51	28.27	204.51	349.29	0.92
G3SD43	55.70	322.88	1.02	116.51	28.27	204.51	349.29	0.92
							Average	**1.00**

Notation:

f_{gpc} = Concrete compressive strength of 150 mm cube (MPa)

P_u = Experimental peak load (kN)

f_y = Yield strength of reinforcement across interface = 250 MPa

bh = Cross sectional area of the interface = 92 x 240 mm^2

V_c = Cohesion contribution, c $(f_{gpc})^{(1/3)}$ bh (kN), where For $f_{gpc} \leq 40$ MPa, c = 0.031 f_{gpc}+0.06, For f_{gpc}>40 MPa, c = 0.0054f_{gpc}+1.0809

V_f = Friction contribution, $\mu[\sigma_n+\rho k f_y]$ bh (kN)

V_d = Dowel contribution, $\alpha\rho\sqrt{f_y f_{gpc}}$ bh (kN), where α = 6.338 $\rho\sqrt{f_y f_{gpc}}$

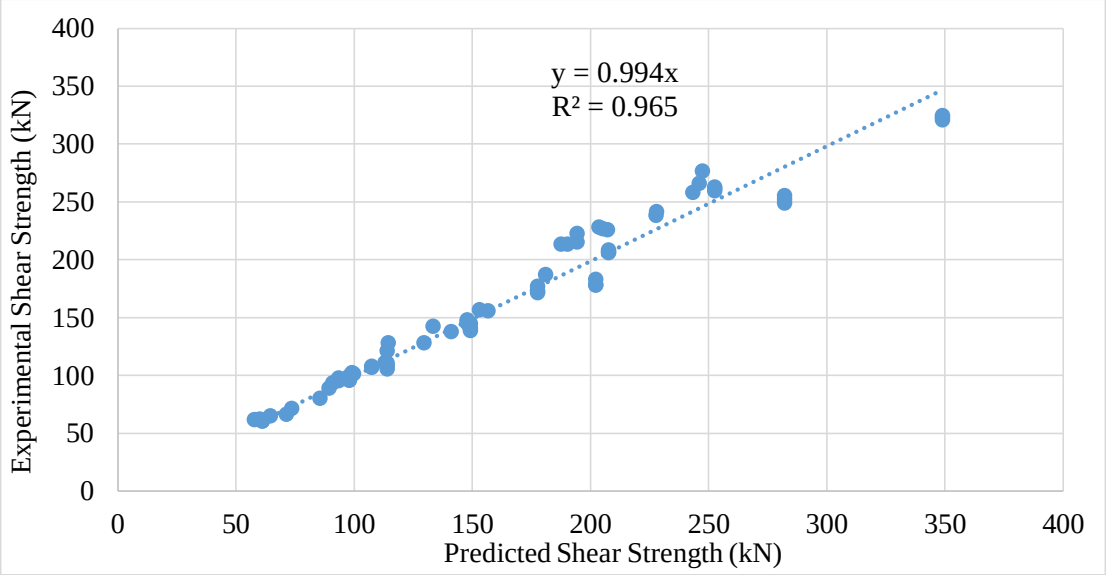

Figure 5.13: Predicted shear strength vs. Experimental shear strength

5.8 COMPARISON OF EXPERIMENTAL RESULTS WITH DIFFERENT THEORIES AND CODES

Shear transfer across the interface is transmitted by friction from compressive stresses, cohesion from aggregate interlocking roughness, and dowel action crossing the surfaces. Different models are available in the literature for calculating the concrete shear transfer strength (Birkeland and Birkeland, 1966, Mattock, 1974, Loov, 1978, Walraven et al., 1987 and Randl, 1997). The outcomes of push-off investigations were used to recommend shear transfer models for concrete. Numerous design expressions were proposed to envisage shear stress at the concrete interface. The majority of design codes considered shear-friction theory for concrete structures (ACI 318, 2019, Euro code 2, 2004, FIB Model Code, 2010 and CSA A23.3, 2019). Table 5.12 presents the shear strength expressions as per different investigators/codes of practice on ordinary Portland cement concrete.

Table.5.12 Shear strength expressions as per different investigators / Codes of practice on conventional concrete

Reference	Shear strength expression	Remarks
Birkeland and Birkeland (1966)	$v_u = \rho f_y \tan\varphi = \rho f_y \mu$	μ = 1.7 for concrete placed monolithically
Mattock (1974)	$v_u = 2.76 + 0.8[\rho f_y + \sigma_n]$	ρ = reinforcement ratio, f_y= Yield strength of reinforcement across interface, σ_n = normal stress
Loov (1978)	$v_u = k\sqrt{f_c[\sigma_n + \rho f_y]}$	σ_n is the clamping stress and k = 0.5 for initially un-cracked shear interfaces.
Walraven, Frenay & Pruijssers (1987)	$v_u = C_1[\rho f_y]^{C_2}$	$C_1 = 0.822 f_C^{0.406}$, $C_2 = 0.159 f_C^{0.303}$
Randl (1997)	$v_u = C f_c^{1/3} + \mu[\sigma_n + \rho k f_y] + \alpha\rho\sqrt{f_y f_c} \le \beta v f_c$	C, μ, k, α, and β are dependent on the roughness at the interface
ACI 318 (2019) Cl. 22.9.4.2 & 3	$v_n = \mu A_{vf} f_y$ $v_n = A_{vf} f_y(\mu \sin\alpha + \cos\alpha)$	μ=1.4λ For monolithic concrete. λ = 1 for normal-weight concrete. ρ_v = greater of 0.75 $\sqrt{f_c'}/f_y$ and 50/f_y (SI Units)
Euro code 2 (2004) Cl. 6.2.5 * Not valid for monolithic Spec	$v_u = C f_{ctd} + \mu\sigma_n + \rho f_y[\mu \sin\alpha + \cos\alpha] \le 0.5 v f_{cd}$	*Surface Type* / *Cohesion Coefficient C MPa* / *Friction Coefficient μ* Very Smooth: 0.025 – 0.10 / 0.50 Smooth: 0.20 / 0.60 Rough: 0.40 / 0.70 Indented: 0.50 / 0.90
FIB Model Code (2010) Cl. 6.3.4	$v_u = \tau_c + \mu(\rho k f_y + \sigma_n) + \alpha\rho\sqrt{f_y f_c} \le \beta v f_c$	*Surface Type* / *C* MPa / *μ* / *Average Roughness Ra* Very Smooth: 0.025 / 0.50 / NA Smooth: 0.35 / 0.60 / <1.50 Rough: 0.45 / 0.70 / ≥ 1.50 Very Rough: 0.50 / 0.90 / ≥ 3.00
CSA A23.3 (2019) Cl. 11.5	$v_u = \phi_c\lambda(c + \mu\sigma) + \Phi_s\rho_v f_y \cos\alpha_f$	c = 1; μ = 1.4 for monolithic concrete. λ = 1 for normal density concrete; $\lambda(c + \mu\sigma) \le 0.25 f_c'$, $\rho_{vmin} = 0.06\sqrt{\frac{f_c'}{f_y}}$
	$v_u = \lambda k\sqrt{\sigma f_c'} + \rho_v f_y \cos\alpha_f$	$\lambda k\sqrt{\sigma f_c'} \le 0.25 f_c'$ k = 0.6 for concrete placed monolithically.

Table.5.13 presents the comparison of shear strength of geopolymer concrete obtained with the shear strength of normal concrete predicted by different shear models/shear equations available in the literature along with the proposed model. The comparison is also shown in figure 5.14 for unreinforced and reinforced shear interfaces. The comparative study indicates that the proposed model (Ref 1) is almost in line with experimental shear strength values and is more accurate than all other models in estimating the shear strength of geopolymer concrete. The available normal concrete shear strength prediction models are highly conservative in estimating the shear strength of unreinforced and reinforced monolithic shear interfaces in geopolymer concrete. The models by Mattock, 1974 and Walraven et al, 1987 came up with better prediction of shear strength of geopolymer concrete in the case of unreinforced and reinforced monolithic interfaces respectively.

Design codes established for conventional concrete are very conservative in estimating the shear strength of geopolymer concrete. Table 5.14 shows the shear stress of GGBS and fly ash-based geopolymer concrete for different grades of concrete and different percentages of stirrup reinforcement for an yield strength of reinforcement f_y = 250 MPa, based on the proposed shear strength model equation of geopolymer concrete (Eq. 5.4). Based on the table, we can interpolate and evaluate the shear stress for the desired grade of concrete and the percentage of stirrup reinforcement.

Table.5.13 Comparison of experimental shear strength of GPC with the shear strength predicted by the design codes/equations

Specimen ID	Shear Stress of GPC v_{up} MPa	Ref 1		Ref 2		Ref 3		Ref 4		Ref 5		Ref 6		Ref 7		Ref 8		Ref 9		Ref 10	
		v_{u1}	v_{up} / v_{u1}	v_{u2}	v_{up} / v_{u2}	v_{u3}	v_{up} / v_{u3}	v_{u4}	v_{up} / v_{u4}	v_{u5}	v_{up} / v_{u5}	v_{u6}	v_{up} / v_{u6}	v_{u7}	v_{up} / v_{u7}	v_{u8}	v_{up} / v_{u8}	v_{u9}	v_{up} / v_{u9}	v_{u10}	v_{up} / v_{u10}
G2SA01	2.79	2.63	1.06	0.00	-	2.76	1.01	0.00	-	0.00	-	1.19	2.34	0.00	-	0.96	2.90	1.04	2.67	0.65	4.29
G1SA01	2.82	2.73	1.03	0.00	-	2.76	1.02	0.00	-	0.00	-	1.20	2.34	0.00	-	0.98	2.89	1.05	2.68	0.65	4.34
G3SB01	2.73	2.78	0.98	0.00	-	2.76	0.99	0.00	-	0.00	-	1.21	2.26	0.00	-	0.98	2.78	1.06	2.58	0.65	4.20
G3SB02	2.78	2.78	1.00	0.00	-	2.76	1.01	0.00	-	0.00	-	1.21	2.30	0.00	-	0.98	2.83	1.06	2.63	0.65	4.28
G3SB03	2.75	2.78	0.99	0.00	-	2.76	1.00	0.00	-	0.00	-	1.21	2.28	0.00	-	0.98	2.80	1.06	2.60	0.65	4.24
G2SA02	2.94	2.93	1.00	0.00	-	2.76	1.07	0.00	-	0.00	-	1.23	2.40	0.00	-	1.00	2.93	1.07	2.74	0.65	4.52
G2SA03	3.01	3.25	0.93	0.00	-	2.76	1.09	0.00	-	0.00	-	1.26	2.39	0.00	-	1.04	2.88	1.10	2.73	0.65	4.63
G1SA02	3.22	3.35	0.96	0.00	-	2.76	1.17	0.00	-	0.00	-	1.27	2.54	0.00	-	1.06	3.05	1.11	2.90	0.65	4.96
G1SA03	3.63	3.88	0.93	0.00	-	2.76	1.31	0.00	-	0.00	-	1.32	2.75	0.00	-	1.12	3.24	1.16	3.14	0.65	5.58
G1SC01	4.03	4.06	0.99	0.00	-	2.76	1.46	0.00	-	0.00	-	1.34	3.02	0.00	-	1.14	3.53	1.17	3.45	0.65	6.20
G1SC02	4.23	4.13	1.02	0.00	-	2.76	1.53	0.00	-	0.00	-	1.34	3.15	0.00	-	1.15	3.69	1.17	3.60	0.65	6.51
G1SC03	4.43	4.24	1.05	0.00	-	2.76	1.61	0.00	-	0.00	-	1.35	3.28	0.00	-	1.16	3.82	1.18	3.75	0.65	6.82
G2SC01	4.32	4.24	1.02	0.00	-	2.76	1.57	0.00	-	0.00	-	1.35	3.20	0.00	-	1.16	3.73	1.18	3.66	0.65	6.65
G3SC01	4.35	4.45	0.98	0.00	-	2.76	1.57	0.00	-	0.00	-	1.37	3.17	0.00	-	1.19	3.67	1.20	3.62	0.65	6.69
G3SC02	4.46	4.45	1.00	0.00	-	2.76	1.62	0.00	-	0.00	-	1.37	3.25	0.00	-	1.19	3.76	1.20	3.71	0.65	6.86
G3SC03	4.35	4.45	0.98	0.00	-	2.76	1.58	0.00	-	0.00	-	1.37	3.17	0.00	-	1.19	3.67	1.20	3.63	0.65	6.69
G2SC02	4.47	4.47	1.00	0.00	-	2.76	1.62	0.00	-	0.00	-	1.38	3.25	0.00	-	1.19	3.75	1.20	3.72	0.65	6.88
G1SD01	4.64	4.50	1.03	0.00	-	2.76	1.68	0.00	-	0.00	-	1.38	3.36	0.00	-	1.20	3.87	1.21	3.84	0.65	7.13
G2SC03	4.58	4.53	1.01	0.00	-	2.76	1.66	0.00	-	0.00	-	1.39	3.30	0.00	-	1.21	3.80	1.21	3.77	0.65	7.05
G2SD01	4.88	4.87	1.00	0.00	-	2.76	1.77	0.00	-	0.00	-	1.45	3.35	0.00	-	1.29	3.77	1.27	3.83	0.65	7.50
G1SD02	4.84	4.88	0.99	0.00	-	2.76	1.75	0.00	-	0.00	-	1.45	3.32	0.00	-	1.30	3.73	1.27	3.80	0.65	7.44
G1SD03	5.04	5.13	0.98	0.00	-	2.76	1.83	0.00	-	0.00	-	1.50	3.36	0.00	-	1.36	3.71	1.31	3.84	0.65	7.75
G2SD02	5.50	5.17	1.06	0.00	-	2.76	1.99	0.00	-	0.00	-	1.51	3.64	0.00	-	1.37	4.02	1.32	4.16	0.65	8.46

Table.5.13 Comparison of experimental shear strength of GPC with the shear strength predicted by the design codes/equations

Specimen ID	Shear Stress of GPC v_{up} MPa	Ref 1		Ref 2		Ref 3		Ref 4		Ref 5		Ref 6		Ref 7		Ref 8		Ref 9		Ref 10	
		v_{u1}	v_{up} / v_{u1}	v_{u2}	v_{up} / v_{u2}	v_{u3}	v_{up} / v_{u3}	v_{u4}	v_{up} / v_{u4}	v_{u5}	v_{up} / v_{u5}	v_{u6}	v_{up} / v_{u6}	v_{u7}	v_{up} / v_{u7}	v_{u8}	v_{up} / v_{u8}	v_{u9}	v_{up} / v_{u9}	v_{u10}	v_{up} / v_{u10}
G3SD01	4.89	5.18	0.94	0.00	-	2.76	1.77	0.00	-	0.00	-	1.51	3.24	0.00	-	1.37	3.57	1.32	3.70	0.65	7.53
G3SD02	4.78	5.18	0.92	0.00	-	2.76	1.73	0.00	-	0.00	-	1.51	3.17	0.00	-	1.37	3.49	1.32	3.62	0.65	7.36
G3SD03	5.00	5.18	0.97	0.00	-	2.76	1.81	0.00	-	0.00	-	1.51	3.31	0.00	-	1.37	3.65	1.32	3.78	0.65	7.69
G2SD03	5.79	5.19	1.12	0.00	-	2.76	2.10	0.00	-	0.00	-	1.51	3.83	0.00	-	1.37	4.22	1.32	4.38	0.65	8.91
G3SB21	4.36	4.44	0.98	1.79	2.43	3.78	1.15	2.66	1.64	3.52	1.24	2.11	2.07	1.79	2.43	1.62	2.69	1.95	2.23	1.82	2.40
G3SB22	4.49	4.44	1.01	1.79	2.50	3.78	1.19	2.66	1.69	3.52	1.27	2.11	2.13	1.79	2.50	1.62	2.77	1.95	2.30	1.82	2.47
G3SB23	4.45	4.44	1.00	1.79	2.48	3.78	1.18	2.66	1.67	3.52	1.26	2.11	2.11	1.79	2.48	1.62	2.74	1.95	2.28	1.82	2.45
G3SC21	6.36	6.77	0.94	1.79	3.55	3.78	1.68	3.21	1.98	4.16	1.53	2.47	2.57	1.79	3.55	1.83	3.49	2.30	2.76	1.82	3.51
G3SC22	6.56	6.77	0.97	1.79	3.66	3.78	1.73	3.21	2.04	4.16	1.58	2.47	2.65	1.79	3.66	1.83	3.59	2.30	2.85	1.82	3.61
G3SC23	6.29	6.77	0.93	1.79	3.51	3.78	1.66	3.21	1.96	4.16	1.51	2.47	2.54	1.79	3.51	1.83	3.44	2.30	2.73	1.82	3.46
G3SD21	7.83	8.06	0.97	1.79	4.37	3.78	2.07	3.71	2.11	4.73	1.66	2.69	2.92	1.79	4.37	2.01	3.90	2.50	3.14	1.82	4.31
G3SD22	8.02	8.06	1.00	1.79	4.48	3.78	2.12	3.71	2.16	4.73	1.70	2.69	2.99	1.79	4.48	2.01	3.99	2.50	3.21	1.82	4.42
G3SD23	7.76	8.06	0.96	1.79	4.33	3.78	2.05	3.71	2.09	4.73	1.64	2.69	2.89	1.79	4.33	2.01	3.86	2.50	3.11	1.82	4.27
G2SA31	5.79	5.87	0.99	2.69	2.15	4.30	1.35	3.19	1.82	4.11	1.41	2.52	2.30	2.69	2.15	1.92	3.01	2.37	2.44	2.40	2.42
G1SA31	6.45	6.05	1.07	2.69	2.40	4.30	1.50	3.24	1.99	4.17	1.54	2.54	2.54	2.69	2.40	1.94	3.33	2.39	2.69	2.40	2.69
G2SA32	6.23	6.40	0.97	2.69	2.32	4.30	1.45	3.33	1.87	4.29	1.45	2.58	2.41	2.69	2.32	1.96	3.17	2.43	2.57	2.40	2.60
G3SB31	6.56	6.71	0.98	2.69	2.44	4.30	1.53	3.41	1.93	4.39	1.49	2.62	2.51	2.69	2.44	1.99	3.30	2.46	2.67	2.40	2.74
G3SB32	6.69	6.71	1.00	2.69	2.49	4.30	1.56	3.41	1.96	4.39	1.52	2.62	2.56	2.69	2.49	1.99	3.37	2.46	2.72	2.40	2.79
G3SB33	6.64	6.71	0.99	2.69	2.47	4.30	1.55	3.41	1.95	4.39	1.51	2.62	2.54	2.69	2.47	1.99	3.34	2.46	2.70	2.40	2.77
G2SA33	7.09	6.94	1.02	2.69	2.64	4.30	1.65	3.47	2.05	4.47	1.59	2.64	2.69	2.69	2.64	2.01	3.54	2.48	2.86	2.40	2.96
G1SA32	7.05	7.11	0.99	2.69	2.62	4.30	1.64	3.51	2.01	4.52	1.56	2.66	2.65	2.69	2.62	2.02	3.50	2.50	2.82	2.40	2.94
G1SA33	8.46	8.21	1.03	2.69	3.15	4.30	1.97	3.72	2.28	4.79	1.77	2.94	2.88	2.69	3.15	2.08	4.07	2.77	3.05	2.40	3.53
G1SC31	9.67	8.51	1.14	2.69	3.60	4.30	2.25	3.78	2.56	4.87	1.99	2.96	3.26	2.69	3.60	2.10	4.60	2.80	3.46	2.40	4.03

Table.5.13 Comparison of experimental shear strength of GPC with the shear strength predicted by the design codes/equations

Specimen ID	Shear Stress of GPC v_{up} MPa	Ref 1		Ref 2		Ref 3		Ref 4		Ref 5		Ref 6		Ref 7		Ref 8		Ref 9		Ref 10	
		v_{u1}	v_{up} / v_{u1}	v_{u2}	v_{up} / v_{u2}	v_{u3}	v_{up} / v_{u3}	v_{u4}	v_{up} / v_{u4}	v_{u5}	v_{up} / v_{u5}	v_{u6}	v_{up} / v_{u6}	v_{u7}	v_{up} / v_{u7}	v_{u8}	v_{up} / v_{u8}	v_{u9}	v_{up} / v_{u9}	v_{u10}	v_{up} / v_{u10}
G1SC32	9.67	8.62	1.12	2.69	3.60	4.30	2.25	3.81	2.54	4.91	1.97	2.97	3.25	2.69	3.60	2.11	4.59	2.81	3.45	2.40	4.03
G1SC33	10.08	8.81	1.14	2.69	3.75	4.30	2.35	3.85	2.62	4.96	2.03	2.99	3.37	2.69	3.75	2.12	4.75	2.82	3.57	2.40	4.20
G2SC31	9.75	8.81	1.11	2.69	3.63	4.30	2.27	3.85	2.53	4.96	1.97	2.99	3.26	2.69	3.63	2.12	4.60	2.82	3.45	2.40	4.07
G2SC32	10.33	9.23	1.12	2.69	3.84	4.30	2.40	3.95	2.61	5.09	2.03	3.03	3.41	2.69	3.84	2.15	4.80	2.86	3.61	2.40	4.31
G1SD31	10.28	9.30	1.11	2.69	3.82	4.30	2.39	3.97	2.59	5.12	2.01	3.04	3.38	2.69	3.82	2.16	4.76	2.87	3.58	2.40	4.29
G2SC33	10.22	9.40	1.09	2.69	3.80	4.30	2.38	4.01	2.55	5.16	1.98	3.05	3.35	2.69	3.80	2.17	4.71	2.88	3.55	2.40	4.26
G3SC31	9.35	9.42	0.99	2.69	3.48	4.30	2.18	4.01	2.33	5.17	1.81	3.06	3.06	2.69	3.48	2.17	4.31	2.88	3.24	2.40	3.90
G3SC32	9.44	9.42	1.00	2.69	3.51	4.30	2.20	4.01	2.35	5.17	1.83	3.06	3.09	2.69	3.51	2.17	4.35	2.88	3.27	2.40	3.94
G3SC33	9.32	9.42	0.99	2.69	3.47	4.30	2.17	4.01	2.32	5.17	1.80	3.06	3.05	2.69	3.47	2.17	4.30	2.88	3.23	2.40	3.89
G2SD31	10.78	10.33	1.04	2.69	4.01	4.30	2.51	4.30	2.51	5.54	1.95	3.17	3.40	2.69	4.01	2.26	4.78	2.99	3.60	2.40	4.50
G1SD32	10.93	10.34	1.06	2.69	4.07	4.30	2.54	4.30	2.54	5.54	1.97	3.17	3.44	2.69	4.07	2.26	4.85	2.99	3.65	2.40	4.56
G1SD33	11.69	11.03	1.06	2.69	4.35	4.30	2.72	4.51	2.59	5.81	2.01	3.26	3.59	2.69	4.35	2.32	5.04	3.07	3.81	2.40	4.87
G2SD32	12.04	11.15	1.08	2.69	4.48	4.30	2.80	4.54	2.65	5.86	2.05	3.27	3.68	2.69	4.48	2.33	5.17	3.08	3.91	2.40	5.02
G2SD33	12.53	11.21	1.12	2.69	4.66	4.30	2.92	4.56	2.75	5.88	2.13	3.28	3.82	2.69	4.66	2.33	5.37	3.09	4.06	2.40	5.23
G3SD31	11.89	11.45	1.04	2.69	4.42	4.30	2.77	4.63	2.57	5.97	1.99	3.30	3.60	2.69	4.42	2.35	5.05	3.11	3.82	2.40	4.96
G3SD32	11.74	11.45	1.03	2.69	4.37	4.30	2.73	4.63	2.54	5.97	1.97	3.30	3.55	2.69	4.37	2.35	4.99	3.11	3.77	2.40	4.90
G3SD33	11.83	11.45	1.03	2.69	4.40	4.30	2.75	4.63	2.56	5.97	1.98	3.30	3.58	2.69	4.40	2.35	5.02	3.11	3.80	2.40	4.93
G3SB41	8.08	9.17	0.88	3.59	2.25	4.81	1.68	3.94	2.05	5.00	1.62	3.07	2.63	3.59	2.25	2.31	3.50	2.92	2.77	2.98	2.71
G3SB42	8.29	9.17	0.90	3.59	2.31	4.81	1.72	3.94	2.11	5.00	1.66	3.07	2.70	3.59	2.31	2.31	3.59	2.92	2.84	2.98	2.78
G3SB43	8.05	9.17	0.88	3.59	2.25	4.81	1.68	3.94	2.05	5.00	1.61	3.07	2.62	3.59	2.25	2.31	3.49	2.92	2.76	2.98	2.70
G3SC41	11.28	12.79	0.88	3.59	3.15	4.81	2.35	4.63	2.43	5.95	1.89	3.61	3.12	3.59	3.15	2.49	4.53	3.44	3.28	2.98	3.78
G3SC42	11.41	12.79	0.89	3.59	3.18	4.81	2.37	4.63	2.46	5.95	1.92	3.61	3.16	3.59	3.18	2.49	4.58	3.44	3.32	2.98	3.83
G3SC43	11.55	12.79	0.90	3.59	3.22	4.81	2.40	4.63	2.49	5.95	1.94	3.61	3.20	3.59	3.22	2.49	4.64	3.44	3.36	2.98	3.88

Table.5.13 Comparison of experimental shear strength of GPC with the shear strength predicted by the design codes/equations

Specimen ID	Shear Stress of GPC v_{up} MPa	Ref 1		Ref 2		Ref 3		Ref 4		Ref 5		Ref 6		Ref 7		Ref 8		Ref 9		Ref 10	
		v_{u1}	v_{up} / v_{u1}	v_{u2}	v_{up} / v_{u2}	v_{u3}	v_{up} / v_{u3}	v_{u4}	v_{up} / v_{u4}	v_{u5}	v_{up} / v_{u5}	v_{u6}	v_{up} / v_{u6}	v_{u7}	v_{up} / v_{u7}	v_{u8}	v_{up} / v_{u8}	v_{u9}	v_{up} / v_{u9}	v_{u10}	v_{up} / v_{u10}
G3SD41	14.69	15.82	0.93	3.59	4.10	4.81	3.05	5.34	2.75	6.97	2.11	3.90	3.77	3.59	4.10	2.67	5.49	3.71	3.96	2.98	4.93
G3SD42	14.53	15.82	0.92	3.59	4.05	4.81	3.02	5.34	2.72	6.97	2.08	3.90	3.73	3.59	4.05	2.67	5.43	3.71	3.92	2.98	4.87
G3SD43	14.62	15.82	0.92	3.59	4.08	4.81	3.04	5.34	2.74	6.97	2.10	3.90	3.75	3.59	4.08	2.67	5.47	3.71	3.95	2.98	4.91
Average		**1.00**		**3.42**		**1.88**		**2.28**		**1.77**		**3.01**		**3.42**		**3.91**		**3.29**		**4.75**	

Reference:

1. Proposed Model
2. Birkeland & Birkeland, 1966
3. Mattock, 1974
4. Loov, 1978
5. Walraven et al., 1987
6. Randl, 1997
7. ACI 318, 2019
8. Euro code 2, 2004
9. FIB Model Code, 2010
10. CSA A23.3., 2019

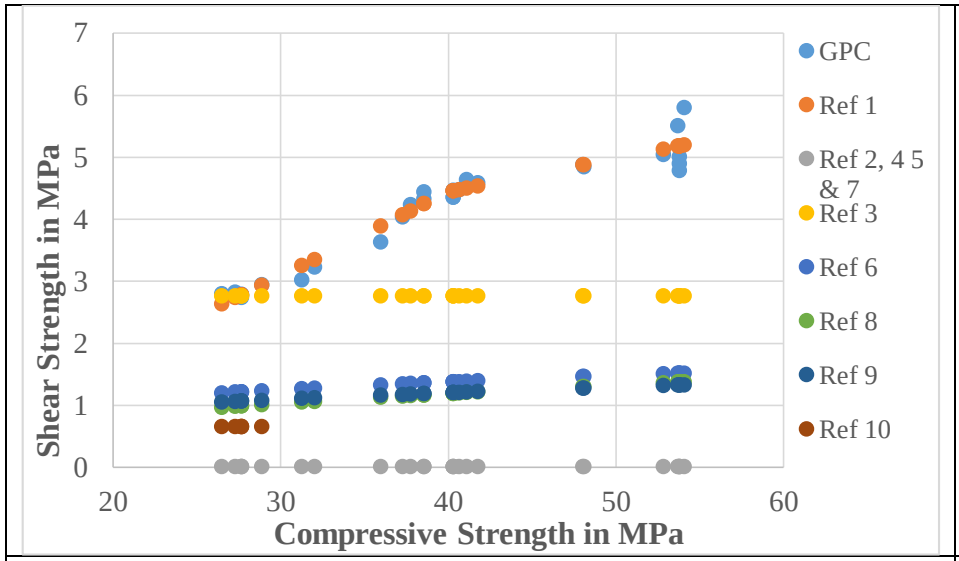

For Unreinforced Push-off specimen

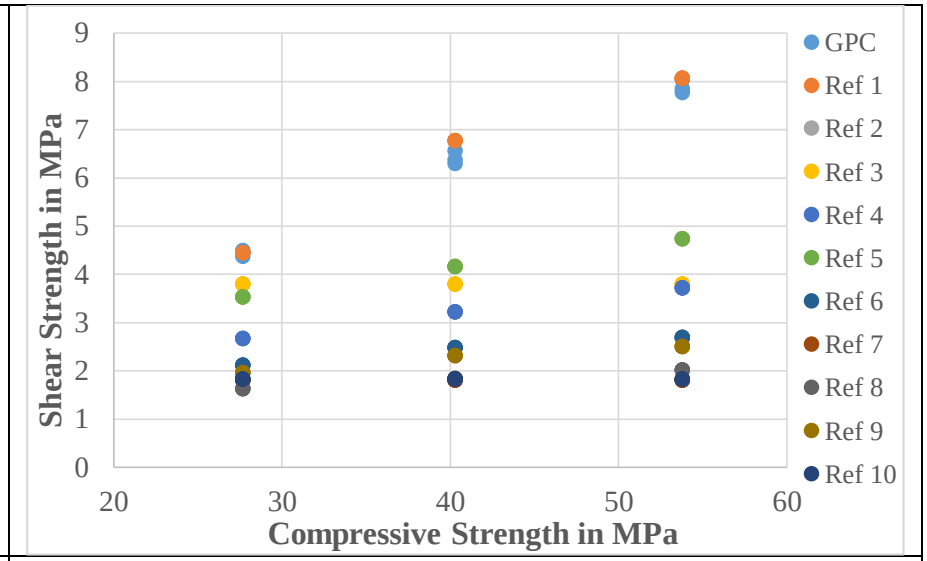

For Reinforced Push-off specimen – 0.51%

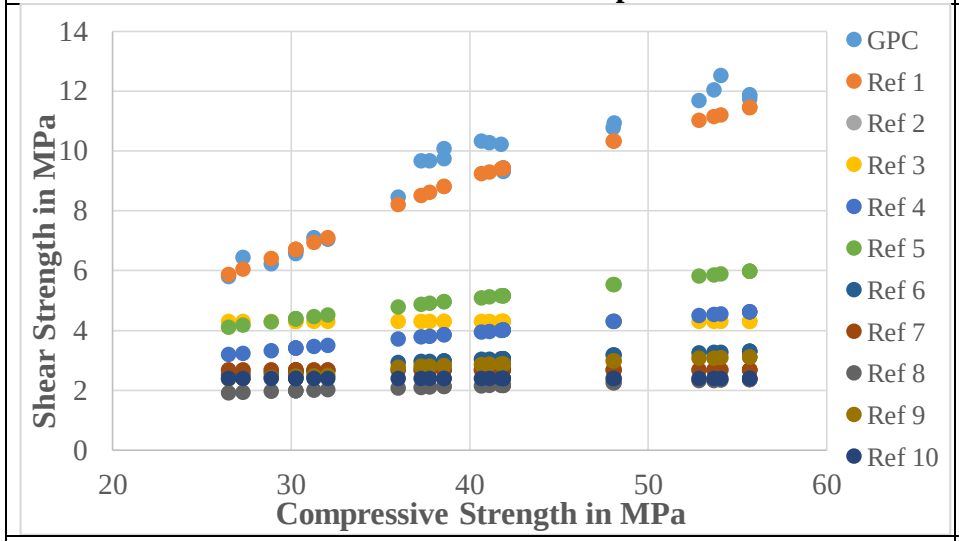

For Reinforced Push-off specimen – 0.77%

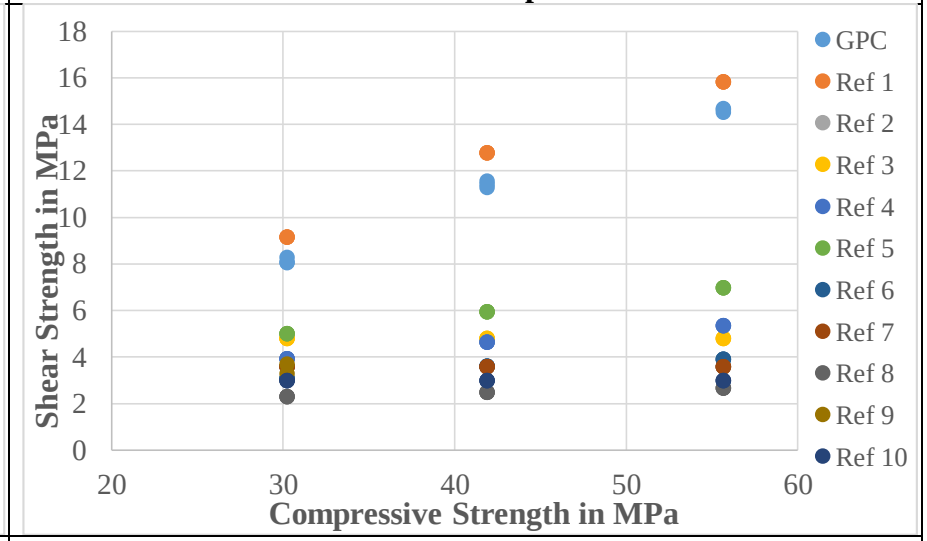

For Reinforced Push-off specimen – 1.02%

Figure 5.14: Comparison of shear strength of GPC predicted by design codes and equations

Table.5.14 Shear Stress of GGBS and fly ash-based GPC for different grades and different % of closed-loop reinforcement crossing the interface based on the proposed model.

% of Reinforcement	Grade of GPC (MPa)								
	20	**25**	**30**	**35**	**40**	**45**	**50**	**55**	**60**
0.15	2.07	2.68	3.33	4.02	4.77	5.06	5.34	5.62	5.90
0.20	2.17	2.80	3.47	4.17	4.94	5.24	5.54	5.84	6.13
0.25	2.29	2.94	3.62	4.34	5.14	5.47	5.78	6.10	6.41
0.30	2.43	3.10	3.80	4.54	5.38	5.73	6.06	6.40	6.73
0.35	2.58	3.28	4.01	4.77	5.65	6.02	6.38	6.75	7.10
0.40	2.75	3.48	4.24	5.03	5.95	6.35	6.74	7.13	7.52
0.45	2.94	3.69	4.49	5.32	6.28	6.72	7.14	7.57	7.99
0.50	3.14	3.93	4.76	5.63	6.64	7.12	7.58	8.04	8.50
0.55	3.35	4.19	5.06	5.97	7.04	7.55	8.06	8.56	9.06
0.60	3.59	4.47	5.39	6.34	7.47	8.03	8.58	9.13	9.67
0.65	3.83	4.77	5.73	6.74	7.93	8.53	9.14	9.73	10.33
0.70	4.10	5.08	6.11	7.16	8.42	9.08	9.73	10.39	11.03
0.75	4.38	5.42	6.50	7.61	8.94	9.66	10.37	11.08	11.79
0.80	4.67	5.78	6.92	8.09	9.49	10.27	11.05	11.82	12.58
0.85	4.99	6.15	7.36	8.60	10.08	10.92	11.76	12.60	13.43
0.90	5.31	6.55	7.83	9.14	10.69	11.61	12.52	13.42	14.33
0.95	5.66	6.97	8.32	9.70	11.34	12.33	13.31	14.29	15.27
1.00	6.01	7.40	8.83	10.29	12.02	13.09	14.15	15.20	16.26
1.05	6.39	7.86	9.37	10.91	12.74	13.88	15.02	16.16	17.29
1.10	6.78	8.33	9.93	11.56	13.48	14.71	15.94	17.16	18.38
1.15	7.19	8.83	10.51	12.23	14.25	15.58	16.89	18.20	19.51
1.20	7.61	9.35	11.12	12.93	15.06	16.48	17.89	19.29	20.69
1.25	8.05	9.88	11.75	13.66	15.90	17.41	18.92	20.42	21.92

The above shear stress does not include the contribution from the reinforcement (A_{steel}) which is not close looped. Contribution from reinforcement that is not closed-looped, towards shear stress = $\mu\rho_{main}kf_y$

5.9 CONCLUSIONS

The following are the conclusions arrived after the study on the shear strength of the monolithic geopolymer concrete interface.

1. The shear strength of monolithic geopolymer concrete interface increased with an increase in the compressive strength of geopolymer concrete.
2. The rate of increase of shear strength decreased for a compressive strength of geopolymer concrete of more than 40 MPa.

3. The average shear strength of monolithic geopolymer concrete interface was about 10%, 16%, 23% and 27% of the total compressive strength of geopolymer concrete for steel percentage with ρ = 0%, 0.51%, 0.77% and 1.02% respectively, across the interface.
4. There is an increase in shear strength of geopolymer concrete by about 56%, 123%, and 170% with the provision of steel percentage of ρ = 0.51%, 0.77%, and 1.02% respectively across the interface.
5. The shear (V_u) across the reinforced monolithic interface in geopolymer concrete specimens is resisted by the combined action of cohesion, friction, and dowel action and can be obtained by the equations given below:

$$V_u = \underbrace{C f_c^{1/3}}_{\text{Cohesion}} + \underbrace{\mu[\sigma_n + \rho k f_y]}_{\text{Friction}} + \underbrace{\alpha\rho\sqrt{f_y f_c}}_{\text{Dowel Action}}$$

$V_u = V_c + V_f + V_d$

Where,

V_c = Shear strength of unreinforced GPC due to cohesion = c $(f_{gpc})^{(1/3)}$ bh, where For $f_{gpc} \leq 40$ MPa, c = 0.031 f_{gpc}+0.06, For f_{gpc}>40 MPa, c = 0.0054f_{gpc}+1.0809

V_f = Shear strength of reinforced GPC due to friction = $\mu[\sigma_n+\rho k f_y]$ bh, where k=0.5 and $f_{gpc} \geq 20$ MPa μ =0.8, $f_{gpc} \geq 35$ MPa μ =1.0, $\rho = \rho_{Main} + \rho_{Stirrups}$ (Randl, 1997)

V_d = Shear Strength due to Dowel contribution = $\alpha\rho\sqrt{f_y f_{gpc}}$ bh, $\rho = \rho_{Stirrups}$ where $\alpha = 6.338\,\rho\sqrt{f_y f_{gpc}}$

6. The proposed shear strength equations are based on cube strength and SI units.
7. The available conventional concrete shear strength prediction models are highly conservative in estimating the shear strength of unreinforced and reinforced monolithic shear interfaces in geopolymer concrete.
8. The models by Mattock, 1974 and Walraven et al., 1987 were able to provide better prediction of shear strength of geopolymer concrete in case of unreinforced and reinforced monolithic interfaces respectively.

CHAPTER 6
EXPERIMENTAL STUDY ON THE SHEAR STRENGTH AT THE MONOLITHIC INTERFACES OF GEOPOLYMER CONCRETE CORBELS / BRACKETS

6.1 INTRODUCTION

Structural members like corbels/brackets are short cantilevers projecting out from the faces of columns. They are cast monolithic with supporting columns and usually used in reinforced / precast concrete structures for supporting vertical and horizontal forces. The corbels in general have a shear span to depth ratio (a/d) less than unity and transfer the loads predominantly through shear. A typical corbel structure with its primary (A_s) and secondary (A_h) reinforcement is shown in figure 6.1. The primary reinforcement influences the ductile failure behavior and the secondary reinforcement influences the shear capacity of the corbels (Mehdi Rezaei et al., 2013).

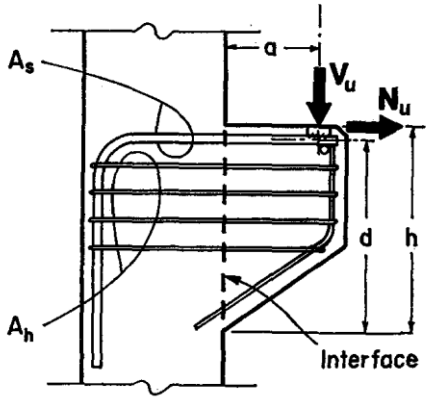

Figure 6.1: A typical corbel/bracket

Corbels exhibit failure modes such as flexural tension which tends to crush concrete because of the yielding of flexural or primary reinforcement. Shear compression failure foaming diagonal cracks i.e., diagonal splitting along the compression strut. Shear friction failure i.e., sliding which results in separation from column or wall face. Splitting failure results because of the vertical load applied at close to cantilever free end. Other failures such as anchorages failure or

bearing failure which causes cracking of concrete under bearing pads due to insufficient size or flexibility also occur. The different failure patterns in corbels are shown in figure 6.2.

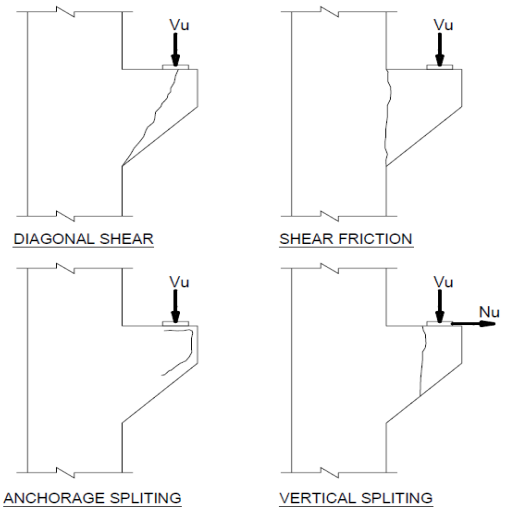

Figure 6.2: Different failure patterns in corbel/bracket

Extensively published research is available on normal, high strength, and fiber-reinforced concrete corbels. However, there are very few studies on the behavior of reinforced geopolymer concrete corbels. This chapter presents the experimental investigation of geopolymer concrete corbels and validates the experimental results using the proposed shear strength model for geopolymer concrete in chapter 5 (Eq. 5.4).

6.2 OBJECTIVES OF THE STUDY

The following are the objectives for the experimental investigations on geopolymer concrete corbels:

1. To study the behavior and the failure pattern of reinforced geopolymer concrete corbels.
2. To study the shear carrying capacity of reinforced geopolymer concrete corbels.
3. To compare the experimental shear strength of corbels with the proposed shear equation for fly ash and GGBS based geopolymer concrete established in chapter 5 (Eq. 5.4).

The parameters of experimental investigation are:

1) Compressive strength of geopolymer concrete (N/mm^2) - Three different strengths- B (20-25 MPa), C (40-45 MPa), and D (50-55 MPa) were tested.
2) Three different percentages of secondary reinforcement (A_h) crossing the monolithic interface of geopolymer concrete corbel, in the form of horizontal stirrups - 0%, 0.53%, and 0.80% of the cross-sectional area at the monolithic interface were tested.

The primary reinforcement (main tension flexural tension reinforcement (A_s)) and shear span to depth (a/d) were kept constant in all the tested corbels.

6.3 EXPERIMENTAL SET-UP

The experimental set-up consisted of casting and testing a total of 45 'Symmetrical Double Corbel (SDC)' specimens made using fly ash and GGBS based geopolymer concrete. The SDC specimens tested assume the geometry and arrangement of reinforcement as shown in figures 6.3 and 6.4 respectively

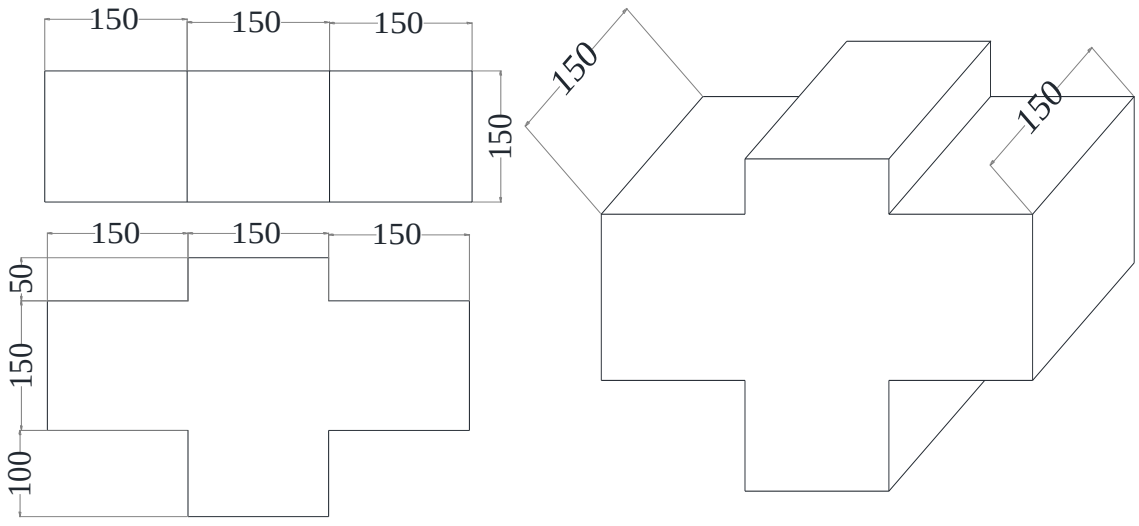

Figure 6.3: SDC specimen geometry

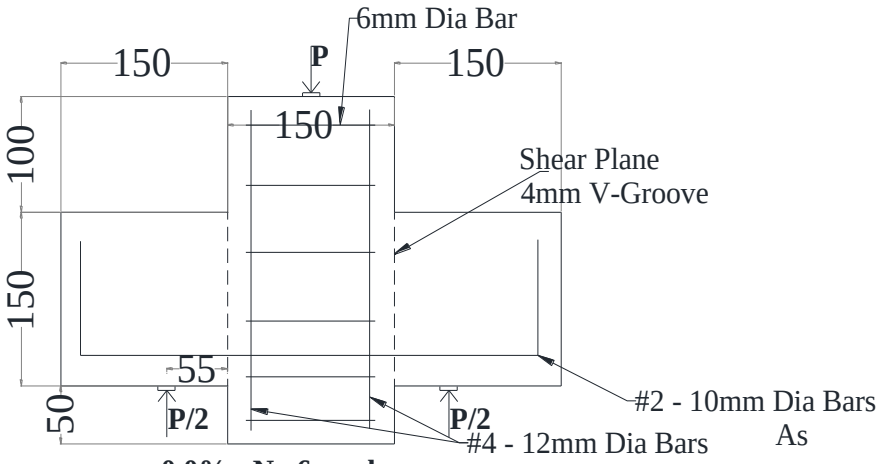

0.0% - No 6mm bars
Shear Reinforcement

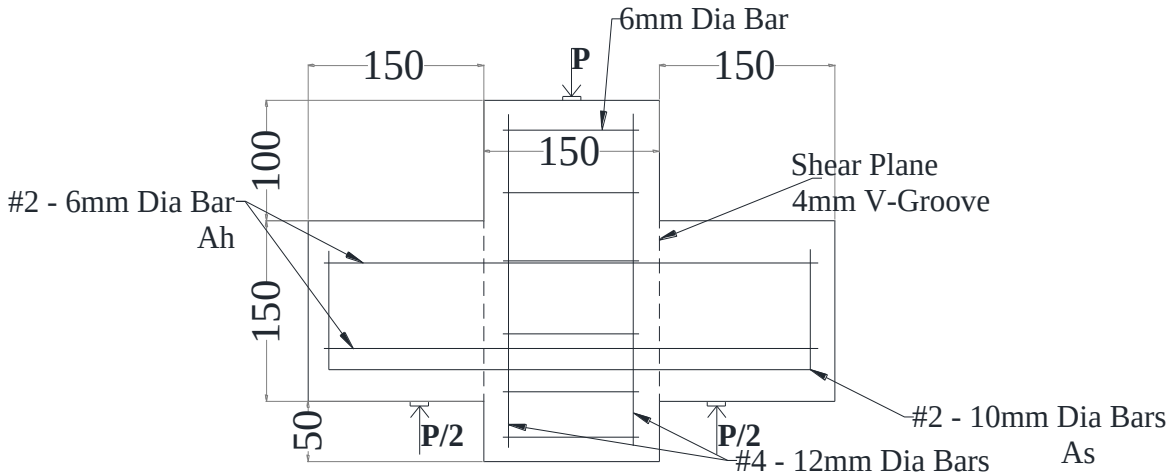

0.53% - 2nos. 6mm bars
Shear Reinforcement

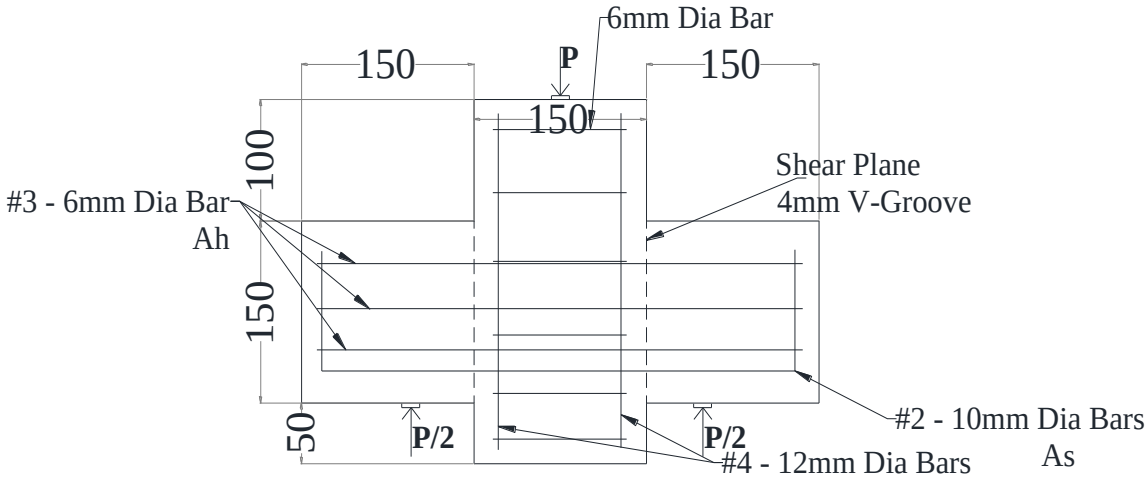

0.80% - 3nos. 6mm bars
Shear Reinforcement

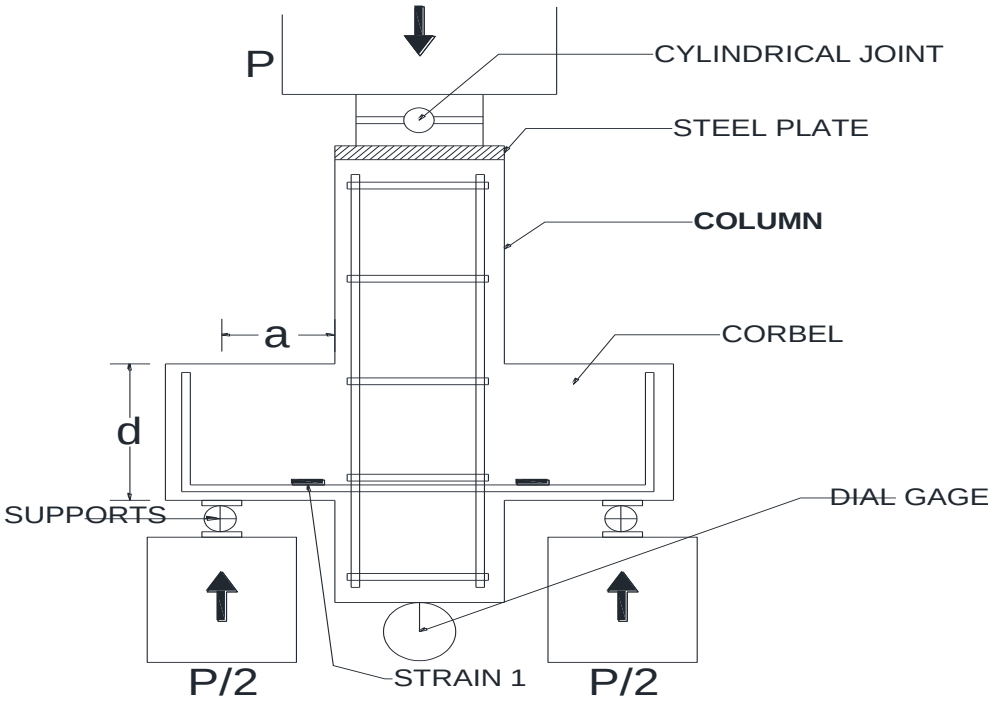

Figure 6.4: SDC specimen reinforcement and load scheme adopted

The schematic diagram of the experimental program shown in figure 6.5 presents the details of variables considered and the number of specimens cast under each variable.

Designation of geopolymer concrete Corbel

There were two variables in the experimental study:

- Strength of GPC mix ---------B (20 – 30 MPa), C (35 – 45 MPa), and D (50 – 60 MPa)
- Stirrups (A_h) percent provided--------S1 (0%), S2 (0.53%), S3 (0.80%)

For each variation there were 3 (or) 6 identical specimens numbered as…1, 2, 3, 4, 5, and 6. Hence each geopolymer concrete corbel was designated based on its mix strength, percent of stirrups, and the identical specimen number.

For example, in the corbel specimen designated GCBS1-3: GC indicates geopolymer concrete corbel, B indicates the corbel was cast using B type mix, S1 indicates the corbel was provided with 0% percent stirrups, and 3-indicates the identical specimen number.

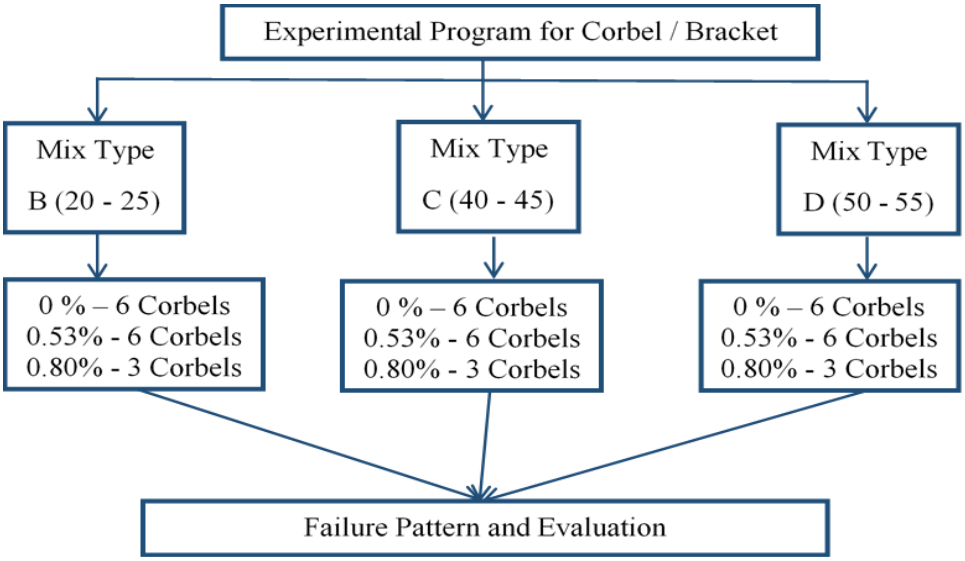

Figure 6.5: Schematic diagram of the experimental program

6.4 MATERIAL DETAILS

6.4.1 Fly ash and GGBS

Binder materials **fly ash** and **GGBS we**re obtained from NTPC Ramagundam thermal power plant, Ramagundam, India, and JSW Cements Pvt ltd, Bilakalagudur, India with a specific gravity of 2.17 and 2.90 respectively. Table 6.1, shows the details of the chemical compositions of fly ash and GGBS.

Table 6.1: Chemical composition of fly ash and GGBS (% by mass)

Binder Material	SiO_2	Al_2O_3	Fe_2O_3	SO_3	CaO	MgO	Na_2O	LOI
Fly ash	60.11	26.53	4.25	0.35	4.00	1.25	0.22	0.88
GGBS	37.73	14.42	1.11	0.39	37.34	8.71	--	1.41

6.4.2 Aggregates

River sand conforming to Zone-II of IS: 383, 2016 was used as fine aggregate. The specific gravity and bulk density of sand are 2.65 & 1.45 g/cm^3 respectively. Well-graded aggregate conforming to IS: 383, 2016 with 20 mm nominal size of granite was used as coarse aggregate 2.80 and 1.5 g/cm^3 were specific gravity and bulk density respectively. Details of river sand are shown in chapter 5.3.2 and 5.3.3

6.4.3 Alkaline activator Solution

A blend of sodium hydroxide and sodium silicate solutions form alkaline activator solution. Sodium hydroxide in the form of pellets with 98% purity was used for investigation. Sodium hydroxide pellets were dissolved in portable water and solutions of molarity (M = 8) were prepared. After cooling, of sodium hydroxide solution was mixed with sodium silicate which was in liquid form and stored at ambient temperature for 24 hrs. with a 1:2.5 ratio at a relative humidity of 65% before casting geopolymer concrete specimens. Potable water was used in the experimental work.

6.4.4 Superplasticizer

Sulphonated naphthalene formaldehyde-based superplasticizer (Conplast SP430) was used for the improvement of workability.

6.5 MIX PROPORTIONS

Parameters used for this study were different grades of geopolymer concrete with a change in binder index. Mix proportions were considered based on work done by G Mallikarjuna Rao et al., 2016. The molarity of sodium hydroxide was 8 M and sodium silicate to sodium hydroxide ratio was 2.5. Mix proportions are shown in Table 6.2

Table 6.2: Mix proportions of geopolymer concrete

Mix Type (Range for Grade of Concrete) N/mm^2	Fly ash (kg/m^3) (F)	GGBS (kg/m^3) (G)	Fine Aggregate (kg/m^3)	Coarse Aggregate (kg/m^3)	NaOH (kg/m^3) M = 8	Na_2SiO_3 (kg/m^3)	Alkaline liquid (kg/m^3) (A)
	Na_2SiO_3/NaOH = 2.5						
B (20 - 25)	294	126	812	965	72	180	252
C (40 - 45)	252	168	812	965	66	165	231
D (50 - 55)	210	210	812	965	60	150	210

6.6 CASTING AND CURING OF GPC CORBELS / BRACKETS

6.6.1 Specimen preparation

A total of 45 'Symmetrical Double Corbel (SDC)' specimens made using fly ash and GGBS based geopolymer concrete were cast and tested. The SDC specimens tested had the geometry and arrangement of reinforcement as shown in Figures 6.3 and 6.4 respectively. Corbels were been cast with three different grades and different percentages of shear or horizontal stirrups i.e., shear reinforcement in the form of closed stirrups was been provided across the shear interface in geopolymer concrete corbels.

All specimens comprised of a column of length 300 mm with two symmetric corbels projecting from the column on either side. The column consisted of longitudinal reinforcement of 4 nos. of diameter 12 mm of 500 MPa yield strength. Horizontal lateral ties were provided in the column of diameter 6 mm, spaced at 75 mm c/c along the length of the column.

In the corbels, the primary tension reinforcement consisted of 2 - 10 mm with yield strength of 500 MPa. Shear reinforcement consisted of 2 legged 6 mm dia. closed stirrups with yield strength of 250 MPa, placed across the shear plane. The number of closed stirrups was varied to change the percent of shear reinforcement across the interface.

The details of reinforcement of corbel specimen cast are shown in Figures 6.4 and 6.6. Design details of the specimen have been mentioned in table 6.3. V grooves of 4 mm deep were made along the vertical direction at the corbel – column junction for ensuring the location and the direction of shear crack.

Table 6.3: Design details of the double corbels/brackets

Specimen ID	Mix Type (Range for the grade of concrete) N/mm^2	Main (Tension) reinforcement A_{main} (A_s)		Horizontal (shear reinforcement) stirrups $A_{stirrups}$ (A_h)		a/d
		Bar details	ρ= A_s/bd	Bar details	ρ= A_h/bd	
GCBS1-1	B (20 - 25)	2 Nos. – 10 mm Dia.	0.74%	NA	0%	0.46
GCBS1-2	B (20 - 25)	2 Nos. – 10 mm Dia.	0.74%	NA	0%	0.46
GCBS1-3	B (20 - 25)	2 Nos. – 10 mm Dia.	0.74%	NA	0%	0.46
GCBS1-4	B (20 - 25)	2 Nos. – 10 mm Dia.	0.74%	NA	0%	0.46
GCBS1-5	B (20 - 25)	2 Nos. – 10 mm Dia.	0.74%	NA	0%	0.46
GCBS1-6	B (20 - 25)	2 Nos. – 10 mm Dia.	0.74%	NA	0%	0.46
GCBS2-1	B (20 - 25)	2 Nos. – 10 mm Dia.	0.74%	2 Nos. – 6 mm Dia.	0.53%	0.46
GCBS2-2	B (20 - 25)	2 Nos. – 10 mm Dia.	0.74%	2 Nos. – 6 mm Dia.	0.53%	0.46
GCBS2-3	B (20 - 25)	2 Nos. – 10 mm Dia.	0.74%	2 Nos. – 6 mm Dia.	0.53%	0.46
GCBS2-4	B (20 - 25)	2 Nos. – 10 mm Dia.	0.74%	2 Nos. – 6 mm Dia.	0.53%	0.46
GCBS2-5	B (20 - 25)	2 Nos. – 10 mm Dia.	0.74%	2 Nos. – 6 mm Dia.	0.53%	0.46
GCBS2-6	B (20 - 25)	2 Nos. – 10 mm Dia.	0.74%	2 Nos. – 6 mm Dia.	0.53%	0.46
GCBS3-1	B (20 - 25)	2 Nos. – 10 mm Dia.	0.74%	3 Nos. – 6 mm Dia.	0.80%	0.46
GCBS3-2	B (20 - 25)	2 Nos. – 10 mm Dia.	0.74%	3 Nos. – 6 mm Dia.	0.80%	0.46
GCBS3-3	B (20 - 25)	2 Nos. – 10 mm Dia.	0.74%	3 Nos. – 6 mm Dia.	0.80%	0.46
GCCS1-1	C (40 - 45)	2 Nos. – 10 mm Dia.	0.74%	NA	0%	0.46
GCCS1-2	C (40 - 45)	2 Nos. – 10 mm Dia.	0.74%	NA	0%	0.46
GCCS1-3	C (40 - 45)	2 Nos. – 10 mm Dia.	0.74%	NA	0%	0.46
GCCS1-4	C (40 - 45)	2 Nos. – 10 mm Dia.	0.74%	NA	0%	0.46
GCCS1-5	C (40 - 45)	2 Nos. – 10 mm Dia.	0.74%	NA	0%	0.46
GCCS1-6	C (40 - 45)	2 Nos. – 10 mm Dia.	0.74%	NA	0%	0.46
GCCS2-1	C (40 - 45)	2 Nos. – 10 mm Dia.	0.74%	2 Nos. – 6 mm Dia.	0.53%	0.46
GCCS2-2	C (40 - 45)	2 Nos. – 10 mm Dia.	0.74%	2 Nos. – 6 mm Dia.	0.53%	0.46
GCCS2-3	C (40 - 45)	2 Nos. – 10 mm Dia.	0.74%	2 Nos. – 6 mm Dia.	0.53%	0.46
GCCS2-4	C (40 - 45)	2 Nos. – 10 mm Dia.	0.74%	2 Nos. – 6 mm Dia.	0.53%	0.46
GCCS2-5	C (40 - 45)	2 Nos. – 10 mm Dia.	0.74%	2 Nos. – 6 mm Dia.	0.53%	0.46
GCCS2-6	C (40 - 45)	2 Nos. – 10 mm Dia.	0.74%	2 Nos. – 6 mm Dia.	0.53%	0.46
GCCS3-1	C (40 - 45)	2 Nos. – 10 mm Dia.	0.74%	3 Nos. – 6 mm Dia.	0.80%	0.46
GCCS3-2	C (40 - 45)	2 Nos. – 10 mm Dia.	0.74%	3 Nos. – 6 mm Dia.	0.80%	0.46
GCCS3-3	C (40 - 45)	2 Nos. – 10 mm Dia.	0.74%	3 Nos. – 6 mm Dia.	0.80%	0.46
GCDS1-1	D (50 - 55)	2 Nos. – 10 mm Dia.	0.74%	NA	0%	0.46
GCDS1-2	D (50 - 55)	2 Nos. – 10 mm Dia.	0.74%	NA	0%	0.46
GCDS1-3	D (50 - 55)	2 Nos. – 10 mm Dia.	0.74%	NA	0%	0.46
GCDS1-4	D (50 - 55)	2 Nos. – 10 mm Dia.	0.74%	NA	0%	0.46
GCDS1-5	D (50 - 55)	2 Nos. – 10 mm Dia.	0.74%	NA	0%	0.46
GCDS1-6	D (50 - 55)	2 Nos. – 10 mm Dia.	0.74%	NA	0%	0.46
GCDS2-1	D (50 - 55)	2 Nos. – 10 mm Dia.	0.74%	2 Nos. – 6 mm Dia.	0.53%	0.46
GCDS2-2	D (50 - 55)	2 Nos. – 10 mm Dia.	0.74%	2 Nos. – 6 mm Dia.	0.53%	0.46
GCDS2-3	D (50 - 55)	2 Nos. – 10 mm Dia.	0.74%	2 Nos. – 6 mm Dia.	0.53%	0.46
GCDS2-4	D (50 - 55)	2 Nos. – 10 mm Dia.	0.74%	2 Nos. – 6 mm Dia.	0.53%	0.46
GCDS2-5	D (50 - 55)	2 Nos. – 10 mm Dia.	0.74%	2 Nos. – 6 mm Dia.	0.53%	0.46

Specimen ID	Mix Type (Range for the grade of concrete) N/mm^2	Main (Tension) reinforcement A_{main} (A_s)		Horizontal (shear reinforcement) stirrups $A_{stirrups}$ (A_h)		a/d
		Bar details	ρ= A_s/bd	Bar details	ρ= A_h/bd	
GCDS2-6	D (50 - 55)	2 Nos. – 10 mm Dia.	0.74%	2 Nos. – 6 mm Dia.	0.53%	0.46
GCDS3-1	D (50 - 55)	2 Nos. – 10 mm Dia.	0.74%	3 Nos. – 6 mm Dia.	0.80%	0.46
GCDS3-2	D (50 - 55)	2 Nos. – 10 mm Dia.	0.74%	3 Nos. – 6 mm Dia.	0.80%	0.46
GCDS3-3	D (50 - 55)	2 Nos. – 10 mm Dia.	0.74%	3 Nos. – 6 mm Dia.	0.80%	0.46

6.6.2 Mixing and casting of Specimen

Separate dry material was assessed and then mixed in a 100 kg capacity rotating drum-type pan mixer. Next, alkaline solution and superplasticizer of optimum dosage were added. Suitable consistent mixing was ensured by continuous mixing of all the constituents for 5 to 7 minutes. The fresh mixes were cohesive and segregation-free. After mixing, the fresh mix was moved into moulds followed by hand vibration for 45 seconds.

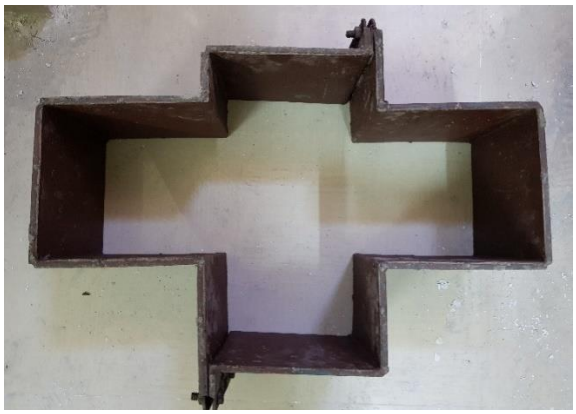

Corbel/Bracket specimen mould

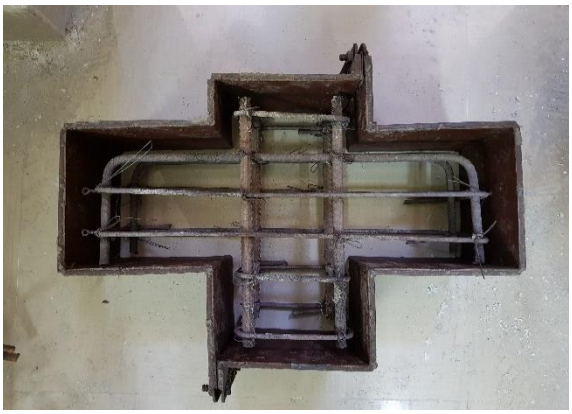

Corbel specimen with reinforcement

Reinforcement configuration

Figure 6.6: SDC specimen casting details

Figure 6.7: Cast specimens left for outdoor curing

6.6.3 Curing of specimens

Specimens were detached from the moulds after 24 hours and air-cured (temperature—35±2°C and relative humidity—75%) up to 28 days as shown in figure 6.7.

6.6.4 Testing of GPC corbels/brackets

For convenience, the corbel specimens were tested in an inverted position as shown in Figures 6.4 and 6.8. The corbels were supported on plain bearing free rollers resting on top of legs of the supporting wedge at a distance 'a = 55 mm' from the face of the column. The vertical load on the column section was subjected by 2000 kN capacity Tinius Olsen Testing (T.O.T) machine located concentrically on top of the column. This setup was assumed to impart only vertical load and no horizontal load was generated.

Figure 6.8: Test setup

As in the case of push-off specimen, 4 mm deep grooves were made at the interfacial zone of column and corbel before the tests. In addition to the corbels, companion cubes were also cast to check the required strength of concrete used for casting the corbel. The average deflection at the interface was measured using L.V.D.T (Linear Variable Differential Transducer) to measure the relative shear slip of the interface. To measure the defection of the column portion owing to flexure behavior development, dial gauge reading was taken at the center of the column. Load (P/2) versus deflection graphs were developed and shown in table 6.4 and figure 6.9.

Table 6.4. Ultimate shear and corresponding deflection of corbel specimens

Description	Ultimate Load kN	% of the increase in Load	Deflection mm	% of the increase in Deflection
GCBS1 - 1	87.11	0	4.10	0
GCBS1 - 3	87.28		4.36	
GCBS1 - 6	88.37		4.61	
Average	**87.59**		**4.36**	
GCBS2 - 1	131.89	52.46	6.25	44.22
GCBS2 - 4	133.83		6.46	
GCBS2 - 6	134.88		6.14	
Average	**133.53**		**6.28**	
GCBS3 - 1	183.07	112.41	7.18	67.02
GCBS3 - 2	185.81		7.33	
GCBS3 - 3	189.26		7.32	
Average	**186.05**		**7.28**	
GCCS1 - 1	142.46	0	5.31	0
GCCS1 - 3	141.65		5.25	
GCCS1 - 5	139.43		5.53	
Average	**141.18**		**5.36**	
GCCS2 - 2	215.46	52.19	7.21	34.24
GCCS2 - 4	212.33		7.12	
GCCS2 - 5	216.78		7.27	
Average	**214.86**		**7.20**	
GCCS3 - 1	271.1	94.35	8.02	51.40
GCCS3 - 2	272.46		8.24	
GCCS3 - 3	279.6		8.1	
Average	**274.39**		**8.12**	
GCDS1 - 3	155.84	0	5.87	0
GCDS1 - 5	157.89		5.97	
GCDS1 - 6	156.56		6.06	

Description	Ultimate Load kN	% of the increase in Load	Deflection mm	% of the increase in Deflection
Average	**156.76**		**5.97**	
GCDS2 - 1	241.13	53.11	7.88	31.96
GCDS2 - 3	237.72		7.96	
GCDS2 - 4	241.23		7.78	
Average	**240.03**		**7.87**	
GCDS3 - 1	317.01	99.52	9.42	55.42
GCDS3 - 2	314.62		9.28	
GCDS3 - 3	306.69		9.12	
Average	**312.77**		**9.27**	

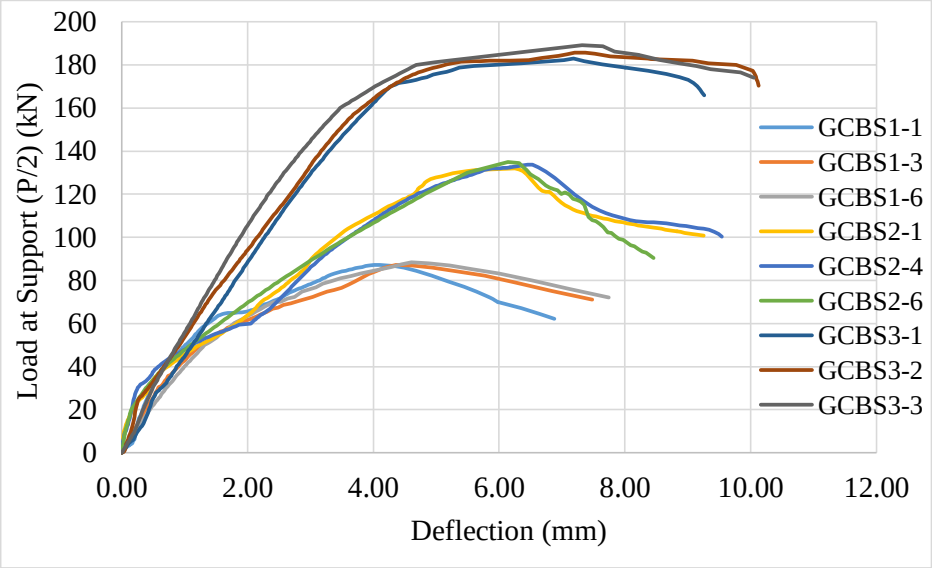

Figure 6.9 (a): Load – deflection curve of corbels for grade B of GPC

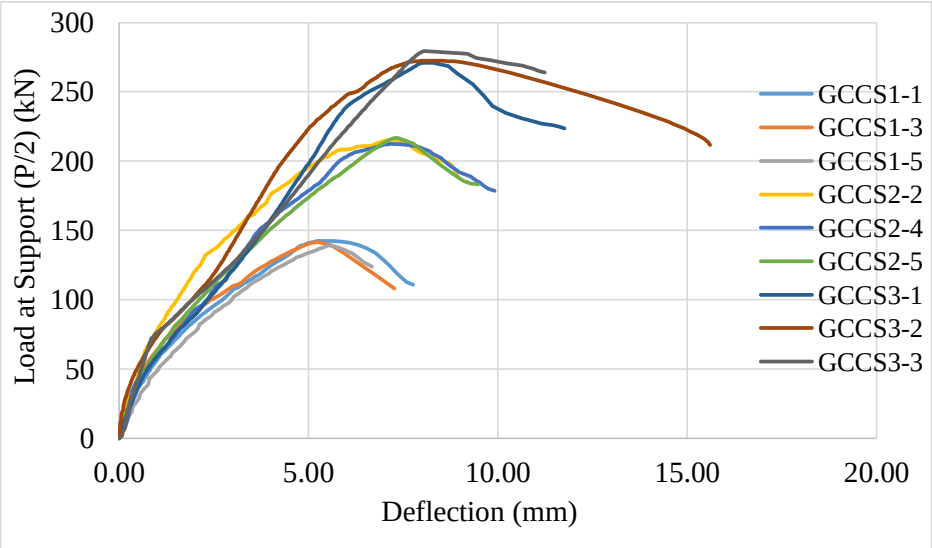

Figure 6.9 (b): Load – deflection curve of corbels for grade C of GPC

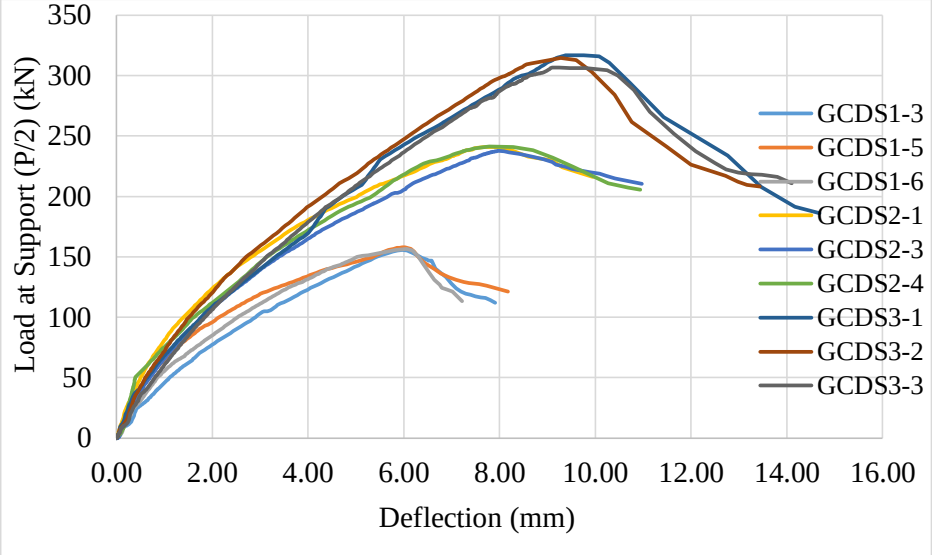

Figure 6.9 (c): Load – deflection curve of corbels for grade C of GPC
Figure 6.9: Load – deflection curves for corbels

The corbel sample was been subjected to incremental loads until point of failure. The failure was characterized by the appearance of cracks near the interface. Since the specimen tested was symmetrical double corbel, 50% of the ultimate load was considered as the shear force at the interface, and the same is shown in table 6.5, and the failure pattern in figure 6.10.

Table. 6.5. Maximum shear force at the interface and corresponding shear stress at the interface of GPC corbels

S.No	Corbel ID	Compressive strength of GPC Mix (f_{gpc})	Closed-loop Stirrups (A_h)		Max shear at the interface (kN)	Shear stress (υ)	υ / f_{gpc}
			Details	A_h%			
1.	GCBS1-1	25.94	NA	0%	87.11	4.09	0.16
2.	GCBS1-2	26.07	NA	0%	84.91	3.99	0.15
3.	GCBS1-3	26.07	NA	0%	87.28	4.10	0.16
4.	GCBS1-4	26.07	NA	0%	85.71	4.02	0.15
5.	GCBS1-5	26.21	NA	0%	84.81	3.98	0.15
6.	GCBS1-6	26.56	NA	0%	88.37	4.15	0.16
7.	GCBS2-1	25.62	2 Nos. – 6 mm Dia.	0.53%	131.89	6.19	0.24
8.	GCBS2-2	25.62	2 Nos. – 6 mm Dia.	0.53%	134.88	6.33	0.25
9.	GCBS2-3	25.62	2 Nos. – 6 mm Dia.	0.53%	130.70	6.14	0.24
10.	GCBS2-4	25.94	2 Nos. – 6 mm Dia.	0.53%	133.83	6.28	0.24
11.	GCBS2-5	26.21	2 Nos. – 6 mm Dia.	0.53%	132.59	6.23	0.24
12.	GCBS2-6	26.56	2 Nos. – 6 mm Dia.	0.53%	134.88	6.33	0.24
13.	GCBS3-1	25.94	3 Nos. – 6 mm Dia.	0.80%	183.07	8.59	0.33
14.	GCBS3-2	26.21	3 Nos. – 6 mm Dia.	0.80%	185.81	8.72	0.33
15.	GCBS3-3	26.56	3 Nos. – 6 mm Dia.	0.80%	189.26	8.89	0.33
16.	GCCS1-1	39.18	NA	0%	142.46	6.69	0.17
17.	GCCS1-2	39.18	NA	0%	147.54	6.93	0.18
18.	GCCS1-3	39.18	NA	0%	141.65	6.65	0.17

S.No	Corbel ID	Compressive strength of GPC Mix (f_{gpc})	Closed-loop Stirrups (A_h)		Max shear at the interface (kN)	Shear stress (υ)	υ / f_{gpc}
			Details	A_h%			
19.	GCCS1-4	40.12	NA	0%	141.62	6.65	0.17
20.	GCCS1-5	40.16	NA	0%	139.43	6.55	0.16
21.	GCCS1-6	40.24	NA	0%	142.60	6.69	0.17
22.	GCCS2-1	39.71	2 Nos. – 6 mm Dia.	0.53%	214.62	10.08	0.25
23.	GCCS2-2	39.71	2 Nos. – 6 mm Dia.	0.53%	215.46	10.12	0.25
24.	GCCS2-3	39.71	2 Nos. – 6 mm Dia.	0.53%	217.66	10.22	0.26
25.	GCCS2-4	40.12	2 Nos. – 6 mm Dia.	0.53%	212.33	9.97	0.25
26.	GCCS2-5	40.16	2 Nos. – 6 mm Dia.	0.53%	216.78	10.18	0.25
27.	GCCS2-6	40.24	2 Nos. – 6 mm Dia.	0.53%	212.58	9.98	0.25
28.	GCCS3-1	40.12	3 Nos. – 6 mm Dia.	0.80%	271.10	12.73	0.32
29.	GCCS3-2	40.16	3 Nos. – 6 mm Dia.	0.80%	272.46	12.79	0.32
30.	GCCS3-3	40.24	3 Nos. – 6 mm Dia.	0.80%	279.60	13.13	0.33
31.	GCDS1-1	53.41	NA	0%	158.07	7.42	0.14
32.	GCDS1-2	53.41	NA	0%	163.43	7.67	0.14
33.	GCDS1-3	53.41	NA	0%	155.84	7.32	0.14
34.	GCDS1-4	54.11	NA	0%	152.89	7.18	0.13
35.	GCDS1-5	54.22	NA	0%	157.89	7.41	0.14
36.	GCDS1-6	54.39	NA	0%	156.56	7.35	0.14
37.	GCDS2-1	53.73	2 Nos. – 6 mm Dia.	0.53%	241.13	11.32	0.21
38.	GCDS2-2	53.73	2 Nos. – 6 mm Dia.	0.53%	249.69	11.72	0.22
39.	GCDS2-3	53.73	2 Nos. – 6 mm Dia.	0.53%	237.72	11.16	0.21
40.	GCDS2-4	54.11	2 Nos. – 6 mm Dia.	0.53%	241.23	11.33	0.21
41.	GCDS2-5	54.22	2 Nos. – 6 mm Dia.	0.53%	232.19	10.90	0.2
42.	GCDS2-6	54.39	2 Nos. – 6 mm Dia.	0.53%	240.99	11.31	0.21
43.	GCDS3-1	54.11	3 Nos. – 6 mm Dia.	0.80%	317.01	14.88	0.28
44.	GCDS3-2	54.22	3 Nos. – 6 mm Dia.	0.80%	314.62	14.77	0.27
45.	GCDS3-3	54.39	3 Nos. – 6 mm Dia.	0.80%	306.69	14.40	0.26

Figure 6.10: Failure pattern of corbel/bracket

6.7 RESULTS AND DISCUSSIONS

All geopolymer concrete corbels were tested under load rate control. There were three phases of response to load-deflection curves. These were elastic - uncracked, elastic – cracked, and ultimate phases, where the first step ends when cracks start which are very fine and invisible. In the elastic – uncracked phase, the deflection increased linearly in all the corbels with a load, since the materials in the compression and tension zones were elastic. After the first crack of the specimen, there was a noticeable decrease in stiffness i.e., a change in slope of the load-deflection curve. It varied from 30% to 35% of the ultimate load in the present investigation.

Elastic - cracked phase, a linear relationship between load and deflection was also observed, but with a decrease in the slope of the load-deflection curve to about 60 - 65% of the ultimate load. After this phase, the slope decreased significantly, and a predominant increase in deflection occurred with a slight increase in the load level until failure. Figure 6.9 shows the load-deflection response of corbels for different grades of geopolymer concrete.

From figure 6.9 (a) and table 6.4, it can be observed that increase in ultimate shear load was up to 52% and 112% for 0.53% & 0.80% of secondary reinforcement at the interface of the corbel and with an increase in 44% and 67% of deflection respectively for grade B of geopolymer concrete where the compressive strength ranges from 20 – 25 N/mm^2. From figure 6.9 (b), it can be observed that the increase in ultimate load was up by 52 and 95% for 0.53 & 0.80% secondary reinforcement crossing interface of corbel, respectively for grade C of geopolymer concrete where compressive strength ranges from 40 – 45 N/mm^2. We can also observe that the compressive strength of geopolymer concrete increased from 20 MPa to 40 MPa and the ultimate shear strength increased by 61%. From figure 6.9 (c), the increase in ultimate shear strength increased by 55% and 100% for 0.53 & 0.80% secondary reinforcement crossing interface of corbel respectively for grade D of geopolymer concrete where compressive strength

ranges from 50 – 55 N/mm^2. It was also observed that the compressive strength of geopolymer concrete increased from 20 MPa to 50 MPa and the ultimate shear strength increased by 79%.

An increase in load-carrying capacity of corbels is found to be significant for corbels with the percentage of secondary reinforcement of 0.53% and 0.80% up to 50% and 100% increase respectively. The shape and area beneath the load-deflection curves are often used as indicators of ductility and toughness respectively. Results from figure 6.9 show that additional secondary reinforcement resulted in an increase in load-carrying capacity as well as ductility of corbels.

During the testing, visible cracks were observed at about 60 - 65% of failure load, near the re-entrant corner of the column corbel interface. With increase in the load, a few more inclined cracks formed well within the shear span and slightly away from the interface. Usually, three types of cracks which develop are distinct: flexural cracks, flexure-shear cracks, and inclined (diagonal) shear cracks. Flexural failure was due to the wide opening of flexural cracks, while diagonal cracks remained fine. In the case of shear failure, flexural cracks remained fine, and failure was characterized by the expansion of one or more shear cracks associated with concrete crushing near the intersection of the sloped edge of the shoulder and the end of the column.

At failure load, one of the flexural cracks extended as a diagonal crack towards the column corbel interface. The type of failure can be categorized under diagonal shear failure. In the absence of horizontal stirrups, the formation was sudden and resulted in wider diagonal cracks. However, the provision of horizontal stirrups made the diagonal cracks propagate slowly towards the column corbel interface. Further, the width of diagonal cracks in stirrup reinforced corbels was small compared to that of corbels with no stirrup reinforcement. Testing of the specimen was stopped at the point where the load could no longer be increased. There were no signs of cracks / crushing in the column location / area. A similar failure pattern was observed by other investigators (Kriz and Raths, 1965, Mattock et al., 1976) who worked on RC corbels.

The variation of shear strength of geopolymer concrete corbels with the corresponding geopolymer concrete compressive strength is shown in figure 6.11. From the variation, it is observed that the shear strength increased with an increase in the compressive strength of geopolymer concrete. Also, the rate of increase of shear strength slightly decreased for a compressive strength of geopolymer concrete that was approximately more than 40 MPa. This was also observed from load-deflection curves where ultimate shear strength increased by 61% for 100% (from 20 MPa to 40 MPa) in concrete strength. Only an 18% increase in shear strength was observed for a 50% (from 40 MPa to 50 MPa) increase in compressive strength.

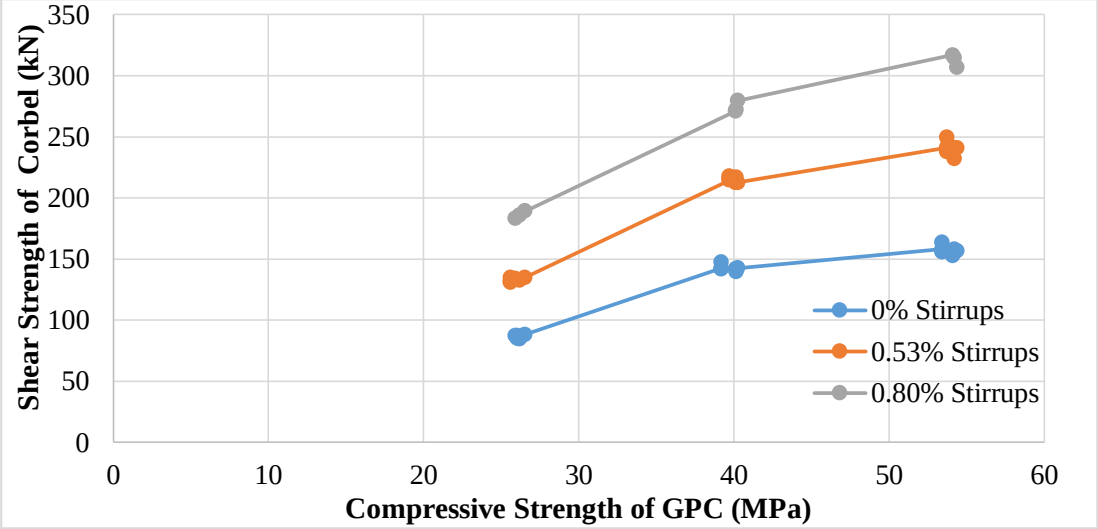

Figure 6.11: Shear strength vs. Compressive strength of GPC corbels

6.7.1 Validation of the proposed analytical expression for shear strength

To predict the shear strength of monolithic geopolymer concrete interface, Eq. 5.4 has been proposed based on tests on the push-off specimens.

The proposed shear strength of monolithic geopolymer concrete interface (V_u) based on Eq. 5.4 is as follows:

$$V_u = V_c + V_f + V_d$$

Where,

V_c = Shear strength of unreinforced GPC due to cohesion = c $(f_{gpc})^{(1/3)}$ bh, where For $f_{gpc} \leq 40$ MPa, c = 0.031 f_{gpc}+0.06, For f_{gpc}>40 MPa, c = 0.0054f_{gpc}+1.0809

V_f = Shear strength of reinforced GPC due to friction = $\mu[\sigma_n+\rho k f_y]$ bh, where k=0.5 and $f_{gpc} \geq 20$ MPa μ =0.8, $f_{gpc} \geq 35$ MPa μ =1.0, $\rho = \rho_{Main} + \rho_{Stirrups}$ (Randl, 1997)

V_d = Shear Strength due to Dowel contribution = $\alpha\rho\sqrt{f_y f_{gpc}}$ bh, $\rho = \rho_{Stirrups}$ where α = 6.338 $\rho\sqrt{f_y f_{gpc}}$

The total percentage of steel carrying both primary (main tension-steel) and secondary (stirrups) was used in the calculation of the shear strength contribution (V_f) of reinforced geopolymer concrete due to friction. As the failure of geopolymer concrete corbels was characterized by diagonal shear cracks, for the calculation of shear strength contribution owing to dowel action, only closed stirrups crossing the interface were considered. The shear capacity calculated from the predicted equation was been compared with that of the experimental shear capacity obtained from the tests of corbel samples. The results of the comparison are given in table 6.6 and the same is shown in figure 6.12.

Table 6.6. Validation of the proposed analytical expression for shear strength at the monolithic interface of corbel

Description	Average compressive strength (f_{gpc}) N/mm^2	% of main steel A_{Main}	% of the steel in stirrups $A_{Stirrups}$	Experimental shear strength of corbel kN	Predicted shear strength based on the monolithic interface of GPC				Experimental / Analytical
					Cohesion contribution of shear strength kN	Frictional contribution of shear strength kN	Dowel contribution of shear strength kN	Predicted shear strength kN	
GCBS1-1	25.94	0.74	0.00	87.11	54.49	31.42	0.00	85.90	1.01
GCBS1-2	26.07	0.74	0.00	84.91	54.83	31.42	0.00	86.25	0.98
GCBS1-3	26.07	0.74	0.00	87.28	54.83	31.42	0.00	86.25	1.01
GCBS1-4	26.07	0.74	0.00	85.71	54.83	31.42	0.00	86.25	0.99
GCBS1-5	26.21	0.74	0.00	84.81	55.20	31.42	0.00	86.62	0.98
GCBS1-6	26.56	0.74	0.00	88.37	56.14	31.42	0.00	87.55	1.01
GCBS2-1	25.62	0.74	0.53	131.89	53.64	42.72	24.37	120.73	1.09
GCBS2-2	25.62	0.74	0.53	134.88	53.64	42.72	24.37	120.73	1.12
GCBS2-3	25.62	0.74	0.53	130.70	53.64	42.72	24.37	120.73	1.08
GCBS2-4	25.94	0.74	0.53	133.83	54.49	42.72	24.67	121.89	1.10
GCBS2-5	26.21	0.74	0.53	132.59	55.20	42.72	24.93	122.86	1.08
GCBS2-6	26.56	0.74	0.53	134.88	56.14	42.72	25.26	124.13	1.09
GCBS3-1	25.94	0.74	0.80	183.07	54.49	48.38	55.52	158.38	1.16
GCBS3-2	26.21	0.74	0.80	185.81	55.20	48.38	56.10	159.68	1.16
GCBS3-3	26.56	0.74	0.80	189.26	56.14	48.38	56.85	161.36	1.17
GCCS1-1	39.18	0.74	0.00	142.46	92.21	39.27	0.00	131.48	1.08
GCCS1-2	39.18	0.74	0.00	147.54	92.21	39.27	0.00	131.48	1.12
GCCS1-3	39.18	0.74	0.00	141.65	92.21	39.27	0.00	131.48	1.08
GCCS1-4	40.12	0.74	0.00	141.62	94.61	39.27	0.00	133.88	1.06
GCCS1-5	40.16	0.74	0.00	139.43	94.66	39.27	0.00	133.93	1.04
GCCS1-6	40.24	0.74	0.00	142.60	94.76	39.27	0.00	134.03	1.06

Table 6.6. Validation of the proposed analytical expression for shear strength at the monolithic interface of corbel

Description	Average compressive strength (f_{gpc}) N/mm^2	% of main steel A_{Main}	% of the steel in stirrups $A_{Stirrups}$	Experimental shear strength of corbel kN	Predicted shear strength based on the monolithic interface of GPC				Experimental / Analytical
					Cohesion contribution of shear strength kN	Frictional contribution of shear strength kN	Dowel contribution of shear strength kN	Predicted shear strength kN	
GCCS2-1	39.71	0.74	0.53	214.62	93.82	53.41	37.77	184.99	1.16
GCCS2-2	39.71	0.74	0.53	215.46	93.82	53.41	37.77	184.99	1.16
GCCS2-3	39.71	0.74	0.53	217.66	93.82	53.41	37.77	184.99	1.18
GCCS2-4	40.12	0.74	0.53	212.33	94.61	53.41	38.16	186.18	1.14
GCCS2-5	40.16	0.74	0.53	216.78	94.66	53.41	38.20	186.27	1.16
GCCS2-6	40.24	0.74	0.53	212.58	94.76	53.41	38.28	186.44	1.14
GCCS3-1	40.12	0.74	0.80	271.10	94.61	60.47	85.87	240.95	1.13
GCCS3-2	40.16	0.74	0.80	272.46	94.66	60.47	85.95	241.09	1.13
GCCS3-3	40.24	0.74	0.80	279.60	94.76	60.47	86.12	241.35	1.16
GCDS1-1	53.41	0.74	0.00	158.07	109.84	39.27	0.00	149.11	1.06
GCDS1-2	53.41	0.74	0.00	163.43	109.84	39.27	0.00	149.11	1.10
GCDS1-3	53.41	0.74	0.00	155.84	109.84	39.27	0.00	149.11	1.05
GCDS1-4	54.11	0.74	0.00	152.89	110.62	39.27	0.00	149.89	1.02
GCDS1-5	54.22	0.74	0.00	157.89	110.74	39.27	0.00	150.01	1.05
GCDS1-6	54.39	0.74	0.00	156.56	110.93	39.27	0.00	150.20	1.04
GCDS2-1	53.73	0.74	0.53	241.13	110.20	53.41	51.11	214.71	1.12
GCDS2-2	53.73	0.74	0.53	249.69	110.20	53.41	51.11	214.71	1.16
GCDS2-3	53.73	0.74	0.53	237.72	110.20	53.41	51.11	214.71	1.11
GCDS2-4	54.11	0.74	0.53	241.23	110.62	53.41	51.47	215.50	1.12
GCDS2-5	54.22	0.74	0.53	232.19	110.74	53.41	51.58	215.72	1.08
GCDS2-6	54.39	0.74	0.53	240.99	110.93	53.41	51.74	216.08	1.12

Table 6.6. Validation of the proposed analytical expression for shear strength at the monolithic interface of corbel

Description	Average compressive strength (f_{gpc}) N/mm^2	% of main steel A_{Main}	% of the steel in stirrups $A_{Stirrups}$	Experimental shear strength of corbel kN	Predicted shear strength based on the monolithic interface of GPC				Experimental / Analytical
					Cohesion contribution of shear strength kN	Frictional contribution of shear strength kN	Dowel contribution of shear strength kN	Predicted shear strength kN	
GCDS3-1	54.11	0.74	0.80	317.01	110.62	60.47	115.81	286.90	1.10
GCDS3-2	54.22	0.74	0.80	314.62	110.74	60.47	116.04	287.26	1.10
GCDS3-3	54.39	0.74	0.80	306.69	110.93	60.47	116.41	287.82	1.07
								Average	**1.09**

From table 6.6 and figure 6.12, it may be observed that there is about a 9% variation in the predicted results compared to experimental shear strength results. Hence it may be concluded that the results of the experimental shear capacity of corbel are well in agreement with the model proposed to predict the interface shear capacity of monolithic fly ash and GGBS based geopolymer concrete. The same may be verified by a graphical representation of experimental capacity versus predicted capacity where the coefficient of correlation comes out to be 0.99.

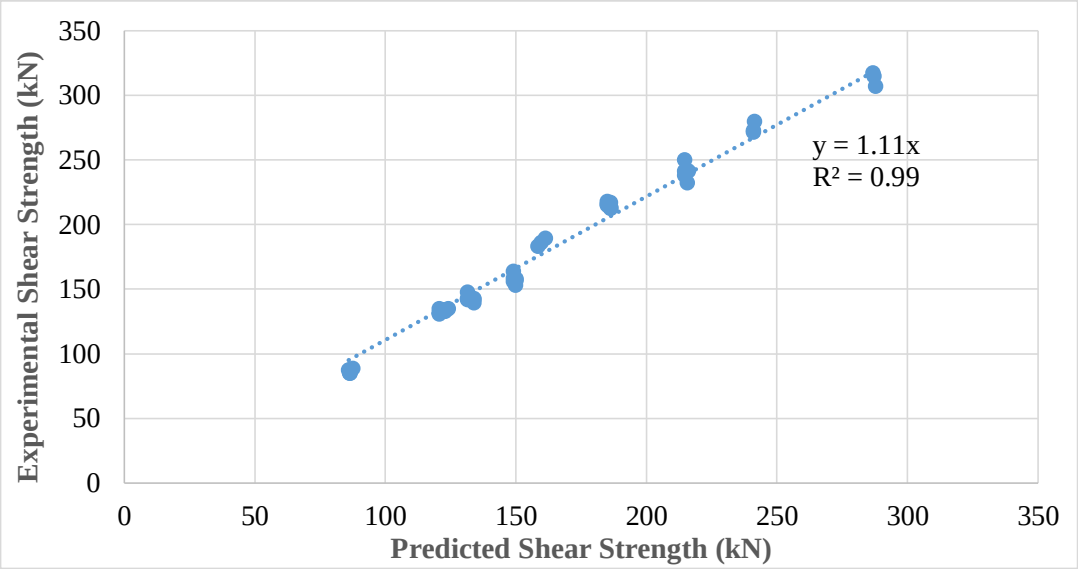

Figure 6.12: Experimental shear strength vs. Predicted shear strength

6.7.2 Comparison of experimental results with different theories and codes

The load Carrying capacity of reinforced concrete corbels can be evaluated by several theories like shear friction theory, truss analogy (strut and tie method), geometrical method of force distribution, and theory of plasticity. A few design codes considered shear – friction theory for evaluating the shear capacity of reinforced corbels, along with strut and tie methodology. Numerous investigations proposed strut and tie methodology in calculating the shear capacity of corbels. Table 6.7 presents the load-carrying capacity of reinforced corbels as per different investigators / Codes of practice on ordinary Portland cement concrete.

Table.6.7 Load carrying capacity of reinforced corbels as per different investigators / Codes of practice on conventional concrete

Reference	Shear strength expression	Remarks
Kriz and Rath, 1965	$V_u = \varphi \text{bd}\sqrt{f_c}F_1F_2$ $F_1 = 6.5(1 - 0.5\frac{d}{a})$ $F_2 = \frac{(1000\rho^{(\frac{1}{3}+\frac{0.4H}{V})})}{10^{\frac{0.8H}{V}}}$	The empirical approach is based on experimental work.
ACI 318, 2019 Cl. 16.5	Shear Friction Strength - $V_u = \emptyset\mu A_v f_y$ Flexural Strength – $V_u = \frac{M_u}{a}$ $M_u = \emptyset\mu f_y A_{sm}\left(d - \frac{a}{2}\right)$ $a = \frac{A_f f_y}{0.85 f_c' b}$ Maximum or permissible shear strength – $V_u = 0.2 f_c' bd$ or 5.5bd or $(3.31+0.08 f_c')bd$	Based on shear friction methodology. The strut and tie model was discussed in Chapter 23 of ACI 318 which is similar to PCI Handbook 2010.
CSA A23.3, 2019 Cl. 11.5	$\upsilon_u = \phi_c\lambda(c + \mu\sigma) + \Phi_s\rho_v f_y \cos\alpha_f$ c = 1; μ = 1.4 for monolithic concrete. λ = 1 for normal density concrete; $\lambda(c + \mu\sigma) \leq 0.25 f_c'$, $\rho_{vmin} = 0.06\sqrt{\frac{f_c'}{f_y}}$	Based on shear friction methodology.
	$\upsilon_u = \lambda k\sqrt{\sigma f_c'} + \rho_v f_y \cos\alpha_f$ $\lambda k\sqrt{\sigma f_c'} \leq 0.25 f_c'$ k = 0.6 for concrete placed monolithically.	
PCI, 2010 7th edition Cl. 5.9.4	Deriving from figure 5.9.4 of PCI handbook – 2010 and Araújo, D.L et al (2016) $V_d = (\sqrt{(1.7\gamma\beta b f_c a)^2 + 6.8 A_s f_y d\gamma^2\beta b f_c} - 1.7\gamma\beta b f_c a)/2$	Based on Strut and Tie Model. Shear Friction methodology is similar to ACI 318 (2014) γ = strength reduction factor = 0.75 β = 0.6 for no Stirrups else 0.75
Hagberg, 1983	$V_{max} = f_c \cos\beta$ $\left[1 - \frac{2 f_c bd}{F_s}\right]\tan^2\beta + \left[\frac{2 f_c bd}{F_s}\right]\tan\beta + 1 = 0$ $F_s = F_{s1} + F_{s2}$ $F_{s1} = A_s f_y$, $F_{s2} = A_h f_y$ $d = \frac{d_1 F_{s1} + d_2 F_{s2}}{F_s}$	Based on Strut and Tie Model.
Euro code 2, 2004 Section J 3	Deriving from figure J 5 of Euro code 2 – 2004 and Araújo, D.L et al (2016) $V_d = (\sqrt{(abk_1\left(1 - \frac{f_c}{250 \times 10^6}\right)\frac{f_c}{\gamma})^2 + 1.6bdA_s f_y k_1\left(1 - \frac{f_c}{250 \times 10^6}\right)\frac{f_c}{\gamma}} - abk_1\left(1 - \frac{f_c}{250 \times 10^6}\right)\frac{f_c}{\gamma}$	Based on Strut and Tie Model. K_1 = 1.18, γ = strength reduction factor = 0.75

To compare the shear transfer capacity of geopolymer concrete corbel with conventional concrete, theoretical shear capacity of the corbel section was been obtained from the shear strength expressions as mentioned in table 6.7. Comparison of experimental shear capacity of geopolymer concrete reinforced corbels with the shear strength predicted by the design codes/equations is presented in table 6.8.

From table 6.8, it may be observed that the interface shear capacity of conventional concrete, when used for geopolymer concrete, underestimates the shear capacity, and the same was observed during the experimental study on geopolymer concrete corbels. The comparison shows that the shear capacity obtained from different theories and codes are varied from 44% to 87% more than the experimental shear strength of geopolymer reinforced corbels.

The comparative study indicates that the proposed model (Ref 1) is almost in line with experimental shear strength values and is more accurate compared to all other models in estimating the shear strength of geopolymer concrete corbels. In general, the shear strength obtained based on strut and tie models is less conservative than the shear strength obtained from shear friction models. Hagberg, 1983 and Euro code 2 seem to give better prediction of shear strength of geopolymer concrete corbels.

Table 6.8. Comparison of experimental shear capacity of GPC reinforced corbels with the shear strength predicted by the design codes/equations

Spec. ID	f_{gpc} N/mm^2	V_{up} kN	Ref 1		Ref 2		Ref 3		Ref 4		Ref 5		Ref 6		Ref 7	
			V_{u1} kN	V_{up} / V_{u1}	V_{u2} kN	V_{up} / V_{u2}	V_{u3} kN	V_{up} / V_{u3}	V_{u4} kN	V_{up} / V_{u4}	V_{u5} kN	V_{up} / V_{u5}	V_{u6} kN	V_{up} / V_{u6}	V_{u7} kN	V_{up} / V_{u7}
GCBS1-1	25.94	87.11	85.90	1.01	67.63	1.29	82.47	1.06	85.32	1.02	86.07	1.01	83.49	1.04	94.58	0.92
GCBS1-2	26.07	84.91	86.25	0.98	67.80	1.25	82.47	1.03	85.32	1.00	86.19	0.99	83.60	1.02	94.68	0.90
GCBS1-3	26.07	87.28	86.25	1.01	67.80	1.29	82.47	1.06	85.32	1.02	86.19	1.01	83.60	1.04	94.68	0.92
GCBS1-4	26.07	85.71	86.25	0.99	67.80	1.26	82.47	1.04	85.32	1.00	86.19	0.99	83.60	1.03	94.68	0.91
GCBS1-5	26.21	84.81	86.62	0.98	67.98	1.25	82.47	1.03	85.32	0.99	86.31	0.98	83.73	1.01	94.79	0.89
GCBS1-6	26.56	88.37	87.55	1.01	68.43	1.29	82.47	1.07	85.32	1.04	86.61	1.02	84.03	1.05	95.06	0.93
GCBS2-1	25.62	131.89	120.73	1.09	80.52	1.64	109.14	1.21	88.68	1.49	112.00	1.18	123.06	1.07	116.39	1.13
GCBS2-2	25.62	134.88	120.73	1.12	80.52	1.68	109.14	1.24	88.68	1.52	112.00	1.20	123.06	1.10	116.39	1.16
GCBS2-3	25.62	130.70	120.73	1.08	80.52	1.62	109.14	1.20	88.68	1.47	112.00	1.17	123.06	1.06	116.39	1.12
GCBS2-4	25.94	133.83	121.89	1.10	81.03	1.65	110.50	1.21	89.78	1.49	112.27	1.19	123.57	1.08	116.61	1.15
GCBS2-5	26.21	132.59	122.86	1.08	81.45	1.63	111.65	1.19	90.72	1.46	112.50	1.18	123.99	1.07	116.80	1.14
GCBS2-6	26.56	134.88	124.13	1.09	81.99	1.65	112.15	1.20	91.93	1.47	112.79	1.20	124.53	1.08	117.03	1.15
GCBS3-1	25.94	183.07	158.38	1.16	86.32	2.12	110.50	1.66	89.78	2.04	122.87	1.49	144.70	1.27	127.63	1.43
GCBS3-2	26.21	185.81	159.68	1.16	86.77	2.14	111.65	1.66	90.72	2.05	123.10	1.51	145.23	1.28	127.80	1.45
GCBS3-3	26.56	189.26	161.36	1.17	87.35	2.17	113.15	1.67	91.93	2.06	123.39	1.53	145.90	1.30	128.02	1.48
GCCS1-1	39.18	142.46	131.48	1.08	83.11	1.71	82.47	1.73	85.32	1.67	95.18	1.50	92.00	1.55	102.52	1.39
GCCS1-2	39.18	147.54	131.48	1.12	83.11	1.78	82.47	1.79	85.32	1.73	95.18	1.55	92.00	1.60	102.52	1.44
GCCS1-3	39.18	141.65	131.48	1.08	83.11	1.70	82.47	1.72	85.32	1.66	95.18	1.49	92.00	1.54	102.52	1.38
GCCS1-4	40.12	141.62	133.88	1.06	84.10	1.68	82.47	1.72	85.32	1.66	95.68	1.48	92.44	1.53	102.94	1.38
GCCS1-5	40.16	139.43	133.93	1.04	84.15	1.66	82.47	1.69	85.32	1.63	95.70	1.46	92.46	1.51	102.96	1.35
GCCS1-6	40.24	142.60	134.03	1.06	84.23	1.69	82.47	1.73	85.32	1.67	95.75	1.49	92.49	1.54	103.00	1.38
GCCS2-1	39.71	214.62	184.99	1.16	100.25	2.14	112.15	1.91	111.04	1.93	121.30	1.77	139.60	1.54	123.44	1.74

Table 6.8. Comparison of experimental shear capacity of GPC reinforced corbels with the shear strength predicted by the design codes/equations

Spec. ID	f_{gpc} N/mm^2	V_{up} kN	Ref 1		Ref 2		Ref 3		Ref 4		Ref 5		Ref 6		Ref 7	
			V_{u1} kN	V_{up} / V_{u1}	V_{u2} kN	V_{up} / V_{u2}	V_{u3} kN	V_{up} / V_{u3}	V_{u4} kN	V_{up} / V_{u4}	V_{u5} kN	V_{up} / V_{u5}	V_{u6} kN	V_{up} / V_{u6}	V_{u7} kN	V_{up} / V_{u7}
GCCS2-2	39.71	215.46	184.99	1.16	100.25	2.15	112.15	1.92	111.04	1.94	121.30	1.78	139.60	1.54	123.44	1.75
GCCS2-3	39.71	217.66	184.99	1.18	100.25	2.17	112.15	1.94	111.04	1.96	121.30	1.79	139.60	1.56	123.44	1.76
GCCS2-4	40.12	212.33	186.18	1.14	100.77	2.11	112.15	1.89	111.04	1.91	121.50	1.75	139.95	1.52	123.58	1.72
GCCS2-5	40.16	216.78	186.27	1.16	100.82	2.15	112.15	1.93	111.04	1.95	121.52	1.78	139.99	1.55	123.59	1.75
GCCS2-6	40.24	212.58	186.44	1.14	100.92	2.11	112.15	1.90	111.04	1.91	121.56	1.75	140.06	1.52	123.62	1.72
GCCS3-1	40.12	271.10	240.95	1.13	107.36	2.53	117.15	2.31	123.90	2.19	132.10	2.05	165.45	1.64	133.90	2.02
GCCS3-2	40.16	272.46	241.09	1.13	107.41	2.54	117.15	2.33	123.90	2.20	132.12	2.06	165.49	1.65	133.91	2.03
GCCS3-3	40.24	279.60	241.35	1.16	107.52	2.60	117.15	2.39	123.90	2.26	132.16	2.12	165.58	1.69	133.93	2.09
GCDS1-1	53.41	158.07	149.11	1.06	97.04	1.63	82.47	1.92	85.32	1.85	101.56	1.56	97.20	1.63	107.79	1.47
GCDS1-2	53.41	163.43	149.11	1.10	97.04	1.68	82.47	1.98	85.32	1.92	101.56	1.61	97.20	1.68	107.79	1.52
GCDS1-3	53.41	155.84	149.11	1.05	97.04	1.61	82.47	1.89	85.32	1.83	101.56	1.53	97.20	1.60	107.79	1.45
GCDS1-4	54.11	152.89	149.89	1.02	97.67	1.57	82.47	1.85	85.32	1.79	101.81	1.50	97.39	1.57	108.00	1.42
GCDS1-5	54.22	157.89	150.01	1.05	97.77	1.61	82.47	1.91	85.32	1.85	101.85	1.55	97.42	1.62	108.03	1.46
GCDS1-6	54.39	156.56	150.20	1.04	97.93	1.60	82.47	1.90	85.32	1.84	101.91	1.54	97.47	1.61	108.08	1.45
GCDS2-1	53.73	241.13	214.71	1.12	116.61	2.07	112.15	2.15	111.04	2.17	127.12	1.90	149.27	1.62	127.19	1.90
GCDS2-2	53.73	249.69	214.71	1.16	116.61	2.14	112.15	2.23	111.04	2.25	127.12	1.96	149.27	1.67	127.19	1.96
GCDS2-3	53.73	237.72	214.71	1.11	116.61	2.04	112.15	2.12	111.04	2.14	127.12	1.87	149.27	1.59	127.19	1.87
GCDS2-4	54.11	241.23	215.50	1.12	117.02	2.06	112.15	2.15	111.04	2.17	127.25	1.90	149.48	1.61	127.26	1.90
GCDS2-5	54.22	232.19	215.72	1.08	117.14	1.98	112.15	2.07	111.04	2.09	127.29	1.82	149.54	1.55	127.29	1.82
GCDS2-6	54.39	240.99	216.08	1.12	117.33	2.05	112.15	2.15	111.04	2.17	127.34	1.89	149.63	1.61	127.32	1.89
GCDS3-1	54.11	317.01	286.90	1.10	124.68	2.54	117.15	2.71	123.90	2.56	137.85	2.30	177.77	1.78	136.89	2.32
GCDS3-2	54.22	314.62	287.26	1.10	124.80	2.52	117.15	2.69	123.90	2.54	137.89	2.28	177.85	1.77	136.91	2.30

Table 6.8. Comparison of experimental shear capacity of GPC reinforced corbels with the shear strength predicted by the design codes/equations

Spec. ID	f_{gpc} N/mm^2	V_{up} kN	Ref 1		Ref 2		Ref 3		Ref 4		Ref 5		Ref 6		Ref 7	
			V_{u1} kN	V_{up} / V_{u1}	V_{u2} kN	V_{up} / V_{u2}	V_{u3} kN	V_{up} / V_{u3}	V_{u4} kN	V_{up} / V_{u4}	V_{u5} kN	V_{up} / V_{u5}	V_{u6} kN	V_{up} / V_{u6}	V_{u7} kN	V_{up} / V_{u7}
GCDS3-3	54.39	306.69	287.82	1.07	125.00	2.45	117.15	2.62	123.90	2.48	137.94	2.22	177.97	1.72	136.94	2.24
Average			**1.09**		**1.87**		**1.77**		**1.80**		**1.58**		**1.44**		**1.52**	

Notations:

f_{gpc} - Average compressive strength (N/mm^2), V_{up} - Experimental shear strength of corbel (kN), V_u- Ultimate shear strength (kN)

1. Proposed model 2. Kriz and Rath, 1965 3. ACI 318, 2019 4. CSA A23.3, 2019

5. PCI, 2010 6. Hagberg, 2013 7. Euro code 2, 2004

6.8 CONCLUSIONS

The following conclusions were arrived at after the study of the shear capacity of geopolymer concrete corbels

1. The ultimate load capacity of corbels increased with an increase in the compressive strength of geopolymer concrete.
2. The ultimate load of corbels increased with an increase in the percentage of closed-loop stirrups (secondary reinforcement).
3. The proposed analytical expression for the shear strength of geopolymer concrete is ably predicts the shear capacity of the corbel. The experimental shear strengths of corbel are about 9% higher than the predicted values of interface shear strength of geopolymer concrete corbels.
4. The shear capacity obtained from different codes and theories underestimates the interface shear capacity of reinforced geopolymer concrete corbels.

CHAPTER 7
CONCLUSIONS

7.1 CONCLUSIONS

Geopolymer concrete is emerging as a sustainable material for use in construction sector. The study of literature on geopolymer concrete has indicated a number of parameters that are affecting its compressive strength. In this thesis an attempt was made to arrive at new unified parameter termed 'Binder index' that can be used to control the strength of geopolymer concrete. Further the thesis came up with experimental investigations on shear strength at the monolithic interface of GGBS and fly ash-based geopolymer concrete and the application to reinforced geopolymer concrete corbels.

The following conclusions were drawn based on three phases of the research work presented in this thesis.

1. The compression and flexural strength of the fly ash and GGBS based geopolymer concrete increases with an increase in GGBS to fly ash ratio. However, the rate of increase of the compressive strength is higher for GGBS to fly ash ratios lower than 1.0.
2. As the molarity of NaOH solution in the alkaline activator increases, the compressive strength, flexural strength, and split tensile strength of the geopolymer concrete also increase. However, the increase in strength is not in proportion to increase in molarity.
3. The compression and flexural strength of geopolymer concrete increase with an increase in A/B ratio. However, the rate of increase of the compressive strength is higher for higher GGBS to fly ash ratios for a constant molarity of NaOH solution in an alkaline activator.
4. The use of higher A/B ratio is beneficial in increasing the strength of geopolymer concrete prepared with low molarity NaOH.
5. The newly proposed parameter called "Binder Index (Bi)" which combines the effects of alkaline to binder content ratio, GGBS to fly ash ratio, and molarity of sodium hydroxide can be considered a single unique parameter to control the compressive strength of geopolymer concrete.

$$\boldsymbol{Bi} = \frac{\boldsymbol{MA}}{\boldsymbol{G}+\boldsymbol{F}}\left[\frac{\boldsymbol{G}}{\boldsymbol{F}}\right]$$

Where, M= Molarity of NaOH, A=alkaline activator (Both NaOH and Na_2SiO_3 together) content, G= GGBS content, F= fly ash content.

6. The strength of geopolymer concrete (both compression and flexural strengths) increases with an increase of binder index. Also, a non-linear variation exists between the binder index and the strengths ((both compression and flexural strengths) f_{gpc} of geopolymer concrete and can be signified by a power equation.

$$\mathbf{f_{gpc} = N[Bi]^{L}}$$

Where N and L are constants.

7. Based on the Phenomenological model, the compressive strength of geopolymer concrete for any binder index can be estimated as follows.

For Binder Index Bi ≤ 10, $\frac{f_{gpc}}{f_{gpc,5.41}} = 0.63\ Bi^{0.25}$

For Binder Index Bi > 10, $\frac{f_{gpc}}{f_{gpc,5.41}} = 0.81\ Bi^{0.10}$

Where f_{gpc} is the compressive strength for any specified Binder Index required and $f_{gpc5.41}$ is the experimentally evaluated strength at a binder index of 5.41.

8. The shear strength of the monolithic geopolymer concrete interface increased with an increase in the compressive strength of geopolymer concrete. And the rate of increase of shear strength decreased for compressive strength of geopolymer concrete of more than 40 MPa.

9. The shear (V_u) across the reinforced monolithic interface in geopolymer concrete specimens is resisted by the combined action of cohesion, friction, and dowel action and can be obtained by the relation:

$$V_u = V_c + V_f + V_d$$

$$V_u = \underbrace{C f_c^{1/3}}_{\text{Cohesion}} + \underbrace{\mu[\sigma_n + \rho k f_y]}_{\text{Friction}} + \underbrace{\alpha\rho\sqrt{f_y f_c}}_{\text{Dowel Action}}$$

Where,

V_c = Shear strength of unreinforced GPC due to cohesion = $c(f_{gpc})^{(1/3)}bh$, where For $f_{gpc} \leq 40$, $c = 0.031\ f_{gpc}+0.06$, For $f_{gpc}>40$, $c = 0.0054f_{gpc}+1.0809$

V_f = Shear strength of reinforced GPC due to friction = $\mu[\sigma_n+\rho k f_y]\ bh$, where k=0.5 and $f_{gpc} \geq 20$MPa $\mu = 0.8$, $f_{gpc} \geq 35$MPa $\mu = 1.0$, $\rho = \rho_{Main} + \rho_{Stirrups}$ (Randl, 1997)

V_d = Shear Strength due to Dowel contribution = $\alpha\rho\sqrt{f_y f_{gpc}}\ bh$, $\rho = \rho_{Stirrups}$ where $\alpha = 6.338\ \rho\sqrt{f_y f_{gpc}}$

10. The proposed shear strength equation are based on cube strength and SI units.
11. The available conventional concrete shear strength prediction models are highly conservative in estimating the shear strength of unreinforced and reinforced monolithic shear interfaces in geopolymer concrete.
12. The ultimate load capacity of corbels increased with an increase in the compressive strength of geopolymer concrete
13. The ultimate load of corbels increased with an increase in the percentage of closed-loop stirrups (secondary reinforcement).
14. The proposed analytical expression for the shear strength of geopolymer concrete was able to predict the shear capacity of the corbel. The experimental shear strengths of corbel are about 9% higher than the predicted values of interface shear strength of geopolymer concrete corbels.
15. The shear capacity obtained from different codes and theories was found to underestimate the interface shear capacity of reinforced geopolymer concrete corbels.

7.2 SPECIFIC CONTRIBUTION MADE IN THIS WORK

1. A New parameter termed “Binder Index (Bi)” was proposed to account for the effects of alkaline to binder content ratio, GGPS to Fly ash ratio, and molarity of sodium hydroxide to control the compressive strength of geopolymer concrete.
2. The proposed parameter ‘Binder index’ has been validated by conducting analytical and experimental studies.
3. A non-linear form of the equation has been proposed between the binder index and the strengths of geopolymer concrete, such as compressive and flexural strength of geopolymer concrete.
4. A Phenomenological model was developed for estimating the compressive strength of geopolymer concrete for any binder index.
5. An expression for the shear strength (V_u) across the unreinforced monolithic interfaces of geopolymer concrete was given in terms of the coefficient of cohesion of geopolymer concrete.
6. An expression for the shear strength (V_u) across the reinforced monolithic interfaces of geopolymer concrete was arrived at in terms of the coefficient of cohesion, friction parameter, and coefficient of dowel action.

7. A comparative study of shear strength expressions given by different investigators / different codes of practice on conventional concrete was made to investigate the efficacy of the proposed analytical expression.
8. The proposed expression for shear strength (V_u) across reinforced / unreinforced monolithic interfaces of geopolymer concrete has been validated by conducting experimental investigations on symmetric double corbel geopolymer concrete specimens.
9. A study of shear strength at the corbel column interface was made by comparing the shear strength predicted by the proposed equation for geopolymer concrete and shear strength expressions given for corbels by different investigators / different codes of practice on conventional concrete.

7.3 LIMITATIONS

1. The research is applicable only to GGBS and fly ash-based geopolymer concrete.
2. The study is limited to the molarity of NaOH solution to 8moles/l and sodium silicate to sodium hydroxide ratio of 2.5.
3. The study of shear strength of GGBS and fly ash-based geopolymer concrete with monolithic interface was performed to yield the strength of reinforcement steel to 250MPa.
4. The study is based on dowel contribution between 0.50% and 1.02% percentages of reinforcement crossing interface.
5. The study is restricted to 0.80% of stirrups (crossing the interface) for the reinforced geopolymer corbels.

7.4 SCOPE FOR FURTHER STUDY

1. A study of the shear strength of geopolymer concrete subjected to elevated temperature may be done to estimate the residual shear strength of geopolymer concrete.
2. A study of the shear strength of fiber-reinforced GGBS and fly ash-based geopolymer concrete with the monolithic interface may be done to evaluate the fiber contribution to shear strength.
3. A study to determine the shear capacity of unsymmetrical double corbel geopolymer concrete.

PUBLICATIONS RELATED TO THE WORK

Journals

1. Sumanth Kumar B, Rama Seshu D (2020), "An Experimental investigation on Shear strength of monolithic Geopolymer Concrete interface", **Journal of Structural Engineering**, CSIR – SERC, ISSN: 0970-0137, Vol. 46, No 6, February – March 2020, pp. 426-433. **(Scopus Indexed)**
2. Sumanth Kumar B, Rama Seshu D (2019), "Binder Index as Criteria for assessing the strength of Geopolymer Concrete", **Journal of Structural Engineering**, CSIR – SERC, ISSN: 0970-0137, Vol. 46, No 1, April – May 2019, pp. 12-16. **(Scopus Indexed)**
3. Sumanth Kumar B, Rama Seshu D (2021) "Comparative Study of Shear friction on Monolithic Geopolymer Concrete", Int. Journal of **Cement Wapno Beton,** 26(1) (2021), 3-11 DOI: https://doi.org/10.32047/CWB.2021.26.1.1 **(SCI Indexed)**
4. Sumanth Kumar B, Rama Seshu D, Shankariah R, Sesha Srinivas B (2020), "A Study on Binder index – A new parameter to predict the strengths of GGBS and Fly ash based Geopolymer Concretes", **ICI Journal,** Vol. 21, Oct-Dec 2020, No.3, pp 23 – 30.

Book Chapters

1. Sumanth Kumar B., Sen A., Rama Seshu D. (2020) "Shear Strength of Fly Ash and GGBS Based Geopolymer Concrete", Advances in Sustainable Construction Materials. **Lecture Notes in Civil Engineering, vol. 68. Springer**, Singapore, April 2020, pp. 105-112. **(Scopus Indexed)**
2. Sumanth Kumar B, Rama Seshu D (2018), **"A Review on Parametric Study of Geopolymer Concrete"**, *Advance in Concrete, Structural and Geotechnical Engineering*, Bloomsbury Publications, ISBN: 978-93-87471-69-6, February 2018, pp. 773 – 777. **(Scopus Indexed)**

Conference Papers

1. Sumanth Kumar B, Arnab Sen, Rama Seshu D, "Behaviour of fly ash and GGBS based reinforced geopolymer corbels" at Second ASCE India Conference on **Challenges of Resilient and Sustainable Infrastructure Development in Emerging Economies (CRSIDE-2020)**.

2. Sumanth Kumar B, Rama Seshu D, “Shear Strength of Monolithic Geopolymer Concrete by ACI 318” at **International Conference on Innovative Trends in Civil Engineering for Sustainable Development (ITCSD-2019).**
3. Sumanth Kumar B, Manjula Ch, Rama Seshu D, “An Appraisal on Shear Strength of Concrete for Different Codes” at **International Conference on Innovative Trends in Civil Engineering for Sustainable Development (ITCSD-2019).**
4. Sumanth Kumar B, Arnab Sen, Rama Seshu D, “Shear Strength of Fly ash and GGBS based Geopolymer Concrete” at National Conference on **Advances in Sustainable Construction Materials (ASCM - 2019).**
5. Sumanth Kumar B, Rama Seshu D, “Geopolymers – Green Binders” at **Telangana State Science Congress (TSSC – 2018).**
6. Sumanth Kumar B, Rama Seshu D, “A Review on Parametric Study of Geopolymer Concrete” at 2nd International Conference on **Advance in Concrete, Structural and Geotechnical Engineering (ACSGE – 2018).**

CHAPTER 8

ANNEXURES

Annexure – I – Design Expressions

Researcher(s) [Year]	Interface Shear Transfer Equations [SI Units]	Notes / Remarks / Limits
Anderson [1960]	For a concrete with 20.7MPa; $v_u = 4.41 + 229\,\rho$ For a concrete with 51.7MPa; $v_u = 5.52 + 276\,\rho$	-
Hanson [1960]	For rough bonded interfaces; $v_u = 3.45 + 121\,\rho$	-
Mattock and Kaar [1961]	$v_u = \frac{18.6}{\left(\frac{x}{d} + 5\right)} + 121\rho$	ρ ≥ 0.15%
Saemann and Washa [1964]	$v_u = \frac{18.6}{(X+5)} + 207\rho\,\frac{33 - X}{X^2 + 6X + 5}$	-
Gaston and Kriz [1964]	For smooth unbonded interfaces; $v_u = 0.30 + 0.78\,\sigma_n$ For smooth bonded interfaces; $v_u = 0.76 + 0.70\,\sigma_n$	-
Birkeland and Birkeland [1966]	$v_u = \rho f_y \mu$	μ = 1.7 for monolithic concrete; μ = 1.4 for artificially roughened joints; μ = 0.8-1.0 for ordinary construction joints. ρ ≤ 1.5% $v_u \leq 5.52\ MPa$ $f_c \geq 27.58\ MPa$
Badoux and Hulsbos [1967]	For construction joints with an intermediate finish; $v_u = \frac{13.79}{11 + \left(\frac{a}{d}\right)} + 137.9\,\rho$ For construction joints with a rough finish $v_u = \frac{24.14}{11 + \left(\frac{a}{d}\right)} + 137.9\,\rho$	-
Birkeland [1968]	$v_u = 2.78\sqrt{\rho f_y}$	-
Mast [1968]	Same as Birkeland and Birkeland [1966] $v_u = \rho f_y \mu$	μ = 1.4 for rough interfaces; μ = 0.7 for smooth interfaces; $v_u \leq 0.15 f_c \mu$

Researcher(s) [Year]	Interface Shear Transfer Equations [SI Units]	Notes / Remarks / Limits
Hofbeck, Ibrahim and Mattock [1969]	Same as Birkeland and Birkeland [1966] $v_u = \rho f_y \mu$	$\rho f_y \leq 4.14\ MPa$
Mattock and Hawkins [1972]	Lower Bound of test results $v_u = 1.38 + 0.8\ (\rho f_y + \sigma_n)$	$\rho f_y + \sigma_n \geq 1.38 MPa$ $v_u \leq [0.3 f_c; 10.34\ Mpa]$
Mattock [1974]	Developed for the mean values of the tests results $v_u = 2.76 + 0.8\ (\rho f_y + \sigma_n)$ $v_u = 2.76\ sin^2\theta + \rho f_s\ (0.8\ sin^2\theta - 0.5 sin2\theta)$ $f_s = 0; 0 \leq \theta < 51.3°$ $f_s = -1.6 f_y \cos(\theta + 38.7°)\ ; 51.3° \leq \theta < 90°$ $f_s = f_y; 90° \leq \theta \leq 180°$	$\rho f_y + \sigma_n \geq 1.38\ MPa$ $v_u \leq [0.3 f_c; 10.34 MPa]$
Hermansen and Cowan [1974]	$v_u = 4.0 + 0.8\ \rho f_y$	-
Mattock, Johal and Chow [1975]	Modified Birkeland [1968] equation $v_u = 2.36 \sqrt{\rho f_y}$	-
Mattock, Li and Wang [1976]	For all lightweight concrete; $v_u = 1.38 + 0.8\ \rho f_y$ For sanded lightweight concrete; $v_u = 1.72 + 0.8\ \rho f_y$	$\rho f_y \geq 1.38\ MPa$ For all lightweight concrete; $v_u \leq [0.2 f_c; 5.52\ MPa]$ For sanded lightweight concrete; $v_u \leq [0.2 f_c; 6.90\ MPa]$
Raths [1977]	For monolithic specimens of normal and lightweight concrete; $v_u = C_s\ 3.11 \sqrt{\rho f_y}$ For smooth interfaces in normal and lightweight concrete; $v_u = C_s\ 2.03 \sqrt{\rho f_y}$	C_s = 1.00 for normal weight concrete; C_s= 0.85 for sand-lightweight concrete C_s= 0.75 for all light weight concrete. $\mu_e = 6.90\ \frac{C_s^2 \mu}{v_u}$
Shaikh [1978]	$v_u = \varphi \rho f_y \mu_e$	C_s = 1.00 for normal weight concrete; C_s = 0.85 for sand-lightweight concrete C_s = 0.75 for all-lightweight concrete. μ = 1.4 for monolithic concrete μ = 1.0 for rough interfaces μ = 0.4 for smooth interfaces $\mu_e = 6.90\ \frac{C_s^2 \mu}{v_u}$

Researcher(s) [Year]	Interface Shear Transfer Equations [SI Units]	Notes / Remarks / Limits
Loov [1978]	$\frac{v_u}{f_c} = k\sqrt{\frac{\rho f_y + \sigma_n}{f_c}}$	For initially uncracked interfaces k = 0.50
Vecchio and Collins [1986]	$v_u = 0.18v_{cimax} + 1.64f_{ci} - 0.82\frac{f_{ci}^2}{v_{cimax}}$ $v_{cimax} = \frac{\sqrt{f_c}}{\left(0.31 + \frac{24w}{a+16}\right)}$	-
Walraven, Frenay and Pruijssers [1987]	$v_u = C_1(\rho f_y)^{C_2}$ $C_1 = 0.822f_c^{0.406}$ $C_2 = 0.159f_c^{0.303}$	-
Mattock [1988]	$v_u = 0.467\, f_c^{0.545} + 0.8\left(\rho f_y + \sigma_n\right)$	$v_u \leq 0.3f_c$
Mau and Hsu [1988]	Same as Loov [1978] $v_u = k\sqrt{(\rho f_y + \sigma_n)f_c}$	For initially cracked and uncracked interfaces; K = 0.66
Lin and Chen [1989]	$v_u = \mu_e\left(\rho f_y + \sigma_n\right)$ $\mu_e = \left(\frac{1.75\sqrt{f_c}}{\rho f_y + \sigma_n}\right)^{0.5} \leq 0.8f_c^{0.25}$	$\rho f_y + \sigma_n \geq 1.38\, MPa$ $v_u \leq [0.3f_c\,;\, 12.46\, MPa]$
Tsoukantas and Tassios [1989]	For smooth interfaces; $v_u = 0.40\sigma_n$ For rough interfaces; $v_u = 0.50\sqrt[3]{f_c^2\sigma_n}$	-
Patnaik [1992]	$v_u = 0.6\sqrt{\left(0.1 + \rho f_y\right)f_c}$	$v_u \leq 0.25f_c$
Loov and Patnaik [1994]	$v_u = k\lambda\sqrt{\left(0.1 + \rho f_y\right)f_c}$	k = 0.5 for composite concrete element k = 0.6 for monolithic concrete. λ = 1.00 for normal weight concrete; λ = 0.85 for sand-lightweight concrete; λ = 0.75 for all lightweight concrete. $v_u \leq 0.25f_c$

Researcher(s) [Year]	Interface Shear Transfer Equations [SI Units]	Notes / Remarks / Limits
Mattock [1994]	For initially cracked, monolithic, normal weight concrete; $v_u = \frac{\sqrt{\rho f_y} f_c^{0.73}}{3.820}$ For composite reinforced concrete elements cast at different times, with a rough interface; $v_u = \frac{\sqrt{\rho f_y} f_c^{0.73}}{3.820} - 0.02 f_c$	$v_u \leq 0.3 f_c$
Randl [1997]	$v_u = C f_c^{1/3} + \mu[\sigma_n + \rho k f_y] + \alpha\rho\sqrt{f_y f_c}$	$v_u \leq \beta v f_c$ For water blasted surfaces (R ≥ 3.0mm); c = 0.4 μ = 0.8 to 1.0 For sand blasted surfaces (R ≥ 0.5mm); c = 0 μ = 0.7 For smooth surfaces; c = 0 μ = 0.5
Ali and White [1999]	$\frac{v_u}{f_c} = 1.47a\sqrt{\frac{\rho f_y + \sigma_n}{f_c}} \leq 1.2b$	-
Valluvan, Kreger and Jirsa [1999]	$v_u = \mu[\sigma_n + \rho f_y]$	$\sigma_n \leq 5.52\ MPa$ $v_u \leq [0.25 f_c\ ;\ 5.52\ MPa]$
Patnaik [2000]	For intentionally roughened surface; $v_u = 0.55\sqrt{(0.25 + \rho f_y) f_c}$	$v_u \leq [0.25 f_c\ ;\ 7.93\ MPa]$ For monolithic concrete (lower bound); $v_u \leq [0.2 f_c\ ;\ 8.96\ MPa]$
	For surface not intentionally roughened; $v_u = 0.5\sqrt{(0.25 + \rho f_y) f_c}$	$v_u \leq [0.2 f_c\ ;\ 5.52\ MPa]$
Kono and Tanaka [2000]	$v_u = k(0.67\rho f_y + 2.84)$	$k = 0.02 f_c + 0.2$ for $f_c \leq 40\ MPa$ else k = 1.0 Not applicable for plain surface and $\rho f_y \geq 7.6\ MPa$

Researcher(s) [Year]	Interface Shear Transfer Equations [SI Units]	Notes / Remarks / Limits
Mattock [2001]	For monolithic concrete and intentionally roughened surfaces; $v_u = k_1 + 0.8\left(\rho f_y + \sigma_n\right)$ $K_1 = \min[0.1\, f_c; 5.52MPa]$ $K_2 = 0.3$ $K_3 = 16.55\ MPa$	$\rho f_y + \sigma_n \geq \frac{K_1}{1.45}$ $v_u \geq 1.55\ K_1$ $v_u \leq [K_2 f_c\ ;\ K_3]$
	For monolithic concrete and intentionally roughened surfaces; $v_u = 2.25\left(\rho f_y + \sigma_n\right)$ $K_1 = 2.76\ MPa$ $K_2 = 0.3$ $K_3 = 16.55\ MPa$	$\rho f_y + \sigma_n \leq \frac{K_1}{1.45}$ $v_u \leq 1.55\ K_1$ $v_u \leq [K_2 f_c\ ;\ K_3]$
	For monolithic sand-lightweight concrete and intentionally roughened surfaces; $K_1 = 1.72\ MPa$ $K_2 = 0.2$ $K_3 = 8.27\ MPa$ For all lightweight monolithic concrete and intentionally roughened surfaces; $K_1 = 1.38\ MPa$ $K_2 = 0.2$ $K_3 = 8.27\ MPa$	
	For concrete placed against hardened concrete not intentionally roughened; $v_u = 0.6\lambda\rho f_y$ For concrete anchored to clean, unpainted, as-rolled structural steel by headed studs or by reinforcing bars; $v_u = 0.7\lambda\rho f_y$	$v_u \leq [0.2 f_c; 5.52\ MPa]$ λ = 1.00 for normal weight concrete; λ = 0.85 for sand-lightweight concrete; λ = 0.75 for all lightweight concrete.
Patnaik [2001]	For smooth concrete interfaces; $v_u = 0.6 + \rho f_y$	$v_u \leq [0.2 f_c; 5.52\ MPa]$
Kahn and Mitchell [2002]	$v_u = 0.55 f_c + 1.4\,\rho f_y$	$v_u \leq 0.2 f_c$
Papanicolaou and Triantafillou [2002]	$f_{ct} = 0.2 f_{ck}^{2/3}\left(0.4 + 0.6\frac{\rho}{2000}\right)$ For smooth interfaces; $v_u = 0.30\left(\rho f_y + \sigma_n\right) + 1.7\sqrt{f_{ct}}$ For rough interfaces; $v_u = 0.45\left(\rho f_y + \sigma_n\right) + 1.4\sqrt{f_{ct}}$	For shear transfer capacity of interfaces between pumice aggregate concrete and high-performance concrete

Researcher(s) [Year]	Interface Shear Transfer Equations [SI Units]	Notes / Remarks / Limits
Gohnert [2003]	$v_u = 0.2090R_Z + 0.7719$	-
Mansur, Vinayagam and Tan [2008]	For normalised clamping forces lower or equal to 0.075; $\frac{v_u}{f_c} = 2.5\left(\frac{\rho f_y}{f_c}\right)$ For normalised clamping forces between 0.075 and 0.270; $\frac{v_u}{f_c} = \frac{0.56}{f_c^{0.385}} + 0.55\left(\frac{\rho f_y}{f_c}\right)$ For normalised clamping forces equal or higher than 0.270 $\frac{v_u}{f_c} = 0.3$	Normalised clamping forces; $\frac{\rho f_y}{f_c}$
Santos and Julio [2009]	When no reinforcement crossing the interface $v_u = C_d f_{ctd} \leq 0.25 f_{cd}$ When reinforcement crossing interface $v_u = \mu_d(\sigma_n + \rho f_y) \leq 0.25 f_{cd}$	$C_d = \frac{1.062 R_{vm}^{0.145}}{\gamma_{coh}}$ (mm) $\mu_d = \frac{1.366 R_{vm}^{0.041}}{\gamma_{fr}}$ (mm) $\gamma_{coh} = 2.6$ and $\gamma_{fr} = 1.2$
Harries, Zeno and Shahrooz [2012]	For interfaces in monolithic concrete; $v_u = 0.075 f_c + 0.002 E_s \rho_v$ For rough cold joint interfaces; $v_u = 0.040 f_c + 0.002 E_s \rho_v$ For cracked interfaces; $v_u = 0.002 E_s \rho_v$	$v_u \leq 0.2 f_c$

Annexure – II – Mix Designs

Mix Proportion for A (20 - 25)

Based on Mix Design proposed by G Mallikarjuna Rao et al (2016)

Assuming Target Strength = 25 Mpa M 8

From Table 2

Binder Quantity = 420 Kg/Cum

Ratio of Flyash : GGBS = 70 : 30

Flyash = 294.00 Kg/Cum

GGBS = 126.00 Kg/Cum

$\frac{\text{Alkaline Solution}}{\text{Binder Ratio}}$ = 0.55

Sodium Silicate : NaOH = 2.5 : 1

Alkaline Solution = 231 Kg/Cum

NaOH Solution = 66.00 Kg/Cum

Sodium Silicate Solution = 165.00 Kg/Cum

$\frac{\text{Total Aggregate}}{\text{Binder}}$ = 4.23

Total Aggregate = 1776.60 Kg/Cum

For 420 Kg/Cum Binder Graph $\frac{\text{Coarse Aggregate}}{\text{Total Aggregate}}$ = 0.543

Coarse Aggregate = 964.69 Kg/Cum

Fine Aggregate = 811.91 Kg/Cum

Mix Proportion for B (20 - 25)

Based on Mix Design proposed by G Mallikarjuna Rao et al (2016)

Assuming Target Strength = 25 Mpa M 8

From Table 2

Binder Quantity = 420 Kg/Cum

Ratio of Flyash : GGBS = 70 : 30

Flyash = 294.00 Kg/Cum

GGBS = 126.00 Kg/Cum

$\frac{\text{Alkaline Solution}}{\text{Binder Ratio}}$ = 0.60

Sodium Silicate : NaOH = 2.5 : 1

Alkaline Solution = 252 Kg/Cum

NaOH Solution = 72.00 Kg/Cum

Sodium Silicate Solution = 180.00 Kg/Cum

$\frac{\text{Total Aggregate}}{\text{Binder}}$ = 4.23

Total Aggregate = 1776.60 Kg/Cum

For 420 Kg/Cum Binder Graph $\frac{\text{Coarse Aggregate}}{\text{Total Aggregate}}$ = 0.543

Coarse Aggregate = 964.69 Kg/Cum

Fine Aggregate = 811.91 Kg/Cum

Mix Proportion for C (40 - 45)

Based on Mix Design proposed by G Mallikarjuna Rao et al (2016)

Assuming Target Strength = 40 Mpa M 8

From Table 2

Binder Quantity = 420 Kg/Cum

Ratio of Flyash : GGBS = 60 : 40

Flyash = 252.00 Kg/Cum

GGBS = 168.00 Kg/Cum

$\frac{\text{Alkaline Solution}}{\text{Binder Ratio}}$ = 0.55

Sodium Silicate : NaOH = 2.5 : 1

Alkaline Solution = 231 Kg/Cum

NaOH Solution = 66.00 Kg/Cum

Sodium Silicate Solution = 165.00 Kg/Cum

$\frac{\text{Total Aggregate}}{\text{Binder}}$ = 4.23

Total Aggregate = 1776.60 Kg/Cum

For 420 Kg/Cum Binder Graph $\frac{\text{Coarse Aggregate}}{\text{Total Aggregate}}$ = 0.543

Coarse Aggregate = 964.69 Kg/Cum

Fine Aggregate = 811.91 Kg/Cum

Mix Proportion for D (50 - 55)

Based on Mix Design proposed by G Mallikarjuna Rao et al (2016)

Assuming Target Strength = 55 Mpa M 8

From Table 2

Binder Quantity = 420 Kg/Cum

Ratio of Flyash : GGBS = 50 : 50

Flyash = 210.00 Kg/Cum

GGBS = 210.00 Kg/Cum

$\frac{\text{Alkaline Solution}}{\text{Binder Ratio}}$ = 0.50

Sodium Silicate : NaOH = 2.5 : 1

Alkaline Solution = 210 Kg/Cum

NaOH Solution = 60.00 Kg/Cum

Sodium Silicate Solution = 150.00 Kg/Cum

$\frac{\text{Total Aggregate}}{\text{Binder}}$ = 4.23

Total Aggregate = 1776.60 Kg/Cum

For 420 Kg/Cum Binder Graph $\frac{\text{Coarse Aggregate}}{\text{Total Aggregate}}$ = 0.543

Coarse Aggregate = 964.69 Kg/Cum

Fine Aggregate = 811.91 Kg/Cum

CHAPTER 9

REFERENCES

1. ACI Committee 318. 2019 Building Code Requirements for Structural Concrete (ACI 318-19) and Commentary (ACI 318R-19). American Concrete Institute, Farmington Hills.
2. Al Bakri, A.M., Kamarudin, H., Bnhussain, M., Nizar, I.K. and Mastura, W.I.W., 2011. Mechanism and chemical reaction of fly ash geopolymer cement-a review. Journal of Asian Scientific Research, 1(5), p.247.
3. Al Bakri, A.M., Kamarudin, H., Bnhussain, M., Nizar, I.K., Rafiza, A.R. and Zarina, Y., 2012. The processing, characterization, and properties of fly ash based geopolymer concrete. Rev. Adv. Mater. Sci, 30(1), pp.90-97.
4. Albitar, M., Ali, M.M. and Visintin, P., 2017. Experimental study on fly ash and lead smelter slag-based geopolymer concrete columns. Construction and Building Materials, 141, pp.104-112.
5. Ali, M.A. and White, R.N., 1999. Enhanced contact model for shear friction of normal and high-strength concrete. Structural Journal, 96(3), pp.348-360.
6. Alkatan, J., 2016. FRP Shear Transfer Reinforcement for Composite Concrete Construction. A Thesis Submitted to University of Windsor, Canada
7. Andalib, R., Hussin, M.W., Majid, M.Z.A., Azrin, M. and Ismail, H.H., 2014. Structural performance of sustainable waste palm oil fuel ash-fly ash geo-polymer concrete beams. Journal of Environmental Treatment Techniques, 2(3), pp.115-119.
8. Anderson, A.R., 1960. Composite designs in precast and cast-in-place concrete. Progressive Architecture, 41(9), pp.172-179.
9. Annapurna, D. and Kishore, R., 2017. Evaluation of mechanical properties of fly ash and GGBS based geopolymer concrete, International Journal of Emerging Technologies and Innovative Research, ISSN: 2349-5162, Vol.4, Issue 12, page no. pp1028-1033.
10. Araújo, D.L., Silva Neto, A.P., Lobo, F.A. and El Debs, M.K., 2016. Comparative analysis of design models for concrete corbels. Revista IBRACON de Estruturas e Materiais, 9(3), pp.435-470.
11. AS3600 – 2002: Concrete Structures, Standards Association of Australia, Sydney, Australia.
12. Badoux, J.C. and Hulsbos, C.L., 1967, December. Horizontal shear connection in composite concrete beams under repeated loads. In Journal Proceedings (Vol. 64, No. 12, pp. 811-819).
13. Bakharev, T., 2005. Geopolymeric materials prepared using Class F fly ash and elevated temperature curing. Cement and concrete research, 35(6), pp.1224-1232.
14. Deepa Balakrishnan S., Thomas John V. and Job Thomas (2013), "Properties of Fly ash based Geo-polymer concrete" – AJER, Volume-2 pp-21-25
15. Barbosa, A.R., Trejo, D. and Nielson, D., 2017. Effect of high-strength reinforcement steel on shear friction behavior. Journal of Bridge Engineering, 22(8), p.04017038.
16. Bhikshma, V. and Kumar, T.N., 2016. Mechanical properties of fly ash based geopolymer concrete with addition of GGBS. The Indian Concrete Journal, pp.64-68.
17. Birkeland, H.W., 1968. Precast and Prestressed Concrete, class notes for course. University of British Columbia.
18. Birkeland, P.W. and Birkeland, H.W., 1966, March. Connections in precast concrete construction. In Journal Proceedings (Vol. 63, No. 3, pp. 345-368).
19. Chang, E.H., 2009. Shear and bond behaviour of reinforced fly ash-based geopolymer concrete beams (Doctoral dissertation, Curtin University).

20. Chi, M. and Huang, R., 2013. Binding mechanism and properties of alkali-activated fly ash/slag mortars. Construction and building materials, 40, pp.291-298.
21. Chindaprasirt, P., Chareerat, T. and Sirivivatnanon, V., 2007. Workability and strength of coarse high calcium fly ash geopolymer. Cement and concrete composites, 29(3), pp.224-229.
22. Chmielewska, B., 2008. Adhesion strength and other mechanical properties of SBR modified concrete. International Journal of Concrete Structures and Materials, 2(1), pp.3-8.
23. CIRSOC, R., 201 (2005). Argentine code of structures of concrete, INTI-CIRSOC, Buenos Aires.
24. FIB Model Code, 2010. Fib model code for concrete structures 2010. Document Competence Center Siegmar Kästl eK, Germany.
25. Collins, F.G. and Sanjayan, J.G., 1999. Workability and mechanical properties of alkali activated slag concrete. Cement and concrete research, 29(3), pp.455-458.
26. Constantinescu, H. and Magureanu, C., 2011. "Study of shear behaviour of high performance concrete using push-off tests". JAES 1 (14) Vol.2, Page 77-82.
27. Dattatreya, J.K., Rajamane, N.P., Sabitha, D., Ambily, P.S. and Nataraja, M.C., 2011. Flexural behaviour of reinforced Geopolymer concrete beams. International journal of civil & structural engineering, 2(1), pp.138-159.
28. Davidovits, J. and Cordi, S.A., 1979. Synthesis of new high temperature geo-polymers for reinforced plastics/composites. Spe Pactec, 79, pp.151-154.
29. Davidovits, J., 1991. Geopolymers: inorganic polymeric new materials. Journal of Thermal Analysis and calorimetry, 37(8), pp.1633-1656.
30. Davidovits, J., 1999, June. Chemistry of geopolymeric systems, terminology. In Geopolymer (Vol. 99, No. 292, pp. 9-39).
31. Deb, P.S., Nath, P. and Sarker, P.K., 2014. The effects of ground granulated blast-furnace slag blending with fly ash and activator content on the workability and strength properties of geopolymer concrete cured at ambient temperature. Materials & Design (1980-2015), 62, pp.32-39.
32. Devika, C.P. and Deepthi, R.N., 2015. Study of flexural behavior of hybrid fibre reinforced geopolymer concrete beam. Int. J. Sci. Res, 4(7), pp.130-135.
33. D Rama Seshu, 2015. A study on bond strength of geopolymer concrete. International Journal of Civil Environmental, Structural, Construction and Architectural Engineering, 9(3), pp.355-358.
34. Douglas, E., Bilodeau, A. and Malhotra, V.M., 1992. Properties and durability of alkali-activated slag concrete. Materials Journal, 89(5), pp.509-516.
35. Dutta, D. and Ghosh, S., 2014. Parametric study of geopolymer paste with the different combination of activators. International Journal of Engineering Innovation & Research, 3(6), pp.786-793.
36. Duxson, P.S.W.M., Mallicoat, S.W., Lukey, G.C., Kriven, W.M. and van Deventer, J.S., 2007. The effect of alkali and Si/Al ratio on the development of mechanical properties of metakaolin-based geopolymers. Colloids and Surfaces A: Physicochemical and Engineering Aspects, 292(1), pp.8-20.
37. Euro code 2 2004. Design of concrete structures - Part 1-1: General rules and rules for buildings. European Committee for Standardization, Avenue Marnix 17, B-1000 Brussels, Belgium. 225 p. (with corrigendum dated of 16 January 2008)
38. Fernández-Jiménez, A. and Puertas, F., 2002. The alkali–silica reaction in alkali-activated granulated slag mortars with reactive aggregate. Cement and Concrete Research, 32(7), pp.1019-1024.
39. Foster, R.M., Brindley, M., Lees, J.M., Ibell, T.J., Morley, C.T., Darby, A.P. and Evernden, M.C., 2017. Experimental investigation of reinforced concrete T-beams strengthened in shear with externally bonded CFRP sheets. Journal of Composites for Construction, 21(2), p.04016086.

40. Ganapati Naidu P, Adiseshu, S. and Satayanarayana, P.V.V., 2012. A study on strength properties of geopolymer concrete with addition of GGBS. International Journal of Engineering Research and Development eISSN, pp.19-28.
41. Ganesan, N., Abraham, R., Raj, S.D. and Sasi, D., 2014. Stress–strain behaviour of confined Geopolymer concrete. Construction and building materials, 73, pp.326-331.
42. Ganesan, N., Indira, P.V. and Santhakumar, A., 2015. Bond behaviour of reinforcing bars embedded in steel fibre reinforced geopolymer concrete. Magazine of Concrete Research, 67(1), pp.9-16.
43. Gartner, E., 2004. Industrially interesting approaches to "low-CO2" cements. Cement and Concrete research, 34(9), pp.1489-1498.
44. Gaston, J.R. and Kriz, L.B., 1964. "Connections in Precast Concrete Structures—Scarf Joints," Journal of the Prestressed Concrete Institute, Vol. 9, No. 3, pp. 37-59.
45. Glukhovsky, V.D., 1957. Soil silicate-based products and structures. Gosstroiizdat Publish. Kiev, USSR.
46. Glukhovsky, V.D., 1959. Soil silicates. Gosstroyizdat, Kiev, USSR 154.
47. Gohnert, M., 2003. Horizontal shear transfer across a roughened surface. Cement and Concrete Composites, 25(3), pp.379-385.
48. Grutzeck, M., Kwan, S. and DiCola, M., 2004. Zeolite formation in alkali-activated cementitious systems. Cement and Concrete Research, 34(6), pp.949-955.
49. Habert, G., Billard, C., Rossi, P., Chen, C. and Roussel, N., 2010. Cement production technology improvement compared to factor 4 objectives. Cement and Concrete Research, 40(5), pp.820-826.
50. Hagberg, T., 1983, January. Design of concrete brackets: on the application of the truss analogy. In Journal Proceedings (Vol. 80, No. 1, pp. 3-12).
51. Hardjito, D. and Rangan, B.V., 2005. Development and properties of low-calcium fly ash-based geopolymer concrete. Curtin University of Technology.
52. Hardjito, D., Wallah, S.E., Sumajouw, D.M. and Rangan, B.V., 2005. Fly ash-based geopolymer concrete. Australian Journal of Structural Engineering, 6(1), pp.77-86.
53. Hardjito, D., Cheak, C.C. and Ing, C.H.L., 2008. Strength and setting times of low calcium fly ash-based geopolymer mortar. Modern applied science, 2(4), pp.3-11.
54. Harries, K.A., Zeno, G. and Shahrooz, B., 2012. Toward an improved understanding of shear-friction behavior. ACI Structural Journal, 109(6), p.835.
55. Hermansen, B.R. and Cowan, J., 1974, February. Modified shear-friction theory for bracket design. In Journal Proceedings (Vol. 71, No. 2, pp. 55-60).
56. Hofbeck, J.A., Ibrahim, I.O. and Mattock, A.H., 1969, February. Shear transfer in reinforced concrete. In Journal Proceedings (Vol. 66, No. 2, pp. 119-128).
57. Ibrahim, W.M.W., Hussin, K., Abdullah, M.M.A.B., Kadir, A.A., Deraman, L.M. and Sandu, A.V., 2017. Influence of foaming agent/water ratio and foam/geopolymer paste ratio to the properties of fly ash-based lightweight geopolymer for brick application. Revista de Chimie, 68(9), pp.1978-1982.
58. IS 2386, 1963 (R2016). Method of test for aggregates for concrete, mechanical properties.
59. IS: 383, 2016. Specification for coarse and fine aggregates from natural sources for concrete.
60. IS 516-1959, (R2004). Method of Tests for Strength of Concrete.
61. IS: 9103–1999, 1999. Concrete Admixtures–Specification.
62. Ismail, I., Bernal, S.A., Provis, J.L., Hamdan, S. and van Deventer, J.S., 2013. Microstructural changes in alkali activated fly ash/slag geopolymers with sulfate exposure. Materials and structures, 46(3), pp.361-373.

63. Jawahar, J.G. and Mounika, G., 2016. Strength properties of fly ash and GGBS based geopolymer concrete. Asian Journal of Civil Engineering (BHRC), 17(1), pp.127-135.
64. Johal, L., 1975. Shear transfer in reinforced concrete with moment or tension acting across the shear plane. PCI journal, 77.
65. Joseph, B. and Mathew, G., 2012. Influence of aggregate content on the behavior of fly ash based geopolymer concrete. Scientia Iranica, 19(5), pp.1188-1194.
66. Joseph, B. and Mathew, G., 2013. Interface Shear Strength of Fly ash based Geopolymer concrete. Annals of the Faculty of Engineering Hunedoara, 11(3), p.105.
67. Jumppanen, U.M., Diederichs, U. and Hinrichsmeyer, K., 1986. Material properties of F-concrete at high temperatures. Research Reports, no. 452, VTT Technical Research Centre of Finland.
68. Junaid, M.T., Kayali, O., Khennane, A. and Black, J., 2015. A mix design procedure for low calcium alkali activated fly ash-based concretes. Construction and Building Materials, 79, pp.301-310.
69. Kahn, L.F. and Mitchell, A.D., 2002. Shear friction tests with high-strength concrete. Structural Journal, 99(1), pp.98-103.
70. Kaneko, Y., Mihashi, H. and Ishihara, S., 2004. Shear failure of plain concrete in strain localized area. In Proceeding of the Fifth International Conference on Fracture Mechanics of Concrete and Concrete Structures, Colorado, USA, VC Li, CKY Leung, KJ Willam and SL Billington (ed.) (pp. 12-16).
71. Karthiyaini, S. and Nagan, S., 2014. Behaviour of geopolymer concrete circular column using glass fiber reinforced polymer. NISCAIR-CSIR, India, ISSN: 0975-1017 (Online), pp 458-464
72. Kathirvel, P. and Kaliyaperumal, S.R.M., 2016. Influence of recycled concrete aggregates on the flexural properties of reinforced alkali activated slag concrete. Construction and Building Materials, 102, pp.51-58.
73. Kreigh, J.D., 1976. Arizona slant shear test: a method to determine epoxy bond strength. ACI Journal, 73(7), pp.372-373.
74. Krishnaraja, A.R., Sathishkumar, N.P., Kumar, T.S. and Kumar, P.D., 2014. Mechanical behaviour of geopolymer concrete under ambient curing. International Journal of Scientific Engineering and Technology, 3(2), pp.130-132.
75. Krivenko, P.V., 1994. Alkaline cements. In Proceedings of the 1st International Conference on Alkaline Cements and Concretes, Kiev, Ukraine, 1994 (Vol. 1, pp. 11-129). Vipol Stock Company.
76. Kriz, L.B. and Raths, C.H., 1965. Connections in precast concrete structures: strength of corbels, J. Prestressed Coner. Inst., 10(1), pp 16-61.
77. Kumar, S., Kumar, R. and Mehrotra, S.P., 2010. Influence of granulated blast furnace slag on the reaction, structure and properties of fly ash based geopolymer. Journal of materials science, 45(3), pp.607-615.
78. Kwon, S.J., Yang, K.H., Hwang, Y.H. and Ashour, A.F., 2017. Shear friction strength of monolithic concrete interfaces. Magazine of Concrete Research, 69(5), pp.230-244.
79. Lăzărescu, A.V., Szilagyi, H., Baeră, C. and Ioani, A., 2017, June. The effect of alkaline activator ratio on the compressive strength of fly ash-based geopolymer paste. In IOP Conference Series: Materials Science and Engineering (Vol. 209, No. 1, p. 012064). IOP Publishing.
80. Lin, I.J. and Chen, Y.L., 1989. Shear transfer across a crack in reinforced high strength concrete. In Proc., 2nd East Asia-Pacific Conf. on Structural Engineering, and Construction (pp. 85-91). Chiang Mai.
81. Loov, R.E., 1978, September. “Design of precast connections”, Paper presented in a seminar organized by Compa International Pte, Ltd.

82. Loov, R.E. and Patnaik, A.K., 1994. Horizontal shear strength of composite concrete beams. The PCI Journal, Chicago IL, pp.48-69.
83. Lund, M.A., 2007. Midge Desktop Audit 2007. Centre for Ecosystem Management, 8.
84. Madheswaran, C.K., Gnanasundar, G. and Gopalakrishnan, N., 2013. Effect of molarity in geopolymer concrete. International Journal of Civil & Structural Engineering, 4(2), pp.106-115.
85. Mallikarjuna Rao G and Rao, T.G., 2015. Final setting time and compressive strength of fly ash and GGBS-based geopolymer paste and mortar. Arabian Journal for Science and Engineering, 40(11), pp.3067-3074.
86. Mallikarjuna Rao G, Rao, T.D., Seshu, R.D. and Venkatesh, A., 2016. Mix proportioning of geopolymer concrete. Cement Wapno Beton, 21(4), pp.274-285.
87. Mallikarjuna Rao, G. and Gunneswara Rao, T.D., 2018. A quantitative method of approach in designing the mix proportions of fly ash and GGBS-based geopolymer concrete. Australian Journal of Civil Engineering, 16(1), pp.53-63.
88. Mansur, M.A., Vinayagam, T. and Tan, K.H., 2008. Shear transfer across a crack in reinforced high-strength concrete. Journal of Materials in Civil Engineering, 20(4), pp.294-302.
89. Mast, R.F., 1968. Auxiliary reinforcement in concrete connections. Journal of the Structural Division, ASCE, 94(6), 1485-1504.
90. Mattock, A.H. and Hawkins, N.M., 1972. Shear transfer in reinforced concrete—recent research. Pci Journal, 17(2), pp.55-75.
91. Mattock, A.H. and Kaar, P.H. - Precast-prestressed concrete bridges, 4. Shear tests of continuous girders, Journal of the PCA R&D Laboratories, Vol. 3, No. 1, pp. 19-46, January 1961.
92. Mattock, A.H., 1975. Effect of aggregate type on single direction shear transfer strength in monolithic concrete. Report SM74-2, Department of Civil Engineering, University of Washington, Seattle, Washington.
93. Mattock, A.H., 1974. Shear Transfer in Concrete Having Reinforcement at an Angle to the Shear Plane. Publication SP-42, Shear in Reinforced Concrete, American Concrete Institute, 1974, pp. 17-42
94. Mattock, A.H., 1981. Cyclic shear transfer and type of interface. Journal of the structural division, 107(10), pp.1945-1964.
95. Mattock, A.H., 1988. Influence of concrete strength and load history on the shear friction capacity of concrete members-comments. Journal Prestressed Concrete Institute, 33(1), pp.165-166.
96. Mattock, A.H., 1994. Effectiveness of loop anchorages for reinforcement in precast concrete members. PCI journal, 39(6).
97. Mattock, A.H., 2001. Shear friction and high-strength concrete. Structural Journal, 98(1), pp.50-59.
98. Mattock, A.H., Chen, K.C. and Soongswang, K., 1976. The behavior of reinforced concrete corbels. PCI Journal, 21(2), pp.52-77.
99. Mattock, A.H., Li, W.K. and Wang, T.C., 1976. Shear transfer in lightweight reinforced concrete. PCI journal, 21(1), pp.20-39.
100. Mehta, R.K., Handfield-Jones, S., Bracegirdle, J. and HALLT, P., 2002. Cement dermatitis and chemical burns. Clinical and experimental dermatology (Print), 27(4), pp.347-348.
101. Momayez, A., Ehsani, M.R., Ramezanianpour, A.A. and Rajaie, H., 2005. Comparison of methods for evaluating bond strength between concrete substrate and repair materials. Cement and concrete research, 35(4), pp.748-757.
102. Morsy, M.S., Alsayed, S.H., Al-Salloum, Y. and Almusallam, T., 2014. Effect of sodium silicate to sodium hydroxide ratios on strength and microstructure of fly ash geopolymer binder. Arabian journal for science and engineering, 39(6), pp.4333-4339.

103. Mourougane, R., Puttappa, C.G., Sashidhar, C. and Muthu, K.U., 2012, June. Shear behaviour of high strength GPC/TVC beams. In Proc. Int. Conf. Adv. Arch. Civ. Eng (Vol. 21, p. 142).
104. Muthadhi, A. and Dhivya, V., 2017. Investigating Strength Properties of Geopolymer Concrete with Quarry Dust. ACI Materials Journal, 114(3), p.355.
105. Nagan, S. and Mohana, R., 2014. Behaviour of geopolymer ferrocement slabs subjected to impact. Iranian Journal of Science and Technology. Transactions of Civil Engineering, 38(C1+), p.223.
106. Nagaraj, V.K. and Babu, D.V., 2018. Formulation and performance evaluation of alkali-activated self-compacting concrete. Asian Journal of Civil Engineering, 19(8), pp.1021-1036.
107. Nath, P. and Sarker, P.K., 2014. Effect of GGBFS on setting, workability and early strength properties of fly ash geopolymer concrete cured in ambient condition. Construction and Building Materials, 66, pp.163-171.
108. Nath, P. and Sarker, P.K., 2017. Flexural strength and elastic modulus of ambient-cured blended low-calcium fly ash geopolymer concrete. Construction and Building Materials, 130, pp.22-31.
109. Nematollahi, B. and Sanjayan, J., 2014. Effect of different superplasticizers and activator combinations on workability and strength of fly ash based geopolymer. Materials & Design, 57, pp.667-672.
110. Ng, T.S., Amin, A. and Foster, S.J., 2013. The behaviour of steel-fibre-reinforced geopolymer concrete beams in shear. Magazine of concrete research, 65(5), pp.308-318.
111. Nugteren, H., Davidovits, J., Antenucci, D., Fernandez-Pereira, C. and Querol, X., 2005, April. Geopolymerization of fly ash. In Proceedings in World of Coal Ash Conference – 2005.
112. Palomo, Á, Alonso, S., Fernandez-Jiménez, A., Sobrados, I. and Sanz, J., 2004. Alkaline activation of fly ashes: NMR study of the reaction products. Journal of the American Ceramic Society, 87(6), pp.1141-1145.
113. Palomo, A., Blanco-Varela, M.T., Granizo, M.L., Puertas, F., Vazquez, T. and Grutzeck, M.W., 1999. Chemical stability of cementitious materials based on metakaolin. Cement and Concrete Research, 29(7), pp.997-1004.
114. Palomo, A., Grutzeck, M.W. and Blanco, M.T., 1999. Alkali-activated fly ashes: a cement for the future. Cement and concrete research, 29(8), pp.1323-1329.
115. Papanicolaou, C.G. and Triantafillou, T.C., 2002. Shear transfer capacity along pumice aggregate concrete and high-performance concrete interfaces. Materials and Structures, 35(4), pp.237-245.
116. Parthiban, K., Saravanarajamohan, K., Shobana, S. and Bhaskar, A.A., 2013. Effect of replacement of slag on the mechanical properties of fly ash based geopolymer concrete. International Journal of Engineering and Technology (IJET), 5(3), pp.2555-2559.
117. Patnaik, A.K., 1992. Horizontal shear strength of composite concrete beams with a rough interface. Degree: Ph. D, University of Calgary (Canada)
118. Patnaik, A.K., 2000. Evaluation of ACI 318-95 Shear-Friction Provisions. Discussion. ACI Structural Journal, 97(3).
119. Patnaik, A.K., 2001. Behavior of composite concrete beams with smooth interface. Journal of Structural Engineering, 127(4), pp.359-366.
120. PCI (Precast/Prestressed Concrete Institute). 2010 PCI Design Handbook, 7th edn. Precast/Prestressed Concrete Institute, Chicago, IL, USA.
121. Phoo-ngernkham, T., Maegawa, A., Mishima, N., Hatanaka, S. and Chindaprasirt, P., 2015. Effects of sodium hydroxide and sodium silicate solutions on compressive and shear bond strengths of FA–GBFS geopolymer. Construction and Building Materials, 91, pp.1-8.

122. Prasad, N.D. and Kumar, Y.H., 2017. Study of Behaviour of Geo-Polymer Concrete with Respect To Its Mechanical Properties of GGBS and fly ash. International Journal of Civil Engineering and Technology, 8(2).
123. Prasanna, K., Lakshminarayan, B., Arun Kumar, M. and Dinesh Kumaran, J.R., 2016. "Fly ash based geopolymer concrete with GGBS". In International Conference on Current Research in Engineering Science and Technology, India. E-ISSN :2348 – 8352, pp 12 - 18
124. Puertas, F., Martínez-Ramírez, S., Alonso, S. and Vazquez, T., 2000. Alkali-activated fly ash/slag cements: strength behaviour and hydration products. Cement and concrete research, 30(10), pp.1625-1632.
125. Purdon, A.O., 1940. The action of alkalis on blast-furnace slag. Journal of the Society of Chemical Industry, 59(9), pp.191-202.
126. Rafeel, A., Vinai, R., Soutsos, M. and Sha, W., 2017. Guidelines for mix proportioning of fly ash/GGBS based alkali activated concretes. Construction and Building Materials, 147, pp.130-142.
127. Rahal, K.N. and Al-Khaleefi, A.L., 2015. Shear-Friction Behavior of Recycled and Natural Aggregate Concrete--An Experimental Investigation. ACI Structural Journal, 112(6).
128. Rahal, K.N., Khaleefi, A.L. and Al-Sanee, A., 2015. An experimental investigation of shear-transfer strength of normal and high strength self-compacting concrete. Engineering Structures, 109, pp.16-25.
129. Rahman, M. and Sarker, P., 2011. Geopolymer concrete columns under combined axial load and biaxial bending. In Proceedings of the CONCRETE 2011 Conference. The Concrete Institute of Australia.
130. Rai, B., Roy, L.B. and Rajjak, M., 2018. A statistical investigation of different parameters influencing compressive strength of fly ash induced geopolymer concrete. Structural Concrete, 19(5), pp.1268-1279.
131. Rajagopalan Gopalakrishnan, 2019. "Durability of alumina silicate concrete based on slag/fly ash blends against corrosion", Engineering, Construction and Architectural Management, Vol. 26 No. 8, pp. 1641-1651.
132. Rajamane, N., Nataraja, M., Lakshmanan, N. and Dattatreya, J., 2011. Rapid chloride permeability test on geopolymer and Portland cement. Ind. Concrete J, 85(10), pp.21-26.
133. Rajamane, N.P., Nataraja, M.C., Lakshmanan, N., Dattatreya, J.K. and Sabitha, D., 2012. Sulphuric acid resistant ecofriendly concrete from geopolymerisation of blast furnace slag. Indian Journal of Engineering and Materials Sciences IJEMS Vol.19 (5), pp 357-367.
134. Rajarajeswari, A. and Dhinakaran, G., 2016. Compressive strength of GGBFS based GPC under thermal curing. Construction and Building Materials, 126, pp.552-559.
135. Rajendran, M. and Soundarapandian, N., 2013. An Experimental Investigation on the Flexural Behavior of Geopolymer Ferrocement Slabs. Journal of Engineering & Technology, 3(2).
136. Rajini, B. and Rao, A.N., 2014. Mechanical properties of geopolymer concrete with fly ash and GGBS as source materials. International Journal of Innovative Research in Science, Engineering and Technology, 3(9), pp.15944-15953.
137. Rama Seshu, D, Shankaraiah, R. and Srinivas, B.S., 2017. A study on the effect of Binder index on compressive strength of Geopolymer concrete. Cement Wapno Beton, 84, pp.211-215.
138. Rama Seshu,D., Shankaraiah, R. and Sesha, S.B., 2019. The Binder Index–A Parameter That Influences the Strength of Geopolymer Concrete. Slovak Journal of Civil Engineering, 27(1), pp.32-38.
139. Ramamohana, B., Gopinathan, P. and Chandrasekhar, I., 2019 "Engineering Properties of GGBS & Fly ash Synthesized Geopolymer Concrete at Different Environmental Conditions by Comparing with Conventional Concrete", International Journal of Recent Technology and Engineering (IJRTE) ISSN: 2277-3878, Volume-7, Issue-5S4, pp 399-407

140. Randl, N., 1997. Investigations on transfer of forces between old and new concrete at different joint roughness. University of Innsbruck: PhD thesis.
141. Randl, N., 2013. Design recommendations for interface shear transfer in fib Model Code 2010. Structural Concrete, 14(3), pp.230-241.
142. Rangan, B.V., 2008. Fly ash-based geopolymer concrete. Curtin University of Technology, Dept of Engineering, Tech. report No.GC4, 2008.
143. Rangan, B.V., 2009. Engineering properties of geopolymer concrete. In Geopolymers (pp. 211-226). Woodhead Publishing.
144. Rao, T.G. and Andal, M., 2014. Cementing efficiency of low calcium fly ash in fly ash concretes. International Journal of Civil, Environmental, Structural, Construction and Architectural Engineering, 7(12), pp.997-1001.
145. Rashad, A.M., 2019. Insulating and fire-resistant behaviour of metakaolin and fly ash geopolymer mortars. Proceedings of the Institution of Civil Engineers-Construction Materials, 172(1), pp.37-44.
146. Raths, C.H., 1977. Reader Comments: Design Proposals for Reinforced Concrete Corbels. PCI Journal, 22(2), pp.93-98.
147. Rostami, H. and Silverstrim, T., 1996, December. Chemically activated fly ash (CAFA): a new type of fly ash based cement. Pittsburgh Coal Conference, Pittsburgh, PA (United States).
148. Saemann, J.C. and Washa, G.W., 1964, November. Horizontal shear connections between precast beams and cast-in-place. In Journal Proceedings (Vol. 61, No. 11, pp. 1383-1410).
149. Santos, P.M. and Júlio, E.N., 2012. A state-of-the-art review on shear-friction. Engineering Structures, 45, pp.435-448.
150. Sarker, P.K., 2011. Bond strength of reinforcing steel embedded in fly ash-based geopolymer concrete. Materials and structures, 44(5), pp.1021-1030.
151. Sarker, P.K., Kelly, S. and Yao, Z., 2014. Effect of fire exposure on cracking, spalling and residual strength of fly ash geopolymer concrete. Materials & Design, 63, pp.584-592.
152. Shaikh, A.F. 1978. Proposed revisions to shear-friction provisions. Precast / Prestressed Concrete Institute, PCI Journal, Vol. 23, No. 2, pp. 12-21
153. Shaw, D.M. and Sneed, L.H., 2014. Interface shear transfer of lightweight-aggregate concretes cast at different times. PCI Journal, 59(3).
154. Shi, C. and Day, R.L., 1999. Early strength development and hydration of alkali-activated blast furnace slag/fly ash blends. Advances in Cement Research, 11(4), pp.189-196.
155. Sofi, M., Van Deventer, J.S.J., Mendis, P.A. and Lukey, G.C., 2007. Bond performance of reinforcing bars in inorganic polymer concrete (IPC). Journal of Materials Science, 42(9), pp.3107-3116.
156. Somna, K., Jaturapitakkul, C., Kajitvichyanukul, P. and Chindaprasirt, P., 2011. NaOH-activated ground fly ash geopolymer cured at ambient temperature. Fuel, 90(6), pp.2118-2124.
157. Song, X.J., Marosszeky, M., Brungs, M. and Munn, R., 2005, April. Durability of fly ash based geopolymer concrete against sulphuric acid attack. In International Conference on Durability of Building Materials and Components (Vol. 10).
158. Srinivasan, S., Karthik, A. and Nagan, D.R.S., 2014. An investigation on flexural behaviour of glass fibre reinforced geopolymer concrete beams. Int. J. Eng. Sci. Res. Technol, 3(4), pp.1963-1968.
159. Standard, C.S.A., A23.3. 2019. Design of concrete structures (sixth edition). Mississauga, Ontario: Canadian Standards Association.
160. Sujatha, T., Kannapiran, K. and Nagan, S., 2012. Strength assessment of heat cured geopolymer concrete slender column. Asian journal of civil engineering (building and housing) Volume 13, Number 5; Page(s) 635 To 646.

161. Sumajouw, D.M., Hardjito, D., Wallah, S. and Rangan, B.V., 2005. Behavior of geopolymer concrete columns under equal load eccentricities. American Concrete Institute: Farmington Hills, MI, USA, pp.577-594.
162. Sumajouw, M. and Rangan, B.V., 2006. Low-calcium fly ash-based geopolymer concrete: reinforced beams and columns, Curtin University of Technology, Report No. EPR-843
163. Teixeira-Pinto, A., Fernandes, P. and Jalali, S., 2002, October. Geopolymer manufacture and application-Main problems when using concrete technology. In Geopolymers 2002 International Conference, Melbourne, Australia, Siloxo Pty. Ltd.
164. Thokchom, S., Ghosh, P. and Ghosh, S., 2009. Acid resistance of fly ash based geopolymer mortars. International Journal of Recent Trends in Engineering, 1(6), p.36.
165. Tsoukantas, S.G. and Tassios, T.P., 1989. Shear resistance of connections between reinforced concrete linear precast elements. Structural Journal, 86(3), pp.242-249.
166. Valluvan, R., Kreger, M.E. and Jirsa, J.O., 1999. Evaluation of ACI 318-95 shear-friction provisions. Structural Journal, 96(4), pp.473-481.
167. Vecchio, F.J. and Collins, M.P., 1986. The modified compression-field theory for reinforced concrete elements subjected to shear. ACI J., 83(2), pp.219-231.
168. Visintin, P., Ali, M.M., Albitar, M. and Lucas, W., 2017. Shear behaviour of geopolymer concrete beams without stirrups. Construction and Building Materials, 148, pp.10-21.
169. Wallah, S.E., Hardjito, D., Sumajouw, D.M.J. and Rangan, B.V., 2005. Sulfate and acid resistance of fly ash-based geopolymer concrete. In Australian Structural Engineering Conference 2005 (p. 733). Engineers Australia.
170. Wallah, S. and Rangan, B.V., 2006. Low-calcium fly ash-based geopolymer concrete: long-term properties. Technical Report no. GC2, Curtin University of Technology, Faculty of Engineering, 2006.
171. Wang, S.D., Pu, X.C., Scrivener, K.L. and Pratt, P.L., 1995. Alkali-activated slag cement and concrete: a review of properties and problems. Advances in cement research, 7(27), pp.93-102.
172. WBCSD, World Business Council for Sustainable Development, 2008. Report on "Sustainable consumption facts and trends—from a business perspective". pp 1-40
173. Xiao, J., Sun, C. and Lange, D.A., 2016. Effect of joint interface conditions on shear transfer behavior of recycled aggregate concrete. Construction and Building Materials, 105, pp.343-355.
174. Yang, K.H., Sim, J.I., Kang, J.H. and Ashour, A.F., 2012. Shear capacity of monolithic concrete joints without transverse reinforcement. Magazine of Concrete Research, 64(9), pp.767-779.
175. Yassin, L.A.G. and Hasan, Q.A.M., 2015. Reinforced Concrete Corbels–State of the Art. Journal of Materials and Engineering Structures «JMES», 2(4), pp.180-205.
176. Yost, J.R., Radlińska, A., Ernst, S., Salera, M. and Martignetti, N.J., 2013. Structural behavior of alkali activated fly ash concrete. Part 2: structural testing and experimental findings. Materials and structures, 46(3), pp.449-462.
177. Zende R, Mamatha. A, 2015. "Study on Fly Ash and GGBS Based Geopolymer Concrete under Ambient Curing". Journal of Emerging Technologies and Innovative Research, 2(7), pp.3082-3087.
178. Zilch, K., and Reinecke, R., "Capacity of Shear Joints between High-Strength Precast Elements and Normal-Strength Cast-in-Place Decks," fibInternational Symposium on High Performance Concrete, Orlando, FL,Sept. 2000.